Universitat Autònoma de Barcelona

Mitochondrial quality control in neurodegenerative diseases: focus on Parkinson's disease and Huntington's disease

Sandra Franco Iborra

Universitat Autònoma de Barcelona

Mitochondrial quality control in neurodegenerative diseases: focus on Parkinson's disease and Huntington's disease

TESI DOCTORAL

2018

Programa de Doctorat en Neurociències

Institut de Neurociències

Tesi realitzada al laboratori de Malalties Neurodegeenratives de l'Institut de Recerca de la Vall d'Hebron (VHIR)

Doctorand	**Director**	**Tutor**
Sandra Franco Iborra	Miquel Vila Bover	José Rodríguez Álvarez

Co-directora	**Co-directora**
Celine Perier	Marta Martínez Vicente

AGRAÏMENTS

En primer lloc vull agraïr al Miquel Vila per l'oportunitat que em va donar de començar a fer la tesi doctoral al seu lab. Gràcies per tenir sempre la porta oberta del teu despatx, per la confiança dipositada en mi i per tot el que m'has ensenyat durant tots aquests anys. A més, he tingut la sort de tenir no només un director de tesis sinó tres! Celine muchas gracias por estar siempre ahí, por ensenyarme tu manera de hacer ciencia (que me encanta!) y por ser siempre tan positiva. En mi manera de trabajar hay un poquito de ti y espero ir pasando este conocimiento a los demás porque en todo laboratorio debería ser obligatorio que hubiera alguien como tu. No solo a nivel profesional pero a nivel personal me has ayudado mucho y siempre que hablamos me siento mucho mejor después. Esta tesis, sin duda, no hubiera sido lo mismo sin ti y yo tampoco. Marta moltes gràcies per la teva infinita paciència, per tenir sempre un moment per mi i per haver-me ajudat en el dia a dia del lab. Gràcies també pels teus consells i per aguantar totes les meves preguntes (sóc incapaç de decidir!)

.

Aquests anys els he passat en el millor laboratori del món amb els millors companys del món! Annabelle tu eres imprescindible para mi día a día en el lab. Gracias por escucharme siempre, todas mis dudas, que si hago esto o hago lo otro y siempre con una sonrisa. Thais, la meva companya de poyata (d'esquena!) m'has fet tots els experiments més entretinguts perquè sempre estaves allà per parlar. I a mi m'encanta parlar, ja ho sabeu! Per mi les dues sou com dues germanes grans que m'heu aconsellat durant tot aquest temps. Ara us hauré de trucar quan no sàpiga que fer! Iria me lo he pasado genial contigo y tus historias, eres la alegría del hemilab! Ariadna, gràcies per estar pendent de mi i preguntar-me sempre com estava i ser la meva companya organitzadora de lab meetings. Albert, hem compartit molts moments junts al lab i molta frustració de l'aplicatiu SIA de la UAB , et desitjo el millor per a aquests últims anys i espero que ens trobem en algun altre lloc. Als meus companys de despatx, els Jordis (Galiano i Bové) gràcies per tot el que he rigut amb vosaltres. Jordi Galiano gairebé em mates d'un espant unes quantes vegades però com a contrapartida ets el millor company per demanar que t'acompanyi al nitrogen líquid. Trobaré molt a faltar els nostres matins a les 8.30 am i els teus "et veig il·lusionada". Jordi Bové, encara estic esperant la meva gorra de l'Arale! Gràcies per tots els moments que em passat junts i rient en el teu estat de bogeria. A la Marta González, la Bea i el Jordi Romero, gràcies per ajudar-me sempre amb un somriure, ha estat un plaer treballar amb vosaltres. Marta me ha hecho mucha gracia conocerte después de haber sido mi profe, echaré de menos nuestras charlas en la reveladora. A les noves adquisicions del lab la Núria, l'Alex, el Marc, la Mercè i l'Alice, que sapigueu que esteu en un lloc immillorable. I també a les persones que van passar pel lab, en especial l'Alba i al Xavi, dos diamants en brut als que els hi desitjo el millor del mon.

Gràcies als nostres veïns del lab de Malalties Mitocondrials, per totes les xerrades al voltant de la màquina de cafè i per la vostra ajuda amb els protocols de DNA mitocondrial. Especialment a la Cora i al Ferran, gràcies als dos per fer més amenes les tardes al lab i també per venir a veure'ns a Brain and Beer, heu estat dels més incondicionals. Hem compartit experiències de lab i viatges i m'encantaria que ens puguèssim trobar a algún altre lloc. Gràcies a la Yolanda també, per estar sempre amb un somriure i disposada a ajudar en tot

.

Gràcies a tots els meus amics de la Uni, Esther, Anna, Xabi, Helena, Laura Luque, Irene ja fa molts anys que ens coneixem i sou totalment imprescindibles per mi. La vida requereix

sempre d’amics que et treguin de birres en els moments baixos i que gaudeixin amb tu de totes les coses bones. I encara que no ens veiem tant però sé que hi sou allà Anna M, Gerard, Uri i Alba gràcies. I evidentment no em puc oblidar del Carlos i l’Iñaki, sempre fent-nos riure i que ja formen part de la familia de ple.

Als meus amics de Brain and Beer, Maca i Marc. Participar en Brain and Beer ha estat unes de les millors experiències de tots aquests anys. Evidentment el millor és haver-nos conegut. Marc, ets una persona molt especial i força peculiar però saps que t’estimem així. Maca, no podria ser la que soy ahora sin haberte conocido, me has ensenyado Carne Cruda y la Cafetera y eso ya irá conmigo para siempre. Eres una persona increíble! Gracias por todas esas calçotadas, barbacoas, tailandeses y las millones de cervezas, aquí o en Bélgica, y todas esas charlas. Y a los friends de Brain ans Beer Andrea, Ananda, Jaume y Marta por apoyarnos siempre.

A Cris y Annece, mis amigas del máster. Aunque ahora estemos separadas hemos pasado unos momentos geniales juntas que no olvidaré jamás. Y siempre hay una excusa para reunirnos en algun lugar del mundo. A Pablo de Equador, por ser tan carinyoso y atento conmigo y enseñarme su cultura.

A mis amigos de IDIBELL, Andrea, Ale, Sónia y Juanjo gracias por haberme integrado en vuestra família y por todos los buenos momentos. Y especialmente a Eva y Patri, sois las dos unos amores y os aprecio muchísimo. Me ha encantado compartir con vosotras todas esas cenas y birras y, especialmente, toda vuestra sabiduría.

Un gracias en mayúsculas a Pablo, por encontrarme. Gracias por compartir conmigo todo este camino, que sabes que a veces no ha sido fácil para mi pero siempre estabas tu para sacarme esa sonrisa. Gracias porque sabes que soy muy pesada siempre preguntándote y siempre piediéndote ayuda y nunca te cansas de estar ahí. La vida contigo es divertida y sé que seguirá siendo así aquí o donde sea que estemos.

I, per acabar, a tota la meva família, i, especialment, als meus pares Miguel i Sílvia i a les meves germanetes Marina i Laia per estar sempre quan us he necessitat. I gràcies perquè sense vosaltres aquesta tesi hagués estat impossible.

Gràcies a totes aquelles que heu compartit un tros del camí amb mi.

TABLE OF CONTENTS

LIST OF TABLES

LIST OF FIGURES

LIST OF ABBREVIATIONS

Only those appearing more than once in the text. The rest, as well as the full name of genes and proteins, are indicated in their first appearance in the text.

6-OHDA	6-hydroxydopamine
AAV	Adeno-associated virus
ATP	Adenosine triphosphate
CAG	Cytosine-adenine-guanine
CMA	Chaperone mediated autophagy
DA	Dopaminergic
ER	Endoplasmic reticulum
HD	Huntington's disease
HEAT	Huntingtin, elongation factor 3, protein phosphatase 2A and TOR1
Htt	Huntingtin
IF	Immunofluorescence
IHQ	Immunohistochemistry
IMM	Inner mitochondrial membrane
IMS	Intermembrane space
iPSC	Induced pluripotent stem cells
LB	Lewy bodies
MDV	Mitochondrial-derived vesicles
MEF	Mouse embryonic fibroblasts
MPP^+	1-methyl-4-phenylpyridinium
MPTP	1-methyl-4-phenyl-1,2,3,6-tetrahydropyridine
mtDNA	Mitochondrial DNA
mtUPR	Mitochondrial unfolded protein response
OMM	Outer mitochondrial membrane
PAS	Pre-autophagosomal structure
PD	Parkinson's disease
PLA	Proximity ligation assay
polyQ	polyglutamines
ROS	Reactive oxygen species
RT	Room temperature
SN	Substantia nigra
SNpc	Substantia nigra pars compacta
TCA	Tricarboxylic acid

TH	Tyrosine hydroxylase
UPS	Ubiquitin-proteasome system

SUMMARY

Summary

In the past years, several important advances have expanded our understanding of the pathways that lead to cell dysfunction and death in Parkinson's disease (PD) and Huntington's disease (HD). Both diseases are movement disorders characterized by the loss of a specific subset of neurons within the basal ganglia, dopaminergic neurons in the substantia nigra pars compacta (SNpc), in the case of PD, and medium spiny neurons in the striatum, in the case of HD,. Despite distinct clinical and pathological features, these two neurodegenerative disorders share critical underlying pathogenic mechanisms such as the presence of misfolded and/or aggregated proteins, oxidative stress and mitochondrial anomalies. Mitochondria are the prime energy source in most eukaryotic cells, but these highly dynamic organelles are also involved in a multitude of cellular events. Disruption of mitochondrial homeostasis and the subsequent mitochondrial dysfunction plays a key role in the pathophysiology of neurodegenerative diseases. Therefore, maintenance of mitochondrial integrity through different surveillance mechanisms is critical for neuronal survival. In this thesis I have studied in depth some mitochondrial quality control mechanisms in the context of PD and HD, in order to broaden the knowledge about the pathomechanisms leading to cell death.

In the first chapter I have studied mitochondrial protein import in *in vitro* and *in vivo* models of PD. *In vitro*, complex I inhibition, a characteristic pathological hallmark in PD, impaired mitochondrial protein import. This was associated with OXPHOS protein downregulation, accumulation of aggregated proteins inside mitochondria and downregulation of mitochondrial chaperones. Therefore, we aimed to reestablish the mitochondrial protein import by overexpressing two key components of the system: translocase of the outer membrane 20 (TOM20) and translocase of the inner membrane 23 (TIM23). Overexpression of TOM20 and TIM23 *in vitro* restored protein import into mitochondria and ameliorated mitochondrial dysfunction and cell death. Complex I inhibition also impaired mitochondrial protein import and led to dopaminergic neurodegeneration *in vivo*. Overexpression of TIM23 partially rescued protein import into mitochondria and slightly protected dopaminergic neurons in the SNpc. On the contrary, TOM20 overexpression did not rescue protein import into mitochondria and exacerbated neurodegeneration in both SNpc and striatum. These results highlight mitochondrial protein import dysfunction and the distinct role of two of their components in the pathogenesis of PD and suggest the need for future studies to target other elements in the system.

In the second chapter, I have studied the role of huntingtin in mitophagy and how the polyglutamine expansion present in mutant huntingtin can affect its function. For such, I worked with differentiated striatal ST-Q7 (as control) and ST-Q111 (as mutant) cells, expressing full length huntingtin. In these conditions, induced mitophagy was not mediated by Parkin recruitment into depolarized mitochondria. Mutant huntingtin impaired induced mitophagy by altering wildtype huntingtin scaffolding activity at different steps of mitophagy process: (i) ULK1 activation through its release from the mTORC1, (ii) Beclin1-Vps15 complex formation, (iii) interaction of the mitophagy adapters OPTN and NDP52 with huntingtin and (iv) with LC3. As a result, mitochondria from ST-Q111 cells exhibited increased damage and altered mitochondrial respiration. These results uncover impaired mitophagy as a potential pathological mechanism linked with HD.

In conclusion, we have discovered new mitochondrial targets for PD and HD emphasizing the important role that mitochondrial quality control plays in neurodegeneration

INTRODUCTION

Preface

This thesis has focused on the study of mitochondrial dysfunction in two neurodegenerative diseases: Parkinson's disease and Huntington's disease. Mitochondrial dysfunction has been long ago linked to the pathogenesis of neurodegenerative disorders. During all these years it has gained attention in the same way that it has lost it. The discovery of new pathways involved in Huntington's disease and Parkinson's disease, has often lead to the idea that mitochondrial dysfunction was a secondary event, arising from an ongoing general dysfunction of cellular homeostasis. Nevertheless, as our knowledge of mitochondria has been advancing and new mitochondrial functions have been discovered, mitochondria came back to the field over and over again. Nowadays, there is no doubt that mitochondrial dysfunction is involved in the pathogenesis of neurodegenerative diseases. Moreover, it is becoming clear that those types of diseases may not arise from a single event but rather comprise a complex network of deleterious events that finally lead to cell death. And mitochondria are one piece of the puzzle without which we could never understand the whole picture. It has been the aim of our work to unravel new pathways affected in two neurodegenerative diseases. Therefore, we have found deficits in mitochondrial protein import in Parkinson's disease and in mitophagy in Huntington's disease. Mitochondrial protein import and mitophagy may seem two very different processes but they both serve a common goal, mitochondrial homeostasis.

1 Introduction

1.1 Mitochondria biology: an overview

1.1.1 Mitochondrial biology: structure and general mitochondrial functions

Mitochondria were first observed more than 150 years ago by Rudolf Albert von Kölliker and described as “thread-like granules” in the cytoplasm of eukaryotic cells. It was more than 100 years later that the origin of mitochondria started to be elucidated. The endosymbiotic hypothesis argues that mitochondria evolved from a bacterial ancestor through the symbiosis within an eukaryotic host cell (Margulis, 1970). From a genetic point of view, mitochondria are a bacterial ancestry originating from within the phylum α-Proteobacteria (*Alphaproteobacteria*) (Gray, 2012). Over the course of time, the bacterium has lost all of its functions as a separate entity and became the mitochondrion. Most eukaryotic cells harbor multiple mitochondria, and the number/volume of mitochondria per cell is regulated to match the bioenergetics demands of each cell type.

Mammalian mitochondria have a ~16-kb multicopy, double-stranded circular genome encoding for 13 protein subunits of the mitochondrial electron transport chain and ATP synthase. The additional genes encode 2 ribosomal RNA (rRNA) and 22 transfer RNA (tRNA), essential components of the mitochondrial translation system (Anderson et al., 1981). This means that the vast majority of the mitochondrial proteome is encoded in the nucleus, synthesized in the cytosol and imported back into the organelle. The majority of the genes encoded by the α-proteobacterium have been transferred to the nucleus via the endosymbiotic gene transfer (Adams and Palmer, 2003).

Mitochondria are double membrane organelle, whose membranes enclose 4 different compartments: outer mitochondrial membrane (OMM), intermembrane space (IMS), inner mitochondrial membrane (IMM) and matrix (**Fig. 1**). The most abundant lipid constituents of the OMM are phosphatidylcholine and phosphatidylethanolamine (Prasai, 2017). The OMM also contains large number of porins, or voltage-dependent anion channels (VDAC), which render the membrane permeable to ions and molecules less than 5 kDa (O’Rourke, 2007). The IMS spans ~20 nm and acts as hub of molecular transport between the cytosol and the mitochondrial matrix (Herrmann and Riemer, 2010). The IMM is permeable only to small uncharged molecules of 100-150 Da or less and is composed by phosphatidylcholine,

phosphatidylethanolamine and also cardiolipin, which is important for IMM organization and for its barrier function. Moreover, the IMM is packed with several proteins, which constitute approximately 76% of the total IMM mass. The most abundant protein complexes are those involved in oxidative phosphorylation. The IMM surface is severalfold larger than the OMM, since it contains invaginations that expand its surface. The IMM surface can be divided into two domains: (i) the inner boundary membrane, which is closely apposed to the OMM, and (ii) the folded cristae membranes, which form invaginations of different shape and size (van der Laan et al., 2016), with different protein composition (Vogel et al., 2006). Cristae junctions connect the folded cristae membranes with the inner boundary membranes (van der Laan et al., 2016). Finally, enclosed by the IMM, the mitochondrial matrix harbors several enzymes and multiple copies of mitochondrial DNA (mtDNA) (Alberts et al., 2002). The mtDNA is highly compacted within the matrix, due to its interaction with several proteins that are crucial for its maintenance, and this structure is called nucleoid (Ngo et al., 2011; Rubio-Cosials et al., 2011).

Mitochondria are classically recognized by their ability to couple cellular respiration to the production of adenosine triphosphate (ATP) in a process termed oxidative phosphorylation (OXPHOS) (**Fig. 1**). This energy transduction occurs via the transport of electrons through a chain of proteins, the respiratory chain, located in the IMM. The respiratory chain is formed by five multimeric protein complexes: reduced nicotinamide adenine dinucleotide (NADH) dehydrogenase-ubiquinone oxidoreductase (complex I, approximately 46 subunits), succinate dehydrogenase-ubiquinone oxidoreductase (complex II, 4 subunits), ubiquinone-cytochrome *c* oxidoreductase (complex III, 11 subunits), cytochrome *c* oxidase (complex IV, 13 subunits), and ATP synthase (complex V, approximately 16 subunits). Additionally, it requires two small electron carriers, the ubiquinone/coenzyme Q and cytochrome c. Glycolysis and tricarboxylic acid cycle (TCA) reactions oxidize carbon to generate electrons. Those electrons are then passed from reduced cofactors to complex I or complex II and flow through the other complexes until being finally transferred to molecular oxygen, thereby producing water. The movement of electrons is linked to the pumping of protons across the IMM, from matrix to the IMS, leading to the production of a proton gradient across the IMM which generates an electrochemical gradient, termed mitochondrial membrane potential. ATP is synthesized by the influx of those protons back into the matrix through the ATP synthase. The generation of ATP through OXPHOS is far more efficient than through the glycolysis pathway, and this is especially crucial in high-energy tissues such as muscle or brain (Mitchell, 1961; Perier and Vila, 2012).

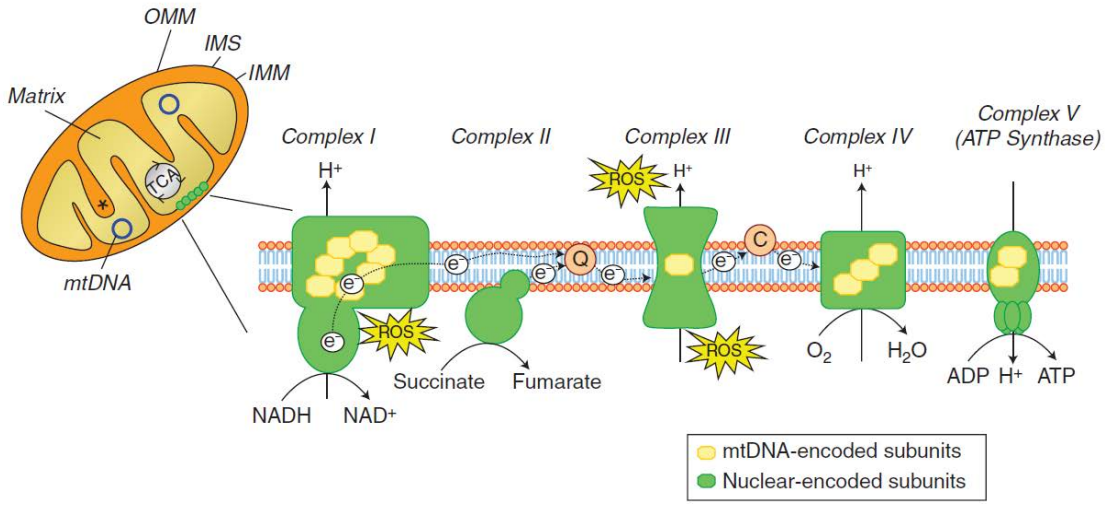

Figure 1 Schematic representation of mitochondrial structure

The scheme represents mitochondrial compartmentalization: outer mitochondrial membrane (OMM), intermembrane space (IMS), inner mitochondrial membrane (IMM) and matrix. The inset shows the electron transport chain, which couples the electron transport to the ATP synthesis. From Perier and Vila 2012.

Besides their main role as energy provider, mitochondria also have key functions in the metabolism of amino acids, fatty acids and steroids, regulation of calcium homeostasis, intracellular signaling, formation of Fe-S clusters and apoptosis.

1.1.2 Mitochondrial quality control systems

Due to the importance and diversity of mitochondrial functions, maintaining mitochondrial homeostasis is vital for cellular and organism health. Moreover, mitochondrial dysfunction is associated with a wide range of human disorders, from inherited mitochondrial diseases to neurodegenerative diseases or cancer (Nunnari and Suomalainen, 2012). Thus, several mechanisms have evolved to constantly survey mitochondrial health and ensure the maintenance and repair of damaged mitochondria (**Fig. 2**). Those mechanisms can act at molecular, protein and organellar levels.

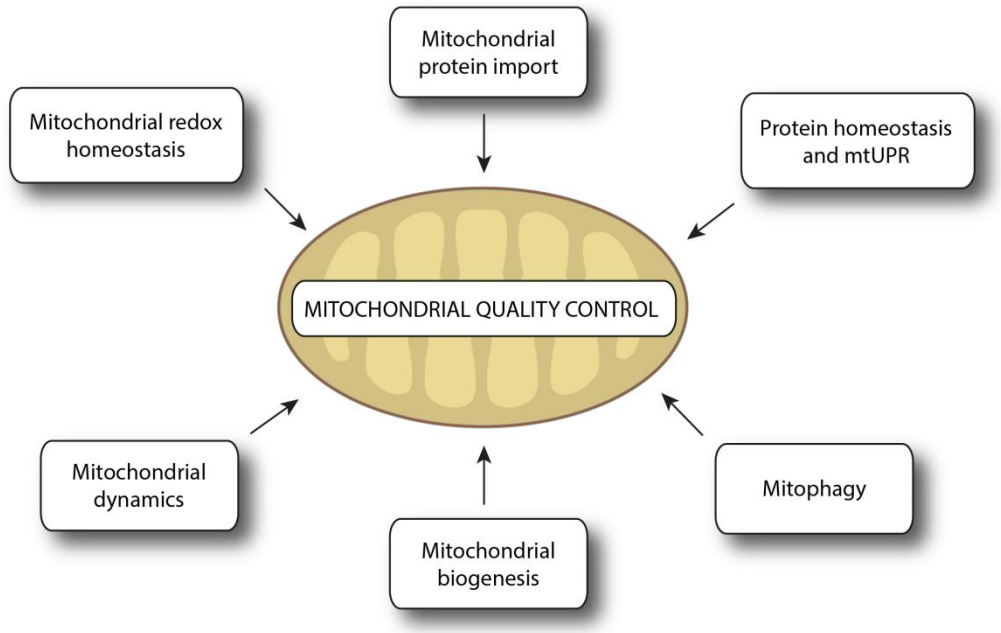

Figure 2. Mitochondrial quality control processes responsible for maintaining mitochondrial integrity and functionality

1.1.2.1 Mitochondrial redox homeostasis

1.1.2.1.1 Reactive oxygen species

Mitochondria are both the target and the source of reactive oxygen species (ROS). ROS are generated due to the incomplete oxidation of oxygen into water, mainly during OXPHOS. ROS play a dual role; they act as signaling molecules in the maintenance of physiological functions (Sena and Chandel, 2012), but in excess they lead to oxidative stress, by damaging lipids, proteins and DNA. The superoxide radical ($^{\bullet}O_2^-$) is the first radical that appears with the reduction of molecular oxygen. Mitochondrial complex I and III are the major sites of superoxide production. Superoxide radical can be transformed into hydrogen peroxide (H_2O_2) by the action of the enzyme superoxide dismutase (SOD) (Halliwell, 1996). Hydrogen peroxide is poorly reactive with most biomolecules, but can react with Fe^{2+} (in the Fenton reaction) to give rise to the hydroxyl radical ($OH^{\bullet}$), probably the most reactive free radical found *in vivo* (Halliwell and Gutteridge, 1984; Liochev, 2013) which can react with virtually all biomolecules. Thus, the existence of antioxidant defenses is highly important to render ROS levels below a toxic threshold.

1.1.2.1.2 Antioxidant defenses

One of the first antioxidant defenses is the enzyme superoxide dismutase (SOD) which accelerates the dismutation of two molecules of superoxide into one molecule of hydrogen peroxide and one molecule of oxygen, thus, reducing the potentially harmful effects of superoxide anion radical. Three SOD isoenzymes have been identified in humans: copper and zinc-containing SOD (CuZnSOD/SOD1), mainly located in the cytosol and nuclear compartments; the manganese-containing SOD (MnSOD/SOD2), a mitochondrial enzyme; and SOD3, a MnSOD located extracellularly (Perry et al., 2010). Even though hydrogen peroxide is a radical with low reactivity, it must be eliminated by the action of enzymes such as catalase, glutathione peroxidases (GPXs), the thioredoxin system, peroxiredoxins (PRDX) and glutaredoxins. GPX couples the reduction of hydrogen peroxide (and other peroxides) to water (or to corresponding alcohols) with the oxidation of reduced glutathione (GSH) to oxidized glutathione (GSSG), which can be converted back to GSH by glutathione reductase (GR). PRDX also couples the reduction of hydrogen peroxide with a cycle of peroxide-dependent oxidation and thiol-dependent reduction of cysteine residues, the latter catalyzed by thioredoxin and thioredoxin reductase. Glutaredoxins have the same function as the thioredoxin system (Chance et al., 1979; Rhee et al., 2005) (**Fig. 3**). Glutathione S-transferases participate in the detoxification of electrophilic compounds by their conjugation with GSH (Hayes et al., 2005). Another group of antioxidants are the non-enzymatic antioxidants such as glutathione, ascorbic acid (vitamin C), α-tocopherol (vitamin E), carotenoids or flavonoids, which are mainly ingested with the diet and act by scavenging free radicals (Forman et al., 2014). The last antioxidant defense layer is the sequestration of “free” transition metals, such as iron or copper, which are capable of stimulating free radical formation and also the direct oxidation of macromolecules. Within cells, iron is stored in the form of ferritin and copper as metallothionein (Rutherford and Bird, 2004). Despite this, antioxidant defenses are not completely efficient and in pathological condition they can be overwhelmed.

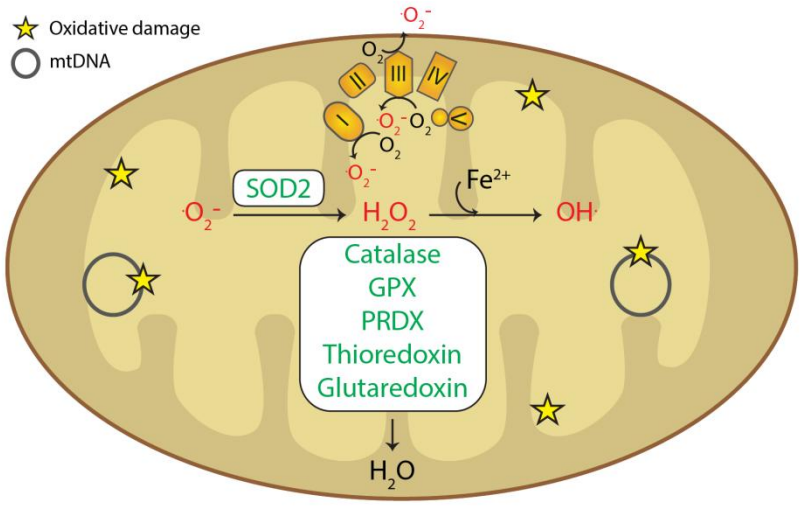

Figure 3. Schematic representation of some of the antioxidant defenses present in the mitocondria.

Superoxide radical arises mainly from complex I and complex III of the electron transport chain. This can lead to increased ROS production and oxidative damage to lipid, proteins and DNA. To maintain ROS levels below a toxic threshold, mitochondria have several antioxidant defenses (depicted in green) which help to maintain ROS production at physiological levels.

1.1.2.2 Mitochondrial protein import machinery

Mitochondrial DNA only encodes for 1% of the total mitochondrial proteome while the remaining 99% is encoded by the nuclear DNA (Wiedemann et al., 2004). Hence, the mitochondrial protein import machinery is essential for the maintenance of mitochondrial function. Most nuclear-encoded mitochondrial proteins are encoded as precursors and maintained in an unfolded conformation to make them translocation-competent. However, precursor proteins can also be imported co-translationally. In any case, precursor proteins in the cytosol must exist in complexes with cytosolic chaperones, such as HSP70, HSP90 (Young et al., 2003) and the recently discovered TOM34 (Faou and Hoogenraad, 2012), to avoid their degradation and aggregation. Moreover, those precursors need to contain information that directs them to the mitochondria and into the correct mitochondrial compartment. The most common signal is the N-terminal targeting sequence called matrix-targeting sequence (MTS), which consists of 10-80 amino acid residues with no sequence identity, but with some characteristic physicochemical properties, such as its potential to form amphipathic helices with one hydrophobic and one positively charged face (Gordon et al., 2000; Roise et al., 1988). There also exist C-terminal targeting sequences and internal signals whose nature remains elusive (Gordon et al., 2000). In this section I will summarize

the different mitochondrial protein import pathways classified according to the protein final destination. Mitochondrial protein import has been reviewed extensively in (Kang et al., 2017a; Wasilewski et al., 2017; Wiedemann and Pfanner, 2017). Classically, the study of the general principles of protein import into mitochondria has been performed in yeast and later it was found that the vast majority of the protein machineries are highly conserved in higher eukaryotes. When the yeast name of the protein changes in humans, I have added the name in brackets.

1.1.2.2.1 Translocation of proteins to the matrix

Most mitochondrial proteins are located within the matrix. For these proteins to be imported, there needs to be cooperation between the two main mitochondrial translocases, the translocase of the outer membrane (TOM) complex on the OMM and the translocase of the inner membrane (TIM23) complex on the IMM. The TOM complex mediates the translocation of nearly all the mitochondrial proteome. It is composed by seven components: (i) Tom70, Tom22 and Tom20, which form the surface receptor and recognize preproteins; (ii) Tom40, a β-barrel protein that conforms the main component of the translocase pore, together with (iii) Tom5, 6, and 7 small associated subunits (Bausewein et al., 2017; Model et al., 2008). The TIM23 complex translocates preproteins through the IMM. Tim50, Tim17 (TIM17A and TIM17B in humans) and Tim21 expose domains to the IMS, Tim23 is the channel forming protein and Mgr2 (ROMO1 in humans) constitutes the lateral gatekeeper. For translocation of the preprotein, TIM23 complex has to associate with the presequence-associated-motor (PAM complex) or import motor, which consists of: (i) mtHsp70 (mortalin in humans), the central chaperone that binds to preproteins and moves them inside the matrix through successive rounds of ATP hydrolysis; (ii) Tim44, (iii) Tim16/Pam16 (MAGMAS in humans) and Tim14/Pam18 (DnaJC15 and DnaJC19 in humans) co-chaperones, (iv) Mge1 (GrpE in humans) and (v) Pam17, which participates in the recruitment of the co-chaperones (van der Laan et al., 2010). In contrast to TOM complex, the translocation of preproteins through the TIM23 complex is energetically driven by the mitochondrial membrane potential and the hydrolysis of ATP (Mokranjac and Neupert, 2010). TIM23 complex interacts with TOM complex during protein translocation to the matrix (Chacinska et al., 2010). Once in the matrix, the mitochondrial-processing peptidase (MPP) is the main peptidase responsible for cleaving the targeting signals of preproteins, leading to the mature polypeptide (**Fig. 4**). A subset of precursors with a specific amino acid motif are further processed by the mitochondrial intermembrane peptidase octapeptidyl aminopeptidase 1 (Oct1), which removes an octapeptide after the cleavage performed by MPP (Gakh et al., 2002). More recently, another peptidase has been discovered, the intermediate cleaving peptidase 55

(Icp55), which removes a unique amino acid after MPP processing to stabilize the mitochondrial proteins (Vögtle et al., 2009).

1.1.2.2.2 Translocation of outer membrane proteins

The insertion of precursors into the OMM can be mediated by TOM complex and sorting and assembly machinery (SAM) complex both located in the OMM. In the case of β-barrel membrane proteins insertion, there is a cooperation of both complexes. The SAM complex, also named TOB (topogenesis of mitochondrial outer membrane β-barrel), is a complex specialized in the insertion of β-barrel proteins, such as VDAC or Tom40 (**Fig. 4**). Interestingly, in yeasts, those β-barrel proteins presumably may move from TOM complex to the intermembrane space, and then to the SAM complex (Wiedemann et al., 2003).

1.1.2.2.3 Translocation of inner membrane proteins

The IMM harbors a variety of proteins, including mitochondrial electron transport chain complexes and ATP synthase. There are three different routes for these proteins once they have been translocated first by the TOM complex: i) through the translocase of the inner mitochondrial membrane 22 (TIM22) complex located in the IMM, ii) through a lateral insertion by the TIM23 complex and iii) in an export-like route from the matrix to the inner membrane (**Fig. 4**) (Neupert and Herrmann, 2007). The TIM22 complex comprises (i) the channel-forming protein Tim22, (ii) the receptor-like protein Tim54, (iii) Tim18, which facilitates the assembly of Tim54 and Tim22, (iv) Sdh3 (SDH3 in humans) which is a subunit of the respiratory chain complex II, and (v) three small TIM chaperones, Tim9, Tim10 and Tim12 (TIMM9, TIMM10A and TIMM10B in humans) (Kerscher et al., 1997; Koehler et al., 1998; Sokol et al., 2014). While this is the case in yeast, in human cells only TIM22 and SDH3 proteins are found and no clear homologues of Tim54 and Tim18 have been identified so far. Besides, no evidence to date reveals the presence of SDHC as a subunit of TIM22 complex. Recent studies, though, have found TIM29 and acylglycerol kinase (AGK) as novel metazoan-specific subunits of TIM22 complex (Callegari et al., 2016; Kang et al., 2016, 2017b; Vukotic et al., 2017).

1.1.2.2.4 Translocation of intermembrane space proteins

Most of the IMS proteins, after their translocation through the TOM complex, are folded in the IMS by the acquisition of cofactors or disulfide bridges which promote their conformational stabilization and assembly. Those proteins share a characteristic feature of

cysteine residues, typically arranged in CX_3C and CX_9C motifs (Sokol et al., 2014). This pathway is known as the mitochondrial import and assembly (MIA) pathway and it is suggested that this folding would prevent the back-translocation of proteins out of the mitochondria. Mia40 (also known as CHCHD4 in humans) is an oxidoreductase that catalyzes the formation of disulfide bonds in imported proteins, thus taking part in the disulfide relay system for IMS protein import (**Fig. 4**). Another key protein is the sulfhydryl oxidase Erv1 (known as Augmenter of Liver Regeneration, ALR in humans), which acts as an electron acceptor during the oxidation reaction (Mesecke et al., 2005; Stojanovski et al., 2012). Other IMS proteins contain an hydrophobic sequence, called bipartite presequence, which is inserted in the inner mitochondrial membrane and then cleaved, thereby releasing the mature protein into the IMS (Glick et al., 1992; Neupert and Herrmann, 2007).

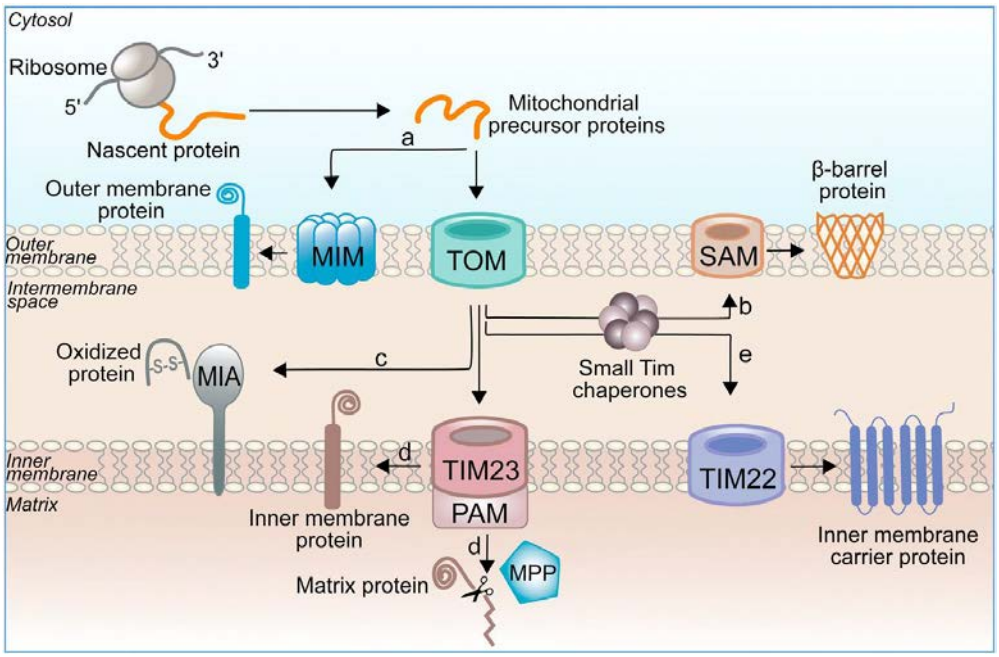

Figure 4. Mitochondrial protein import pathways

Nuclear-encoded mitochondrial proteins are synthesized in the cytosol and delivered as precursors to the translocase of the outer membrane (TOM) complex. Depending on their final destinations, precursors can follow different pathways. **a**) Precursors with α-helical transmembrane segments are directed to the insertase of the OMM (MIM) for assembly. **b**) β-barrel precursors are inserted through the sorting and assembly machinery (SAM) complex with the help of the small TIM chaperones. **c**) IMS proteins are folded via the mitochondrial import and assembly (MIA) pathway. **d**) Precursors with cleavable N-terminal presequences are directed to the IMM and the matrix through the translocase of the inner membrane 23 (TIM23) complex and actively imported to the matrix via the presequence-associated motor (PAM). Once in the matrix, the presequences are recognized and cleaved by the mitochondrial-processing peptidase (MPP). **e**) Hydrophobic precursors with internal targeting signals are transported through the IMS by small TIM chaperones and delivered to TIM22. From Wasilewski et al., 2017.

1.1.2.3 Protein homeostasis within mitochondria and mtUPR

Mitochondrial proteome needs to be surveilled for proper organization and function. In mitochondria, this has an enhanced difficulty, since most of the proteins are nuclear-encoded and are transported into mitochondria as precursors, which have to be, in some cases, cleaved, and assembled in multiprotein complexes. When this process is hampered somehow, there is a need for those proteins to be degraded to avoid the generation of mitochondrial aggregates. For these functions to take place, mitochondria have their specific protein quality control machinery, composed by chaperones and proteases. Upon proteostatic stress, mitochondria have to signal the nucleus so as to elicit a transcriptional program, known as mitochondrial unfolded protein response (mtUPR), aimed to restore mitochondrial integrity and function.

1.1.2.3.1 Chaperones

Mitochondrial protein import is under the surveillance of molecular chaperones. These proteins stabilize or assist the acquisition of the active conformation of other proteins without being part of their final structure, in order to avoid misfolding or aggregation of the newly transported precursors (Kim et al., 2013). Mortalin (also known as mtHsp70 or Grp75) is a chaperone crucial for the trafficking of proteins into the mitochondrial matrix, since it forms the core of the import motor between the TIM23 complex and the matrix. This chaperone binds to the unfolded polypeptide chain driving its translocation into the matrix via an ATP-dependent process (Horst et al., 1997). Heat shock protein 60 and 10 (HSP60 and HSP10, respectively) machineries form two stacked rings in the mitochondrial matrix that allow the accommodation of the unfolded polypeptide following the hydrolysis of ATP, assisting henceforth its proper folding (Okamoto et al., 2015). Tumor necrosis factor receptor-associated protein 1 (TRAP1), another molecular chaperone present in the matrix, was first identified as a member of the heat shock protein 90 (HSP90) family because of its high degree of sequence and structural similarity. HSP90 and TRAP1 both have an N-terminal targeting sequence and an ATP-binding domain, but TRAP1 displays different functional characteristics (Song et al., 1995) and is thought to play an important role in preventing ROS-dependent cell death (Gesualdi et al., 2007). In the IMS, the small TIM chaperones assist the transfer of polypeptides through this compartment (Webb et al., 2006).

1.1.2.3.2 Proteases

Proteases degrade misfolded and damaged proteins, as well as process proteins that have been imported into mitochondria. Besides their role in protein trafficking through the mitochondria, protease-mediated quality control represents another layer of defense against misfolded or damaged proteins as a result of ROS and also against non-assembled proteins due to mitonuclear imbalance (Quirós et al., 2015). There are different types of proteases: (i) ATP-dependent proteases, (ii) ATP independent proteases and (iii) oligopeptidases (Gumeni and Trougakos, 2016). **Figure 5** illustrates their mitochondrial localization and function.

ATP-dependent proteases hydrolyse ATP to disassemble, unfold and sequester their substrates in compartments where they are degraded. Both iAAA and mAAA (ATPases associated with diverse cellular activities) proteases are inserted in the inner mitochondrial membrane, with iAAA facing the IMS and mAAA facing the matrix. Both participate in the quality control and turnover of OXPHOS proteins (Gerdes et al., 2012). Lon protease and Clp protease proteolytic subunit (CLPP) are both serine peptidases acting in the mitochondrial matrix (Haynes et al., 2007; Quirós et al., 2014). Lon protease not only degrades oxidized and damaged proteins but is also associated with mitochondrial DNA regulation, by targeting mitochondrial transcription factor A (TFAM) for degradation (Matsushima et al., 2010). The Lon protease homozygous deletion in mouse causes embryonic lethality, underscoring its crucial role in cellular homeostasis (Quirós et al., 2014). CLPP forms a complex in the mitochondrial matrix with the chaperone ATP-dependent Clp protease ATP-binding subunit ClpX-like (CLPX) (Baker and Sauer, 2012). CLPP substrates have not been unraveled in mammals but it has been associated with the degradation of unfolded proteins (Broadley and Hartl, 2008). Similarly, CLPP homozygous deletion in mice leads to infertility, mtDNA accumulation, inflammation and impaired survival (Gispert et al., 2013).

Two ATP-independent proteases act in the mitochondria, high temperature requirement A2 (HTRA2, also called Omi) and ATP23, which are located in the IMS and participate in the protein quality control of this compartment (Clausen et al., 2011; Quirós et al., 2015). HTRA2 is a serine protease whose expression levels are increased during stress conditions (Gray et al., 2000). Moreover, HTRA2 also has a role during apoptosis, since it can be released from the IMS to relieve the inhibition of cytosolic caspases by binding to inhibitors of apoptosis proteins (IAPs) in the cytosol (Hegde et al., 2002; Verhagen et al., 2002). HTRA2 can also mediate caspase-independent cell death through its own protease activity (Hegde et al., 2002). However, mice lacking expression of HTRA2 develop specific neurodegeneration of

striatal neurons together with a parkinsonian phenotype leading to early death, challenging the notion that HTRA2 is a major regulator of apoptotic cell death (Martins et al., 2004). One mutation (G399S) and one polymorphism (A141S) in the HTRA2 gene were identified in PD patients (Strauss et al., 2005). Conversely, other studies reported lack of association of HtrA2 variants with PD (Krüger et al., 2011; Simon-Sanchez and Singleton, 2008a).

Once the ATP-dependent proteases act, oligopeptidases such as the presequence protease (PITRM1, also known as PreP) and the mitochondrial oligopeptidase M (MEP, also known as neurolysin) further process the substrates. Human PITRM1 is a metalloendoprotease, which has been implicated in Alzheimer's Disease, due to its role in the degradation of amyloid β-peptides (Mossmann et al., 2014).

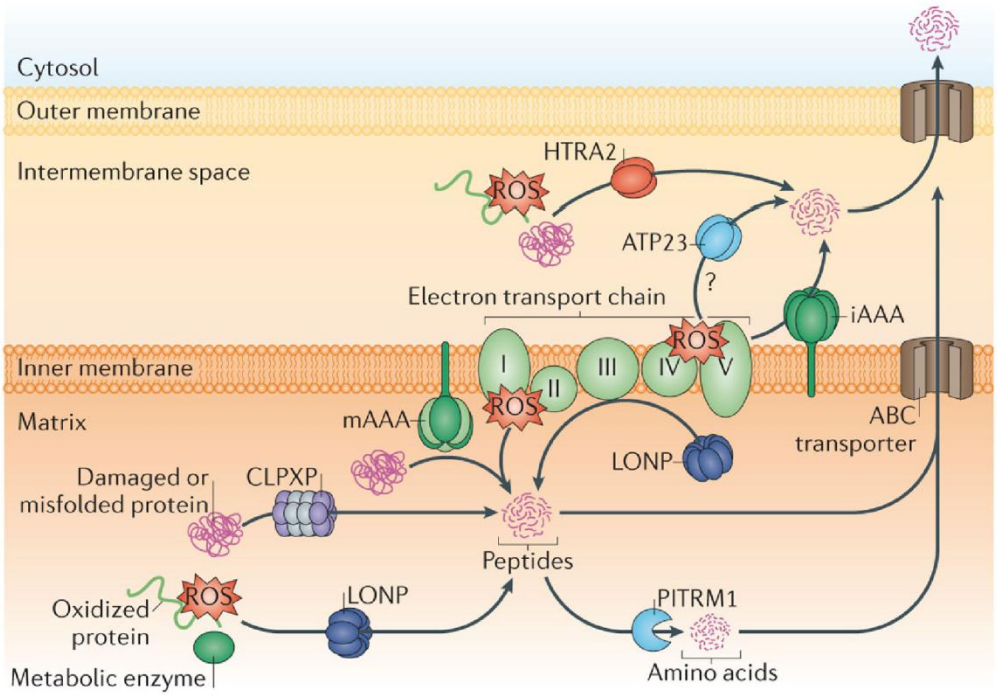

Figure 5. Mitochondrial proteases.

Mitoproteases degrade defective proteins in different mitochondrial compartments. Lon protease (LONP) and the complex formed by CLPP and CLPX (CLPXP) act in the matrix together with mAAA proteases. iAAA proteases function in the IMS together with HTRA2 and ATP23. ATP23 and iAAA proteases participate in the maintenance of the respiratory chain (although the role of ATP23 is not completely clear, indicated by the question mark in the figure). Proteolysis generates peptides, which can be exported to the cytosol through ATP-binding cassette transporter (ABC) or further degraded into amino acids by the oligopeptidase presequence protease (PITRM1). From Quirós et al., 2015.

Furthermore, some of these proteases are highly regulated and have other functions, such as protein import, cardiolipin metabolism, mitochondrial gene expression and mitochondrial DNA stability (Quirós et al., 2015).

1.1.2.3.3 The mitochondrial unfolded protein response

As discussed above, the mitochondrial proteome is encoded by both mitochondrial and nuclear DNA. Proteostatic stress can arise for a variety of reasons: (i) when there is a high input of nuclear-encoded mitochondrial proteins that need to be folded, (ii) imbalance between the nuclear and the mitochondrial genome, or (iii) oxidative stress that modifies endogenous mitochondrial proteins. Mitochondria have developed their own mechanisms (such as the one present in the endoplasmic reticulum, ER) to respond to this proteostatic stress, called the mitochondrial unfolded protein response (mtUPR). This response is a mechanism of mitochondrial to nucleus communication (Martinus et al., 1996) to activate a transcriptional program for mitochondrial homeostasis (Zhao et al., 2002).

Although the first characterization was made in mammalian cells, the following studies have used *C.elegans* to further analyze the mtUPR. One of the suggested models for mtUPR activation in *C.elegans* is based on Clpp-1 (*C.elegans* homolog of CLPP protease) dependent degradation, which generates small peptides that are pumped out through HAF-1 transporter and contribute to the downstream signaling of mtUPR by triggering the relocalization of transcription factor DVE-1 and the ubiquitin-like protein UBL-5 to the nucleus (Haynes et al., 2007, 2010; Haynes and Ron, 2010). HAF-1 is also suggested to work by modulating ATFS-1 import. ATFS-1 is a bZIP transcription factor normally imported into mitochondria and degraded by Lon protease. ATFS-1 has also a nuclear localization signal and upon mtUPR activation, its trafficking to mitochondria is impaired, leading to its translocation into the nucleus and subsequent transcriptional activation of several genes that are protective against mitochondrial dysfunction (Nargund et al., 2012). Therefore, ATFS-1 functions as a sensor of mitochondrial import efficiency, implying that any condition that hampers mitochondrial protein import activity could potentially activate mtUPR (Chacinska et al., 2009; Nargund et al., 2012).

While the mtUPR has been extensively investigated in *C.elegans*, it is not clear how this response occurs in mammals. In cell lines, different interventions activate CHOP and C/EBPβ transcription factors, which heterodimerize, bind to target promoters on a CHOP binding site, and activate the expression of mtUPR genes (Aldridge et al., 2007). Recently, ATF5, a bZIP transcription factor, was proposed to act like ATFS-1 in *C.elegans* (Fiorese et

al., 2016). In summary, mtUPR is emerging as a stress response pathway, which coordinates two different compartments, the nuclear and the mitochondrial, to promote mitochondrial health. **Figure 6** summarizes the different mtUPR responses in *C.elegans* and mammals.

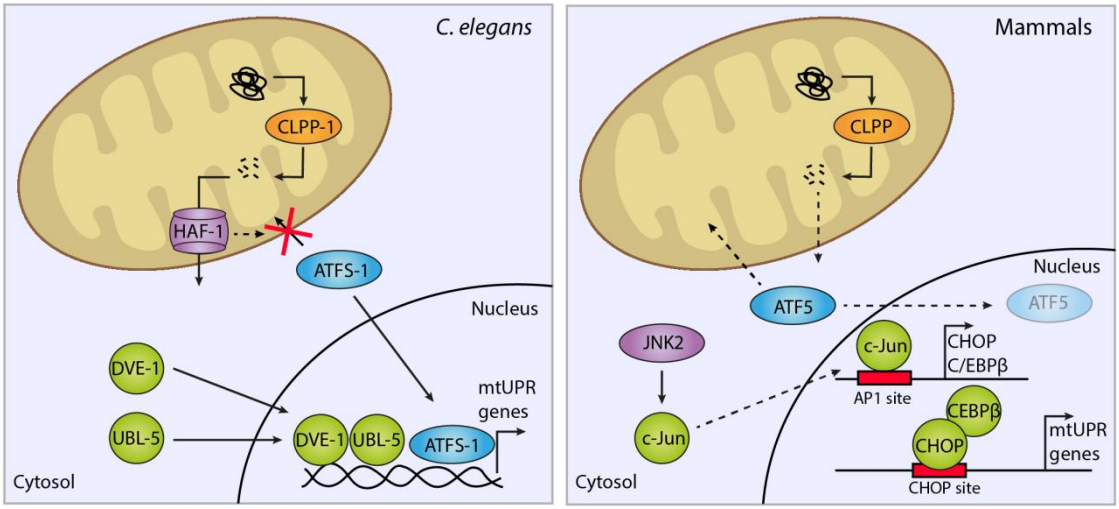

Figure 6. mtUPR in *C.elegans* and mammals.

In ***C.elegans***, extrusion of small peptides generated by CLPP-1 via HAF-1 transporter leads to the translocation of DVE-1 and UBL-5 transcription factors. Attenuation of protein import induces the translocation of ATFS-1 transcription factor to the nucleus, leading to the transcriptional activation of mtUPR genes. In **mammals**, the homologue of HAF-1 is unknown, while ATF5 was found to act like ATFS-1 in *C.elegans*. For mtUPR transcriptional activation, the kinase JNK2 (c-Jun N-terminal kinase 2) and the transcription factor c-Jun are needed to induce CHOP and C/EBPβ transcription through the binding to AP1 sites. CHOP and C/EBPβ transcription factors activate the expression of mtUPR genes. Dashed lines indicate unknown pathways.

1.1.2.4 Mitochondrial dynamics: the balance between fusion and fission

Mitochondria are dynamic organelles whose structure varies constantly from a tubular network to individual mitochondria. This mitochondrial network is regulated by the balance between mitochondrial fusion, fission, *de novo* mitochondrial biogenesis, and the elimination of unwanted mitochondria by mitophagy (Ploumi et al., 2017). While mitochondrial fusion is believed to favor mitochondrial biogenesis by the exchange of new proteins and mtDNA between the merging organelles, mitochondrial fission is considered to be a process that isolates dysfunctional mitochondria so that they can be cleared by mitophagy. Additionally, mitochondrial dynamics have been regarded as a mechanism to regulate metabolic and bioenergetic status of the cell (Liesa and Shirihai, 2013; Wai and Langer, 2016).

1.1.2.4.1 Mitochondrial fusion

Mitofusin 1 and mitofusin 2 (MFN1 and MFN2) are dynamin-like GTPases that control OMM fusion, whereas optic atrophy 1 (OPA1) is the dynamin-like GTPase in charge of IMM fusion (**Fig. 7**) (Mishra and Chan, 2014; Sebastián et al., 2017). Both MFNs have redundant roles but with certain specific features: (i) MFN1, but not MFN2, is needed for OPA1-mediated IMM fusion (Cipolat et al., 2004); (ii) MFN2 mutations cause Charcot-Marie-Tooth disease type 2A, a peripheral neuropathy characterized by progressive degeneration of the peripheral nerves (Züchner et al., 2004); and (iii) in addition to its role in mitochondrial fusion, MFN2 plays also a key role in mitochondria-ER tethering (de Brito and Scorrano, 2008). mitoPLD is a mitochondrial phospholipase possibly required for OMM fusion (Huang and Frohman, 2009). mitoPLD localizes into the OMM, where cleaves cardiolipin to generate phosphatidic acid, a fusogenic lipid, and this activity is required for MFN-mediated mitochondrial fusion (Choi et al., 2006).

For the complete fusion of mitochondria, IMM must fuse as well. OPA1 is a dynamin-like GTPase protein anchored to the IMM and exposed to the IMS, which mediates IMM fusion and controls cristae morphogenesis (**Fig. 7**) (Olichon et al., 2006). Different OPA1 variants, determined by alternative-splicing and proteolytic cleavage, control the balance between fusion and fission. It is becoming clear that regulated proteolysis is a key facet of OPA regulation. Membrane-bound long OPA1 (L-OPA1) can be processed at two protease cleavage sites to generate short-OPA1 (S-OPA1). The zinc metalloprotease OMA1 (overlapping activity with m-AAA protease) cleaves OPA1 at S1 site and the ATP-dependent protease YME1L (yeast mitochondrial DNA escape 1-like) cleaves OPA1 at S2 site (MacVicar and Langer, 2016). Proteolytic processing is central for OPA1 activity, since the balance between L-OPA1 and S-OPA1 maintains normal mitochondrial morphology. L-OPA1 is sufficient to mediate complete mitochondrial fusion (Anand et al., 2014; Wai et al., 2015), whereas the activation of OMA1-dependent processing of OPA1 in absence of YME1L leads to mitochondrial fission (Anand et al., 2014). The existence of two proteases that can fine tune OPA1 activity highlights the importance of OPA1 processing upon different physiological stimulus.

1.1.2.4.2 Mitochondrial fission

Mitochondrial fission facilitates (i) the segregation of damaged mitochondria from a healthy network and (ii) mitochondrial transport through neuronal processes. Dynamin-related protein 1 (DRP1) is a cytosolic protein that is recruited to the OMM, where it oligomerizes to

form ring-like structures, which upon GTP hydrolysis facilitate membrane constriction (Koirala et al., 2013). Additional adaptors are required for DRP1 recruitment to the mitochondrial surface, such as mitochondrial fission protein 1 (FIS1), mitochondrial fission factor (MFF) and mitochondrial dynamics proteins of 49 and 51 kDa (MiD49 and MiD51) (Losón et al., 2013). FIS1 is the mitochondrial adaptor in yeast but in metazoans it is not required for fission (Osellame et al., 2016). Instead, MFF is postulated as a strong candidate to act as a DRP1 receptor (**Fig. 7**) (Losón et al., 2013). Mitochondrial fission occurs at ER-mitochondrial contact sites, where ER tubules mediate constriction before DRP1 recruitment, indicating a role for ER tubules in defining division sites (Friedman et al., 2011). Less-well understood is the fission of the IMM and whether DRP1-mediated OMM constriction can also lead IMM scission is still unknown. However, as reported above, S-OPA1 fragment accumulation does favor mitochondrial fission. This discovery opens a new area of study in the field of mitochondrial fission, since more investigation is needed to understand the precise role of S-OPA1 together with its processing-peptidases, in regulating mitochondrial dynamics.

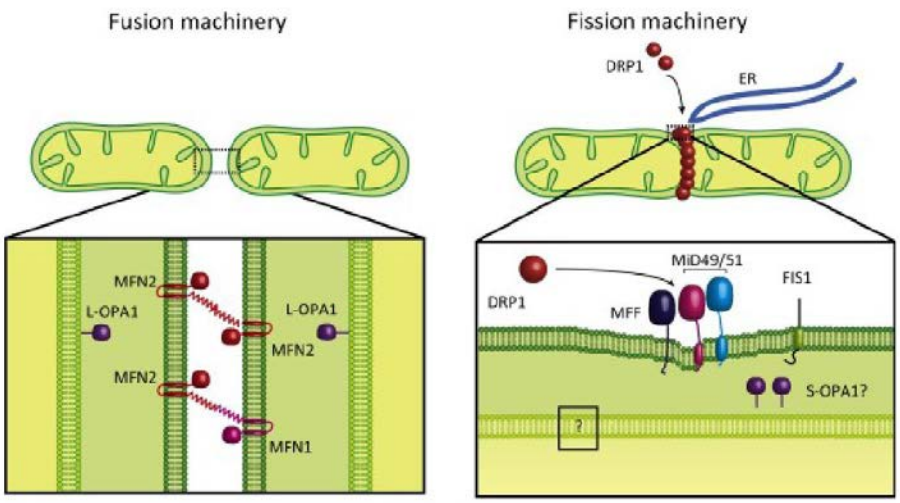

Figure 7. Mitochondrial fusion and fission machinery.

Homo- or heterodimerization of MFN1 and MFN2 are required for OMM fusion, while L-OPA1 isoform is needed for IMM fusion. For mitochondrial fission DRP1 is recruited to the OMM in the presence of MFF, MiD49 and/or MiD51. Mitochondrial fission occurs at ER-mitochondria contact sites. S-OPA1 isoforms could contribute to IMM fission, but this is still under investigation. Adapted from Wai and Langer, 2016.

1.1.2.5 Mitochondrial biogenesis

Mitochondrial biogenesis requires a complex coordination of the nuclear and mitochondrial expression programs. Peroxisome proliferator-activated receptor gamma coactivator 1-alpha (PGC-1α) is the master regulator of mitochondrial biogenesis; it interacts with and coactivates several transcription factors such as nuclear respiratory factors 1 and 2 (NRF1 and NRF2), estrogen related receptor alpha (ERRα), YY1, myocyte enhancer factor 2C (MEF2C) peroxisome proliferator-activated receptors (PPAR) and many others, coordinating mitochondrial biogenesis and oxidative metabolism (Scarpulla, 2006, 2011; Wu et al., 1999). NRF1 and NRF2 frequently work together up-regulate the transcription of several nuclear-encoded genes with essential mitochondrial functions, and to induce the expression of TFAM (Virbasius et al., 1993), which initiates the transcription and replication of mtDNA given its ability to bind and bend DNA without sequence specificity (Ekstrand et al., 2004). Through the regulation of TFAM levels, PGC-1α can regulate the expression of mitochondrial genes (Scarpulla, 2008).

1.1.2.6 Mitophagy

Mitophagy is the only known pathway that targets selectively the degradation of an entire mitochondrion. Specifically, mitophagy is a type of selective macroautophagy, hereafter referred to as autophagy (**Fig. 8**). Autophagy is a conserved mechanism whereby intracytosolic components, such as proteins, aggregates or organelles, are delivered to lysosomes for degradation (Cuervo and Macian, 2012; Martinez-Vicente, 2015). For such, the cargo is sequestered into a double-membrane vesicle, the autophagosome, that subsequently fuses with lysosomes for degradation and recycling (Klionsky and Emr, 2000) (**Fig. 9**).

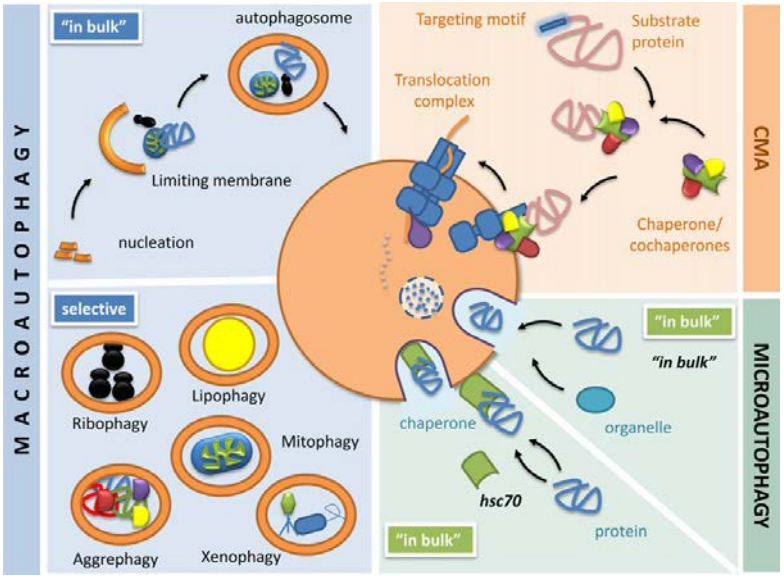

Figure 8. Types of autophagy.

There are three major types of autophagy (i) chaperone-mediated autophagy (CMA), based on the recognition by chaperones of a targeting motif in the protein to be degraded, (ii) microautophagy, characterized by the direct engulfment of cytosolic components through invaginations of the lysosomal membrane, even though recent studies suggest that it can occur in a selective manner depending on the interaction of the substrates with a chaperone, and (iii) macroautophagy, involving the engulfment of cytosolic regions inside double membrane vesicles that fuse with the lysosomes to degrade their content. Macroautophagy can be divided in "in bulk" or selective and specific examples are highlighted. From Cuervo and Macian, 2012.

The mammalian target of rapamycin (mTOR) is the master regulator of autophagy. Under basal conditions, mTOR Complex 1 (mTORC1, formed by mTOR, regulatory-associated protein TOR (Raptor) and mLST8) binds to and inhibits ULK1 activity. For autophagy initiation mTORC1-ULK1 dissociation is needed (Ganley et al., 2009; Hosokawa et al., 2009; Jung et al., 2009), therefore ULK1 can trigger the translocation of the Vps34 complex to the preautophagosomal structure (PAS) (Axe et al., 2008; Di Bartolomeo et al., 2010; Russell et al., 2013). Vps34 complex is formed by beclin 1, AMBRA, Vps34, Vps15 and Atg14L. Vps34 generates PI3P (phosphatidylinositol 3-phosphate), thus forming the PAS, which represents a signaling platform that initiates autophagosome nucleation (Axe et al., 2008). There are two different ubiquitination-like cascades in charge of autophagosome elongation, one is driven by Atg12-Atg5-Atg16L and the other is based on protein-lipid conjugation. Both mechanisms lead to elongation of the membrane via the lipidation of light chain 3 (LC3-I) protein with phospholipid phosphatidylethanolamine to form LC3-II (He and Klionsky, 2009). Since autophagy is a selective process, there are autophagy receptors that recognize

specific cargos. Those receptors have two differential recognition sites. On one hand, they are able to recognize degradation signals on cargo proteins and, on the other hand, they can also bind LC3/GABARAP proteins on the forming autophagosome via the LIR motif (LC3 interacting region) (Stolz et al., 2014). According to the substrate to be eliminated, different autophagy pathways have been described, such as aggrephagy (protein aggregates), ribophagy (ribosomes), pexophagy (peroxisomes), liposomes (lipophagy), reticulophagy (ER), nucleophagy (nuclear envelope), lysophagy (lisosomes) and mitophagy (mitochondria) (Deng et al., 2017).

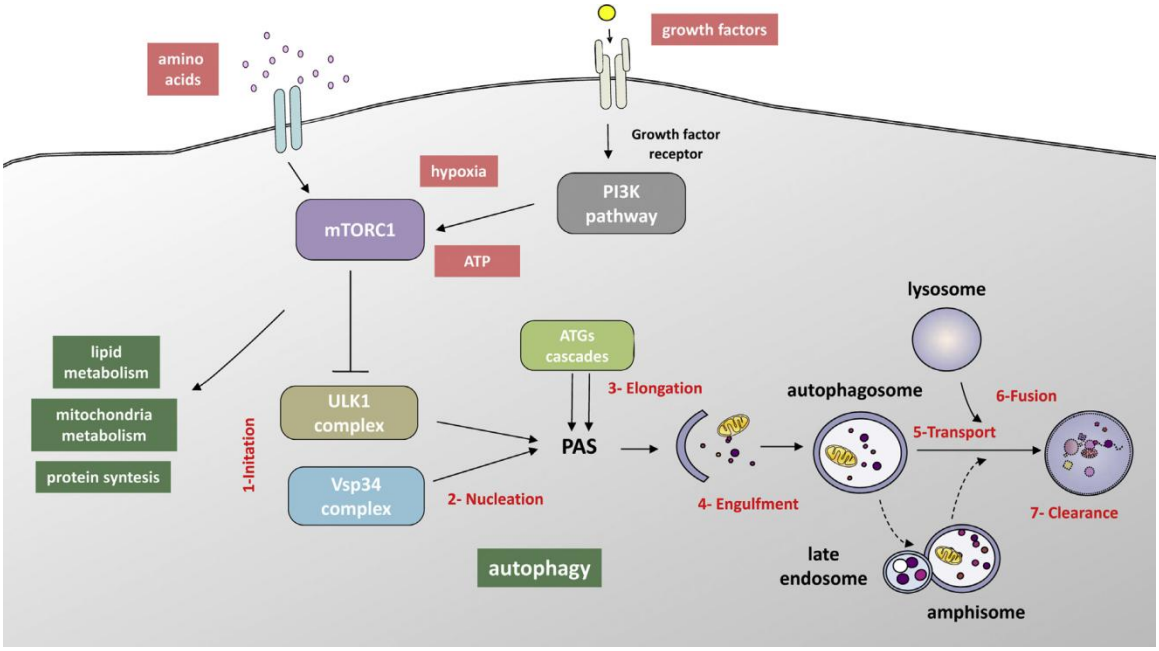

Figure 9. Autophagy regulation and steps

mTORC1 is the main (negative) regulator of autophagy induction through its role in nutrient sensing. When nutrients and energy become limiting, in response to growth factors or upon other cell stressors (like hypoxia), mTORC1 is inhibited. Upon inhibition, ULK1 and Vps34 complex are activated and initiate the nucleation of the PAS structure, the elongation through the ATGs cascade and the engulfment of the cargo to be degraded. Mitcrotubule-based transport machinery allows fusion between autophagosomes, endosomes and lysosomes to degrade the sequestered material. From Martínez-Vicente 2015.

The general mitophagy pathway consists of three steps: (i) recognition of mitochondria that needs to be cleared, (ii) formation of the autophagic membrane that surrounds the organelle, and (iii) fusion of mitoautophagosomes with lysosomes. Besides mitophagy, other forms of partial mitochondrial degradation have been described (Martinez-Vicente, 2017). OMM proteins can be degraded through Parkin-dependent polyubiquitination and degradation by the proteasome (Chan et al., 2011). More recently, parts of the mitochondria have been

found to bud of independently from the fission machinery. These vesicles are called mitochondria-derived vesicles (MDV), which are targeted to the lysosome for degradation (Roberts et al., 2016; Soubannier et al., 2012). PTEN-induced putative kinase 1 (PINK1) and Parkin might play a regulatory role in the formation of MDV after mitochondrial depolarization (McLelland et al., 2014). Despite this, PINK1 and Parkin have been extensively studied for their role in mitophagy.

1.1.2.6.1 PINK1/Parkin-dependent mitophagy mechanisms

The most studied pathway to flag mitochondria for degradation involves PINK1 and Parkin and has been reviewed elsewhere (McWilliams and Muqit, 2017; Misgeld and Schwarz, 2017; Pickrell and Youle, 2015). Briefly, PINK1 is constitutively imported and degraded inside healthy mitochondria, so upon loss of mitochondrial membrane potential or some blockade in the mitochondrial import system, full-length PINK1 accumulates in the OMM of dysfunctional mitochondria (Vives-Bauza et al., 2010) forming a complex with the TOM complex (Lazarou et al., 2012). Upon PINK1 stabilization in the mitochondrial surface, it phosphorylates ubiquitin chains linked to the OMM proteins at serine 65, which stimulates the recruitment and activation of Parkin (Kazlauskaite et al., 2014; Koyano et al., 2014). Moreover, PINK1 also phosphorylates Parkin at serine 65, which stimulates Parkin's E3 ligase activity (Kim et al., 2008; Shiba-Fukushima et al., 2012). Both PINK1-mediated phosphorylation events are required for full Parkin activation. PINK1 has other substrates whose phosphorylation is also linked to the mitophagy process. Miro phosphorylation activates its Parkin-dependent proteasomal degradation leading to an arrest in mitochondrial motility (Wang et al., 2011), though others failed to replicate it (Birsa et al., 2014). MFN2 phosphorylation was suggested to recruit Parkin (Chen and Dorn, 2013), while others have reported that MFN1 and MFN2 are polyubiquitinated in a PINK1/Parkin-dependent manner, which serves as a signal for ubiquitin proteasome system (UPS) degradation (Gegg et al., 2010; Tanaka et al., 2010). In this model, the presence of phospho-ubiquitins in the OMM stimulates Parkin recruitment towards damaged mitochondria and, at the same time, PINK1-dependent phosphorylation of Parkin leads to its activation and polyubiquitination of proteins on the mitochondrial surface. Thereby, Parkin generates more substrates for PINK1 to be phosphorylated and all together feeds a feedforward mechanism aimed to tag dysfunctional mitochondria (**Fig. 10**) (Bingol and Sheng, 2016).

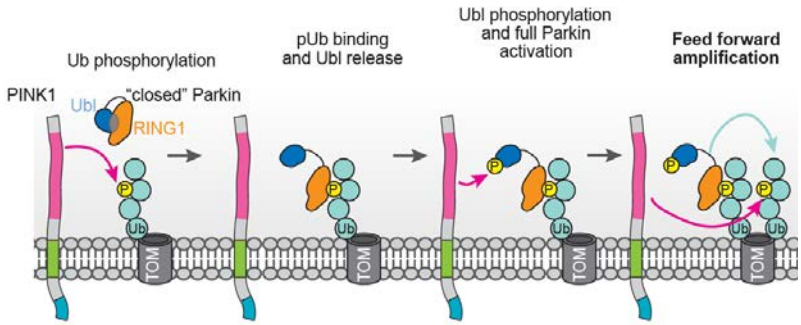

Figure 10. Proposed mechanism for PINK1-dependent Parkin recruitment to the mitochondria.

Adapted from Bingol and Sheng, 2016.

Once recruited to the OMM and activated, Parkin ubiquitinates many substrates with K48- and K63-linked ubiquitin chains. K63-linked chains are proposed to act as the label for autophagy and are recognized by different autophagy receptors, while K48-linked chains have been suggested to be the principal signal for UPS degradation (Akutsu et al., 2016; Yamano et al., 2016). To date, five different autophagy receptors have been described to recognize polyubiquitinated signals in PINK1/Parkin-mediated mitophagy: p62, NBR1, Optineurin (OPTN), NDP52 and TAX1BP1. Of those, p62 has been the classical receptor for selective autophagy, but a recent work by Lazarou *et al*. has shown that OPTN and NDP52 are indeed the primary receptors for PINK1/Parkin-mediated mitophagy. Mitophagy receptors connect the mitochondria to be eliminated with LC3-II, the main component of the autophagosomal membrane, and can recruit as well different components of the autophagosome machinery such as ULK1, WIPI1 (WD repeat domain phosphoinositide-interacting protein 1) and DFCP1 (double FYVE domain containing protein 1) (Lazarou et al., 2015b). OPTN and NDP52 also recruit and activate TANK-binding kinase 1 (TBK1) to damaged mitochondria. TBK1-dependent OPTN and NDP52 phosphorylation recruits more mitophagy adapters and enhances their binding to ubiquitin chains (Heo et al., 2015; Richter et al., 2016). Mitophagy is also kept in check by deubiquitinating enzymes, such as USP15, USP30 and USP35, which remove ubiquitin tags acting as potential brakes for the pathway (Bingol et al., 2014; Cornelissen et al., 2014; Wang et al., 2015b). Recently, the essential role of Parkin in mitophagy has been challenged, since in its absence other E3-ubiquitin ligases can polyubiquitinate OMM proteins (Szargel et al., 2016). Besides, PINK1 has been reported to be dispensable for basal mitophagy *in vivo* (McWilliams et al., 2018). Therefore, other forms of mitophagy, PINK1/Parkin-independent must exist.

1.1.2.6.2 PINK1/Parkin-independent mitophagy mechanisms

Mitophagy extends well beyond the so known PINK1-Parkin pathway. Nix (also known as BNIP3L), is induced upon hypoxia together with B-cell lymphoma 2 nineteen kilodalton interacting protein 3 (BNIP3), triggering the mitochondrial permeability transition pore opening, depolarization and LC3/GABARAP recruitment for the autophagosome formation (Novak et al., 2010; Zhang and Ney, 2009). Nix was first described as a mitophagy receptor during reticulocyte maturation when mitochondria are eliminated from the erythrocyte (Sandoval et al., 2008; Schweers et al., 2007). FUND1 (Fun14 domain containing 1) has also been implicated in hypoxia-induced mitophagy. FUND1 phosphorylation regulates the affinity of FUND1-LC3 interaction, where dephosphorylation increases this interaction and mitophagy (Liu et al., 2012). Of note, all these proteins are OMM proteins that act directly as mitophagy receptors. Moreover, other mitochondrial proteins have been described to recruit the autophagosomal machinery (Martinez-Vicente, 2017). Cardiolipin (CL) is a phospholipid mostly present in the IMM. However, it was found to contains an LC3-binding motif and to be translocated into the OMM, where it can function as a mitophagy receptor by binding LC3-II (Chu et al., 2013). This translocation seems to be directed by depolarization (Maguire et al., 2017). An overview of the different proteins that act as mitophagy receptors can be found in **Figure 11**.

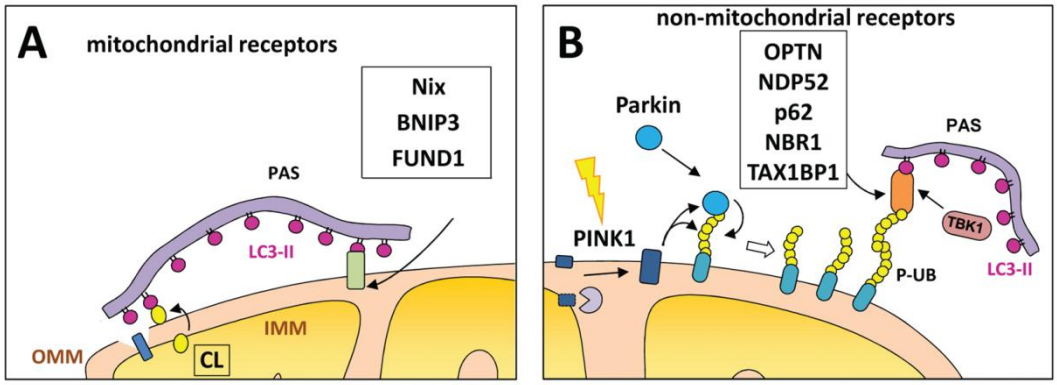

Figure 11. Mechanisms of mitophagy.

A) Mitochondrial components that act as mitophagy receptors, and **B)** non-mitochondrial receptors. All these mitophagy receptors recognize mitochondria to be degraded and link them to LC3-II in the PAS. Adapted from Martínez-Vicente, 2017.

1.1.3 Mitochondrial quality control dysfunction and neurodegenerative diseases

Neurons are highly dependent on mitochondrial function to maintain energy-intensive functions such as membrane excitability, neurotransmission and plasticity: the brain consumes 20% of the total oxygen and about a quarter of the total glucose used by the body for energy supply. Thus, improper functioning of mitochondria has devastating effects on neuronal survival (Court and Coleman, 2012). In fact, a growing body of evidence suggests the involvement of mitochondrial abnormalities in age-related neurodegenerative diseases. One classical mechanism is the generation of mitochondrial ROS which has been identified as an important factor for disease progression and cell death (Lin and Beal, 2006). However, given the importance of mitochondria quality control, it is not surprising that its dysfunction is also present in neurodegenerative disorders.

Mitochondrial quality control is especially important in neurons, since their mitochondria have longer half-life than in other cell types (Miwa et al., 2008; O'Toole et al., 2008). Moreover, neuronal morphology is complex and characterized by long axons and elaborated dendrites, thus delineating different compartments with specific energetic demands (Li et al., 2004; MacAskill et al., 2010). As a result, correct handling of mitochondrial dynamics, mitochondrial biogenesis and mitophagy is essential to maintain a healthy mitochondrial pool, and alterations in this processes have started to be unraveled in different neurodegenerative diseases (Martinez-Vicente, 2017; Schon and Przedborski, 2011). Nonetheless, all these processes supporting organellar quality control are also intimately connected to mitochondrial protein homeostasis (Rugarli and Langer, 2012). In this way, while the implication of mitochondrial dysfunction in the pathogenesis of a myriad of neurodegenerative diseases has been studied for more than 20 years; the specific implication of mitochondrial quality control dysfunction is quite recent and has only started to be elucidated.

Next I will focus on the contribution of mitochondrial dysfunction specifically in the field of Parkinson's disease and Huntington's disease.

1.2 Parkinson’s disease

1.2.1 Etiology and pathological hallmarks

1.2.1.1 Epidemiology

In 1817, James Parkinson described for the first time the symptoms of a disease that was later named Parkinson’s disease in his “An Essay on the Shaking Palsy” (Parkinson, 2002). Parkinson's disease (PD) is the second most common neurodegenerative disorder after Alzheimer’s disease affecting 1% of the population above 60 years (Pringsheim et al., 2014). Prevalence of PD is higher in Europe, North America and South America compared with African, Asian and Arab countries. Age is the greatest risk factor for PD and gender has been established to be another well defined risk factor, with the male-to-female ratio being approximately 3:2. With an ageing population and the expectancy of life increasing year after year, the prevalence of PD is expected to increase by more than 50% by 2030 (Dorsey et al., 2007). PD cases are mostly sporadic and seem to arise from an intricate relationship between genetic and environmental factors. Noteworthy, genetic studies in the 90s revealed the existence of monogenic forms of PD. Since then, PD has been identified as a genetically heterogeneous disease where several monogenic forms of the disease and numerous genetic risk factors have been identified. **Table 1** summarizes the most relevant PD-associated genes. Several excellent reviews have been written recently covering the field of PD genetics (Brás et al., 2015; Deng et al., 2018; Klein and Westenberger, 2012).

Table 1 PD-associated genes

Loci	Protein	Inheritance	References
SNCA (PARK1/4)	α-synuclein	AD Risk locus	Bostantjopoulou et al., 2001; Polymeropoulos et al., 1997; Singleton et al., 2003; Zarranz et al., 2004
LRRK2 (PARK8)	Leucine-rich repeat kinase 2	AD Risk locus	Paisán-Ruíz et al., 2004; Zimprich et al., 2004
VPS35 (PARK17)	Vacuolar protein sorting 35	AD	Vilariño-Güell et al., 2011; Zimprich et al., 2011
CHCHD2 (PARK22)	Coiled-coil-helix-coiled-coil-helix domain containing 2	AD	Funayama et al., 2015
PINK1 (PARK6)	PTEN-induced putative kinase 1	AR	Hatano et al., 2004; Valente et al., 2004
Parkin (PARK2)	RBR E3 ubiquitin protein ligase	AR	Kitada et al., 1998
DJ-1 (PARK7)	DJ-1	AR	Bonifati et al., 2003
ATP13A2 (PARK9)	ATPase 13A2	AR	Ramirez et al., 2006
PLA2G6 (PARK14)	Phospholipase A2 isoform e	AR	Paisan-Ruiz et al., 2008
FBXO7 (PARK15)	FBXO7	AR	Shojaee et al., 2008
DNAJC6 (PARK19)	DnaJ heat shock protein family (Hsp40) member C6	AR	Edvardson et al., 2012
SYNJ1 (PARK20)	synaptojanin-1	AR	Krebs et al., 2013
GBA1	Glucocerebrosidase	Risk locus	Aharon-Peretz et al., 2004; Tayebi et al., 2001
MAPT	Microtubule-associated protein tau	Risk locus	Pascale et al., 2016

AD: autosomal dominant; AR: autosomal recessive

Since the advent of genome-wide association studies (GWAS) many risk loci have been identified, besides the ones named on the table (Hernandez et al., 2016). Even though the risk conferred by these alleles may be modest, when combined in an individual can be considerable.

1.2.1.2 Pathology

The classical neuropathological feature of PD is the progressive and profound loss of neuromelanin containing dopaminergic neurons in the substantia nigra (SN) pars compacta (SNpc). The most affected area is generally the ventrolateral tier, which projects to the dorsal putamen of the striatum (Fearnley and Lees, 1991) (**Fig. 12**). Neuronal degeneration in PD is not restricted to SN or to neurons containing Lewy bodies, but also to other neuronal populations such as cholinergic neurons in the basal forebrain and the midbrain tegmentum, serotonergic neurons in the raphe nuclei and noradrenergic neurons in the locus coeruleus (Hirsch et al., 2003).

Another neuropathological hallmark of PD is the presence of eosinophilic, intracytoplasmic, proteinaceous inclusions, called Lewy bodies (LBs, **Fig. 12**). Classical LBs are spherical structures with a hyaline appearance on hematoxylin and eosin that stain strongly for α-synuclein. Moreover, LBs also contain ubiquitin, phosphorylated neurofilaments, Parkin, components of the ubiquitin-proteasome system, molecular chaperones and lipids (Uversky, 2007). Some years ago, Braak presented a staging system for PD based on a specific pattern of α-synuclein pathology/Lewy pathology spreading. According to Braak, neuronal damage in PD occurs in a spreading and caudal-to-rostral pattern from enteric and peripheral autonomic nervous system to neocortex (Braak et al., 2003, 2004).

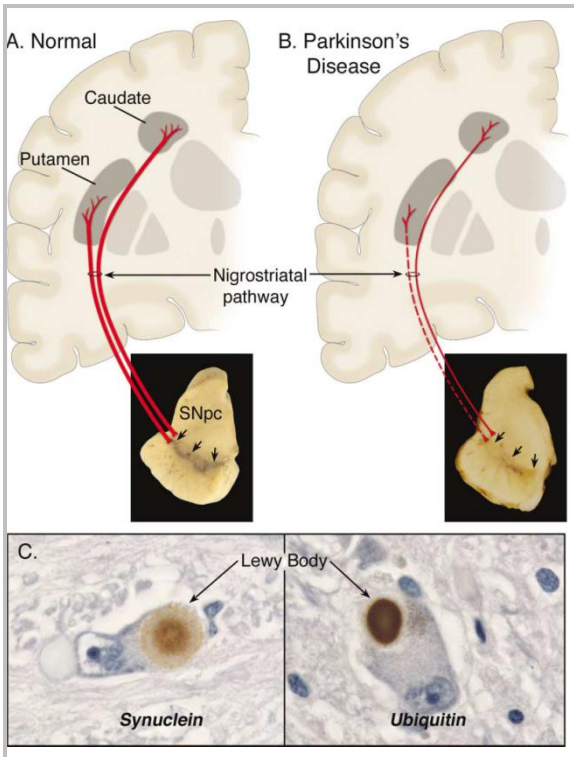

Figure 12. PD neuropathology.

A) Schematic representation of the normal nigrostriatal pathway. Dopaminergic neurons have their bodies in the substantia nigra pars compacta and project to the basal ganglia (caudate and putamen = striatum). **B**) Schematic representation of the dopaminergic pathway in a PD patient. There is a marked loss of dopaminergic neurons that project to the putamen (dashed line) and, to a lesser extent, of the ones projecting to the caudate. Loss of dopaminergic neurons can be observed macroscopically by the depigmentation of the substantia nigra. **C**) Immunohistochemical labeling of Lewy bodies in a SNpc dopaminergic neuron, positive for α-synuclein and ubiquitin. From Dauer and Przedborski, 2003.

1.2.1.3 Clinical features and therapies

1.2.1.3.1 Clinical features

PD is characterized by the presence of motor and non-motor symptoms. Usually, the disease is diagnosed by the first motor symptoms which have been estimated to appear when up to 60% of the dopaminergic neurons in the SN are lost (Brownell et al., 1998; Wüllner et al., 1994) leading to a depletion of dopamine concentrations in the striatum below 60-70%. The classical motor symptoms that base the diagnosis criteria are resting tremor, bradykinesia, muscular rigidity, postural instability and gait impairment (Fahn, 2003). Together, these manifestations define the syndrome of parkinsonism, of which PD is the major cause, but other neurodegenerative disorders or non-degenerative conditions are also accompanied by parkinsonism. Those PD manifestations arise from the cellular loss within the SNpc and the concomitant dysfunction of the basal ganglia. As the disease progresses, there is a worsening of motor features and complications related to long-term symptomatic treatment emerge (Coelho and Ferreira, 2012). Before the onset of motor symptoms, patients may present a variety of non-motor symptoms, which can start even 10 years before the diagnosis, characterized by constipation, hyposmia (loss of smell), depression and rapid eye movement (REM) sleep behavior disorder (RBD) (Pont-Sunyer et al., 2015). Non-motor symptoms progress in both severity and diversity as the disease advances (Schapira et al.,

2017) and contribute substantially to disability in the later stages of the disease, being the main determinants of quality of life and institutionalization (Coelho and Ferreira, 2012). Dementia is the major symptom in the late course of the disease occurring in 83% of patients with more than 20 years of disease duration (Hely et al., 2008).

1.2.1.3.2 Therapies

Currently, there is no treatment that can halt or stop the progression of the disease and/or the neurodegenerative process and only symptomatic treatments are available. Drugs that increase intracerebral dopamine concentrations or stimulate dopamine receptors are the gold standard for the management of motor symptoms. One of the most famous treatments is L-Dopa or Levodopa, which is the standard and initial therapy for patients. Motor symptoms respond initially well to the replacement therapy but later on, patients experience a wearing-off effect characterized by shorter duration of responses to individual doses, together with motor complications (Connolly and Lang, 2014). Deep brain stimulation of either the subthalamic nucleus or globus pallidus internus is effective for the treatment of motor symptoms, as well as some specific non-motor fluctuations (Fasano et al., 2012). Regarding non-motor symptoms therapy, numerous pharmacotherapies are available mostly using drugs already approved for another indication to treat the concrete symptom (Oertel, 2017).

1.2.1.4 Experimental models

Experimental models of PD can be found in a variety of organisms such as yeasts (Tenreiro et al., 2017), *C.elegans* (Martinez et al., 2017a), flies (Guo, 2012), rodents (Terzioglu and Galter, 2008) and even nonhuman primates (Porras et al., 2012). However, few, if any, PD-model is able to recapitulate all the major clinical and pathologic features of PD. Even though, each model has contributed to the advance in the understanding of the neurobiology of PD and the development of new therapies.

1.2.1.4.1 Genetic models

The majority of the genetic models are created based on the knowledge of targets associated with potential mechanisms leading to PD. However, most genetic models in rodents show very subtle phenotype with no overt loss of dopaminergic neurons (Lee et al., 2012). Since PD patients show no degeneration at least until their fifth decade of life, it

raises the possibility that those genetic models have no enough time to develop pathology given their shorter lifespan.

1.2.1.4.2 Pharmacological models

In contrast to the genetic models, pharmacological or toxin models mimic the nigrostriatal dopaminergic degeneration and display some motor deficits. Some of the toxic agents that have been used to model PD are 6-hydroxydopamine (6-OHDA, (Bové and Perier, 2012)), 1-methyl-4-phenyl-1,2,3,6-tetrahydropyridine (MPTP), rotenone (Betarbet et al., 2000), paraquat (Brooks et al., 1999) and amphetamine-type psychostimulants (Kogan et al., 1976). Despite their widespread use, pharmacological models have some drawbacks: (i) the degeneration takes place during days, nor years, (ii) toxins cause damage mainly to dopaminergic neurons but not to other disease-linked neuronal types and (iii) there is no LB pathology. In the next section I will describe in detail the MPTP mouse model, since it is the model I have used to test neuroprotective strategies for PD.

1.2.1.4.2.1 MPTP model

MPTP was first discovered in humans, after a group of young drug abusers developed a parkinsonian syndrome due to the intravenous injection of a narcotic meperidine analogue contaminated with MPTP (Langston et al., 1983). MPTP is in a fact a protoxin that can cross the blood brain barrier and enter the brain, where it is converted by the monoamine oxidase B (MAO-B) to its active metabolite, 1-methyl-4-phenylpyridinium ion (MPP^+). MPP^+ enters the dopaminergic neurons through the dopamine transporter and once in the cytoplasm inhibits complex I activity (Javitch et al., 1985) (**Fig. 13**).

MPTP has been used to model PD in a variety of species, though the most popular ones are the mouse and monkey. The mouse MPTP model is widely used to study the mechanisms of dopaminergic cell death linked to PD (Bové et al., 2014; Perier et al., 2005a, 2007; Ramonet et al., 2013; Vila et al., 2001; Vila and Przedborski, 2003). MPTP is mainly administered via systemic route through subcutaneous or intraperitoneal injections. Regarding the regime of administration, the best characterized regimens are the acute and sub-acute. The acute regimen consists of four injections of 20 mg/kg every 2 hours, leading to 90% dopamine depletion in the striatum and 70% of dopaminergic cell loss in SNpc in a non-apoptotic fashion (Jackson-Lewis et al., 1995). The sub-acute regimen implies one intraperitoneal injection of 30 mg/kg daily for five consecutive days (Tatton and Kish, 1997), and causes a 40-50% of dopamine depletion in striatum and 30-40% cell loss in the SN (Perier et al.,

2007). In the sub-acute regimen, neurons die by apoptosis and the lesion is stabilized within 21 days after MPTP administration. Although MPTP is able to induce the characteristic dopaminergic cell loss, what is lacking in this model is the presence of LB. Until the development of models that can converge most of the pathological hallmarks of PD, MPTP mouse model will continue to be the gold standard model to study the molecular pathways to cell death and to test neuroprotective strategies.

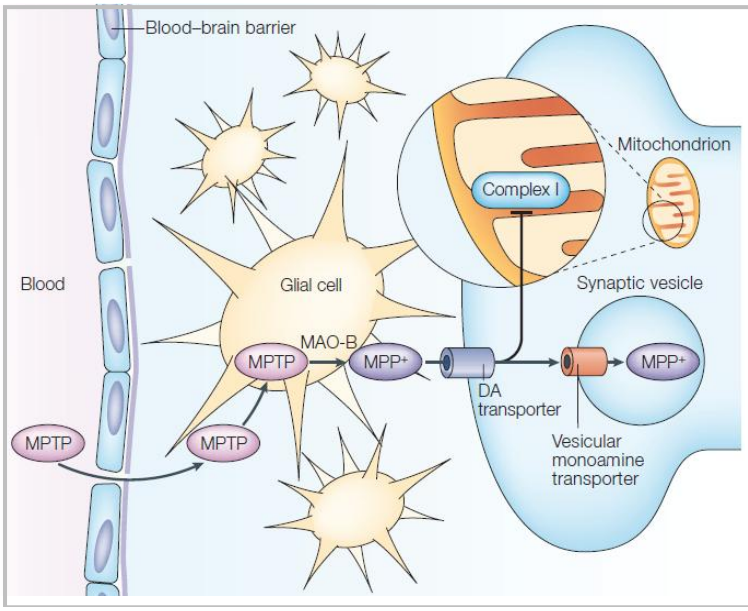

Figure 13. MPTP metabolism.

MPTP is a protoxin that rapidly crosses the blood-brain barrier and is metabolized in glial cells by the enzyme MAO-B to the active toxin, MPP^+. The active compound MPP^+ is taken up by dopamine (DA) transporters inside dopaminergic neurons, where MPP^+ inhibits complex I of the electron transport chain. From Vila and Przedborski, 2003.

1.2.1.5 Pathogenesis

1.2.1.5.1 Hallmarks of Parkinson's disease

To date, several key molecular pathways have been linked to the pathogenesis of PD. Protein misfolding, aggregation and impairment of protein clearance pathways are classical hallmarks of PD. In fact, decreased lysosomal enzyme levels (Chu et al., 2009; Dehay et al., 2010), and markers of chaperone-mediated autophagy (CMA) (Alvarez-Erviti et al., 2010) together with autophagosome accumulation (Anglade et al., 1997) are classically observed in the SN of PD patients. α-synuclein aggregation is the paradigmatic example of altered protein homeostasis present in PD. During the pathogenic process, soluble α-synuclein monomers form oligomers that combine to form protofibrils and, eventually, large insoluble α-synuclein aggregates, which conform LBs (Kim and Lee, 2008). Aggregated α-synuclein interferes with several cellular mechanisms leading to disruption of neuronal homeostasis (Sheng and Cai, 2012). For instance, α-synuclein impairs the UPS and lysosomal functions, leading to defective clearance of abnormal α-synuclein species and other substrates (Dehay et al., 2013). Dysfunctions in protein degradation and turnover, in turn, may affect synaptic

function (Tai and Schuman, 2008). In this toxic environment, neuroinflammation is another contributor to the pathogenesis. Some evidences suggest that α-synuclein induces the innate and adaptive immunity in PD (Hirsch and Hunot, 2009; Ransohoff, 2016) while others point out that neuroinflammation could promote α-synuclein misfolding (Gao et al., 2008). Since this thesis is focused on the role of mitochondrial dysfunction in the context of PD and HD, I have dedicated a section to describe in detail the evidences of mitochondrial dysfunction in each neurodegenerative disease.

1.2.1.5.2 Mitochondrial dysfunction in Parkinson's disease

The identification of genes related to familial forms of PD boosted the field of mitochondrial dysfunction, since most of the proteins encoded by those genes participate in the maintenance of mitochondrial homeostasis. **Table 2** summarizes some of the evidences linking PD-associated genes with mitochondria. However, mitochondrial deficits were already described more than ten years before the discovery of PD-associated α-synuclein mutations. **Table 3** summarizes some of the alterations related with mitochondria that have been described in PD patients and PD models.

Table 2. PD-associated genes and their relationship with mitochondria

Gene	Evidence	Model	References
α-synuclein	Direct interaction with mitochondria and accumulation.	Rat, HeLa cells, MEF, striatum and SN from PD patients	Banerjee et al., 2010; Devi et al., 2008a; Nakamura et al., 2011
	Complex I inhibition	Striatum and SN from PD patients, rat, mouse, MN9D cells.	Devi et al., 2008a; Liu et al., 2009a; Loeb et al., 2010
	Mutations lead to increased mtDNA damage, mitophagy and mitochondrial fission.	Zebrafish, Drosophila, mouse	Butler et al., 2012; Choubey et al., 2011; Kamp et al., 2010; Martin et al., 2006; O'Donnell et al., 2014;
LRRK2	Mitochondrial dysfunction and altered mitochondrial dynamics.	*C.elegans*, Drosophila, mouse and neurons derived from IPSc from PD patients.	Ng et al., 2012; Niu et al., 2012; Saha et al., 2009; Wang et al., 2012b

VPS35	Abnormal cargo trafficking by MDVs	Rat, mouse, human fibroblasts.	Wang et al., 2015a
PINK1/Parkin	Decreased complex I activity, impaired respiration, decreased ATP synthesis, morphological abnormalities and mitophagy defects.	PD patients, mouse, Drosophila, PC12 cells.	Burman et al., 2012; Cui et al., 2010; Greene et al., 2003; Liu et al., 2009b; Morais et al., 2009; Müftüoglu et al., 2004; Scarffe et al., 2014; Ziviani et al., 2010
Parkin	Defects in mitochondrial biogenesis through PGC-1α downregulation.	Mouse, PD patients	Pacelli et al., 2011; Shin et al., 2011; Stevens et al., 2015
DJ-1	Impaired mitochondrial respiration, reduced membrane potential, increased ROS levels and altered mitochondrial morphology and mitophagy.	Mice, rat, MN9D and M17 cells, hippocampal neurons and PD patients.	Gao et al., 2012; Krebiehl et al., 2010; Wang et al., 2012a.
FBXO7	Deficiencies in Parkin translocation to mitochondria, ubiquitination of MFN1 and mitophagy.	Drosophila	Burchell et al., 2013
PLA2G6	Respiratory chain dysfunction, reduced ATP synthesis and abnormal mitochondrial morphology.	Drosophila	Kinghorn et al., 2015
ATP13A2	Increased fragmentation and increased ROS production.	Mouse cortical neurons and SH-SY5Y cells	Gusdon et al., 2012
HSP9 (mortalin)*	Mitochondrial dysfunction: increased ROS, decreased membrane potential, alterations in mitochondrial network and respiration and mitochondrial loss.	Yeast, human cell lines, fibroblasts.	Burbulla et al., 2010; Goswami et al., 2012
HTRA2*	Striatal neurodegeneration and parkinsonian phenotype.	Mice	Martins et al., 2004

* There is some controversy on whether there is an association of these genes with risk of PD (Chung et al., 2017; Freimann et al., 2013; Krüger et al., 2011; Simon-Sanchez and Singleton, 2008b).

Table 3. Mitochondria-associated alterations in PD

Evidence	Model	References
Complex I dysfunction - Complex I inhibitor MPTP causes parkinsonism - Reduced activity in SN, peripheral tissues and cybrid cells. - Oxidation of catalytic subunits	PD patients	Blin et al., 1994; Haas et al., 1995; Keeney et al., 2006; Krige et al., 1992; Langston et al., 1983; Parker et al., 1989, 2008; Schapira et al., 1990; Swerdlow et al., 1996
Mitochondrial DNA alterations - Deletions - POLG mutations are associated with parkinsonism. - mtDNA deletions are not sufficient per se to trigger SNpc dopaminergic cell death.	Human SNpc dopaminergic neurons, mice	Bender et al., 2006; Dai et al., 2014; Davidzon et al., 2006; Kraytsberg et al., 2006; Luoma et al., 2004; Perier et al., 2013
ROS-mediated damage - Cardiolipin peroxidation. - Damage to lysosomal membranes. - Damage to nuclear and mtDNA	Mouse, PD patients.	Dehay et al., 2010; Hoang et al., 2009; Perier et al., 2005a; Sanders et al., 2014
Mitochondrial protein import - α-synuclein is imported into the mitochondria through TOM40 complex. - Decreased TOM40 protein levels. - α-synuclein interaction with TOM20.	PD patients, mouse, human DA primary neuronal cultures	Bender et al., 2013; Devi et al., 2008a; Di Maio et al., 2016
Mitochondrial dynamics - Parkinsonian neurotoxins 6-OHDA, rotenone and MPP+ induce mitochondrial fission and cell death. - Drp1 inhibition prevents mitochondrial fragmentation and DA neurodegeneration in PD models.	Neuronal cultures: CSM14.1, BE(2)-M17, and primary cultures from rat and mouse. Rat, mouse.	Barsoum et al., 2006; Bido et al., 2017; Gomez-Lazaro et al., 2008; Meuer et al., 2007; Ramonet et al., 2013; Rappold et al., 2014; Su and Qi, 2013
Mitophagy - Inefficient removal of Miro from damaged mitochondria. - Impaired mitophagy	Fibroblasts and neurons derived from IPSc from PD patients.	Hsieh et al., 2016
Mitochondrial biogenesis - Decreased PGC-1α levels. - PGC-1α loss increases the sensitivity to MPTP-induced dopaminergic cell death	PD patients, mouse	Shin et al., 2011; St-Pierre et al., 2006; Zheng et al., 2010

For the past 30 years mitochondrial dysfunction has been regarded as a central pathogenic hallmark for this devastating disease. However, different aspects of mitochondrial biology have come to focus during all this years, ranging from bioenergetics, oxidative stress and, more recently, mitophagy. Recent developments highlight the increasing potential of mitochondria to defend themselves against various threats (Perier et al., 2010, 2013). In fact, novel, critical roles of mitochondrial proteases have emerged in neuronal physiology and pathology, representing an early mechanism aimed to mitigate mitochondrial stress. Once the first line of defense has been overcome, mitochondrial dynamics, in terms of mitochondrial fission and fusion, mitochondrial biogenesis and mitophagy, play an important role in maintaining a healthy organelle population. Thus, impairments in these quality control systems may lead to the accumulation of defective mitochondria, as well as inefficient mitochondrial transport and distribution, leading to synaptic and neuronal degeneration. But, still, as we advance in the field of mitochondrial physiology, new questions arise. How are all the mitochondrial quality control mechanisms, at the protein and the organelle levels, inter-connected? Which are the mechanisms that establish the difference between damaged mitochondria and mitochondria that have to be labeled for degradation? Being able to answer these and other questions could help us to develop new and better therapeutic strategies that target mitochondrial quality control mechanisms which could benefit not only patients with Parkinson's disease, but also with other neurodegenerative disorders.

1.3 Huntington's disease

1.3.1 Etiology and pathological hallmarks

1.3.1.1 Epidemiology and therapy

In the 19th century, chorea and its hereditary nature were already noticed, but it was George Huntington's description that led to the eponymous designation of the disease Huntington's disease (Huntington, 1872). Huntington's disease (HD) is an autosomal dominant neurodegenerative disorder with a prevalence of 10.6-13.7 individuals per 100.000 in Western populations (Bates et al., 2015). HD is caused by an abnormal cytosine-adenine-guanine (CAG) trinucleotide repeat expansion, coding for the amino acid glutamine, in the exon 1 of the huntingtin gene (*HTT*) (The Huntington's Disease Collaborative Research Group., 1993). Normal population display between 16 and 20 repeats, while affected individuals display an expanded polyglutamine (polyQ) tract of more than 35 glutamines, at the amino terminus end of the huntingtin protein (Htt), which is associated with protein

aggregation and a gain-of-function toxicity. However, loss of function and/or dominant negative effect may also contribute to the pathology (Cattaneo et al., 2005; Rubinsztein and C., 2003). The age at onset of diagnostic motor manifestations in HD is inversely correlated with the length of the CAG expansion. Accordingly, there is a reduced penetrance within individuals having less than 40 repeats, while 40 or more are associated with nearly full penetrance by the age of 65 years (Hendricks et al., 2009). Nevertheless, there is a huge inter-individual variability in age of onset of symptoms between carriers with similar CAG expansion, thus the existence of other candidate modifier genes has been proposed (Holmans et al., 2017). The median age at onset is 40 years and the disease is fatal after 15-20 years of the onset of symptoms. No current treatments are available to halt or delay the progression of the disease and just two drugs have been licensed by the US Food and Drug Administration for specific use in HD patients, which are tetrabenazine, approved in 2008 for the treatment of chorea (Huntington Study Group, 2006) and deutetrabenazide, with the same mechanism of action but increased half-life (Frank et al., 2016).

1.3.1.2 Clinical features

HD carriers present a premanifest phase, in which they are clinically indistinguishable from a healthy control (presymptomatic stage) and then progress to develop subtle motor, cognitive and behavioral changes (prodromal stage). With the onset of the motor symptoms, HD patients enter into the manifest phase, which will inexorably progress until death (Ross et al., 2014).

HD classically manifests with a triad of signs and symptoms, including motor, cognitive and behavioral features. Motor disorder in HD is characterized by two motor alterations, (i) presence of involuntary movements (hyperkinetic phase), such as chorea and, (ii) impairment of voluntary movements (hypokinetic phase), such as incoordination, bradykinesia and rigidity (Dorsey et al., 2013). Cognitive disorders appear years before the diagnosis and are characterized by impaired emotion recognition, processing speed, visuospatial and executive function, among others (Papoutsi et al., 2014; Stout et al., 2011). Neuropsychiatric disorders are also present in the premanifest phase (Tabrizi et al., 2009) and generally comprise depression, irritability and apathy (Craufurd et al., 2001).

1.3.1.3 Pathology

HD typically develops with striatal neurodegeneration. Specifically there is a massive loss of gamma-aminobutyric acid (GABA)ergic medium spiny neurons, which project to the globus pallidus and the SN (Reiner et al., 1988). On the contrary, large interneurons are generally spared (Waldvogel et al., 2014). Striatal loss may start more than 10 years before the onset of symptoms (Tabrizi et al., 2013). HD also develops with atrophy of the cerebral cortex, subcortical white matter, thalamus, specific hypothalamic nuclei and other brain regions (Waldvogel et al., 2014) (**Fig. 14**). One of the neuropathological hallmarks of HD is the presence of cytoplasmic aggregates and nuclear inclusions of mutant Htt throughout the brain (Davies et al., 1997; DiFiglia et al., 1997). Those aggregates can sequester other proteins, giving rise to deficits in several pathways.

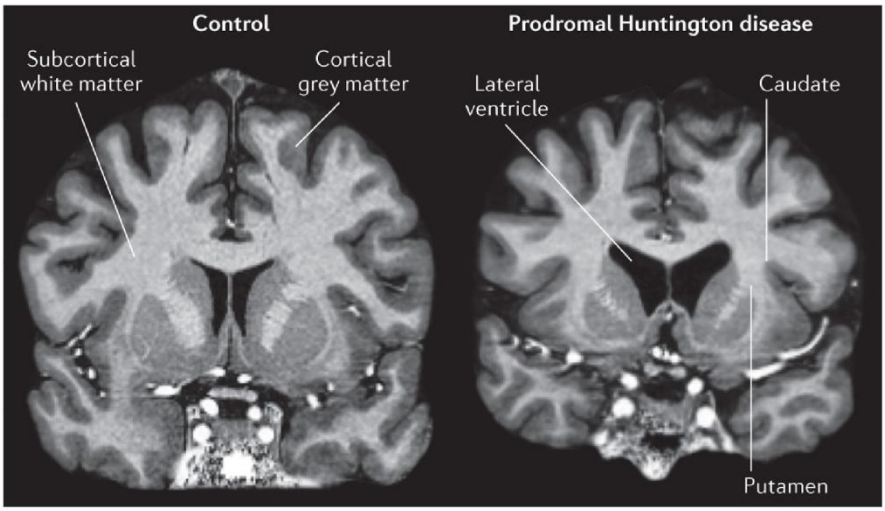

Figure 14. Brain neuroimaging.

HD is characterized by bilateral atrophy of caudate and putamen. There is a concomitant increase in size of the lateral ventricle. Additionally subtle changes in the cortical gray matter can be found together with an atrophy of the subcortical white matter. From Bates et al., 2015.

1.3.2 Huntingtin pathogenic mechanisms

Htt is a 348 kDa protein, ubiquitously expressed and essential for mammal embryonic development (Duyao et al., 1995; Nasir et al., 1995; Zeitlin et al., 1995). Adult loss of Htt leads to neurodegeneration, demonstrating its essential role in maintaining neuronal function and survival (Dragatsis et al., 2000). Htt is composed by α-helical HEAT (Huntingtin, elongation factor 3, protein phosphatase 2A and TOR1) repeats, which consists of 50 amino acids forming a helical hairpin (**Fig. 15**). In Htt, those HEAT repeats stack to form an

elongated superhelix with an hydrophobic core (Li et al., 2006). Generally, HEAT repeat proteins mediate protein-protein interactions, which is consistent with the multiple interaction partners of Htt (Li and Li, 2004), suggesting that acts as an scaffolding protein. To date, Htt has been proposed to be involved in transcriptional regulation (Luthi-Carter and Cha, 2003), axonal trafficking of vesicles, autophagosomes and mitochondria (Gauthier et al., 2004; Trushina et al., 2004; Wong and Holzbaur, 2014) nuclear export/import, ubiquitin-mediated proteolysis and regulation of the endosomal and autophagic system among many other cellular mechanisms (Martin et al., 2014). Moreover, Htt can shuttle between the nucleus and the cytoplasm. It is suggested that upon polyQ expansion there is a conformational transition leading to a specific toxic conformation. Some studies support this hypothesis, revealing that the expanded polyQ stretch presents a β-hairpin containing β-sheets conformation (Hoop et al., 2016; Peters-Libeu et al., 2012) leading to aggregate inclusions. However, other data suggest the presence of cellular malfunctioning prior to Htt aggregation, implying that soluble forms may also exert a role in cellular toxicity. In fact, it is also believed that Htt inclusions may act as a pro-survival mechanism to isolate those soluble toxic forms (Arrasate and Finkbeiner, 2012). Another toxic mechanism linked to Htt aroused by the discovery of N-terminal fragments of the expanded protein in HD patients' inclusions (DiFiglia et al., 1997) (**Fig. 15**). N-terminal Htt fragments aggregate faster and are more toxic than the unfragmented protein, as observed in several models (Kim et al., 2001; Wang et al., 2008; Wellington et al., 2002). Not only N-terminal Htt fragments containing the polyQ stretch are toxic, but also C-terminal fragments (El-Daher et al., 2015). Therefore, it is becoming clear that Htt fragments also participate in the deleterious cascade leading to HD.

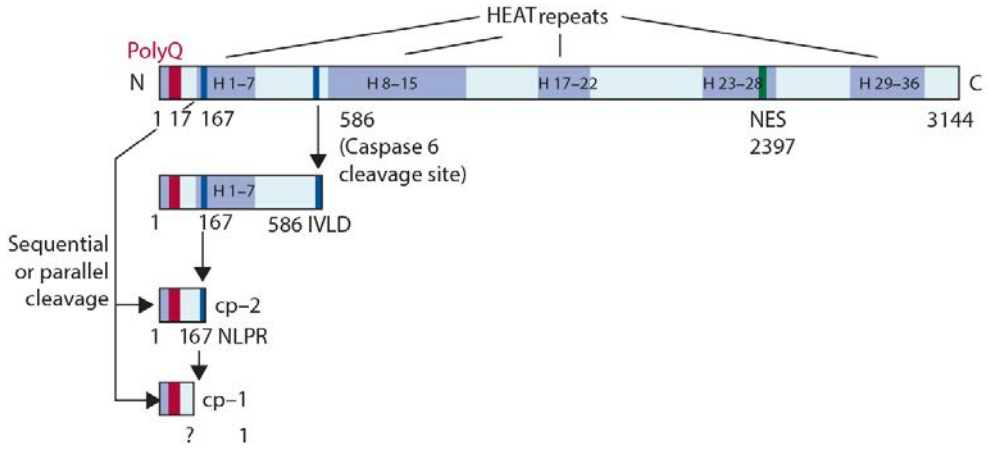

Figure 15. Huntingtin structure and cleavage.

Human Htt protein is composed by several HEAT domains. The polyQ stretch is present in the N-terminus of the protein. Proteolytic cleavage by caspase 6 and other unknown proteases forms toxic N-terminal fragments (such as cp-1 or cp-2). IVLD and NLPR are amino acid cleavage sequences. NES = nuclear export signal. Adapted from Ross and Tabrizi, 2011.

1.3.3 Experimental models

1.3.3.1 Toxic models

HD can be modeled using toxic or genetic models. Toxic models were widely used before the discovery of the genetic mutation underlying HD. Those models were based first on the observation of striatum as the primary degenerative region in HD brains, thus using ibotenic acid (Hantraye et al., 1990) and kainic acid (Coyle and Schwarcz, 1976), which led to excitotoxic cell death. With the discovery that striatal interneurons did not degenerate as much as GABAergic neurons, quinolinic acid supplanted the first toxins, since it has relatively low toxicity to striatal interneurons (Schwarcz et al., 2010). Mitochondrial toxins, such as malonate and 3-nitropropionic acid, were later used due to its ability to inhibit the electron transport chain (Ferrante, 2009). As for the toxic models of PD, these kind of models have the limitation of producing an acute lesion, which hardly represent the progressive nature of HD.

1.3.3.2 Genetic models

HTT gene is very large: it has 67 exons and is ~170 kb large (Ambrose et al., 1994). This makes working with this gene very challenging. The variety of HD genetic models that exist reflect different approaches aimed to model this “difficult” gene. Rodent models are the most

widely used and can be divided into those expressing truncated fragments of mutant *HTT* and those expressing full length mutant *HTT*. R6/1, R6/2 and N171-82Q express truncated N-terminal fragments of mutant *HTT* and present more robust and rapidly progressive phenotype. R6/1 mice and R6/2 mice express exon 1 of human *HTT* with originally 116 and 144 CAG repeats, respectively (Mangiarini et al., 1996). The N171-82Q mice express truncated *HTT* cDNA with 82 CAG repeats (Schilling et al., 1999). Full length mouse models were developed using two different strategies. HdhQ111 (Wheeler et al., 2002), CAG140 (Menalled et al., 2003) and HdhQ150 (Lin et al., 2001) mouse models have an expanded CAG repeat knocked in into the endogenous mouse *Htt* locus. The second strategy consisted in introducing the full-length mutant human *HTT* gene either using yeast artificial chromosome technology, as in the YAC128HD mice (Hodgson et al., 1999), or bacterial artificial chromosome technology, as in the BACHD mice (Gray et al., 2008)

Several cell lines have been used to model the pathologic events in HD, from non-neuronal to neuronal (Cisbani and Cicchetti, 2012). The ST*Hdh*$^{Q7/Q7}$, ST*Hdh*$^{Q7/Q111}$ and ST*Hdh*$^{Q111/Q111}$ cell lines have been widely used in the field of HD research and have enable the discovery of several HD-related pathways (Gines et al., 2003a, 2003b; Seong et al., 2005; Xifró et al., 2008). These cell lines were derived from striatal primordia (Trettel et al., 2000) of HD knock in mouse model with a chimeric exon 1. These cell lines express wild type and mutant Htt at endogenous levels (Wheeler et al., 2000) and are the model used in this thesis to study mitophagy in the context of mutant Htt. A new promising field is starting with the development of inducible pluripotent stem cells (iPSC) derived from HD patients (Camnasio et al., 2012) or murine models (Ritch et al., 2012).

1.3.4 Pathogenic cellular mechanisms in Huntington's disease

1.3.4.1 Hallmarks of Huntington disease

Several mechanisms contribute to the pathogenic features of HD. **Figure 16** shows a schematic representation of the pathogenic cellular mechanisms in HD. Under normal conditions, the integrity of the proteome is maintained through molecular chaperones and clearance machineries, such as the UPS and autophagy. Wild type Htt is ubiquitinated at K6, K9 and K15, thus leading to its degradation by the proteasome. Thus, Htt is a target for UPS-mediated degradation (Kalchman et al., 1996) but can also be degraded by lysosomes. Upon polyQ expansion, UPS-mediated degradation of mutant Htt is impaired leading to mutant Htt accumulation into insoluble, ubiquitin-containing aggregates (Ortega and Lucas,

2014; Waelter et al., 2001). Conversely, autophagy is induced, since mutant Htt sequesters and inactivates mTOR (Ravikumar et al., 2004). While the number of autophagosomes increases, there is a deficit in cargo recognition (Martinez-Vicente et al., 2010) and aggregated proteins, such as mutant Htt, and damaged organelles are not degraded. This has a major impact on mutant Htt degradation, since upon polyQ expansion it is preferentially degraded by autophagy and several post-translational modifications target the mutant protein to this particular pathway (Jeong et al., 2009; Sarkar and Rubinsztein, 2008). Moreover, changes in expression levels of autophagy proteins have been reported in striatum from HD patients (Hodges et al., 2006). In fact, alterations in transcriptional regulation are another pathogenic hallmark, which occurs early in the course of the disease (Cha, 2007). Mutant Htt interacts with and disrupts components of the general transcriptional machinery affecting both promoter accessibility and recruitment of RNA polymerase II (Seredenina and Luthi-Carter, 2012). Particularly, mutant Htt interferes with the PGC-1α transcriptional pathway, impairing its ability to activate downstream genes (Cui et al., 2006; Dickey et al., 2016; Weydt et al., 2006). Recently, Htt has been shown to interact with peroxisome proliferator-activated transcription factor δ (PPARδ), a downstream PGC-1α gene, while mutant Htt represses its activation (Dickey et al., 2016). Htt protein also interacts with several proteins involved in vesicular trafficking while these interactions are impaired in the presence of the mutant protein (Jones and Hughes, 2011). General axonal transport is also hampered by mutant Htt leading to alterations in neurotransmitter release and perturbed neuronal activity, which underlies the cognitive and physical decline observed in HD patients (Gauthier et al., 2004; Morfini et al., 2009)

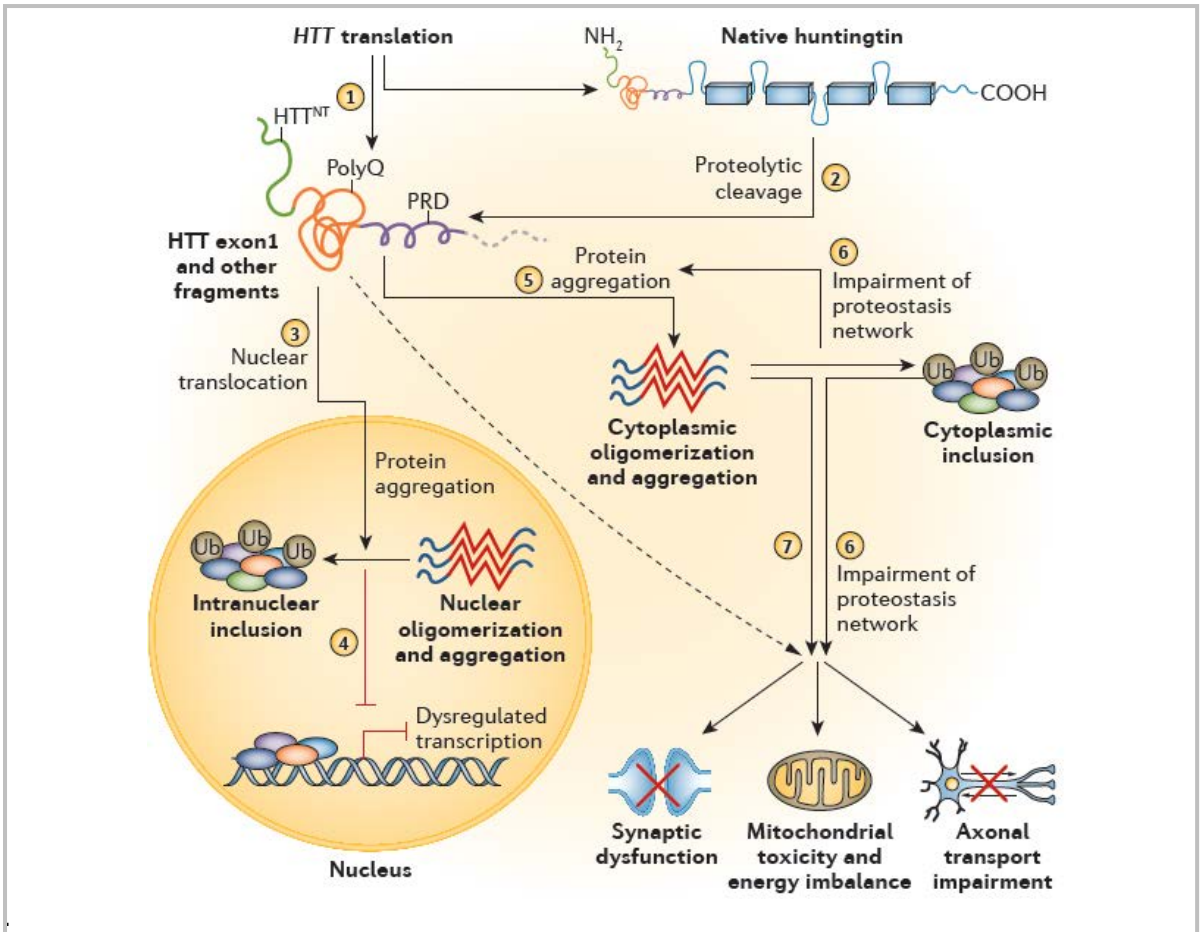

Figure 16. Pathogenic cellular mechanisms of huntingtin.

(**1**) *HTT* translation leads to full length huntingtin (Htt) protein and N-terminal fragments due to aberrant splicing. (**2**) Full-length Htt can also give rise to Htt fragments through proteolytic cleavage. (**3 and 4**) Htt aberrant fragments can enter the nucleus, aggregate and form nuclear inclusions, which can lead to transcriptional dysregulation. (**5**) Htt can oligomerize and aggregate in the cytosol as well. (**6**) The impairment of the proteostasis network can exacerbate Htt aggregation. (**7**) Mutant Htt and its fragments result in additional global cellular impairments, including synaptic dysfunction, mitochondrial toxicity and decreased axonal transport. PRD, proline rich domain, Ub, ubiquitin. From Bates et al., 2015.

1.3.4.2 Mitochondrial dysfunction in Huntington's disease

Pioneering studies in the 80's and early 90's unraveled the presence of biochemical abnormalities in the respiratory chain enzymes in mitochondria from striatal HD patients. Since then, accumulating evidence indicate that mitochondria is a key player in HD pathogenesis. **Table 4** summarizes different mitochondrial alterations present in HD patients or HD models.

Table 4. Mitochondria-associated alterations in HD

Evidence	Model	References
Bioenergetics - Glucose hypometabolism in caudate nuclei. - Increased lactate levels. - Impaired energy metabolism.	HD patients	Grafton et al., 1992; Jenkins et al., 1993
OXPHOS deficiencies - Reduced complex II, III and IV activity in striatum.	HD patients, mouse, rat	Brennan et al., 1985; Damiano et al., 2013; Gu et al., 1996
Membrane potential - Reduced membrane potential. - Calcium-dependent mitochondrial depolarization and swelling	HD patients' lymphoblasts, mouse, rat and ST-Q7/111 cells	Gellerich et al., 2008; Guo et al., 2016; Panov et al., 2002, 2003; Ventura et al., 2013
ATP - Reduced ATP levels and increased phosphocreatine levels .	HD patients' lymphoblasts, mouse and ST-Q7/111 cells	Mochel et al., 2012; Naia et al., 2015, 2016
Mitochondrial DNA - Increased frequency of mtDNA lesions and depletions.	HD patients (striatum and skin fibroblasts)	Siddiqui et al., 2012
Oxidative stress - Lipofucsin accumulation - Increased protein, lipid and DNA oxidation. - Aconitase, creatine kinase, citrate synthase and ATP synthase oxidation and reduced activity.	HD patients, mouse	Browne et al., 1997; Perluigi et al., 2005; Sorolla et al., 2010; Stack et al., 2008; Tabrizi et al., 1999
Mitochondrial quality control defects - Impaired mitochondrial protein import. - Impaired mitochondrial disulfide relay system for IMS import.	Mouse, primary cortical and striatal neurons and ST-Q7 and ST-Q111 cells	Napoli et al., 2013; Yano et al., 2014
Mitochondrial dynamics - Increased Drp1 and Fis1 levels and decreased mitofusins levels. - Mitochondrial fragmentation. - DRP1-mutant HTT interaction leading to increased DRP1 enzymatic activity.	HD patients, mouse, rat	Kim et al., 2010; Liot et al., 2009; Shirendeb et al., 2011, 2012; Song et al., 2011

Mitochondrial biogenesis - Impairment of PGC-1α transcriptional pathway. - Repression of peroxisome proliferator-activated transcription factor δ (PPARδ).	Mouse, HEK293T, striatal cells, mouse primary cortical neurons, iPSCs differentiated into medium spiny neuron.	Cui et al., 2006; Dickey et al., 2016; Weydt et al., 2006
Mitophagy - Impairment of cargo sequestration step in autophagy. - Blockade of mitochondria-containing autophagosome formation.	ST-Q18, ST-Q111 and MEF.	Khalil et al., 2015; Martinez-Vicente et al., 2010
Trafficking - Trafficking abnormalities. - Altered mitochondrial motility and accumulation adjacent to aggregates. - Impaired mitcrotubule protein association with mitochondria. - Altered autophagosomal motility preventing autophagosomal fusion with lysosomes.	Drosophila, mouse, rat and mouse primary embryonic striatal and cortical neurons	Chang et al., 2006; Gunawardena et al., 2003; Orr et al., 2008; Shirendeb et al., 2012; Song et al., 2011; Trushina et al., 2004; Wong and Holzbaur, 2014

In summary, even though HD is a disorder whose primary cause is known, many molecular changes and cellular consequences underlie the disease pathogenesis. In addition to folding, aggregation and clearance pathways, other mechanisms are also emerging which can have an important role in disease pathogenesis and disease progression. Mitochondrial impairment is one of the main characteristics that neurodegenerative diseases share, probably because neurons are highly dependent on mitochondrial function. In the case of HD, modulation of mitochondrial health has been shown to protect striatal neurons against mutant Htt toxicity. For instance, restoring complex IV activity in HD transgenic mice (Bae et al., 2005), PGC-1α overexpression in *in vitro* and *in vivo* models of HD (Cui et al., 2006; Weydt et al., 2006) upregulation of SOD2 (Madhavan et al., 2008) or inhibition of mitochondrial fission (Guo et al., 2013) have led to neuroprotection. Interestingly, either full-length or small mutant Htt fragments have been reported to directly interact with OMM and alter mitochondrial function (Choo et al., 2004; Gutekunst et al., 1998; Orr et al., 2008) but the mechanism remains elusive. On the other hand, mutant Htt has been reported to interact and block TIM23 complex, located in the IMM, but how Htt can reach the inner membrane remains also unknown. Finally, how all these mechanisms taking place on the outside and the inside of mitochondria act in concert to generate neuronal degeneration is also a matter of further study.

AIM AND OBJECTIVES

2 Aim and objectives

The main aim of this study is to deepen our understanding of the pathophysiology of Parkinson's disease and Huntington's disease in order to develop new mitochondrial therapeutic targets for these type of diseases. Since we focus on two different neurodegenerative diseases, the specific objectives are:

OBJECTIVE 1. To determine the role of mitochondrial protein import and protein quality control systems in *in vitro* and *in vivo* models of PD and their potential as therapeutic targets. To achieve this objective we have established the next specific objectives:

a) To study the integrity of mitochondrial protein import system in midbrain human *post-mortem* tissue from PD patients as well as in complex I-deficient mice and complex I-deficient dopaminergic neuroblastoma cells, all models of PD.
b) To analyze the consequences of mitochondrial protein import failure in complex I-deficient mice and dopaminergic neuroblastoma cells, by means of OXPHOS protein levels, presence of mitochondrial aggregated proteins, mtUPR activation, mitochondrial membrane potential, ROS production, cell death and nigrostriatal degeneration.
c) To evaluate the therapeutic potential of genetic rescue of the activity of the mitochondrial protein import system in complex I-deficient mice and neuroblastoma cell lines. For neuroblastoma cells we have overexpressed two different key translocases proteins, TIM23 and TOM20, either transiently or stably, and assessed cell death. For complex I-deficient mice, we have stereotaxically delivered adeno-associated virus encoding for the same two key translocases proteins and assessed the integrity of the dopaminergic nigrostriatal system.

OBJECTIVE 2. To study how the HD-related cellular alterations affect quality control surveillance systems in mitochondria. Since Htt has been recently described as a scaffold protein for selective macroautophagy, our aim is to study the failure of mitochondria turnover by mitophagy in an *in vitro* neuronal model of HD using differentiated cells and working with the endogenous proteins. To achieve this objective we have established the next specific objectives:

a) To evaluate mitophagy mechanism in an *in vitro* model of HD. For such we have used different state-of-the art techniques to measure mitophagy in differentiated striatal cell lines expressing exon 1 of the human Htt protein with either 7 or 111 glutamine repeats (ST-Q7 or ST-Q111).

b) To determine how mutant Htt expressing 111 glutamine repeats can affect the mitophagy system. To do so, we have used differentiated ST-Q7 and ST-Q111 cells and we have analyzed each of the steps that make up the mitophagy mechanism: (i) labeling of damaged mitochondria, (ii) formation of the initiation, nucleation and elongation complexes, and (iii) interaction of mitophagy adapters and the autophagosome membrane. We have analysed the role of Htt protein and its key interactions with the autophagy/mitophagy machinery.

c) To analyse the consequences of an impaired mitophagy activity in differentiated ST-Q7 and ST-Q111 cells by means of bioenergetic status, ROS production and mitochondrial membrane potential.

MATERIALS AND METHODS

3 Materials and Methods

3.1 Reagents and antibodies

The following chemicals were used: MPTP (Ref. M0896), MPP^+ (Ref. D048), rotenone (Ref. R-8875), CCCP (carbonyl cyanide 3-chlorophenyl hydrazone, Ref. C2759), oligomycin (Ref. 75351), antimycin A (Ref. A8674) and the lysosomal inhibitors chloroquine (Ref. C6628) and bafilomycin A1 (Ref. B1793) were from Sigma-Aldrich. The following reagents were also used: MitoTracker™ Deep Red FM (Molecular Probes, Ref. M22426), CM-H_2DCFDA (Life Technologies, Ref. C6827), Cell Rox® Green Reagent (Thermo Fisher, Ref. C10444) and TMRM (Tetramethylrhodamine methyl ester, Sigma-Aldrich, Ref. T668).

A complete list of the primary and secondary antibodies used is summarized on **Table 5**, **6** and **7**.

Table 5. List of primary antibodies used in Chapter I

Antibody	Species	Source	Reference	Dilution
Tim23	mouse monoclonal	BD Biosciences	611222	WB: 1:1000 IF cells: 1:300 IF tissue: 1:1000 IHC: 1:320
Tom20	mouse monoclonal	Abcam	ab56783	WB: 1:1000 IF: 1:300 IHC: 1:320
Total OXPHOS	mouse monoclonal	Abcam/Mitoscience	ab110411/MS601	1:1000
Complex IV sub IV (COX IV)	rabbit polyclonal	Abcam	ab16056	WB: 1:1000 IF cells: 1:300 IF tissue: 1:500
eGFP	rabbit polyclonal	Novus Biologicals	NBP2-37821	1:1000
Ndufs3	mouse monoclonal	Abcam	ab110246	WB: 1:1000 IF: 1:200
ClpX	rabbit monoclonal	Abcam	ab168338	1:2000

Grp75	mouse monoclonal	abcam	ab2799	1:1000
TH	mouse monoclonal	Chemicon	MAB 5280	IF: 1:1000
TH	rabbit polyclonal	Calbiochem	657012	IHC: 1:2000/ 1:5000
VDAC1/Porin	rabbit polyclonal	Abcam	ab15895	1:2000
α-Tubulin	mouse monoclonal	Sigma-Aldrich	T5168	1:5000
β-actin	mouse monoclonal	Sigma-Aldrich	A5441	1:5000

WB: western blot, IF: immunofluorescence, IHC: immunohistochemistry

Table 6. List of primary antibodies used in Chapter II

Antibody	Specie	Source	Reference	Dilution
LC3	rabbit polyclonal	Novus	NB2220	WB: 1:2000 PLA: 1:100
LAMP-1	rat monoclonal	Santa Cruz	sc-19992	IF: 1:200
PINK1	Rabbit polyclonal	Novus	BC100-494SS	1:2000
Parkin	Rabbit polyclonal	Abcam	ab15954	WB: 1:2000 IF: 1:200
Total-UB	Rabbit polyclonal	Sigma-Aldrich	U 5379	1:2000
poly-UB K63	rabbit monoclonal	Cell Signaling	5621S	1:2000
ULK1	Rabbit polyclonal	Novus	NBP2-24738SS	WB: 1:2000 PLA: 1:100
ULK1 S555	rabbit monoclonal	Cell Signaling	5869P	1:2000
ULK1 S317	rabbit monoclonal	Cell Signaling	12753S	WB: 1:2000 PLA: 1:100
ULK1 S757	Rabbit polyclonal	Cell Signaling	6888S	1:2000

OPTN	Rabbit polyclonal	Proteintech	10837-1-AP	1:100
Htt	mouse monoclonal	Chemicon	MAB2166	1:100
NDP52/CALCOCO2	mouse monoclonal	Santa Cruz	sc-376540	PLA: 1:100 IF: 1:100
p62 C-term	Guinea pig polyclonal	Progen	GP62-C	IP: 1:350
NBR1	mouse monoclonal	Abnova	H00004077-M01	IP: 1:350
anti-DNA	mouse monoclonal	Progen	AC-30-10	1:100
Beclin 1	mouse monoclonal	Santa Cruz	48341	1:100
Vps15 (PIK3R4)	rabbit polyclonal	Novus	NBP1-30463	1:100
mTOR [GT649]	mouse monoclonal	Genetex	GTX630198	1:100
VDAC1/Porin	Rabbit polyclonal	Abcam	ab15895	1:2000
β-actin	mouse monoclonal	Sigma-Aldrich	A5441	1:5000

WB: western blot, PLA: proximity ligation assay, IF: immunofluorescence, IP: immunoprecipitation,

Table 7. List of secondary antibodies used in Chapter I and II

Antibody	**Source**	**Reference**
Goat anti-mouse HRP	GE Healthcare	NXA931
Donkey anti-rabbit HRP	GE Healthcare	NA934V
Donkey anti-rat HRP	GE Healthcare	NA935V
Goat anti-guinea pig HRP	Santa Cruz	sc-2438

Goat anti-mouse biotinylated	Vector Laboratories	BA9200
Goat anti-rabbit biotinylated	Vector Laboratories	BA1000
Alexa Fluor® 488 goat anti-mouse	Thermo Fisher	A11001
Alexa Fluor® 488 goat anti-rabbit	Thermo Fisher	A11008
Alexa Fluor® 488 donkey anti-rat	Thermo Fisher	A21208
Alexa Fluor® 594 goat anti-mouse	Thermo Fisher	A11005
Alexa Fluor® 594 goat anti-rabbit	Thermo Fisher	A11012

3.2 Human experiments

3.2.1 *Post-mortem* brain homogenates

Postmortem human brain samples were obtained from the New York Brain Bank at Columbia University and the University of Barcelona Brain Bank. SN was dissected from ventral midbrain samples from 5 control subjects and 9 PD patients (mean age at death = 72 ± 4.3 years, cold postmortem interval = 6.47 ± 2.72 hours and frozen postmortem interval = 10.63 ± 2.82 hours). Total tissue proteins were isolated in a buffer containing 50 mM Tris-HCl (pH 7, Sigma-Aldrich, Ref. T6066), 150 mM NaCl (Sigma-Aldrich, Ref. S3014), 5 mM EDTA (Ethylenediaminetetraacetic acid, Sigma-Aldrich, Ref. E5134), 1% SDS (Sodium dodecyl sulfate, Sigma-Aldrich, Ref. L3771), 1% Nonidet P-40 (Sigma-Aldrich, Ref. I8896) and protease inhibitors (Complete mini Protease Inhibitor Cocktail, Sigma-Aldrich, Ref. 11836153001).

3.3 Mouse experiments

3.3.1 Animal handling

We used C57BL/6Ncrl background male mice. Animals were housed under controlled conditions (22^{o}C ± 1^{o}C; 12h light/dark cycle) with food and water available *ad libitum*. All the animal procedures and methods employed in this study followed the Guide for the Care and

Use of Laboratory Animals (Guide, 8th edition, 2011, NIH) and European (2010/63/UE), Spanish (RD53/2013) and Catalan (Decret 214/97) legislation. All the procedures had been approved by the Vall d'Hebron Institute of Research Animal Ethical Experimental Committee.

3.3.2 AAV vector production and stereotaxic delivery

For adeno-associated virus (AAV) delivery, human TIM23 and human TOM20 cDNA sequences cloned into a pCMV6-XL5 vector were obtained from Origene (Origene Technologies, Ref SC116167 and SC114860 respectively) and AAV of serotype 2/9 were produced at the UPV-CBATEG (Autonomous University of Barcelona, UAB, Spain).

One microliter of viral suspension was stereotaxically delivered to the area just above the SN of 8-week-old C57BL/6Ncrl mice (-2.9 AP, -1.3 L and -4.2 DV) at a flow rate of 0.2 µL/min. At day 28 post AAV injections, animals were either euthanized, to analyze TIM23 and TOM20 overexpression, or treated with saline or MPTP, as indicated (**Fig. 17**).

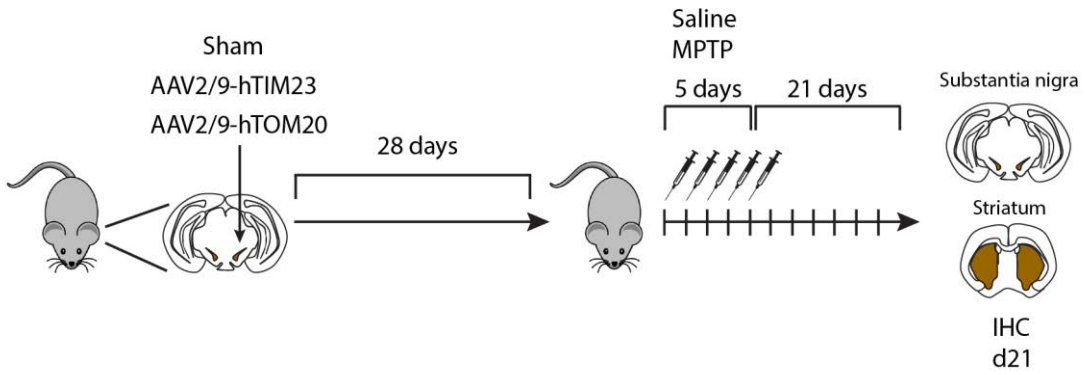

Figure 17. Diagram representing the workflow and experiments performed with AAV-injected mice.

IHC: immunohistochemistry.

3.3.3 MPTP administration to mice

8-week-old mice were treated following a sub-acute regimen (Jackson-Lewis and Przedborski, 2007), which consisted of one intra-peritoneal injection of MPTP-HCl (30 mg/kg, Sigma-Aldrich, Ref. M0896) per day, during five consecutive days. Animals were euthanized at day 0, 1, 2, 4, 7 and 21 after the last injection. Control mice received saline injections only (**Fig. 18**).

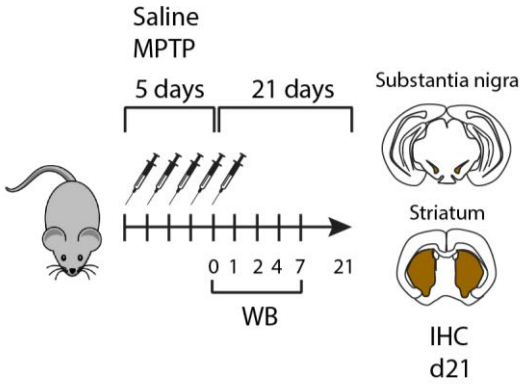

Figure 18. Diagram representing the workflow and experiments performed with MPTP-intoxicated mice.

IHC: immunohistochemistry, WB: western blot.

3.3.4 Tissue collection

For biochemical analysis, ventral midbrain was removed from the mice and resuspended in RIPA buffer containing 50 mM Tris-HCl pH 7, 150 mM NaCl, 5 mM EDTA, 1% SDS, 1% Nonidet P-40 and proteases inhibitors. Tissue was homogenized performing 10 go/back movements with a 18G syringe and 10 go/back movements with a 23G syringe. The suspension was centrifuged at 13.000 rpm for 30 min at 4^{o}C in order to separate the pellet, which contains the debris, from the supernatant, which contains all the proteins. Samples were sonicated for 5 sec and total protein concentration was determined by the bicinchoninic assay method (Thermo Scientific, Reagent A Ref. 23228 and Reagent B Ref. 23224) with BSA (Bovine Serum Albumin, Thermo Fisher Ref. 23209) as a standard protein.

For histological analysis, mice were anesthetized with an intraperitoneal injection of 0.2 mL of 5% pentobarbital (Ref. 37689). We used a 9 mL/min flow rate of NaCl 0.9% (Frasenius Kabi) during 3 minutes and 4% paraformaldehyde (Panreac, Ref. A3697.9010) diluted in 0.2 M phosphate buffer containing 0.15M sodium phosphate dibasic and 0.05M of sodium phosphate monobasic (Sigma-Aldrich, Ref. S0876 and S9638 respectively) during 8 min. Brains were removed and incubated 24h in 4% ice-cold paraformaldehyde at 4^{o}C and 48h more in 30% sucrose (Sigma-Aldrich, Ref. S9378) at 4^{o}C. Brains were frozen in 2-methylbutane (Honeywell, Ref. M3263) between -30 and -40^{o}C and stored at -80^{o}C.

3.4 Cell culture and treatments

3.4.1 BE(2)-M17

Human neuroblastoma dopaminergic cell line BE(2)-M17 (Sigma-Aldrich, Ref. 95011816) was grown in Minimal Essential Medium optimized (Opti-MEM, Gibco, Thermo Fisher, Ref. 31985062) supplemented with 10% inactivated fetal bovine serum (Thermo Fisher, Ref 26140-079), 1% penicillin-streptomycin (Sigma-Aldrich, Ref P4333) and 0.5 mg/mL active geneticin (Thermo Fisher, Ref 11558616) and maintained at 37°C in humidified 95% air/5%CO_2 incubator.

MPP^+ was diluted in water and added at 80% of cell confluence at the following concentrations: 0.12 mM, 0.25 mM, 0.5 mM, 1 mM, 2 mM and 5 mM for 24h.

3.4.2 ST-Q7 and ST-Q111 cells

ST*Hdh*$^{Q7/Q7}$ (ST-Q7) and ST*Hdh*$^{Q111/Q111}$ (ST-Q111) were obtained from Coriell Institute (Ref. CH00097 and CH00095, respectively). ST-Q7 and ST-Q111 cells were grown in Dulbecco's Modified Eagle Medium (DMEM, Gibco, Thermo Fisher, Ref. 41966-029) supplemented with 10% inactivated fetal bovine serum, 1% penicillin-streptomycin and 0.4 mg/mL active geneticin and maintained at 33°C in humidified 95% air/5%CO_2 incubator. For differentiation, cells were supplemented with dopamine (DOPA) cocktail consisting on 10 ng/mL α-FGF-acidic mouse recombinant (Fibroblast growth factor, Sigma-Aldrich, Ref. SRP3197-50U), 250 µM IBMx (3-isobutyl-1-methylxanthine, Sigma-Aldrich, Ref. I5879), 200 nM TPA/PMA (Phorbol 12-myristate 13-acetate, Sigma-Aldrich, Ref. P1585), 50 µM Forskolin (Sigma Aldrich, Ref. F6886) and 20 µM dopamine hydrochloride (Sigma-Aldrich, Ref. H8502) during at least 24h.

3.4.3 SH-SY5Y

Human neuroblastoma SH-SY5Y cell line was obtained from ATCC (CRL-2266™) and grown in Dulbecco's Modified Eagle Medium supplemented with 10% inactivated fetal bovine serum and 1% penicillin-streptomycin and maintained at 37°C in humidified 95% air/5%CO_2 incubator.

For biochemical studies cells were washed twice with ice-cold PBS solution containing 137 mM NaCl, 2.7 mM KCl, 10 mM Na_2HPO_4 and 1.8 mM KH_2PO_4 at pH 7.4 (Sigma-Aldrich, Ref. P9333, S7907 and P5655, respectively) before detaching them with a cellular scraper. Cell suspension was centrifuged at 800g for 5 min at 4^{o}C. Supernatant was discarded and the pellet was resuspended in PBS. We repeated the centrifugation step two more times and finally cell suspension was resuspended in RIPA buffer to which we added freshly proteases inhibitors (HALT Protease inhibitor cocktail EDTA free, Thermo Scientific, Ref. 1862209) and 1 mM PMSF (Sigma Aldrich, Ref. P7626). Homogenates were incubated on ice for 15 min and samples were sonicated. Total protein concentration was determined by the bicinchoninic assay method with BSA as a standard protein.

3.5 Transfections

3.5.1 Bacterial transformation and DNA purification

For the production of mitoGFP plasmid, the mitochondrial targeting sequence of Aconitase 2 was cut using BAMHI and EcoRI as restriction sites. EGFP was recovered from the vector pEGFPN2 by EcoR I and Not I digestion. Mitochondrial targeting sequence (Bam HI - EcoRI) and EGFP (EcoRI - Not I) were cloned into the pcDNA3 vector using the BamHI and Not I cloning site. Human TIM23 and TOM20 plasmids cloned into a pCMV6-XL5 vector were obtained from Origene (Origene Technologies, Ref SC116167 and SC114860). mKeima-Red-Mito7 (mitoKeima) plasmid was obtained from Addgene (Ref. 56018).

Competent bacterial samples XL Blue were transformed with 1-2 µL of cDNA (TIM23 or TOM20) by incubation 10 min on ice followed by a thermal shock at 42^{o}C for 3 min. Bacterial colonies were let to grow overnight in Luria-Broth (LB, Invitrogen Ref 12795027) agar (Alfa Aesar, Ref. A10752) plates supplemented with Ampicillin (100 µg/mL, Sigma-Aldrich, Ref. A9518) at 37^{o}C. One individual colony was picked with a pipette tip and thrown into LB medium supplemented with Ampicillin and let on agitation overnight at 37^{o}C. Plasmid purification was performed with NucleoBond R Xtra Midi (Clontech Laboratories, Ref. 740410.50).

3.5.2 Transfections

For mitoGFP, TIM23 and TOM20 plasmid transfection in BE(2)-M17 cells, Lipofectamine 2000 (Thermo Fisher, Ref. 11668-019) was used. For cells seeded in a 12-well plate, 0.8 µg of DNA were transfected using a DNA:lipofectamine ratio between 1:1.5 and 1:2. DNA and lipofectamine were diluted separately in Opti-MEM medium (without serum or antibiotics) and the mixture was incubated for 5 minutes prior to the mixing of DNA and lipofectamine. After 20-25 minutes of incubation at room temperature (RT), the DNA-lipofectamine mix was added to each well. We added the same amount of lipofectamine also in non-transfected condition. 4-5 hours after transfection, medium was changed to the corresponding growing medium.

For mitoKeima transfection in ST-Q7 and ST-Q111 cells, Lipofectamine 3000 (Thermo Fisher, Ref. L3000015) was used. For cells seeded in a 12-well plate, we transfected 30 µg of DNA using a DNA:lipofectamine ratio 1:1.5 and following the same protocol as for BE(2)-M17 cells.

3.6 Generation of TOM20 stable cell line

Human TOMM20 (Myc-DDK tagged) and pLenti-C-Myc-DDK-P2A-Puro lentiviral particles were obtained from Origene (Origene Technologies, RC210746L3V and PS100092V). 8µg/mL of polybrene (Hexadimethrine bromide, Sigma-Aldrich, Ref. H9268) was added to the medium 1-2h before lentiviral transduction. Lentiviral particles were added at a MOI (multiplicity of infection) of 5 and incubated for 18-20h at 37^{o}C in humidified 95% air/ 5% CO_2 incubator. Two days after transduction, medium with puromycin (selection marker, Life Technologies, Ref. A11138-03) at 1µg/mL was added and stable cell lines were obtained after 4-7 days.

3.7 Quantitative Real-Time PCR (RT-qPCR)

BE(2)-M17 cells treated with MPP^+ or vehicle were trypsinized and centrifuged at 300g for 5 minutes. The pellet was washed with PBS and centrifuged again at 300g for 5 minutes. For mRNA extraction we used the RNeasy Mini Kit (Qiagen, Ref. 74106) according to manufacturer's instructions. Total mRNA concentration was measured on a Nanodrop 1000 (Nucliber). One µg of total mRNA was reverse-transcribed with Oligo(dT) by using

SuperScript III™ first-strand system for RT-PCR (Invitrogen, Ref. 18080051) or the High Capacity cDNA Reverse Transcription Kit (Applied Biosystems, Ref. 4368814) in a final volume of 20 uL following manufacturer's instructions.

The expression of the genes of interest was analyzed using Taqman Universal Master Mix II with UNG (Roche Applied Biosystems, Ref. 4440038) and fluorescence-labelled specific probes (**Table 8**) on a 7900HT SDS (Applied Biosystems). 2.5 ng of cDNA were used to measure mRNA levels. Relative quantification was carried out using the 2-deltadeltaCt method using the software ABI PRISM 7900HT SDS version 2.2 (Applied Biosystems).

Table 8. List of RT-qPCR probes used

Gene	Specie	Taqman ref.
TIM23	Human	#Hs00197056_m1
TOM20	Human	#Hs00740685_sH
CLPX	Human	#Hs01101010_m1
HSP9	Human	#Hs00269818_m1
RPLP0	Human	#4326314E

3.8 Immunohistochemistry in tissue

SN and striatum coronal serial sections were cut at either 20 µm or 30 µm using a cryostat (Leica CM 3050 S) and incubated in 0.1 M phosphate buffer containing 0.01% sodium azide (Sigma-Aldrich, Ref. S8032) until used.

3.8.1 TIM23/TOM20 immunohistochemistry in Substantia Nigra

To assess TIM23 and TOM20 expression in SN we used 6 regularly spaced 20 µm-thick sections spanning the entire SNpc. Free-floating sections were incubated in 10% methanol (Panreac, Ref. 131091), 3% H_2O_2 (Sigma-Aldrich, Ref. H1009) in TBS (100 mM TrisBase and 150 mM NaCl) for 5 min at RT. Since both antibodies are raised on mouse, we used the Vector® M.O.M™ Immunodetection kit (Vector Laboratories, Ref. BMK-2202) according to manufacturer's instructions. Briefly, tissues were incubated in M.O.M Mouse Ig Blocking

Reagent for 1h at RT and then incubated overnight at 4ºC with primary antibodies anti-Tim23 and anti-Tom20 diluted in M.O.M diluent. Sections were incubated with anti-mouse biotinylated secondary antibody diluted in M.O.M diluent for 1h at RT, followed by signal amplification using the avidin-biotin complex (ABC Standard, Thermo Fisher, Ref. 32020) method. For developing we used 3,3'-diaminobenzidine tetrahydrochloride (DAB Enhanced, Sigma-Aldrich, Ref. 3939). Sections were mounted onto superfrost ultra plus slides (Menzel-Gläser, Ref.10417002) and air-dried overnight at RT. Slides were dehydrated by a short sequential incubation with ethanol 70%, ethanol 95%, ethanol 100% and xylene (Panreac, Ref. A2476), and coverslips (24x60mm, Menzel-Gläser, Ref. 781753) were mounted with DPX (Sigma, Ref. 06522).

3.8.2 Tyrosine hydroxylase-immunostaining in SN and Striatum

To assess tyrosine hydroxylase (TH) expression in SN we used 12 regularly spaced 30 µm-thick sections spanning the entire SNpc, while for striatum we used 4 representative 30 µm-thick sections covering different striatal anatomical levels. Tissue was incubated for 5 min in 10% methanol, 3% H_2O_2 in TBS prior to blocking with 5% normal goat serum (Vector Laboratories, Ref. S100) in TBS for 1h at RT. Sections were incubated with anti-TH antibody at 1:2000 for SN and 1:5000 for striatum in 2% normal goat serum in TBS for 48h in agitation at 4^{o}C. Then, anti-rabbit biotinylated secondary antibody was applied, diluted in 2% normal goat serum in TBS at 1:1000 for SN and at 1:2000 for striatum for 1h at RT, followed by signal amplification using the avidin-biotin complex (ABC Standard for SN and ABC Ultra-sensitive Plus for striatum, Thermo Fisher, Ref. 32050) method. For developing we used 3,3'-diaminobenzidine tetrahydrochloride (DAB Enhanced). Sections were mounted onto superfrost ultra plus slides and air-dried overnight at RT. Slides were dehydrated by a short sequential incubation with ethanol 70%, ethanol 95%, ethanol 100% and xylene, and coverslips were mounted with DPX. For SN, we performed a Nissl counterstaining with Cresyl Violet (Sigma-Aldrich, Ref. C5042) for 10 minutes prior to the dehydration step.

3.8.3 Quantitative morphology

To assess the integrity of the nigrostriatal pathway, we quantified TH-positive neurons and fibers in the SNpc and striatal immunostained sections (Bové et al., 2014; Perier et al., 2007; Recasens et al., 2014).

3.8.3.1 TH-positive striatal fibers

Striatal TH innervation was assessed by optical densitometry (OD) in 4 representative sections of the striatal volume (**Fig. 19**). Sections were scanned in an Epson Perfection V750 PRO scanner and Sigma Scan software (Systate Software, Inc) was used to quantify the grey intensity in the striatum (Str) compared to the blank, which in our case was represented by the cortex (Ctx). In this way, OD was assessed with the formula OD=-log (Istr/Ictx).

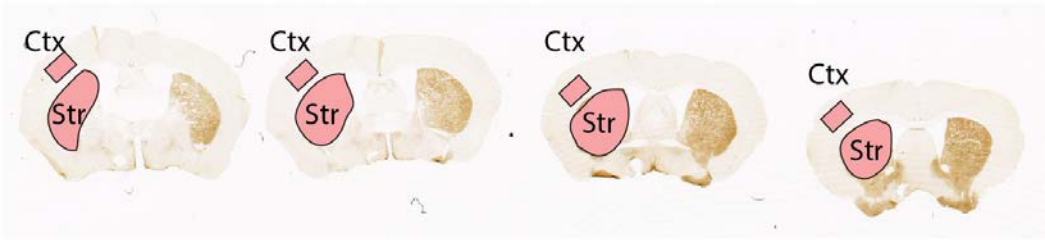

Figure 19. TH-immunohistochemistry in 4-regularly spaced 30 µm-thick sections corresponding to different striatal anatomical levels.

Ctx, cortex; Str, Striatum.

3.8.3.2 TH-positive SNpc neurons

To assess the total number of TH-positive SNpc neurons, we used stereology in 12 regularly spaced 30 µm-thick sections covering the entire SNpc. For such, we used the StereoInvestigator software (MBF Bioscience) where we delineated the SNpc for each slide (**Fig. 20**) and probes for stereological counting were applied to the map obtained (size of counting frame was 50x50 µm spaced 125x100 µm) using a Zeiss Axio Imager D1 microscope (Carl Zeiss Microscopy).

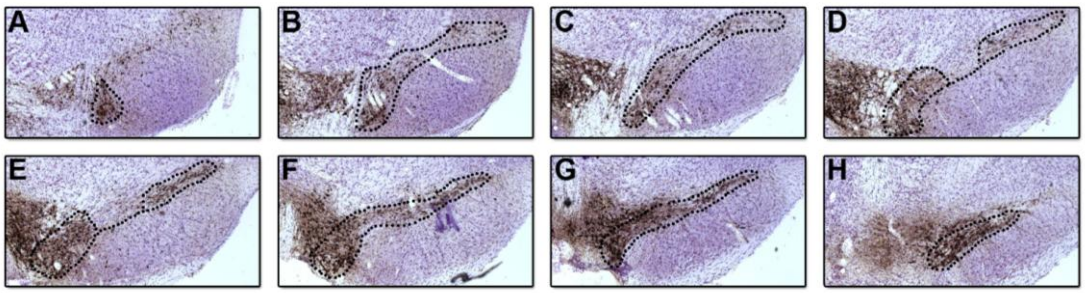

Figure 20. Coronal sections across the entire SNpc from caudal (A) to rostral (H).

Photomicrograph in (**A**) corresponds to the first caudal section to consider for stereology counting. The interval between each section corresponds to a fourth section interval. The brown colour represents TH-positive neurons and the purple colour, the Nissl staining.

Each TH-positive cell that had its nucleus included within the counting frame was counted (**Fig. 21**). Using the optical fractionator method, we estimated the total number of TH-positive cells in the SNpc of each hemisphere.

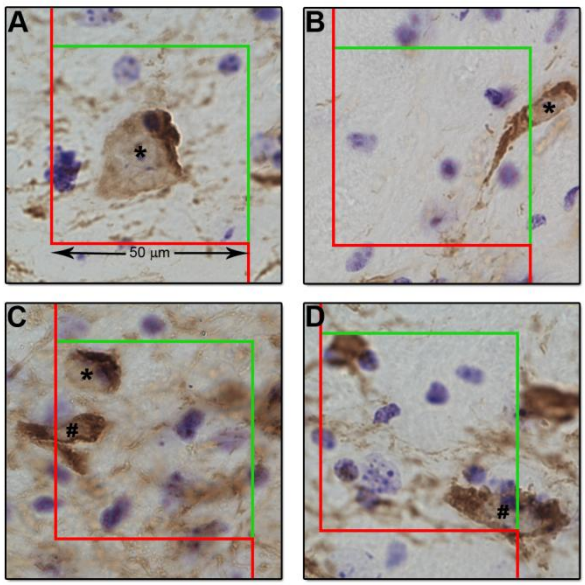

Figure 21. Stereological counting using optical fractionator.

(**A-D**) Illustrate the way we count TH-positive cells with a bicolour 50 µm-squared counting frame. Every nucleus of TH-positive cell inside the counting frame (asterisk in **A** and **C**) or touching the green line (asterisk in **B**) has to be count. Every nucleus of TH-positive cell touching the red line (pound sign in C) has to be excluded from the counting. (**D**) If the nucleus of TH-positive cell crosses both, green and red lines, the cell has to be excluded (pound sign in **D**).

3.9 Immunofluorescence in tissue

Immunostaining was performed on 20 or 30 µm-thick free-floating sections. Tissue sections were incubated with blocking solution containing 5% normal goat serum and 0.1% triton x-100 (Sigma, Ref. T9284) in PBS for 1h at RT. Then, sections were incubated with the corresponding primary antibodies in 2% normal goat serum and 0.1% triton x-100 in PBS

overnight at 4^{o}C and with the corresponding secondary Alexa antibodies for 1h at RT. For nuclei staining Hoechst 33342 (Invitrogen, Ref. H3570) was used at 1:20000 dilution in PBS for 10 min. Sections were mounted onto superfrost ultra plus slides using DAKO Fluorescent Mounting Medium (DAKO, Ref. S3023).

Images were acquired using an Olympus BX61 fluorescence microscope connected to a Olympus DP70 camera and cellSens software (Olympus Corporation) or using an Olympus FV1000 confocal microscope connected to FV 4.1 software (Olympus Corporation). We created ROIs corresponding to TH-positive neurons, in which we analyzed COX IV intensity using ImageJ 1.50a (National Institutes of Health, USA).

3.10 Immunofluorescence in cells

Cells were seeded in 16 mm of diameter coverslips (Menzel Gläser, Ref. #1). Cells were fixed in 4% paraformaldehyde for 30 minutes at RT. Following the incubation with blocking solution containing normal goat serum 3%, triton x-100, 0.1% in PBS for 1h at RT, the corresponding primary antibodies were used diluted in the same blocking solution overnight at 4^{o}C. Then, cells were incubated 1h at RT with the corresponding Alexa secondary antibodies, diluted in blocking solution. Nuclei were stained with 10 µM Hoechst 33342 in PBS for 10 min at RT. Slides were mounted onto superfrost ultra plus slides using DAKO Fluorescent Mounting Medium. Images were acquired using an Olympus FV1000 confocal microscope. Intensity analysis was performed by drawing a ROI to each cell and measuring its intensity using ImageJ 1.50a. When immunofluorescence analysis was performed on TIM23 and TOM20 transient transfected cells, intensity was only measured in those cells overexpressing TIM23 or TOM20.

Colocalization analysis of LAMP1-mitochondria was done with single cells quantifying the overlapping signal of LAMP-1 and Mitotracker in the cytosol area. For such, we used the Pearson's correlation coefficient and the percentage of lysosomes that were positive for mitochondria by using ImageJ 1.50a software. At least 50 single cells were quantified in each condition.

3.11 Immunoblot

Human, mouse and cellular protein extracts homogenized in RIPA buffer were sonicated and heated at 95^{o}C for 5 min after adding loading buffer 6x containing Tris 500 mM, 30% glycerol (Sigma-Aldrich, Ref. G5516), 10% SDS and 0.6 M DTT (Roche, Ref. 10708984001). Proteins were resolved by SDS-PAGE on different percentage of polyacrylamide gels, ranging from 7% to 15% and run around 90 min at 120V in running buffer (25 mM Trizma R Base, 192 mM glycine and 1% SDS, Sigma-Aldrich, Ref. T6066, G7126 and L3771, respectively). Protein All Blue Standards ladder (Biorad, Ref. 161-0373) was used as a ladder. Resolved proteins were transferred onto nitrocellulose membranes (GE Healthcare, Ref. 10600002) during 90 minutes at 200 mA per gel in transfer buffer (25mM Trizma R Base, 192mM glycine and 20% methanol) and then blocked with 5% non-fat milk powder (Sigma-Aldrich, Ref. 70166) in PBS for 1h at room temperature. Membranes were incubated with the corresponding primary antibodies diluted in 4% bovine serum albumin (Sigma-Aldrich, Ref. A4503) in PBS overnight at 4^{o}C. Then, we proceeded to the incubation with the corresponding secondary antibodies coupled with horseradish peroxidase and diluted in 5% milk in PBS for 1h at RT. Finally, proteins were visualized using either West Pico SuperSignal Substrate or SuperSignal West Femto (Thermo Fisher, Ref. 34080 and 34095, respectively) on an ImageQuant RT ECL imaging system (GE Healthcare). Immunoblots were quantified by densitometry using ImageJ 1.50a.

3.12 mtDNA copy number

3.12.1 Cells

BE(2)-M17 cells were trypsinized, centrifuged at 300 g for 5 minutes. The pellet was washed with PBS and centrifuged again at 300g for 5 minutes. After the addition of Proteinase K (Sigma-Aldrich, Ref. P2308), purification of total (genomic and mitochondrial) DNA was performed using the QIAamp DNA Mini Kit (Qiagen, Ref. 51306) according to manufacturer's instructions. Total DNA concentration was measured using a Nanodrop 1000 and diluted at 100 ng/µL in distilled H_2O.

To quantify mtDNA content, we analysed relative mtDNA (*12S* rRNA gene) versus nuclear DNA (*RNaseP* single copy gene) copy number. The sequences for 12S primers were: 5'-CCACGGGAAACAGCAGTGAT-3' (forward) and 5'-CTATTGACTTGGGTTAATCGTGTGA-3' (reverse) and the FAM-labeled probe sequence was FAM-5'-TGCCAGCCACCGCG-3'-

MGB. For RNAseP we used a commercial assay RNAseP Control Reagent VIC-TAMRA (Applied Biosystems Ref. 4316849). A standard curve with cloned-12S and RNAseP amplicons was used for absolute quantification of mtDNA and nuclear DNA in the samples. Real-time PCR was performed on an ABI PRISM 7900HT and SDS version 2.2 software using Taqman Universal Master Mix II with UNG.

3.12.2 Tissue

Ventral midbrain tissue was used for purification of total (genomic and mitochondrial) DNA with the QIAamp DNA Mini Kit (Qiagen, Ref. 51306) according to manufacturer's instructions. Total DNA concentration was measured using a Nanodrop 1000 and diluted at 100 ng/µL in distilled H_2O.

To quantify mtDNA content, we analysed relative mtDNA (*16S* rRNA gene and *ND4* gene) versus nuclear DNA (*ANG1* gene) copy number. The sequences for 16S primers were: 5'-AATGGTTCGTTTGTTCAACGATT-3' (forward) and 5'-AGAAACCGACCTGGATTGCTC-3' (reverse) and the FAM-labeled probe sequence was 5'-FAM-AAGTCCTACGTGATC TGAGTT-MGB-3'. The sequences for ND4 primers were: 5'-TGCATCAATCATAATCCAA ACTCCATGA -3' (forward) and 5'-GGCAGAATAGGAGTGATGATGTGA-3' (reverse) and the VIC-labeled probe sequence was 5'-VIC-CCGACATCATTACCGGGTTTTCCTCTTG-3' Tamra. For ANG1 we used a commercial assay A (Applied Biosystems Ref. Mm00833184_s1). A standard curve with cloned-16S, ND4 and ANG1 amplicons was used for absolute quantification of mtDNA and nuclear DNA in the samples. Real-time PCR was performed on an ABI PRISM 7900HT and SDS version 2.2 software using Taqman Universal Master Mix II with UNG.

3.13 Mitochondrial enrichment

Mitochondria were isolated from BE(2)-M17 cells as previously described on Frezza *et al*. (Frezza et al., 2007). Briefly, cells were washed once with PBS and detached them using a cell scraper. Cell suspension was centrifuged at 600g at 4^{o}C for 5 min and the supernatant was discarded. Pellet was resuspended in ice-cold IBc buffer (10 mM Tris-MOPS (Sigma, Ref. M5162), 1mM EGTA/Tris (Sigma, Ref. E4378) and 0.2 M sucrose in H_2O at pH 7.4). To homogenize we used a Teflon pestle operated at 1600 rpm and stroked the cell suspension placed in a glass potter during 30-40 times. Cell suspension was centrifuged at 600g for 10

min at 4^{o}C and the supernatant was further centrifuged at 7000g for 10 min at 4^{o}C. Pellet was washed with ice-cold IBc buffer and centrifuged again at 7000g for 10 min at 4^{o}C. Finally, the pellet containing mitochondria was resuspended in an adequate volume of IBc buffer. Next, we determined the mitochondrial protein concentration by the bicinchoninic assay method with BSA as a standard protein.

3.14 Mitochondrial protein aggregation

For assessing the presence of insoluble proteins in mitochondria, we resuspended the isolated mitochondria at a final concentration of 1mg/mL in lysis buffer containing 25mM Tris-HCl at pH 7.4, 300mM NaCl, 5mM EDTA, proteases inhibitors and 1mM PMSF. An equal volume of lysis buffer containing 1% Nonidet P-40 was added to mitochondrial dilution. Samples were incubated on ice during 10 min and then, centrifuged at 20.000g for 30 min at 4^{o}C. We collected both the supernatant, which is the soluble fraction, and the pellet, which represents the NP-40-insoluble aggregate. The insoluble fraction was washed with PBS and centrifuged again at 20.000g for 15 min at 4^{o}C. The pellet was resuspended in loading buffer 4x containing blue 4x (100 mM Tris, 30% glycerol, 4% SDS and 0.2% bromophenol blue, Sigma-Aldrich Ref. B6131), 25 mM DTT in running buffer and both soluble and insoluble fractions were separated on 15% SDS-PAGE gels for western blot analysis using Total OXPHOS antibody. This protocol was adapted from Moisoi *et al* (Moisoi et al., 2009a).

3.15 Membrane potential

BE(2)-M17 cells were seeded in 12-well plates and, upon 80% confluence, treated with either vehicle or MPP^{+} at 1 mM for 24h. Cells were washed twice with pre-warmed PBS and TMRM probe (reconstituted in DMSO, Life Technologies, Ref. C6827) was added to the medium at 1 µM and incubated for 30 min in cell incubator. Cells were washed twice with pre-warmed PBS and recollected with a cell scraper in medium. Using a FACSAria flow cytometer (BD Biosciences) 10.000 cells were acquired and fluorescence was read at 561 nm laser with 582/15 emission filter. Membrane potential was analyzed as mean fluorescence intensity (MFI) and represented either as MFI or as fold change compared to the corresponding controls using the FCS Express (v3 De Novo Software^{TM}).

3.16 Mitochondrial pOTC import assay

Human ornithine transcarbamylase (OTC) precursor cDNA in pGEM-3Zf(+)-pOTC plasmid was transcribed and translated in vitro using the TNT-coupled reticulocyte lysate system (Promega) in the presence of l-[35S]methionine (PerkinElmer). Following translation, [35S]methionine-labeled pOTC was incubated with isolated mitochondria at 37°C for the indicated times, and mitochondria containing imported OTC were collected by centrifugation at 9,000g for 10 min and subjected to SDS-PAGE. The radioactive polypeptides on the gel were visualized using a Personal Molecular Imager FX (Biorad). Cleaved mature OTC (mOTC), which represents the completion of import into the mitochondrial matrix and migrates faster than pOTC on SDS-PAGE, was quantified using ImageJ 1.50. The data are presented as the percentage of mOTC compared to total [35S]pOTC.

3.17 Seahorse XF24 mitochondrial respiration analysis

Oxygen consumption rate (OCR) was measured using the Seahorse XF24 equipment (Seahorse bioscience Inc., North Billerica, MA, USA). ST-Q7 and ST-Q111 cells were seeded in Seahorse XF24 Cell Culture Microplate (Seahorse Biosciences, Ref. 100777-004). Striatal cells were seeded on XF24 microplates and differentiated and treated with the corresponding treatments. Cells were rinsed once and incubated in 700 µl of XF assay buffer (DMEM without $NaHCO_3$, 2 mM glutamax; pH 7.4, 5 mM glucose, 1 mM sodium pyruvate), then equilibrated for 1 h at 37°C in a non-CO_2 incubator. All medium and solutions of mitochondrial complex inhibitors were adjusted to pH 7.4 on the day of assay. Following three baseline measurements of OCR, mitochondrial complex inhibitors were sequentially injected into each well. Three OCR readings were taken after addition of each inhibitor and before automated injection of the subsequent inhibitor. Mitochondrial complex inhibitors, in order of injection, included oligomycin (1 µM) to inhibit complex V (i.e., ATP synthase), CCCP (0.5 µM each time) to uncouple the proton gradient, antimycin A (1.0 µM) to inhibit complex III, and rotenone (1.0 µM) to inhibit complex I. OCR were automatically calculated, recorded, and plotted by Seahorse XF24 software version 1.8 (Seahorse Bioscience, Billerica, MA, USA). At the end of each assay, cells were washed once with an excess of RT DPBS, lysed with ice-cold RIPA buffer and the protein content estimated by the bicinchoninic assay method with BSA as a standard protein.

3.18 Cell death

3.18.1 Cell death analysis using MTT

Cell death was analyzed using the MTT Cell Proliferation Assay (ATCC bioproducts, Ref. 30-1010K) following manufacturer's instructions. $3x10^3$ BE(2)-M17 cells were seeded in 96-well plates and, upon 80% confluence, treated with either vehicle or different MPP^+ concentrations for 24h. 10 µL of MTT Reagent was added to each well and the plate was further incubated for 3h at 37°C in humidified 95% air/5%CO_2 incubator. When the purple precipitate is visible, 100 µL of Detergent reagent was added to all wells and the plate was swirled gently and left in the dark for 3h. MTT is reduced by metabolically active cells generating an intracellular purple formazan that can be quantified by spectrophotometric means at 590 nm absorbance in an spectrophotometer (ELx800, Biotek Instruments, Inc.).

3.18.2 Cell death analysis using propidium iodide

Cell death was analyzed as number of propidium iodide positive cells. All measurements and analyses were performed using FACSAria flow cytometer. BE(2)-M17 cells were seeded in 12-well plates, transfected with hTIM23 or hTOM20 and treated with either vehicle or MPP^+ at 5 mM for 24h. Cells were detached and propidium iodide (Invitrogen, Ref. P3566) was added at 1:1000 dilution. Using a FACSAria flow cytometer 10.000 cells were acquired and fluorescence was read at 488 nm laser with 610/20 emission filter. Cell death was analyzed as the number of PI positive cells and represented as fold change compared to the corresponding controls using the FCS Express (v3 De Novo Software™).

3.19 ROS

3.19.1 Fluorometer analysis

BE(2)-M17 cells were seeded in 12-well plates and, upon 80% confluence, treated with either vehicle or MPP+ at 1 mM for 24h. Cells were washed twice with pre-warmed PBS and 10µM CM-H_2DCFDA probe (reconstituted in DMSO) was added in Opti-MEM medium and incubated for 30 min in cell incubator. Cells were washed twice with pre-warmed PBS and lysed using a cell lysis buffer containing 20 mM Tris-HCl, 150 mM NaCl, 1 mM Na_2EDTA, 1 mM Na_2EGTA and 1% of triton in H_2O. Plates were shaken at room temperature for 5

minutes. From each well, 50uL of cell lysate was loaded per triplicate into a 96-well black microplate (Corning Incorporated, Ref. 3631) and read immediately with 485/20 nm excitation and 528/20 nm emission wavelengths in the spectrofluorometer (FLx800, Biotek Instruments, Inc.). Fluorescence values were corrected with protein concentration and represented as fold change compared to the corresponding controls.

3.19.2 Flow cytometry analysis

Cells were seeded in 12-well plates and, upon 80% confluence, treated with the corresponding reagents. Cells were washed twice with pre-warmed PBS and either 50 μM of CM-H_2DCFDA probe or 50 μM CellROX was added in medium and incubated for 30 min in a cell incubator. Cells were washed twice with pre-warmed PBS and recollected with a cell scraper in medium. Using a FACSAria flow cytometer, 10.000 cells were acquired and fluorescence was read at 488 nm laser with 530/30 emission filter. ROS was analyzed as mean fluorescence intensity (MFI) and represented either as MFI or as a percentage compared to the corresponding controls using the FCS Express v3.

3.19.3 Immunofluorescence analysis

Cells were seeded in 16 mm of diameter coverslips and 5 μM of CellROX was added in medium and incubated for 30 min in a cell incubator. We followed the same protocol as the one for immunofluorescence. Images were acquired using an Olympus FV1000 confocal microscope.

3.20 Proximity Ligation Assay (PLA)

PLA was performed in 3% formaldehyde-fixed cells (Sigma Aldrich, Ref. F1635) following manufacturer's instructions. Briefly, samples were blocked for 30 min at RT and incubated with specific primary antibodies overnight. Secondary antibodies anti-mouse PLUS and anti-rabbit MINUS conjugated with oligonucleotides were added to the reaction (Duolink PLA Probe anti-mouse PLUS and anti-rabbit MINUS, Duolink, Sigma Aldrich, Ref. DUO92001 and DUO92005 respectively) and incubated for 1h at 37^{o}C. Ligation reagents were added and incubated for 30 min at 37^{o}C. If the two PLA probes are close enough, a closed oligonucleotide circle will be generated. Amplification solution, containing nucleotides and

fluorescently labeled oligonucleotides, and polymerase were added and incubated for 100 min at 37^{o}C. The oligonucleotide arm of one of the PLA probes acts as a primer for rolling-circle amplification reaction using the ligated circle as a template. This generates a concatemeric product where the fluorescently labeled oligonucleotides will hybridize (Detection Reagent RED, Duolink, Sigma Aldrich, Ref. DUO92008). The proximity ligation signal is observed as fluorescence spots and was analysed by confocal microscopy using an Olympus FV1000 confocal microscope. The corresponding control experiments were performed under identical experimental conditions. Quantification was performed by analyzing the number of dots per cell and the area fraction that these dots occupy per cell using ImageJ 1.50a.

3.21 Immunoprecipitation

ST-Q7 and ST-Q111 cells seeded in 6-well plates, upon 80% confluence, were recollected in PBS using a cell scraper and centrifuged at 800g at 4^{o}C for 5 min. Pellet was resuspended in IP buffer containing 0.01% triton x-100 in PBS and protease inhibitors (Thermo Scientific, Ref. 78415). 1:2 mixture of Dynabeads® protein A and protein G (Thermo Scientific, Ref. 10001D and 10003D, respectively) was incubated with the corresponding antibody, together with 5 mM BS^{3} (bis(sulfosuccinimidyl)suberate, Sigma Aldrich, Ref. S5799), to crosslink the antibody to the Dynabeads®, in IP buffer and let rocking 30 min at RT. The supernatant was discarded using a magnetic particle concentrator (DynaMag^{TM}-2, Invitrogen, Ref. 4211) and BS^{3} was inactivated with 50mM Tris-HCl pH 7.4 for 15 min. Dynabeads® were washed three times with IP buffer and incubated with the corresponding cell lysate for 90 min at 4^{o}C. For elution, samples were incubated in elution buffer containing 0.2 M glycine pH 2.5, LB6x and 16 mM DTT 10 min at 70^{o}C. Immunoprecipitates or whole-cell extracts were analyzed by standard immunoblotting.

3.22 Statistical analysis

The values were expressed as the mean ± standard error of the mean (SEM). The significant differences (*p<0.05, **p<0.01, ***p<0.001) when comparing two groups were determined by a two-tailed unpaired Student's t test. When comparing more than two groups, significant differences were determined by one-way or two-way ANOVA followed by Tukey's post hoc test. Statistical analyses were performed using GraphPad Prism 6.

RESULTS

4 Results

4.1 Chapter I: PD and mitochondrial protein import

4.1.1 Mitochondrial protein import deficiency in human substantia nigra in PD.

Mitochondrial proteome is mostly encoded by the nuclear DNA, thereby mitochondrial proteins must be imported from the cytoplasm to the different mitochondrial compartments (Pfanner and Neupert, 1990). Some previous studies have linked α-synuclein to the mitochondrial protein import machinery (Bender et al., 2013; Devi et al., 2008b). To test the possibility that mitochondrial protein import was impaired in the context of PD, we analyzed the expression levels of two nuclear-encoded mitochondrial proteins, NADH (reduced form of nicotinamide adenine dinucleotide)–ubiquinone oxidoreductase core subunit S3 (NDUFS3) and cytochrome c oxidase subunit IV (COX IV) by immunoblotting. NDUFS3 protein levels were decreased in SN protein homogenates from PD patients compared to age-matched controls, while COX IV protein levels had a tendency to decrease, though not significant (**Fig. 22A**). These results are in agreement with a previous work in which they reported decreased NDUFS3 immunofluorescence intensity in substantia nigra sections from PD patients (Di Maio et al., 2016). To further determine whether mitochondrial protein import machinery was impaired in the SN of PD patients, we then analyzed the expression of TIM23 and TOM20 in *post-mortem* samples from PD patients and control individuals. Since the majority of the mitochondrial proteins reside in the mitochondrial matrix, they are imported through the TOM complex in the outer membrane and through the TIM23 complex in the inner membrane (Wiedemann and Pfanner, 2017). Thus, TIM23 and TOM20 protein levels are a good readout of the mitochondrial protein import. TIM23 and TOM20 protein levels were decreased in SN protein homogenates from PD patients compared to age-matched controls (**Fig. 22B**). All together, these results suggest an impairment of mitochondrial protein import in PD patients.

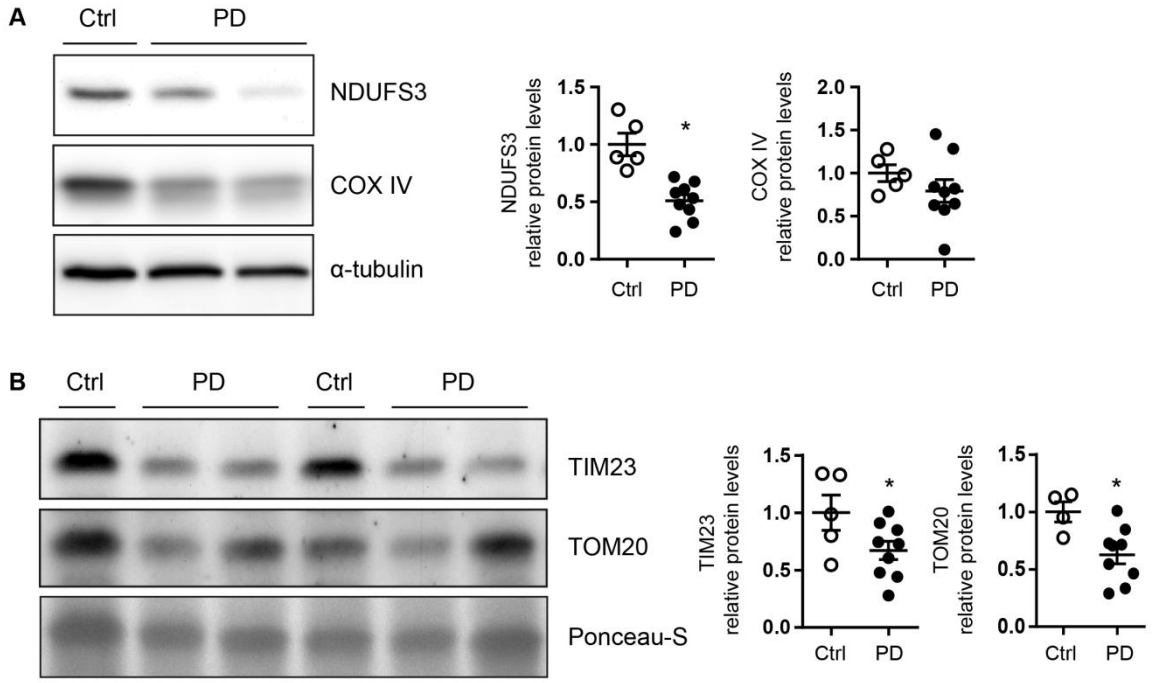

Figure 22. Mitochondrial protein import deficiency in human substantia nigra in PD.

(**A**) Representative immunoblots of COX IV, NDUFS3 and α-tubulin protein levels in substantia nigra homogenates from control (Ctrl, n=5) and PD patients (n=9). Protein levels were normalized relative to α-tubulin. (**B**) Representative immunoblots of TIM23 and TOM20 protein levels in substantia nigra homogenates from Ctrl (n=4-5) and PD patients (n=9). Protein levels were normalized relative to Ponceau-S. (**A-B**) Quantification is depicted as fold change to Ctrl. Data are presented as mean ± s.e.m. * P < 0.05 compared with Ctrl after unpaired Student's t test.

4.1.2 Complex I inhibition impairs mitochondrial protein import

The above data obtained in human *post-mortem* tissue suggest that mitochondrial protein import dysfunction is associated with dopaminergic cell death in PD. Yet, human *post-mortem* studies can hardly provide mechanistic clues for such hypothesis. To explore in more detail the functional significance of mitochondrial protein import dysfunction in dopaminergic cell death, additional experiments were performed in human dopaminergic BE(2)-M17 neuroblastoma cell line intoxicated with parkinsonian neurotoxin MPP^+, the active metabolite of MPTP (Dehay et al., 2010).

As similarly observed in human *post-mortem* tissue, TIM23 and TOM20 protein levels were decreased in cells treated with increasing MPP^+ concentrations (**Fig. 23A**). Reduced TIM23 protein levels were associated with a drop in the mRNA content, whereas TOM20 mRNA levels did not correlate with reduced protein levels (**Fig. 23B**), suggesting that different mechanisms regulate mitochondrial expression levels of both proteins.

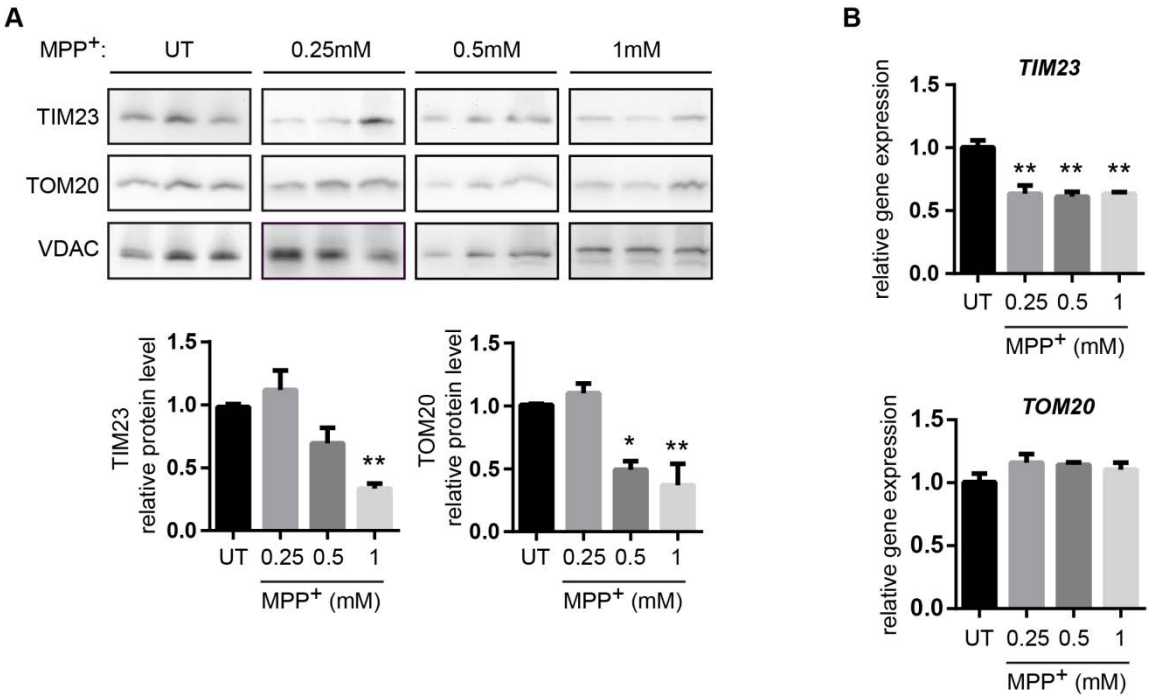

Figure 23. Complex I inhibition leads to a decrease in translocases levels.

(**A**) Representative immunoblots of TIM23, TOM20 and VDAC protein levels in BE(2)-M17 cells untreated (UT) or treated with MPP^+ (0.25 mM, 0.5 mM or 1 mM, 24h). Protein levels were normalized relative to VDAC (n=3 independent experiments). (**B**) *TIM23* and *TOM20* gene expression in BE(2)-M17 cells UT or treated with MPP^+ (0.25 mM, 0.5 mM or 1 mM, 24h). Gene expression levels were normalized relative to *RPLP0* (n=3 independent experiments). (**A-B**) Quantification is depicted as fold change to UT condition. Data are presented as mean ± s.e.m. * $P < 0.05$, ** $P < 0.01$ compared with UT condition after one-way ANOVA test followed by Tukey's post hoc test.

To study mitochondrial protein import dysfunction in BE(2)-M17 dopaminergic cells upon complex I inhibition, we used (i) confocal imaging and immunoblotting of mitochondrially targeted GFP (mitoGFP), (ii) a direct assay of mitochondrial protein import in isolated mitochondria, and (iii) confocal measurements of mitochondrial localization of endogenous, nuclear-encoded, and imported proteins NDUFS3 and COX IV. Initial characterization of mitochondrial protein import upon complex I inhibition was performed using mitoGFP. This construct contains a mitochondrial-targeting sequence that has to be cleaved inside the mitochondria in order to release the mature fluorescent protein. MitoGFP intensity levels appeared decreased in the mitochondria of transfected cells following MPP^+ intoxication at 1 mM (**Fig. 24A**). Processing of mitoGFP inside mitochondria leads to a slight drop in its molecular weight, thus making the precursor and the mature protein distinguishable by immunoblotting. Decreased mitoGFP fluorescence intensity in MPP^+-intoxicated cells corresponded to a reduction in the mitoGFP intra-mitochondrial processing by ~35%, as

quantified by western blot analysis (**Fig. 24B**). These results suggest that mitochondrial import of proteins containing a mitochondrial-targeting sequence is impaired upon complex I inhibition. To address whether MPP^+ directly inhibits mitochondrial protein import machinery, we used the classical biochemical approach for analyzing protein import (Mokranjac and Neupert, 2007; Stojanovski et al., 2017). This method consists on isolating mitochondria and assessing mitochondrial protein import *in organello* using radio-labeled human ornithine transcarbamylase (OTC). In this system, MPP^+ intoxication inhibited import by 50% as observed by the reduction in the mature OTC form (**Fig. 24C**). To study the impact of mitochondrial protein import deficiency in endogenous mitochondrial proteins, we examined the levels of nuclear-encoded, mitochondrially targeted NDUFS3 and COX IV, and found a decrease in both imported proteins after MPP^+ treatment (**Fig. 24D**). We also report that mitochondrial mass, reflected by mtDNA copy number, did not change in MPP^+-treated cells (**Fig. 24E**). We conclude that the import activity deficiency is not caused by a diminution of mitochondrial mass, but rather due to an intrinsic defect inside each mitochondrion.

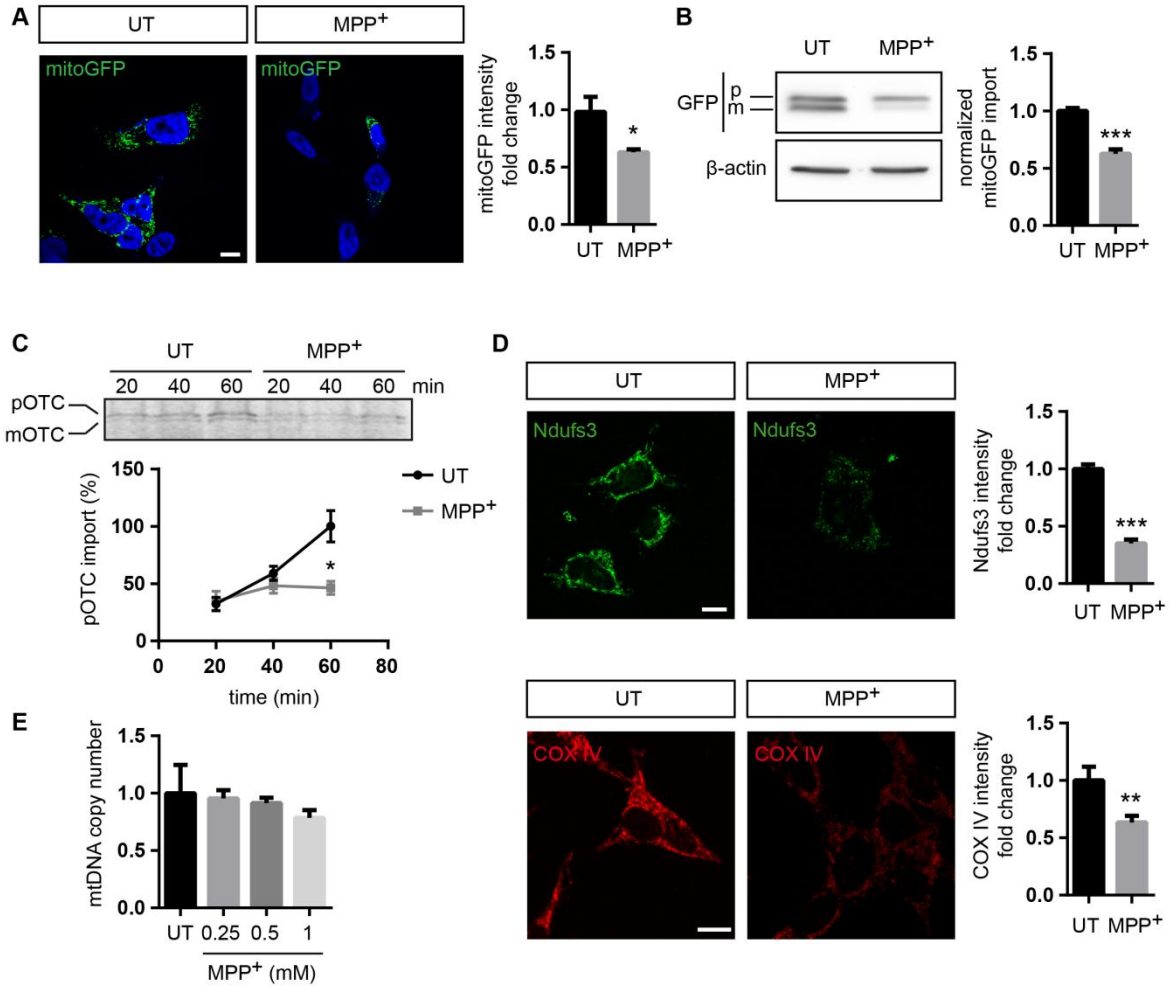

Figure 24. Complex I inhibition impairs mitochondrial protein import activity.

(**A**) Representative images of mitoGFP-transfected BE(2)-M17 cells untreated (UT) or treated with MPP^+ (1 mM, 24h, n= 3 independent experiments). Quantification is depicted as the fold change of mitoGFP intensity per cell compared with UT condition. A minimum of 35 cells were analyzed per condition. Scale bar: 10 µm. (**B**) Representative immunoblots of GFP and β-actin protein levels in BE(2)-M17 cells UT or treated with MPP^+ (1 mM, 24h). mitoGFP import was calculated as the ratio of mature (m) GFP compared to the sum of precursor (p) and mature GFP (total GFP; n=5 independent experiments). (**C**) Representative immunoblots of radiolabelled OTC in isolated mitochondria UT or treated with MPP^+ (1 mM) at different time points. pOTC import was calculated as the percentage of mature (m) OTC compared to the sum of precursor (p) and mature OTC (n=3 independent experiments). (**D**) Representative images of NDUFS3 and COX IV immunofluorescence in BE(2)-M17 cells UT or treated with MPP^+ (1 mM, 24h). Quantification is represented as the fold change in NDUFS3 or COX IV intensity compared with UT condition. A minimum of 35 cells were analyzed per condition. Scale bar: 10 µm. (**E**) Quantification of mitochondrial DNA (mtDNA) copy number in BE(2)-M17 cells UT or treated with MPP^+ (0.25 mM, 0.5 mM and 1 mM, 24h, n=3 independent experiments). mtDNA copy number was measured by quantitative RT-PCR and expressed as the ratio of mtDNA (*12S* copy number) to nuclear DNA (*RNAseP* copy number). (**A-E**) Quantification is depicted as fold change to UT condition. Data are presented as mean ± s.e.m. * $P < 0.05$, ** $P < 0.01$, ***$P < 0.001$ compared with UT condition after (**A-D**) unpaired Student's t test, (**E**) one-way ANOVA test followed by Tukey's post hoc test.

MPP^+-induced cell death occured at the highest dose of MPP^+ used (5 mM, **Fig. 25**). Interestingly, decreased levels of TIM23 and TOM20, as well as mitochondrial import inhibition, occured at a lower MPP^+ concentration (1 mM), suggesting that mitochondrial import inhibition might be instrumental in the demise of dopaminergic neurons in PD. All together, these results demonstrate that complex I inhibition impairs mitochondrial protein import in dopaminergic cells.

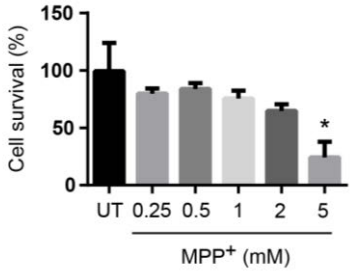

Figure 25. Complex I inhibition leads to a dose-dependent cell death.

In vitro sensitivity of BE(2)-M17 cells to increasing MPP^+ concentrations for 24h (n=4 independent experiments). Cell survival was determined by MTT assay. Quantification is depicted as the % of cell survival relative to UT condition. Data are presented as mean ± s.e.m. * $P < 0.05$ compared with UT condition after one-way ANOVA test followed by Tukey's post hoc test.

4.1.3 Complex I inhibition leads to a decrease in OXPHOS protein levels and protein aggregation inside mitochondria

To determine the consequences of mitochondrial protein import impairment following MPP^+ intoxication, we first assessed the protein levels of various OXPHOS subunits, as the majority of them are encoded both by the nuclear and the mitochondrial genome. We analyzed NADH:ubiquinone oxidoreductase subunit B8 (NDUFB8, complex I), succinate dehydrogenase complex iron sulfur subunit B (SDHB, complex II), ubiquinol-cytochrome c reductase core protein 2 (UQCRC2, complex III) and ATP synthase F1 subunit alpha (ATP5A, complex V), which are nuclear-encoded, while cytochrome c oxidase subunit II (COX II, complex IV) is encoded by the mtDNA (Larsson, 2010). Upon MPP^+ intoxication, we found a downregulation of all the proteins, except ATP5A (**Fig. 26A**). We further assessed the consequences of mitochondrial import impairment following complex I inhibition, and we observed that MPP^+-treated cells exhibited an enrichment in detergent-insoluble mitochondrial proteins SDHB and ATP5A (**Fig. 26B**), indicating an increase of aggregated intra-mitochondrial proteins. The observed increase of aggregated intra-mitochondrial proteins may be due to (i) an imbalance of OXPHOS subunits stoichiometry due to the import deficit or, (ii) an impairment of intra-mitochondrial protein quality control system. Interestingly, MPP^+-treated cells exhibited a transcriptional activation of mitochondrial chaperones *CLPX* and *HSP9* (**Fig. 26C**), which was not observed at protein levels (**Fig. 26D**), suggesting that import defects might impair the translocation of chaperones of mtUPR into the mitochondria and the subsequent mtUPR activation (Haynes and Ron, 2010). These results indicate that mitochondrial protein import deficiency and intra-mitochondrial protein aggregation occur in an *in vitro* paradigm of PD, below the toxic threshold (5 mM MPP^+), thus suggesting that occur prior to cell death (**Fig. 25**). These findings set the stage to study whether restoration of mitochondrial protein import can attenuate mitochondrial dysfunction and cell loss in this pathological situation.

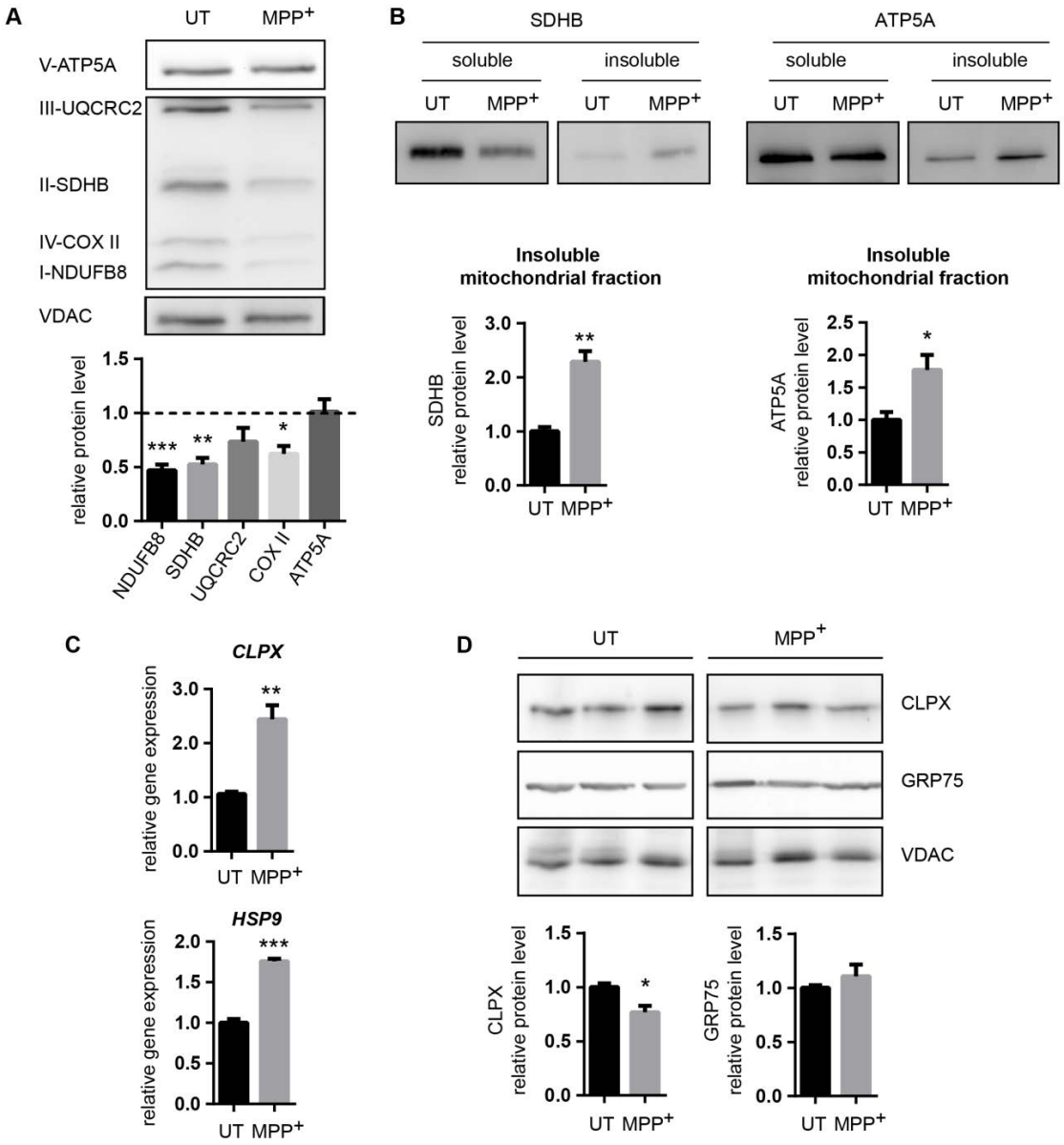

Figure 26. Complex I inhibition leads to a decrease in OXPHOS protein levels and protein aggregation inside mitochondria.

(**A**) Representative immunoblots of ATP5A (complex V), UQCRC2 (complex III), SDHB (complex II), COX II (complex IV), NDUFB8 (complex I) and VDAC protein levels in BE(2)-M17 cells untreated (UT) or treated with MPP^+ (1 mM, 24h). Protein levels were normalized relative to VDAC (n=3 independent experiments). (**B**) Representative immunoblots of SDHB and ATP5A protein levels in soluble and insoluble mitochondria-isolated fractions of BE(2)-M17 cells UT or treated with MPP^+ (1 mM, 24h, n=3 independent experiments). (**C**) *CLPX* and *HSP9* gene expression in BE(2)-M17 cells UT or treated with MPP^+ (1 mM, 24h). Gene expression levels were normalized relative to *RPLP0* (n=3 independent experiments). (**D**) Representative immunoblots of CLPX and GRP75 protein levels in BE(2)-M17 cells UT or treated with MPP^+ (1 mM, 24h). Protein levels were normalized relative to VDAC (n=4 independent experiments). (**A-D**) Quantification is depicted as fold change to UT condition. Data are presented as mean ± s.e.m. * P < 0.05, ** P < 0.01, ***P < 0.001 compared with UT condition after unpaired Student's t test.

4.1.4 TIM23 or TOM20 overexpression restores mitochondrial protein import in dopaminergic cells.

Since TIM23 and TOM20 are integral parts of the transport machinery and were downregulated upon MPP^+-induced complex I inhibition, we first examined whether transient overexpression of either pCMV6-XL5-TIM23 (TIM23) or pCMV6-XL5-TOM20 (TOM20) could prevent the impairment of the import system. We focused on a mitochondrial endogenous protein which is not inhibited directly by MPP^+. Therefore, we performed immunofluorescence analysis of COX IV, a mitochondrial protein nuclearly encoded. Upon MPP^+ intoxication there is a ~40% decrease in COX IV immunofluorescence intensity (**Fig. 24D**). TIM23 overexpression prevented the decrease in COX IV immunofluorescence intensity induced by MPP^+ (**Fig. 27A**), indicating that MPP^+-induced impairment in protein import was prevented. TOM20 overexpression also preserved COX IV immunofluorescence intensity after MPP^+ toxicity, even at higher levels than control cells (**Fig. 27B**).

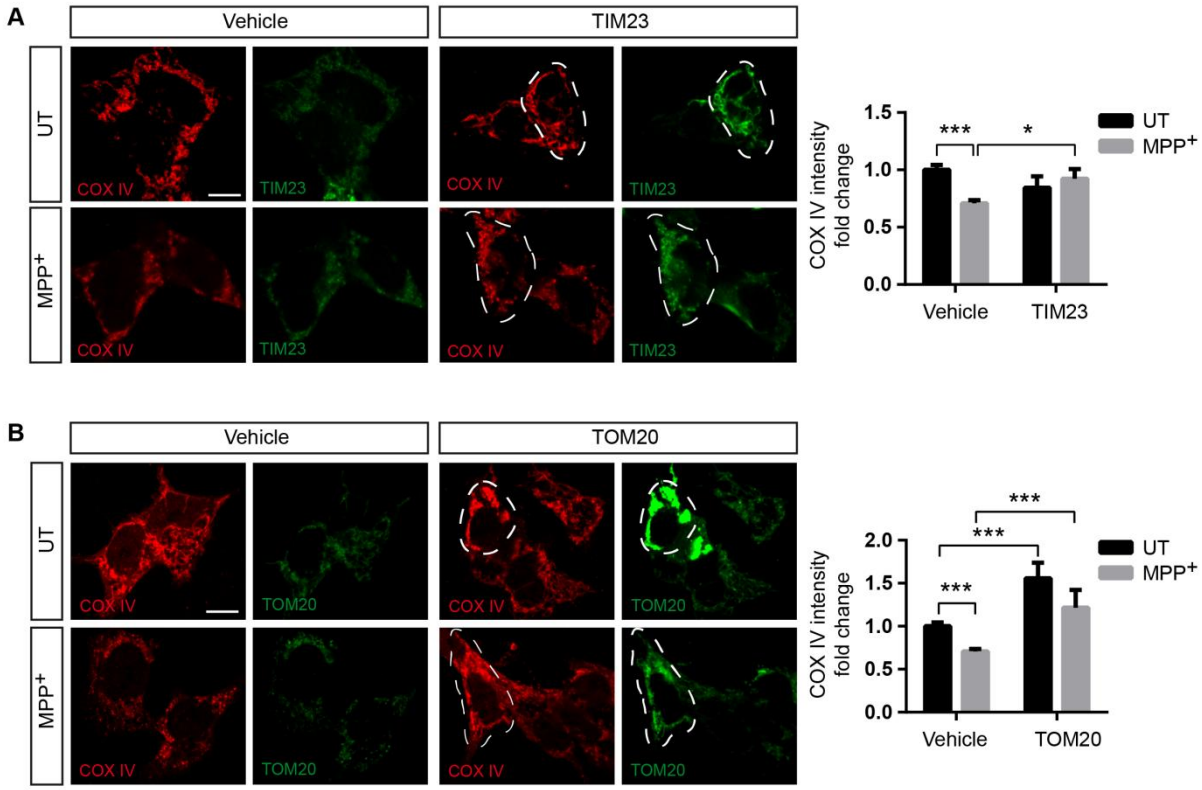

Figure 27. TIM23 or TOM20 transient overexpression restores mitochondrial protein import upon complex I inhibition in BE(2)-M17 cells.

(**A**) Representative images of COX IV and TIM23 immunofluorescence in vehicle- or pCMV6-XL5-TIM23 (TIM23)-transfected BE(2)-M17 cells untreated (UT) or treated with MPP^+ (1 mM, 24h). Quantification is depicted as the fold change in COX IV intensity compared with vehicle-transfected UT condition. Dashed line shows TIM23-overexpressing cells. Scale bar: 10 μm. (**B**) Representative

images of COX IV and TOM20 immunostained in vehicle- or pCMV6-XL5-TOM20 (TOM20)-transfected BE(2)-M17 cells UT or treated with MPP^+ (1 mM, 24h). Quantification is depicted as the fold change in COX IV intensity compared with vehicle-transfected UT condition. Dashed line shows TOM20-overexpressing cells. Scale bar: 10 μm. (**A-B**) Data are presented as mean ± s.e.m. * P < 0.05, ** P < 0.01, ***P < 0.001 after two-way ANOVA followed by Tukey's post hoc test.

Although TIM23 or TOM20 overexpression overcame COX IV downregulation after MPP^+ intoxication, mitoGFP experiments failed to show this effect. When we overexpressed mitoGFP together with TIM23 or TOM20 in a complex I-deficient environment, there was no restoration of mitoGFP intra-mitochondrial processing or mitoGFP intensity (**Fig. 28A and B**). This could be explained in part because of the differences in transfection efficiencies due to the transfection of two plasmids instead of one. Thus, TIM23 or TOM20 overexpression can restore mitochondrial import upon complex I inhibition.

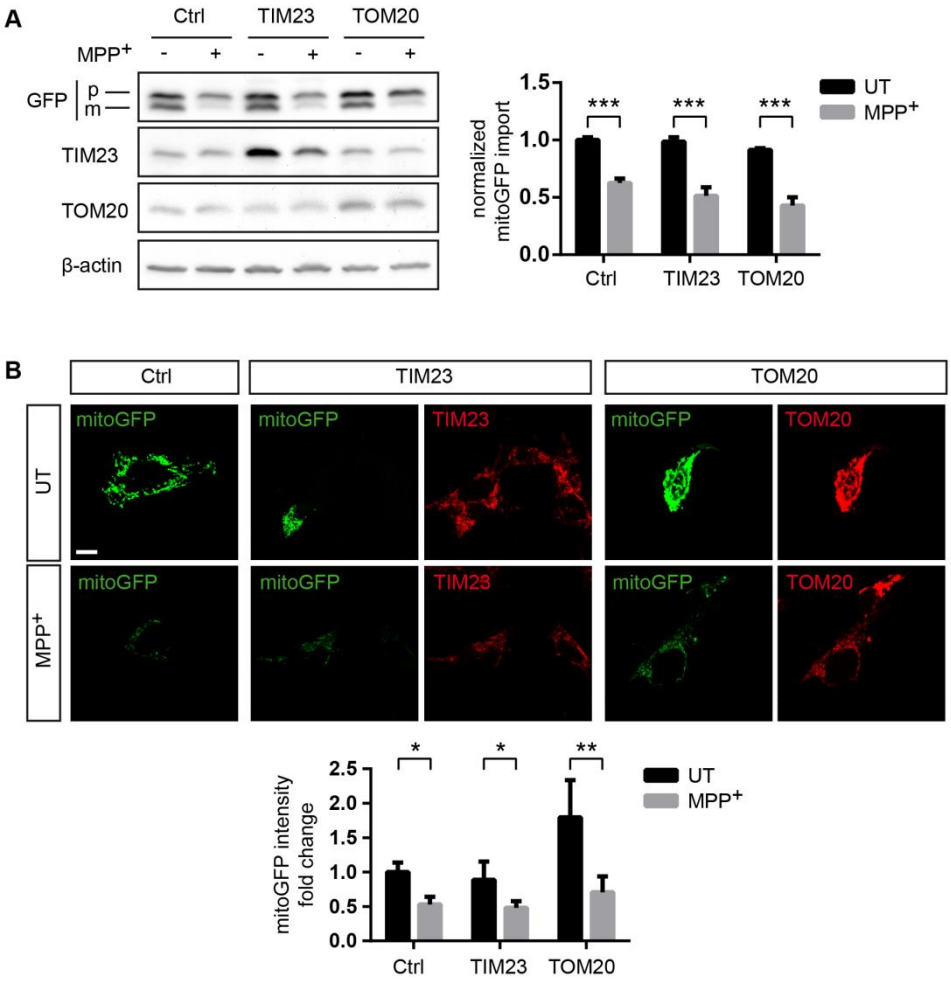

Figure 28. TIM23 or TOM20 transient overexpression does not restore mitoGFP mitochondrial processing upon complex I inhibition in BE(2)-M17 cells.

(**A**) Representative immunoblots of GFP, TIM23 and TOM20 protein levels in mitoGFP-transfected BE(2)-M17 cells alone (Ctrl) or together with pCMV6-XL5-TIM23 (TIM23) or pCMV6-XL5-TOM20 (TOM20), untreated (UT) or treated with MPP^+ (1 mM, 24h). mitoGFP import was calculated as the ratio of mature (m) GFP compared to the sum of precursor (p) and mature GFP (total GFP) and quantification is depicted as fold change to Ctrl UT condition (n=3 independent experiments). (**B**) Representative images of mitoGFP, TIM23 and TOM20 immunostained in mitoGFP-transfected BE(2)-M17 cells alone (Ctrl) or together with TIM23 or TOM20, untreated (UT) or treated with MPP^+ (1 mM, 24h). Quantification is depicted as the fold change in mitoGFP intensity compared with Ctrl UT condition. Scale bar: 10 μm. (**A-B**) Data are presented as mean ± s.e.m. * $P < 0.05$, ** $P < 0.01$, ***$P < 0.001$ after two-way ANOVA followed by Tukey's post hoc test.

4.1.5 Analysis of membrane potential, ROS production and cell death upon complex I inhibition in transient TIM23 or TOM20 overexpressing cells.

One of the main functional consequences of complex I inhibition is the generation of reactive oxygen species (ROS) together with the loss of mitochondrial membrane potential (Nakai et al., 2003; Perier et al., 2005b). Thus, we examined ROS levels and mitochondrial membrane potential upon TOM20 or TIM23 transient overexpression. Complex I inhibition resulted in a 3-fold increase in ROS levels. TOM20 overexpression reduced ~33% ROS production after MPP^+ intoxication (**Fig. 29A**) similarly to TIM23 overexpression (**Fig. 29B**). Complex I inhibition reduced 40% mitochondrial membrane potential. TOM20 overexpression partially rescued mitochondrial membrane potential (**Fig. 29C**) while TIM23 overexpression did not (**Fig. 29D**). All in all, TOM20 overexpression protected against complex I-induced mitochondrial dysfunction, whereas TIM23 effect was milder. However, TOM20 overexpression only displayed a partial protection against complex I-induced mitochondrial dysfunction. This indicates that other mechanisms beyond protein import contribute to the mitochondrial demise observed after MPP^+ intoxication.

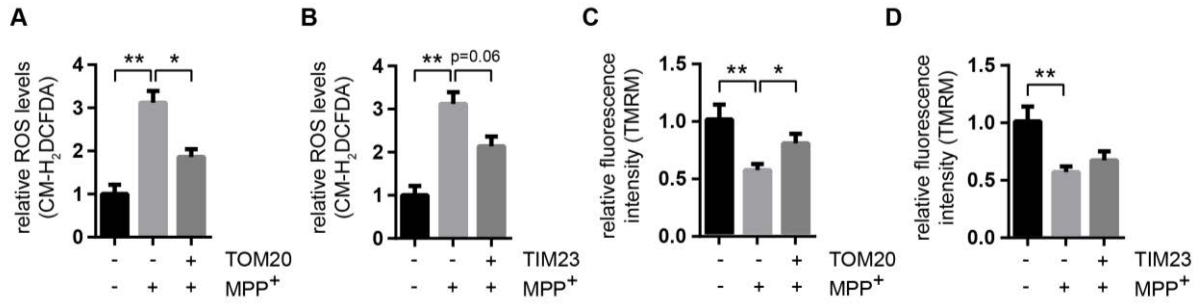

Figure 29. Analysis of membrane potential and ROS production in transient TOM20 or TIM23 overexpressing cells.

(**A-B**) ROS production measured as CM-H_2DCFDA fluorescence intensity in (**A**) pCMV6-XL5-TOM20-transfected (TOM20) and (**B**) pCMV6-XL5-TIM23-transfected (TIM23) BE(2)-M17 cells untreated or treated with MPP^+ (1 mM, 24h). Quantification is depicted as the fold change in fluorescence intensity compared with vehicle-transfected UT condition (n=3 independent experiments). (**C-D**) Mitochondrial membrane potential measured as TMRM fluorescence intensity in (**C**) TOM20-transfected and (**D**) TIM23-transfected BE(2)-M17 cells untreated or treated with MPP+ (1 mM, 24h). Quantification is represented as the fold change in fluorescence intensity compared with vehicle-transfected UT condition (n=5 independent experiments). (**A-D**) Data are presented as mean ± s.e.m. * $P < 0.05$, ** $P < 0.01$ after repeated measures one-way ANOVA followed by Tukey's post hoc test.

As reported above, 5 mM MPP^+ induced a massive cell death in BE(2)-M17 cells (**Fig. 25**). When transiently overexpressing TOM20, we observed an unexpected increase of cell death at basal level (**Fig. 30A**), potentially masking a protective effect of TOM20 overexpression against MPP^+ intoxication. Nonetheless, MPP^+ did not induce further cell death in TOM20-overexpressing cells, which might suggest a protective role of TOM20 overexpression. To distinguish the effect of cell death induced by TOM20 overexpression to the one induced by MPP^+, we compared each group to its own control. This comparison shows that TOM20 overexpression exerted a partial protection against MPP^+-induced cell death (**Fig. 30B**). It is notable that there was a massive expression of TOM20 24h after transfection, which was maintained at 48h (~3.7 fold and ~2.5 fold after 24 and 48 h of transfection respectively,(**Fig. 30C and D**). This condition poorly reflects the physiological situation in the cell, and may explain the increased cell death observed at basal level compared to vehicle-transfected cells. To overcome the toxic effect of TOM20 transient transfection, we developed a lentiviral (LV)-TOM20 stable cell line. MPP^+-induced cell death (5 mM) was reduced ~25% in LV-TOM20 stable cells compared with empty vector (EV) cell line (**Fig. 30E**).

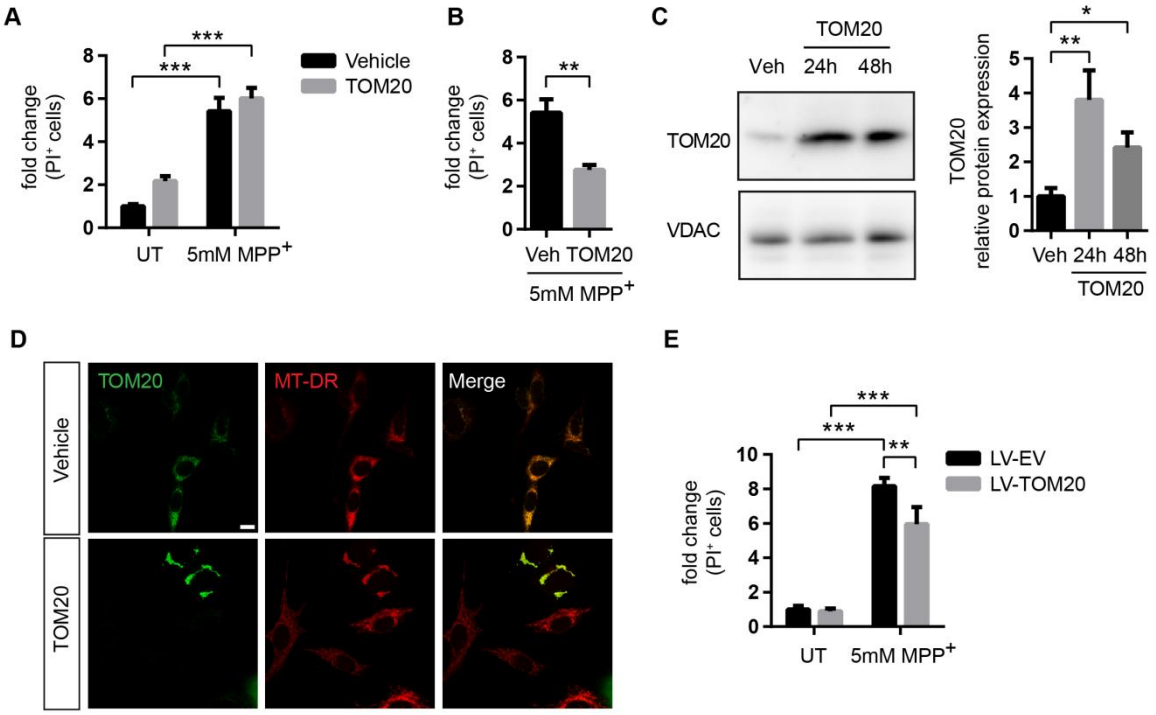

Figure 30. TOM20 transient or stable overexpression protects against complex I-induced cell death.

(**A-B**) Cell death measured as propidium iodide (PI) positive cells in vehicle- or pCMV6-XL5-TOM20-(TOM20)-transfected cells untreated or treated with MPP^+ (5 mM, 24h, n=5 independent experiments). Quantification is represented as (**A**) the fold change in the percentage of PI positive cells compared with vehicle-transfected UT condition or (**B**) compared with each control condition. (**C**) Representative immunoblots of TOM20 and VDAC protein levels in vehicle (Veh)- or TOM20-transfected BE(2)-M17 cells (n=3 independent experiments). Protein levels were normalized relative to VDAC and quantification is depicted as fold change to Veh condition (n=3 independent experiments). (**D**) Representative images of TOM20 and MitoTracker® DeepRed (MT-DR) immunofluorescence in vehicle or TOM20-transfected BE(2)-M17 cells. (**E**) Cell death measured as propidium iodide (PI) positive cells in empty vector (EV) or lentiviral (LV)-TOM20 stable cell lines untreated or treated with MPP^+ (5 mM, 24h). Quantification is depicted as the fold change in the percentage of PI positive cells compared with EV UT condition (n=4 independent experiments). (**A-C and E**) Data are presented as mean ± s.e.m. * P < 0.05, ** P < 0.01, ***P < 0.001 after (**A and E**) two way ANOVA followed by Tukey's post hoc test, (**B**) unpaired Student's t test or (**C**) one way ANOVA followed by Tukey's post hoc test.

TIM23 transient overexpression partially protected against MPP^+-induced cell death, although its overexpression also produced cell death in UT conditions (**Fig. 31 A and B**). Again, there was an excessive expression of TIM23 at both 24 and 48h post-transfection (~9 fold and ~6 fold after 24h and 48h of transfection respectively, Fig. **31C and D**).

Unfortunately, we were not able to develop a stable cell line for TIM23 to confirm such results. Overall, we show that TOM20 transient and stable overexpression mitigated complex I-dependent mitochondrial dysfunction and cell death, whereas TIM23 transient overexpression partially rescued MPP^+-induced cell death.

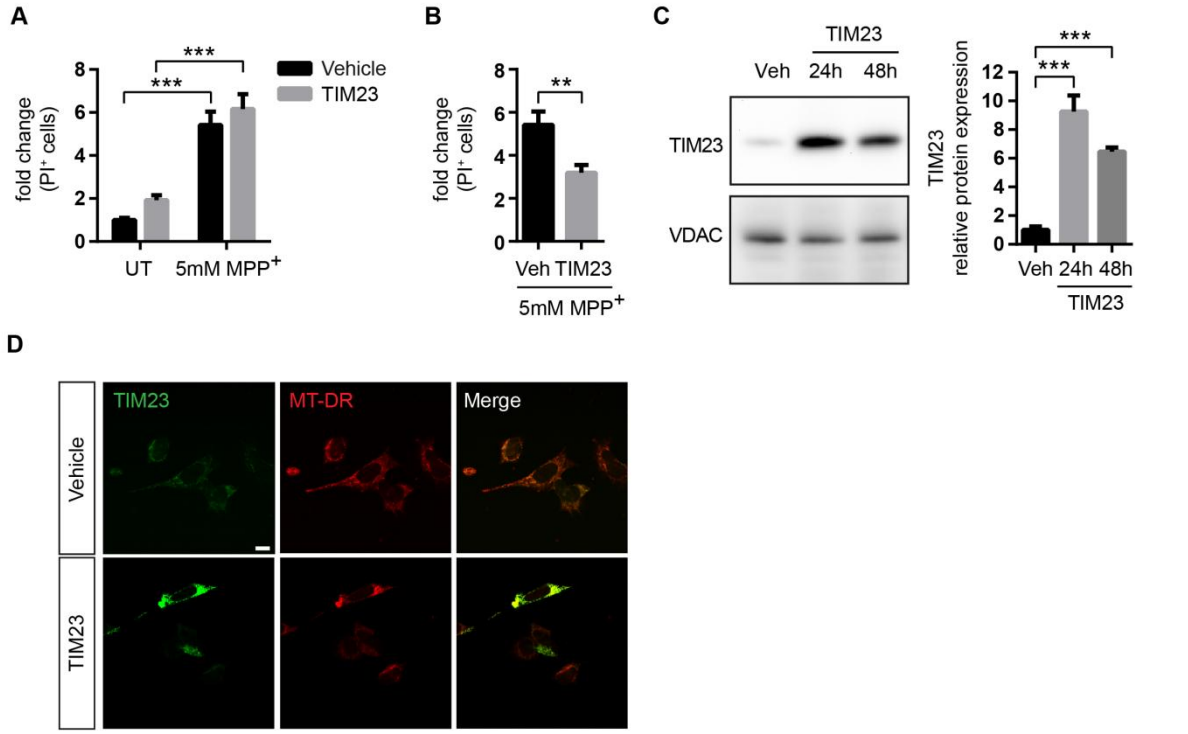

Figure 31. TIM23 transient or stable overexpression partially protects against complex I-induced cell death.

(**A-B**) Cell death measured as propidium iodide (PI) positive cells in vehicle- or pCMV6-XL5-TIM23 (TIM23)-transfected cells untreated or treated with MPP^+ (5 mM, 24h, n=5 independent experiments). Quantification is depicted as (**A**) the fold change in the percentage of PI positive cells compared with vehicle-transfected UT condition or (**B**) compared with each control condition. (**C**) Representative immunoblots of TIM23 and VDAC protein levels in vehicle (Veh)- or TIM23-transfected BE(2)-M17 cells (n=3 independent experiments). Protein levels were normalized relative to VDAC and quantification is depicted as fold change to Veh condition (n=3 independent experiments). (**D**) Representative images of TIM23 and MitoTracker® DeepRed (MT-DR) immunofluorescence in vehicle or TIM23-transfected BE(2)-M17 cells. (**A-C**) Data are presented as mean ± s.e.m. ***P < 0.001 after (**A**) two way ANOVA followed by Tukey's post hoc test, (**B**) unpaired Student's t test or (**C**) one way ANOVA followed by Tukey's post hoc test.

4.1.6 Mitochondrial protein import impairment precedes dopaminergic neuron degeneration in the MPTP mouse model of Parkinson's disease.

Our *in vitro* data show that mitochondrial protein import deficiency parallels MPP^+-induced dopaminergic injury. In particular, our results suggest that TIM23 and TOM20 deficiency are involved in dopaminergic neurodegeneration. To determine the relevance of mitochondrial protein import in an *in vivo* situation, we assessed TIM23 and TOM20 protein levels in the 1-methyl-4-phenyl-1,2,3,6-tetrahydropyridine (MPTP) mouse model of PD. Eight to ten week old mice were treated with a sub-acute MPTP regimen (30 mg/kg per day for five consecutive days) and euthanized at different time points after the last MPTP administration. Mitochondrial parkinsonian neurotoxin MPTP reproduces several PD-linked cellular alterations, such as inhibition of mitochondrial complex I (Nicklas et al., 1985), increased ROS production (Hasegawa et al., 1990; Rossetti et al., 1988), oxidative damage to lipids, DNA and proteins (Hoang et al., 2009; Perier et al., 2005b, 2010; Ramonet et al., 2013), activation of mitochondria-dependent apoptotic pathways and dopaminergic cell death (Perier et al., 2005b, 2007; Vila et al., 2001). Here we found that MPTP induced a decrease of TIM23 protein levels in the ventral midbrain of intoxicated mice (**Fig. 32A**). TIM23 protein levels were decreased as early as at day 0 post-MPTP, preceding dopaminergic cell death in this model, which occurs between days 2 and 4 after the last MPTP administration (Perier et al., 2005b, 2007; Vila et al., 2001). This ~50% decrease was maintained throughout the neurodegenerative process that usually lasts until day 7 post-MPTP (**Fig. 32A**). The deficit of TOM20 protein levels started at day 2, at the same time of dopaminergic cell death in this model (**Fig. 32A**). Immunohistochemistry of TIM23 and TOM20 revealed a specific decrease within SNpc dopaminergic neurons in these animals as early as 2 days after MPTP intoxication (**Fig. 32B**). Because dopaminergic cell death might be associated with a decrease of mitochondrial mass per cell, we analyzed the mitochondrial mass by measuring the mtDNA copy number. No changes in mitochondrial mass were observed after MPTP intoxication (**Fig. 32C**), suggesting a specific downregulation of TIM23 and TOM20 translocases.

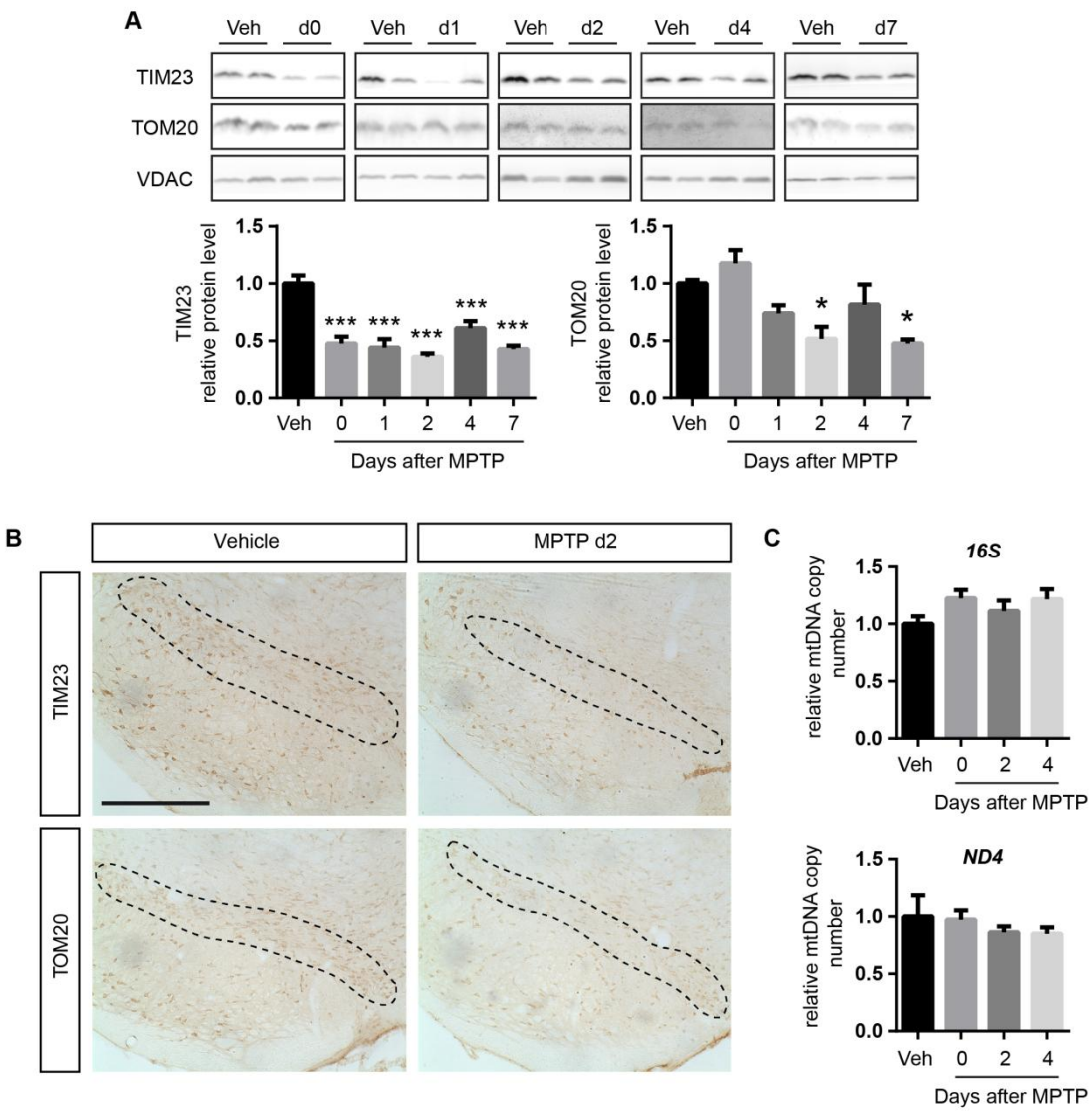

Figure 32. Mitochondrial translocases loss precedes dopaminergic neuron degeneration upon MPTP intoxication.

(**A**) Representative immunoblots of TIM23, TOM20 and VDAC protein levels in ventral midbrain of vehicle- (Veh, n=5) and MPTP-treated (n=6-7) mice euthanized at different time points. Protein levels were normalized relative to VDAC and quantification is depicted as fold change to vehicle condition. (**B**) Representative images of TIM23 and TOM20 immunohistochemistry in ventral midbrain sections from vehicle- and MPTP-treated mice euthanized at day 2 after the last injection. Dashed lines enclose substantia nigra. Scale bar: 500 µm. (**C**) Quantification of mitochondrial DNA (mtDNA) copy number in ventral midbrain samples of vehicle- (n=6) and MPTP-treated (n=7-8) mice euthanized at different time points. mtDNA copy number was measured by quantitative RT-PCR and expressed as the ratio of mtDNA (*16S* and *ND4* copy number) to nuclear DNA (*ANG1* copy number). (**A and C**) Data are presented as mean ± s.e.m. * P < 0.05, ** P < 0.01, *** P < 0.001 compared with vehicle after one-way ANOVA followed by Tukey's post hoc test.

In parallel, MPTP intoxication was associated with reduced mitochondrial protein import in tyrosine-hydroxylase (TH) positive neurons of the SN at day 2 post-MPTP, as shown by decrease intensity in mitochondrially localized COX IV (**Fig 33**). Deficit of imported proteins following MPTP intoxication could then not be simply attributed to a reduction of mitochondrial mass (**Fig. 32C**) or a reduced number of dopaminergic cells in these animals, as it occurred prior to dopaminergic cell death. These results indicate that mitochondrial import system is impaired in SNpc dopaminergic neurons early following MPTP intoxication, within a time-frame compatible to influence the fate of dopaminergic neurons in this pathological situation.

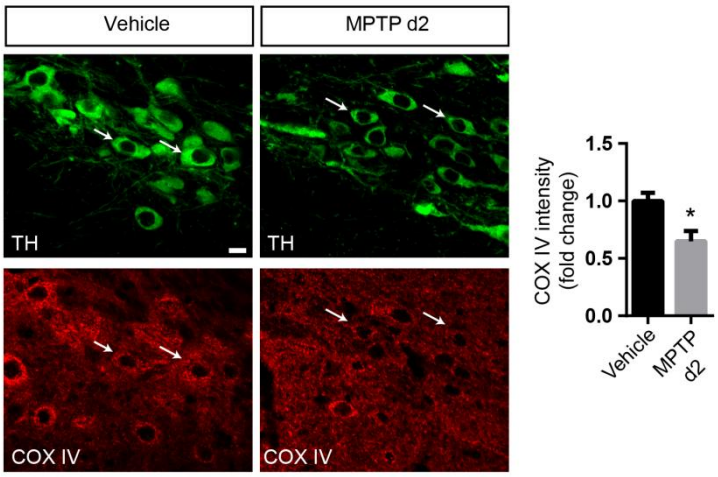

Figure 33. Mitochondrial protein import is hampered upon MPTP intoxication.

Representative images of tyrosine hydroxylase (TH) and COX IV immunostained in ventral midbrain sections from vehicle- (n=5) or MPTP-treated (n=5) mice euthanized at day 2 after the last injection. Quantification is depicted as the fold change of COX IV intensity in TH positive neurons compared to vehicle condition. White arrows indicate representative neurons. A minimum of 36 neurons were analyzed per animal. Data are presented as mean ± s.e.m. * $P < 0.05$ compared to vehicle after unpaired Student's t test.

4.1.7 Mitochondrial protein import and nigrostriatal dopaminergic system integrity upon MPTP intoxication in TIM23- or TOM20-overexpressing mice.

Since TIM23 and TOM20 overexpression *in vitro* led to a partial protection in MPP^+-induced cell death, we further assessed whether TIM23 and TOM20 decreased levels have an instrumental role in MPTP-induced neurodegeneration. For such we overexpressed TIM23 or TOM20 in the SNpc of saline and MPTP-treated mice by means of adenoassociated viral (AAV) vectors. Mice received single unilateral stereotaxic injections of AAV-TIM23 or AAV-TOM20 in the SNpc. Sham, TIM23- and TOM20-overexpressing mice were treated with either saline or MPTP and we assessed (i) the mitochondrial protein import system by COX IV immunofluorescence, and (ii) the integrity of the nigrostriatal dopaminergic system at day 21 after the last MPTP injection, once the dopaminergic lesion is stabilized (Vila et al., 2001). Four weeks after viral vector delivery, ventral midbrain samples ipsilateral to AAV-TIM23 injections displayed a 53% ± 2,92 transduction efficiency (**Fig. 34A**). MPTP intoxication induced a reduction in mitochondrial protein import as determined by the decrease in the mitochondrially localized COX IV protein which was reversed by the overexpression of TIM23 (**Fig. 34B**). In sham-injected mice, MPTP produced a ~50% depletion of striatal dopaminergic terminals, as assessed by optical densitometry of striatal tyrosine hydroxylase (TH)-positive fibers (**Fig. 34C**). Overexpression of TIM23 did not prevent the loss in striatal terminals induced by MPTP (**Fig. 34C**). When analyzing SN cell bodies, MPTP killed ~35% of SNpc dopaminergic neurons, as determined by stereological cell counts of SNpc TH-positive cells (**Fig. 34D**). In contrast, TIM23-overexpressing mice exhibited a mild attenuation of MPTP-induced nigrostriatal dopaminergic denervation at the level of SNpc dopaminergic cell bodies (**Fig. 34D**).

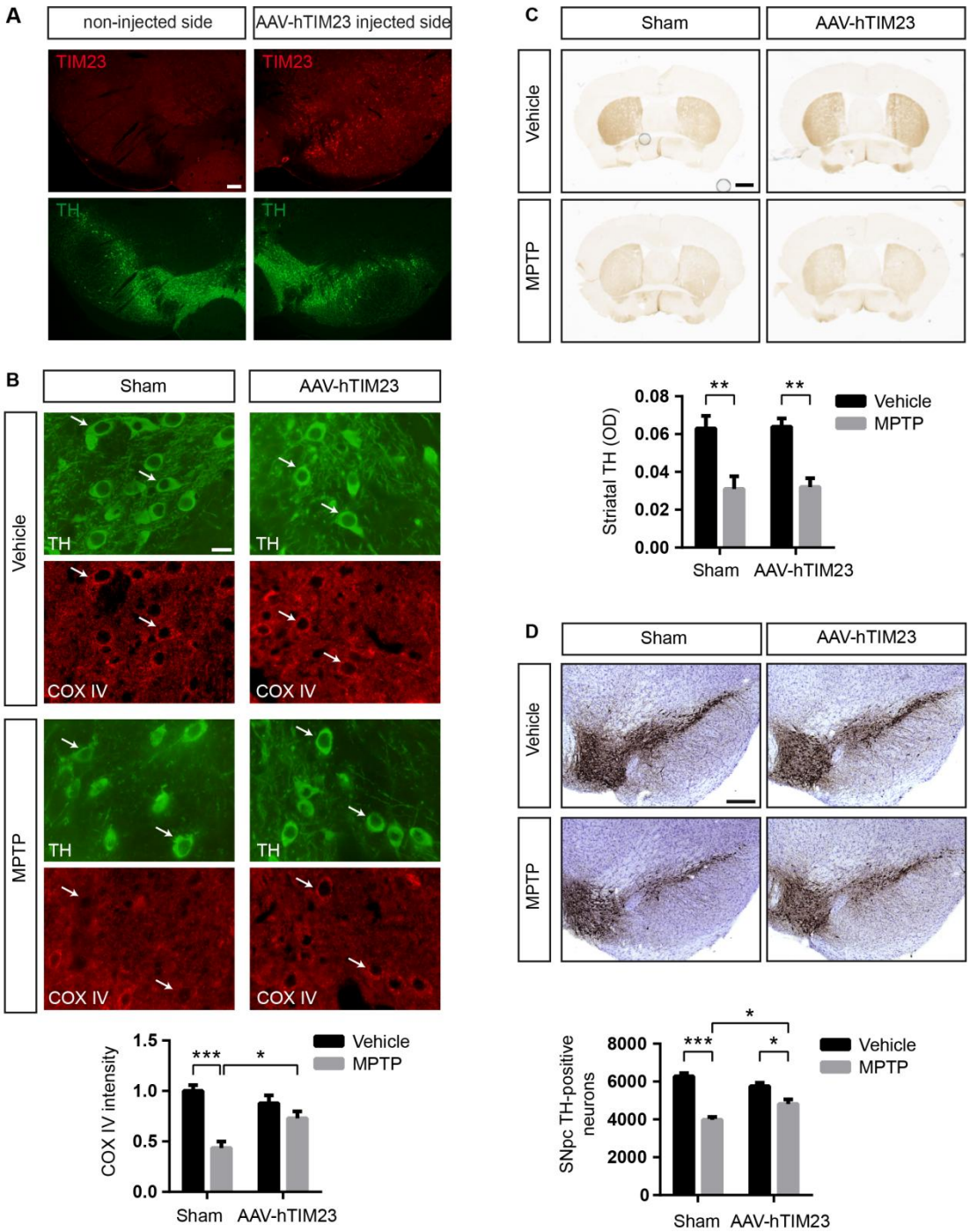

Figure 34. TIM23 overexpression slightly attenuates MPTP-induced dopaminergic neuron injury *in vivo*.

(**A**) Representative images of TIM23 and TH immunofluorescence in ventral midbrain sections from AAV-hTIM23 mice (n=3). Scale bar: 150 μm. (**B**) Representative images of TH and COX IV immunohistochemistry in ventral midbrain sections from sham- and AAV-hTIM23-injected mice treated with vehicle or MPTP (Sham-Vehicle n=5; Sham-MPTP n=6; AAV-hTIM23-Vehicle n=5; AAV-hTIM23-MPTP n=6). Scale bar: 50 μm. Quantification is depicted as the fold change in COX IV intensity compared with sham-injected vehicle-treated group. (**C**) Representative photomicrographs of TH immunohistochemistry in striatum from sham- and AAV-hTIM23-injected mice treated with vehicle

or MPTP (Sham-Vehicle n=7; Sham-MPTP n=5; AAV-hTIM23-Vehicle n=8; AAV-hTIM23-MPTP n=8). Quantification is represented as the optical densitometry of striatal TH immunoreactivity in the different experimental groups at day 21 post MPTP. Scale bar: 500 µm. (**D**) Representative photomicrographs of TH immunohistochemistry SNpc from sham- and AAV-hTIM23-injected mice treated with vehicle or MPTP (Sham-Vehicle n=14; Sham-MPTP n=10; AAV-hTIM23-Vehicle n=7; AAV-hTIM23-MPTP n=8). Quantification is depicted as the stereological cell counts of SNpc TH-immunoreactive neurons in the different experimental groups at day 21 post MPTP. Scale bar: 500 µm. (**B-D**) Data are presented as mean ± s.e.m. * $P < 0.05$, ** $P < 0.01$, *** $P < 0.001$ after two-way ANOVA followed by Tukey's post hoc test.

TOM20 overexpression led to a 63% ± 4,81 transduction efficiency in ventral midbrain samples ipsilateral to AAV-TOM20 injection (**Fig. 35A**). In contrast to TIM23 overexpression, TOM20 overexpression did not reverse the mitochondrial protein import deficit induced by MPTP (**Fig. 35B**). Similarly, TOM20 did not protect against MPTP-induced striatal TH loss or SNpc dopaminergic cell death (**Fig. 35C and D**). Strikingly, TOM20 overexpression seemed to induce even further dopaminergic cell death compared to sham animals (**Fig. 35C and D**). These results seem in contradiction with our *in vitro* data showing that TOM20 overexpression attenuates cell death after complex I inhibition.

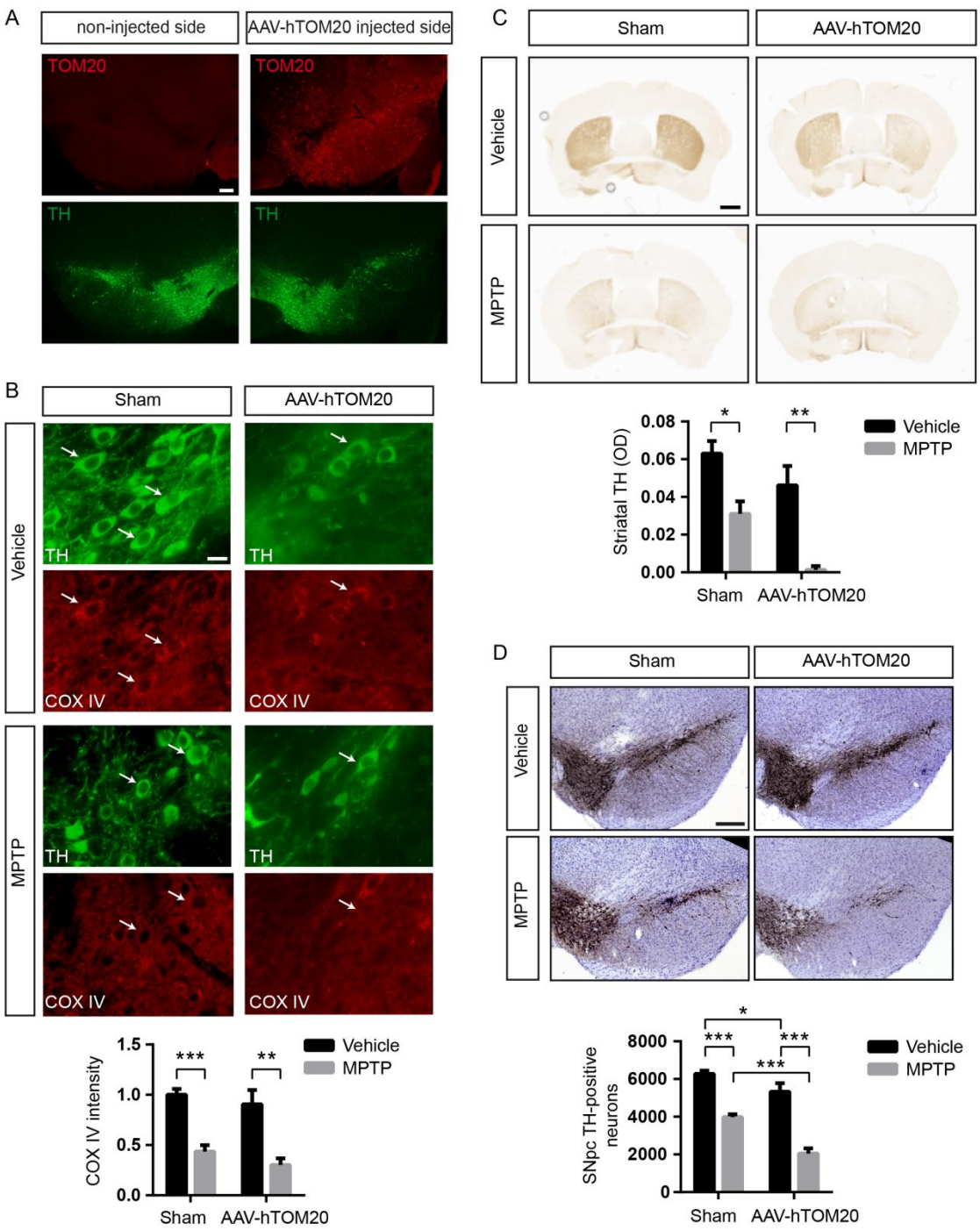

Figure 35. TOM20 overexpression cannot attenuate MPTP-induced dopaminergic neuron injury *in vivo*.

(**A**) Representative images of TOM20 and TH immunofluorescence in AAV-hTOM20 mice (n=2). Scale bar: 150 µm. (**B**) Representative images of TH and COX IV immunohistochemistry in ventral midbrain sections from sham- and AAV-hTOM20-injected mice treated with vehicle or MPTP (Sham-Vehicle n=5; Sham-MPTP n=6; AAV-hTOM20-Vehicle n=4; AAV-hTOM20-MPTP n=4). Scale bar: 50 µm. Quantification is depicted as the fold change in COX IV intensity compared with sham-injected vehicle-treated group. (**C**) Representative photomicrographs of TH immunohistochemistry in striatum from sham- and AAV-hTOM20-injected mice treated with vehicle or MPTP (Sham-Vehicle n=7; Sham-

MPTP n=5; AAV-hTOM20-Vehicle n=8; AAV-hTOM20-MPTP n=7). Quantification is depicted as the optical densitometry of striatal TH immunoreactivity in the different experimental groups at day 21 post MPTP. Scale bar: 500 µm. (**D**) Representative photomicrographs of TH immunohistochemistry in SNpc from sham- and AAV-hTOM20-injected mice treated with vehicle or MPTP (Sham-Vehicle n=14; Sham-MPTP n=10; AAV-hTOM20-Vehicle n=7; AAV-hTOM20-MPTP n=7). Quantification is represented as the stereological cell counts of SNpc TH-immunoreactive neurons in the different experimental groups at day 21 post MPTP. Scale bar: 500 µm. (**A-D**) Data are presented as mean ± s.e.m. * $P < 0.05$, ** $P < 0.01$, *** $P < 0.001$ after (**B-D**) two-way ANOVA followed by Tukey's post hoc test.

Taken together, these results show that TIM23 overexpression in SNpc partially protects against cell body degeneration but not axonal degeneration. Strikingly, TOM20 overexpression is able to induce neuroprotection *in vitro*, but not in vivo, neither at the level of SN cell bodies nor striatal terminals.

4.2 Chapter II: mitophagy and HD

4.2.1 Mitophagy is affected in ST-Q111 cells

Here we investigated the genuine role of Htt in neuronal mitophagy in differentiated striatal neurons. To date, the studies of Htt's role in autophagy have been done in mitotic dividing cells and mostly non-neuronal models with overexpression of different proteins involved in the mitophagy process. Now we know that mitophagy process taking place in neurons under basal or induced conditions may differ from those mechanisms proposed in cellular models, where Parkin and PINK1 are artificially overexpressed (Rakovic et al., 2013; Van Laar et al., 2011). Thus, we first studied whether the clearance of mitochondria inside the lysosomes under basal and induced conditions was affected in a HD cellular model in a situation as close as possible to the physiological neuronal conditions. For such, we used differentiated striatal neurons derived from a knock-in mouse expressing human exon 1 carrying a polyQ tract with 7 glutamines ST*Hdh*-Q7 (ST-Q7, control) or 111 glutamines ST*Hdh*-Q111 (ST-Q111, mutant) inserted into the endogenous mouse *Htt* gene. We first analyzed mitochondrial clearance measured by different alternative methods: (i) colocalization of mitochondria with lysosomes by confocal microscopy, (ii) expression and analysis of the pH-dependent fluorescent mitochondrial protein mitoKeima and (iii) quantification of mitochondrial mass with anti-DNA fluorescence labelling.

Mitophagy can be detected as the amount of mitochondria engulfed within an autophagosome, or also inside a lysosome if lysosomal proteolysis has been properly inhibited. Under basal conditions, the amount of lysosomes loaded with mitochondrial material (in the presence of lysosomal inhibitors to avoid completion of the degradation) was similar between control and mutant striatal cells. However, after mild (rotenone 1 μM, 4h) and acute (CCCP 10 μM, 24h) mitochondrial depolarization, control cells showed a clear increase in the number of lysosomes colocalizing with mitochondria but no increase was observed in ST-Q111 cells, indicating that mitophagy was not being completed as efficiently as in control cells when mutant Htt was present (**Fig. 36A**). This assay reveals that less amount of mitochondria is being engulfed and digested through selective mitophagy after induction of mitochondrial depolarization.

To further analyze mitochondrial clearance in our differentiated striatal cell line, we took advantage of Keima, a pH-dependent fluorescent protein, relatively resistant to lysosomal degradation (Katayama et al., 2011; Lazarou et al., 2015b). Keima is expressed within the mitochondria, so when mitochondria are engulfed by the autophagosomes and then the

autophagosomes are fused with the lysosomes, Keima is released into the lysosomal lumen. Interestingly, the emission spectrum of Keima peaks at 620 nm and its excitation has a bimodal spectrum, peaking at 440 and 586 nm depending on the pH. At physiological pH of mitochondria (pH 8.0) Keima is excited by the 440 nm light, while at acidic lysosomal pH (pH 4.5) there is a shift towards a 586 nm light excitation (Katayama et al., 2011). Since once in the lysosomal lumen the protein shifts to red excitation and is resistant to lysosomal degradation, the signal released upon red-laser excitation is a reporter of mitochondria engulfed inside a lysosome. We transfected the mitochondrial matrix-localizing Keima (mitoKeima) in differentiated ST-Q7 and ST-Q111 cells and induced a mild or acute mitochondrial depolarization. In those conditions, mitochondria are delivered into lysosomes and Keima is present in the lysosomal lumen. For such, we analyzed the mitoKeima intensity upon ~586 nm excitation. In ST-Q7 cells there was an increase in mitoKeima intensity, concomitant with the severity of the mitochondrial insult, indicating that mitochondria are being contained into lysosomes upon depolarization. In ST-Q111 cells there were no changes and even a tendency towards a decrease in mitoKeima intensity, suggesting an alteration in the mitophagy process (**Fig. 36B**).

As another measure of mitochondrial degradation, we quantified mtDNA as reported in Lazarou *et al.*, using quantification of mtDNA as a reporter of mitochondrial mass (Lazarou et al., 2015a). For such, we immunostained differentiated ST-Q7 and ST-Q111 cells with anti-DNA antibody upon mild and acute mitochondrial depolarization. The anti-DNA antibody used preferentially stains mtDNA (Legros et al., 2004). In ST-Q7 cells there was a loss of DNA intensity upon rotenone and CCCP treatment, indicative of mitochondrial removal upon damage. However, no significant changes were observed in ST-Q111 cells, further implying that mitochondria are not being degraded with the same efficiency as ST-Q7 upon stress-induction (**Fig. 36C**).

These results indicate that induced mitophagy, but not basal mitophagy, is impaired in differentiated ST-Q111 cells, suggesting that mutant Htt might directly or indirectly affect the efficiency of this process.

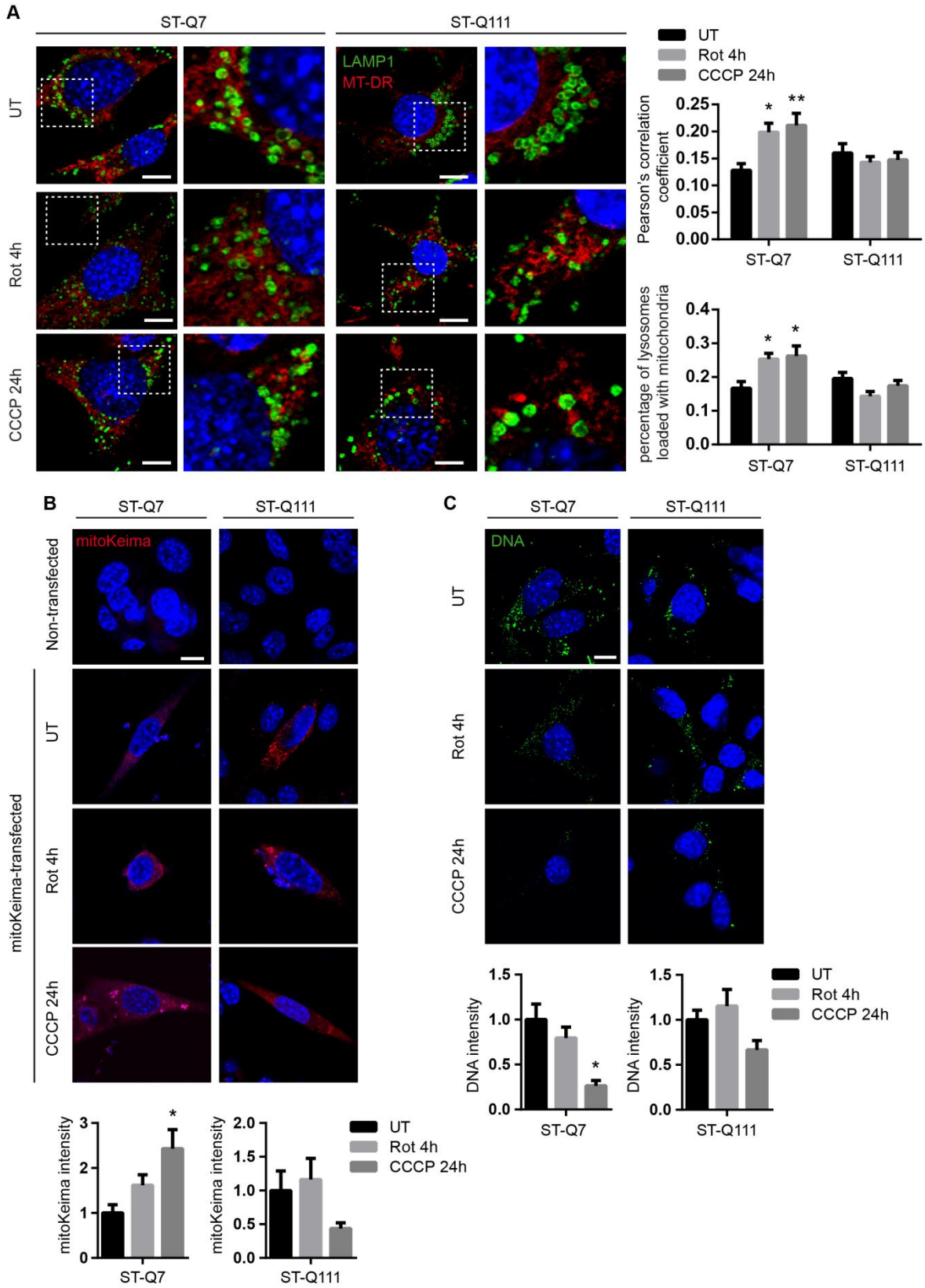

Figure 36. Mitophagy is affected in ST-Q111 cells.

(**A**) Representative images of LAMP1 and MitoTracker® DeepRed immunostained ST-Q7 and ST-Q111 cells untreated (UT) or treated with rotenone (Rot, 1 μM, 4h) or CCCP (10 μM, 24h). Insets show higher magnification images. Colocalization degree was quantified using the Pearson's

correlation coefficient and the ratio of LAMP1-stained lysosomes loaded with MitoTracker® DeepRed-stained mitochondria. A minimum of 30 cells were analyzed per condition. (**B**) Representative images of non-transfected or mitoKeima-transfected ST-Q7 and ST-Q111 cells UT or treated with Rot (1 μM, 4h) or CCCP (10 μM, 24h). Lysosomal-positive mitoKeima signal was calculated as the ratio of intensity (594 nm-light excitation) per cell area, represented as the fold change compared with mitoKeima-transfected UT conditions. A minimum of 20 cells were analyzed per condition. (**C**) Representative images of ST-Q7 and ST-Q111 cells immunostained with anti-DNA UT or treated with Rot (1 μM, 4h) or CCCP (10 μM, 24h). Quantification is represented as the fold change in DNA intensity compared with UT conditions. 15 to 50 cells were analyzed per condition. (**A-C**) Scale bar: 10 μm. Data are presented as mean ± s.e.m. * $P < 0.05$, ** $P < 0.01$ compared to UT condition after (**A**) two-way ANOVA followed by Tukey's post hoc test (**B-C**) one-way ANOVA test followed by Tukey's post hoc test.

4.2.2 Mitophagy in differentiated striatal cells is not mediated by Parkin translocation to mitochondria

To study how the presence of mutant Htt could affect the mitophagy process we analyzed the different steps of the mitophagy mechanism. We first checked whether mutant Htt could be involved in the initiation of the mitophagy process. According to many studies published in the last years, the initiation of mitophagy process starts with the retention of full-length PINK1 protein on the mitochondrial surface. PINK1 is normally imported inside mitochondria and degraded. Upon loss in the mitochondrial membrane potential, PINK1 becomes stabilized and activated on the OMM (Matsuda et al., 2010; Narendra et al., 2010b; Vives-Bauza et al., 2010). Upon activation, PINK1 phosphorylates ubiquitin molecules present on the OMM at their serine 65. Moreover, PINK1 also phosphorylates Parkin at its serine 65 of the ubiquitin-like domain, leading to Parkin E3 ubiquitin ligase activity activation. In addition, Parkin binds with high affinity to phospho-ubiquitin, thereby recruiting Parkin onto OMM. In fact, phospho-ubiquitin is essential for the full activation of Parkin and all together leads to stimulation of Parkin activity (Kane et al., 2014; Kazlauskaite et al., 2014; Koyano et al., 2014). Active Parkin ubiquitinates a variety of substrates present on the OMM either elongating pre-existing ubiquitin chains or ubiquitinating substrates *de novo*. These ubiquitin chains will be subsequently phosphorylated by PINK1, generating a feedforward mechanism in which PINK1 is essential for the phosphorylation of ubiquitin and Parkin, while Parkin has an amplifier role (Martinez-Vicente, 2017; McWilliams and Muqit, 2017). Thus we investigated whether PINK1 and Parkin levels could be affected in ST-Q111 upon induction of mitophagy. In our cellular model, we did not detect differences in the amount of total PINK1 levels in total cellular homogenates in differentiated ST-Q7 cells upon mild or acute

depolarization. However, in differentiated ST-Q111 cells, basal PINK1 protein levels were slightly increased but again, no changes were observed upon rotenone- or CCCP-induced mitophagy (**Fig. 37A**).

Following the mitophagy initiation pathway, we also studied Parkin translocation to mitochondrial membrane as a marker of mitophagy induction. Depolarization induced by various effectors did not alter Parkin protein levels in total homogenate but more importantly, we were unable to detect Parkin protein translocation to mitochondria using two distinct methods. Parkin protein was not detected by immunoblot in isolated mitochondrial fractions; instead all Parkin protein remained cytosolic (**Fig. 37B**). By confocal immunofluorescence under basal conditions and after mild and severe depolarization, endogenous Parkin protein also remained cytosolic and was not detected in mitochondria labeled with mitochondrial probe MitoTracker® DeepRed in neither differentiated ST-Q7 nor ST-Q111 cell lines (**Fig. 37C**). This scenario is similar to those observed in other neuronal and non-neuronal cells where endogenous Parkin translocation to mitochondria is not detectable (Cai et al., 2012; Rakovic et al., 2013; Sterky et al., 2011; Van Laar et al., 2011). Even the artificial overexpression of Parkin protein tagged to a fluorescent protein (EGFP) could not promote a clear translocation of EGFP-Parkin from the cytosol to the mitochondria at short time and mild depolarization (Rot 4h). Only after 24h with strong depolarization induced by CCCP 10 µM it was possible to observe a partial translocation of EGFP-Parkin from a diffuse cytosolic distribution to a mitochondrial localization (**Fig 37D**). This recruitment of overexpressed-EGFP-Parkin was only detectable in less than 50% of both differentiated striatal cells ST-Q7 (42,7% ± 11,75) and ST-Q111 (46,3% ± 11,18) after this strong and prolonged depolarization, while the remaining cells still showed non-mitochondrial localization of EGFP-Parkin.

Since under Parkin overexpression some studies could detect a clear mitochondrial localization using other cell lines (Ashrafi et al., 2014; Cai et al., 2012; Joselin et al., 2012; Rakovic et al., 2013), we tested whether other neuronal cells could present Parkin translocation under these conditions. For such we used two human immortalized neuroblastoma cell lines, BE(2)-M17 and SH-SY5Y cell lines. SH-SY5Y cell line exhibits some markers of noradrenergic neurons, while BE(2)-M17 cell line expresses adrenergic properties. Under artificial overexpression of EGFP-Parkin and after 4h of rotenone treatment some BE(2)-M17 cells started to show Parkin translocation to the mitochondria. After total depolarization (CCCP 10 µM, 24h) the number of cells presenting mitochondrial EGFP-Parkin was close to 97% in both cell lines (**Fig. 37E**), indicating that these cells are

more predisposed to induce mitochondrial EGFP-Parkin recruitment upon severe depolarization compared to striatal cells.

According to these results, and in correlation with other studies, Parkin endogenous levels in striatal neurons seem too low in mitochondria to trigger the feedforward amplification mechanism of Parkin binding to phospho-ubiquitin and ubiquitination of the substrates. This means that probably neuronal mitophagy takes place in a slower and less robust process in contrast with other models used to study mitophagy in which Parkin is overexpressed. However, despite the low levels of Parkin and the apparent undetectable recruitment of Parkin to the mitochondrial membrane, mitophagy process takes place and mitochondria are engulfed by autophagosomes and fused with lysosomes (**Fig. 36A**).

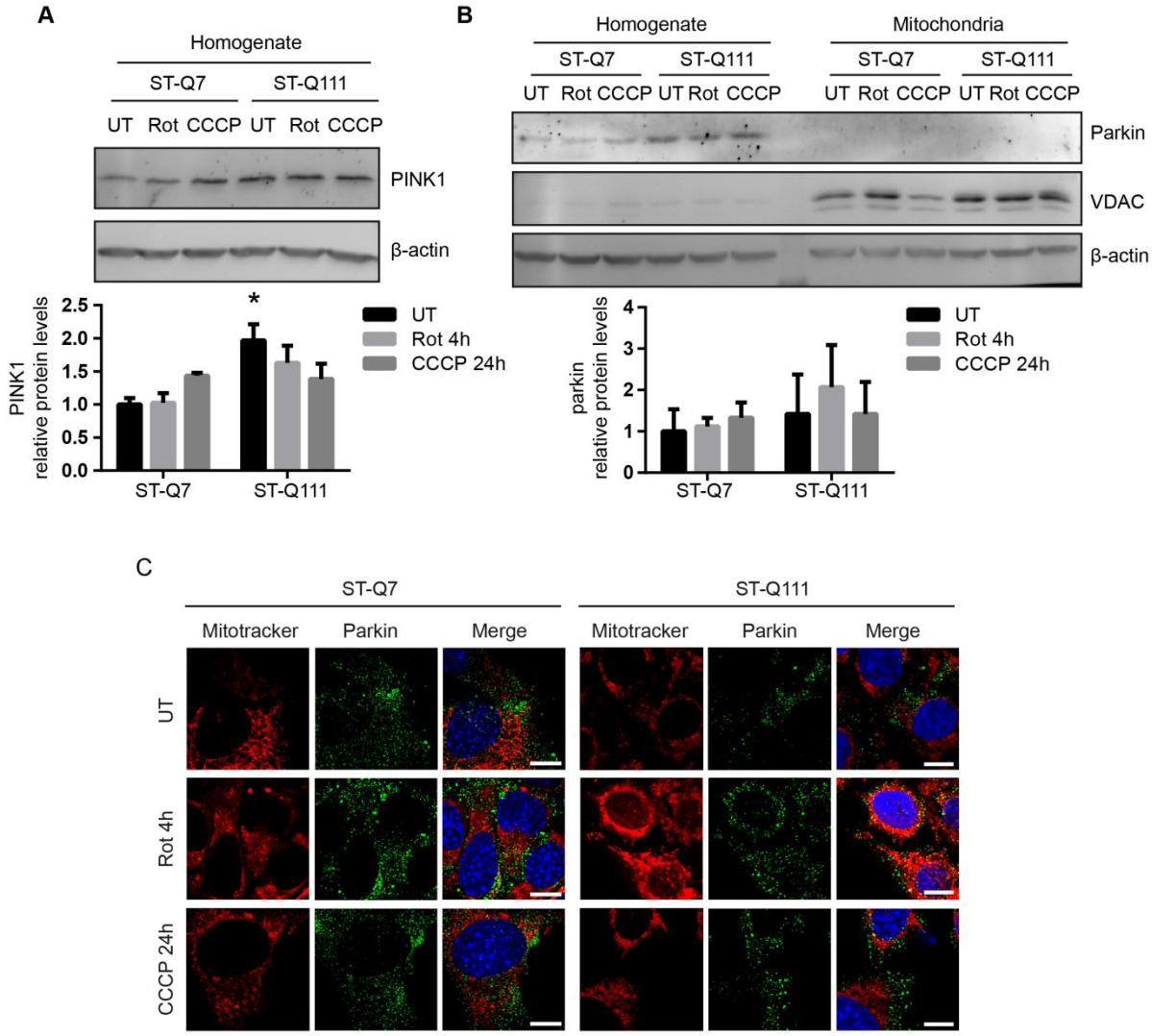

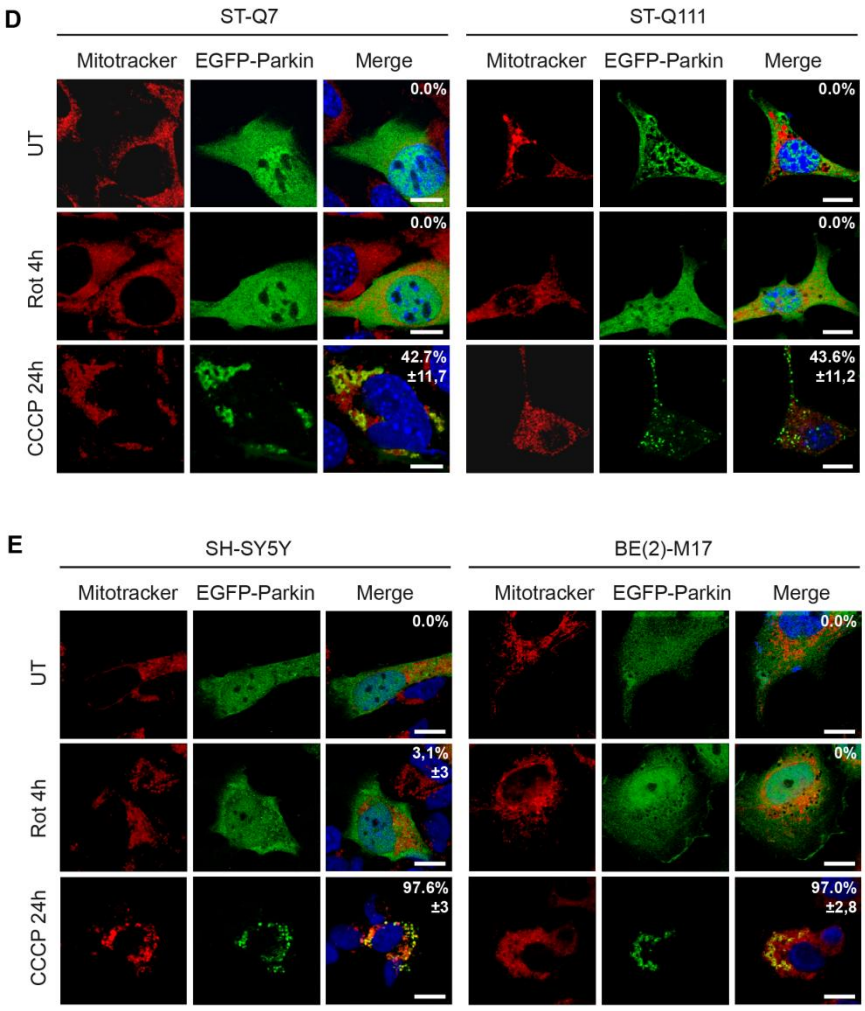

Figure 37. Mitophagy in differentiated striatal cells is not mediated by Parkin translocation to mitochondria.

(**A**) Representative immunoblots of PINK1 protein levels in total homogenates from ST-Q7 and ST-Q111 cells untreated (UT) or treated with rotenone (Rot, 1 μM, 4h) or CCCP (10 μM, 24h). Protein levels were normalized relative to β-actin and quantification is depicted as fold change to ST-Q7 untreated. **B**) Representative immunoblots of Parkin protein levels in total homogenates and isolated mitochondria from ST-Q7 and ST-Q111 cells untreated UT or treated with Rot (1 μM, 4h) or CCCP (10 μM, 24h). Protein levels were normalized relative to β-actin and quantification is depicted as fold change to ST-Q7 untreated. (**C**) Representative images of MitoTracker® DeepRed and Parkin immunostained ST-Q7 and ST-Q111 cells UT or treated with Rot (1 μM, 4h) or CCCP (10 μM, 24h). (**D**) Representative images of MitoTracker® DeepRed and EGFP-Parkin immunostained ST-Q7 and ST-Q111 cells UT or treated with Rot (1 μM, 4h) or CCCP (10 μM, 24h). (**E**) Representative images of MitoTracker® DeepRed and EGFP-Parkin immunostained SH-SY5Y and BE(2)-M17 cells UT or treated with Rot (1 μM, 4h) or CCCP (10 μM, 24h). (**A-B**) Data are presented as mean ± s.e.m. from three independent experiments. * $P < 0.05$ compared to ST-Q7 untreated after two-way ANOVA test followed by Tukey's post hoc test. **(C-E**) Scale bars: 10 μm. A minimum of cells 30 were analyzed per

condition. Data are presented as mean ± s.e.m. of the percentage of cells with endogenous Parkin or EGFP-Parkin colocalizing with MitoTracker® DeepRed labeled mitochondria.

4.2.3 Characterization of the mitochondrial polyubiquitination status in ST-Q7 and ST-Q111 cells

The ubiquitin code signals for almost every process in cells. A particular protein can be modified at one or multiple lysine (K) residues with one ubiquitin or with an ubiquitin chain. The way ubiquitin moieties conjugate through one of their lysine residues adds another level of complexity to the ubiquitin code (Akutsu et al., 2016). During classical PINK1/Parkin mediated mitophagy, Parkin is recruited at the outer mitochondrial membrane and can promote the ubiquitination of several proteins, due to its E3 ubiquitin ligase activity (Matsuda et al., 2010; Sarraf et al., 2013). Parkin can form different types of polyubiquitin chains, one of them is the K63-linked chains, which has been classically awarded as a tag for selective autophagy and can be recognized by different autophagy receptors (Akutsu et al., 2016; Yamano et al., 2016).

We aimed to analyze whether the ubiquitination step in mitophagy was affected in the presence of mutant Htt. For such, we analyzed the polyubiquitination pattern of mitochondrial isolated fractions before and after mitophagy induction. We could not detect any change in total ubiquitin protein levels upon mild or strong depolarization in homogenate or in isolated mitochondria from ST-Q7 and ST-Q111 cells (**Fig 38A**). Since ubiquitin chains are linked to different cellular process, we studied specifically K63-linked ubiquitin chains. In isolated mitochondria from differentiated ST-Q7, upon mild and strong depolarization, there was a tendency towards the increase in poly-ubiquitin K63 levels, while in ST-Q111 there was no increase and, even, a rather decrease in the poly-ubiquitin K63 signal upon CCCP, though not significant (**Fig. 38B**), suggesting that the autophagy-specific K63-poly-ubiquitination step might be altered in ST-Q111 cells.

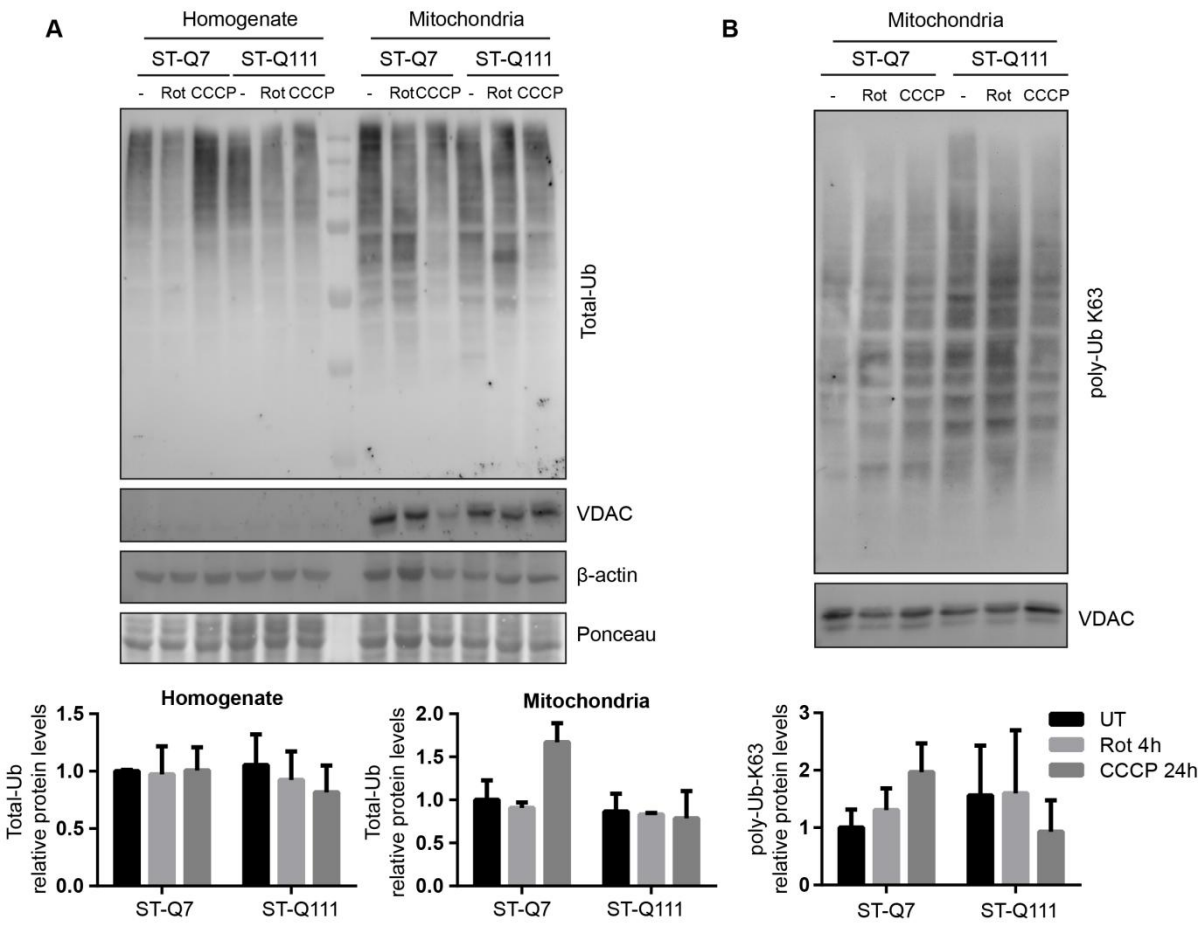

Figure 38. Characterization of the mitochondrial polyubiquitination status in ST-Q7 and ST-Q111 cells.

(**A**) Representative immunoblots of total-Ubiquitin (Ub) protein levels in total homogenates (n=3 independent experiments) or isolated mitochondrial fractions (n=2 independent experiments) from ST-Q7 and ST-Q111 cells untreated (-) or treated with rotenone (Rot, 1 µM, 4h) or CCCP (10 µM, 24h). Protein levels were normalized relative to Ponceau, for total homogenate, or VDAC, for mitochondrial fractions. (**B**) Representative immunoblots of poly-Ubiquitin (Ub) K63 protein levels in isolated mitochondrial fractions from ST-Q7 and ST-Q111 cells untreated (-) or treated with Rot (1 µM, 4h) or CCCP (10 µM, 24h). Protein levels were normalized relative to VDAC (n=3 independent experiments). (**A-B**) Quantification is depicted as fold change to ST-Q7 untreated. Data are presented as mean ± s.e.m. from three independent experiments. * $P < 0.05$ compared to ST-Q7 untreated after two-way ANOVA test followed by Tukey's post hoc test.

4.2.4 Mutant Htt alters the autophagy initiation step

We next checked the effect of mutant Htt in the autophagy initiation complex. Autophagy initiation is coordinated by unc-51 like kinase 1 (ULK1) which forms a complex with Atg13 and FIP200 to regulate the initial step of autophagy induction in mammalian cells. Under

basal conditions, ULK1 protein is bound to the mTORC1 (mammalian target of rapamycin complex 1) and inactivated by the mTOR-mediated phosphorylation at S757 (Kim et al., 2011). Another protein involved in autophagy regulation is AMPK, which maintains energy homeostasis through the sensing of the energy status of the cell (Hardie, 2007). In order to induce autophagy, ULK1 must be activated and released from the mTORC1, losing the mTOR-mediated inhibiting phosphorylation at S757. Simultaneously, AMPK activates ULK1 through physical interaction (Lee et al., 2010b) and phosphorylation of different residues (S555, S777, S317) (Egan et al., 2011; Kim et al., 2011). Previous studies showed that Htt has a key role as a scaffolding protein binding active ULK1 in its C-terminal domain, competing with mTORC1 for the ULK1 binding and promoting the initiation of autophagy (Ochaba et al., 2014; Rui et al., 2015).

In order to check the ability of ULK1 to be released from the mTORC1 and how the presence of the polyQ tract with 111 glutamines might affect this step, we analyzed the interaction of ULK1 with mTOR. We also assessed the ability of ULK1 to shift towards the Htt scaffolding complex by evaluating ULK1 and Htt interaction. For such, we used the Proximity Ligation Assay (PLA) technology since immunoprecipitation with the endogenous proteins was technically not feasible due to low amount of these proteins and the fragility of their interaction. PLA allows the observation and quantification by immunofluorescence of protein-protein interactions within the cell. In differentiated ST-Q111 cells, ULK1-mTOR interaction was more stable after depolarization compared to ST-Q7 cells, in which ULK1-mTOR interaction decreased upon depolarization to allow ULK1 activation. These results suggest that in mutant cells ULK1 remains more inactive and bound to mTOR than in WT cells (**Fig. 39A**). In a similar way, the interaction of ULK1 with Htt was clearly increased in ST-Q7 cells after depolarization, but this interaction was not promoted in ST-Q111 after depolarization, confirming that ULK1 has less affinity for mutant Htt (**Fig. 39B**).

While ULK1 remains bound to the mTORC1, it is inactivated by the phosphorylation mediated by mTOR kinase activity at S757 (Kim et al., 2011). We observed that this inactivating phosphorylation was again more abundant after depolarization when mutant Htt was present (**Fig. 39C**) in correlation with higher presence of mTOR-ULK1 interaction. In parallel, AMPK activates ULK1 by phosphorylating at least four sites (Egan et al., 2011). We observed that mutant Htt was not interfering with the phosphorylation of ULK1 mediated by AMPK (S555) since similar rates of phosphorylation were detected after depolarization in both cell lines (**Fig. 39C**). Even though the phosphorylation of ULK1 mediated by AMPK was not perturbed by the presence of mutant Htt, we detected lower amount of active ULK1 (phosphorylated at S317) bound to Htt after depolarization in ST-Q111 cells (**Fig. 39D**). All

together, these results suggest that the extended polyQ tract present in mutant Htt is somehow interfering with the proper interaction of active ULK1 from the mTORC1 complex to the Htt scaffolding complex, a step necessary to initiate autophagy.

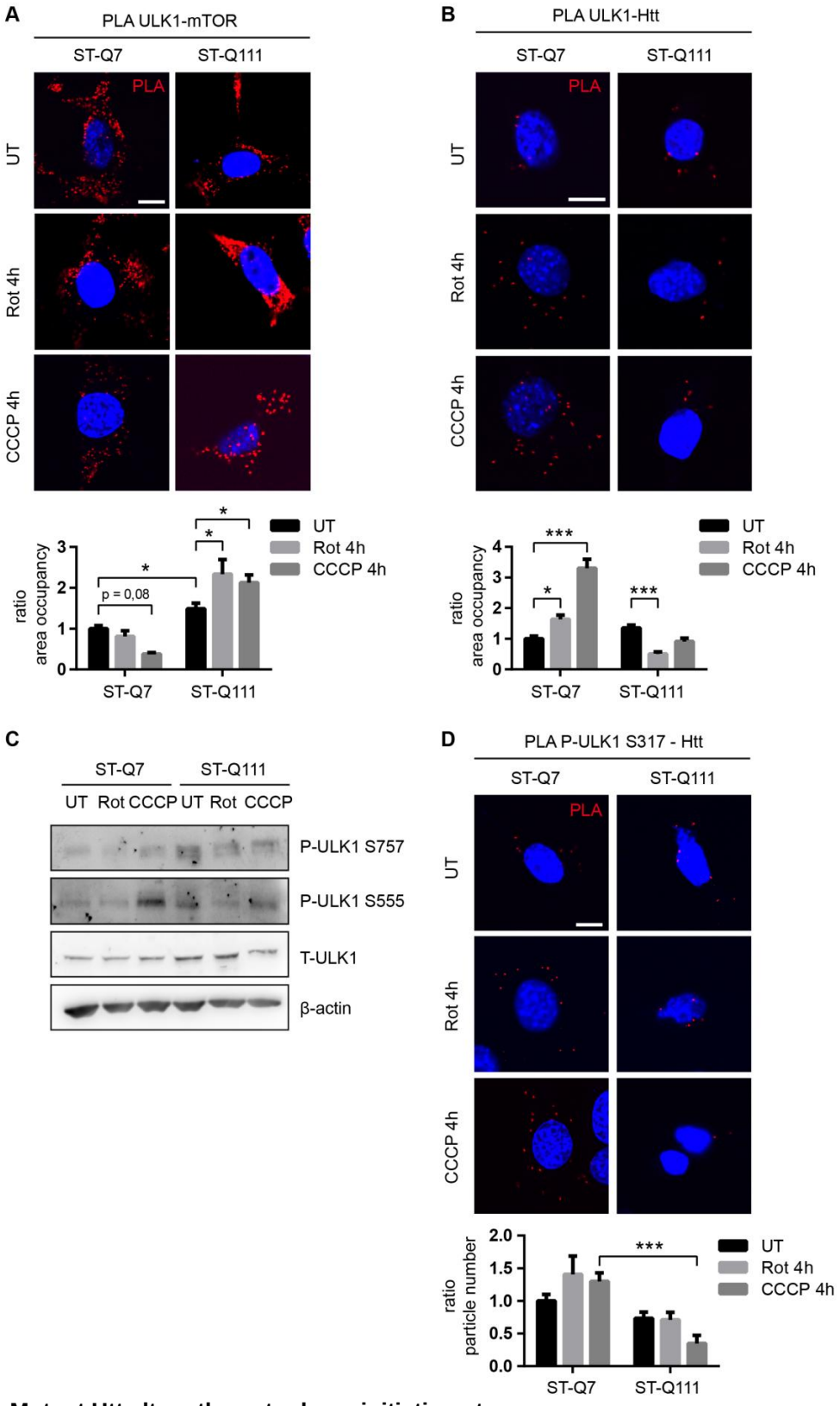

Figure 39. Mutant Htt alters the autophagy initiation step.

(**A**) ULK1-mTOR interaction detected by PLA in ST-Q7 and ST-Q111 cells untreated (UT) or treated with rotenone (Rot, 1 μM, 4h) or CCCP (10 μM, 4h). 24 to 85 cells were analyzed per condition. (**B**) ULK1-Htt interaction detected by PLA in ST-Q7 and ST-Q111 cells UT or treated with Rot (1 μM, 4h) or CCCP (10 μM, 4h). 35 to 115 cells were analyzed per condition. (**C**) Representative immunoblots of Phospho-ULK1-S757, Phospho-ULK1-S555, total ULK1 (T-ULK1) and β-actin protein levels in total homogenates from ST-Q7 and ST-Q111 cells UT or treated with Rot (1 μM, 4h) or CCCP (10 μM, 24h). (**D**) Phospho-ULK1 S317-Htt interaction detected by PLA in ST-Q7 and ST-Q111 cells UT or treated with Rot (1 μM, 4h) and CCCP (10 μM, 4h). (**A-B, D**) Scale bars: 10 μm. PLA interaction was quantified as a ratio of area occupancy by the PLA signal or number of particles represented as the fold change compared with ST-Q7 UT condition. Data are presented as mean ± s.e.m. * $P < 0.05$, ** $P < 0.01$, *** $P < 0.001$ after two-way ANOVA test followed by Tukey's post hoc test.

Following its activation, ULK1 phosphorylates beclin 1, a component of the autophagy initiation complex that generates phosphatidylinositol-3-phosphate (PtdIns3P). PtdIns3P activates the phosphatidylinositol 3-kinase class III (PI3KC3 or Vps34) (Russell et al., 2013). The complex of beclin 1, Vps15, PI3KC3 and others is responsible for the autophagosome formation (Matsunaga et al., 2010). A recent work by Ashkenazi *et al*. has shown how ataxin 3, the protein altered in spinocerebellar ataxia type 3, binds through its wild type polyQ domain to beclin 1. Ataxin 3 is a deubiquitinase, therefore protects Beclin 1 from its degradation by the proteasome since it removes the ubiquitins that signal for proteasomal degradation. Authors showed that extended polyQ tracts, such as the ones present in mutant Htt, bind to beclin 1 to a greater extent than wild type forms, thus competing with the physiological binding of ataxin 3. This observation, suggests that the presence of mutant Htt could interfere and compete in the normal beclin 1/ataxin 3 interaction, promoting beclin 1 degradation by the UPS (Ashkenazi et al., 2017). Lower levels of beclin 1 are associated to lower autophagy induction (He et al., 2015; Tassa et al., 2003). Using PLA technology, we have investigated the possible influence of mutant Htt in the formation of the beclin 1-Vps15-Vps34 (PI3KC3) complex as one of the initial protein complex required for the initiation of autophagy. At basal levels, beclin 1-Vps15 interaction was downregulated in the presence of mutant Htt. Upon depolarization, differentiated ST-Q7 cells showed an increased beclin 1-Vps15 interaction, meaning that the beclin 1 initiation complex was being assembled, while differentiated ST-Q111 cells displayed a downregulation (**Fig. 40**). These results further confirm that expanded polyQ tracts present in mutant Htt hamper the formation of the autophagy initiation complex.

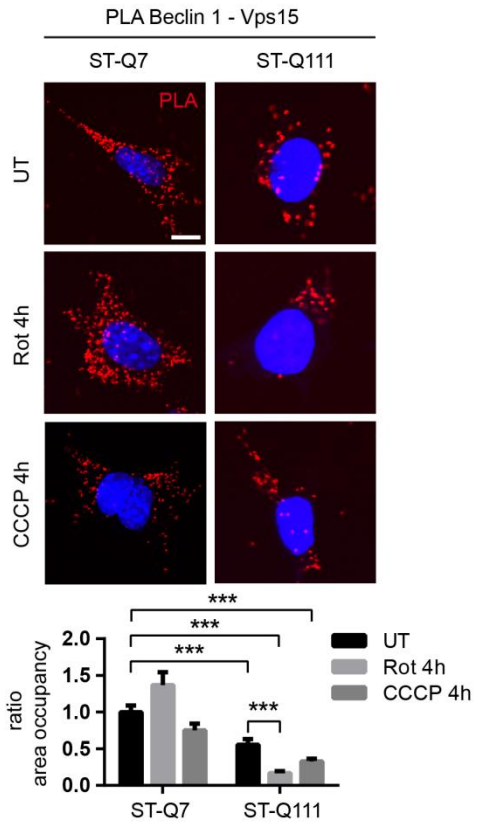

Figure 40. Mutant Htt alters the formation of the nucleation complex.

Beclin 1 - Vps15 interaction detected by PLA in ST-Q7 and ST-Q111 cells untreated (UT) or treated with Rot (1 μM, 4h) and CCCP (10 μM, 4h). Scale bar: 10 μm. PLA interaction was quantified as a ratio of area occupancy by the PLA signal or number of particles represented as the fold change compared with ST-Q7 untreated condition. Data are presented as mean ± s.e.m. *** $P < 0.001$ after two-way ANOVA test followed by Tukey's post hoc test.

4.2.5 polyQ tract in mutant Htt affects the scaffolding role of Htt during mitophagy

Previously, we and others have shown that in addition to the interaction with ULK1, Htt can also interact with the adaptor of selective autophagy p62 (Martinez-Vicente et al., 2010; Ochaba et al., 2014; Rui et al., 2015). Besides p62, different protein adapters for selective autophagy like NDP52, OPTN and NBR1 have been identified (Yoshii and Mizushima, 2015). During mitophagy, these adapters are able to recognize two types of macromolecules (i) polyubiquitinated OMM proteins, through the ubiquitin-binding domain (UBD), present on the mitochondrial surface and, simultaneously, (ii) LC3-II, through the LC3-interacting region (LIR), present on the autophagosome structure. In this way, adapters can recruit the

autophagy machinery and promote the elongation of the isolated membrane engulfing the mitochondria (Wild et al., 2014).

Whereas some studies have shown the requirement of p62 for mitophagy (Geisler et al., 2010; Lee et al., 2010a), others have reported that lack of p62 does not hamper mitophagy (Narendra et al., 2010a; Okatsu et al., 2010). In a recent study, Lazarou and coworkers have shown that optineurin (OPTN) and NDP52 are indeed the primary receptors for mitophagy. These receptors are recruited to mitochondria by the phospho-ubiquitin signal mediated by PINK1 (which is essential), and enhanced by Parkin (which is important to amplify the signal, but not essential) (Lazarou et al., 2015b). Accordingly, and as previously proposed, p62 and NBR1 can participate in mitophagy as adapters but are not essential (Narendra et al., 2010a).

Htt has been identified as a mitophagy scaffold due to its ability to couple the induction of autophagy, through ULK1 binding, and cargo recruitment into autophagosomes, through p62 binding (Rui et al., 2015). Therefore, we first checked whether those mitophagy receptors that have been shown to be essential are also able to directly interact with Htt scaffolding complex. To test this, we used PLA technology again to detect *in vivo* interaction between Htt and OPTN and NDP52. According to previous works (Hattula and Peränen, 2000) and to protein-protein interaction predictions Htt might interact with both adapter proteins. We confirmed this interaction with both proteins and detected lower OPTN-Htt interaction after depolarization only when Htt was carrying the mutant polyQ tract (**Fig. 41A-B**). Moreover, NDP52-Htt interaction upon mutant polyQ presence was below the detection threshold (**Fig. 41B**), while NDP52 expression was detected by immunofluorescence in both ST-Q7 and ST-Q111 cells (**Fig. 41C**). Therefore, we confirmed that the lack of PLA signal is due to an impairment in NDP52-Htt interaction and not a loss of NDP52 expression upon mutant Htt. These results showed that the interaction between the two essential adapters of mitophagy and Htt is influenced by the number of glutamines in the polyQ tract and, in the case of ND52, the interaction is totally abolished when mutant Htt is present.

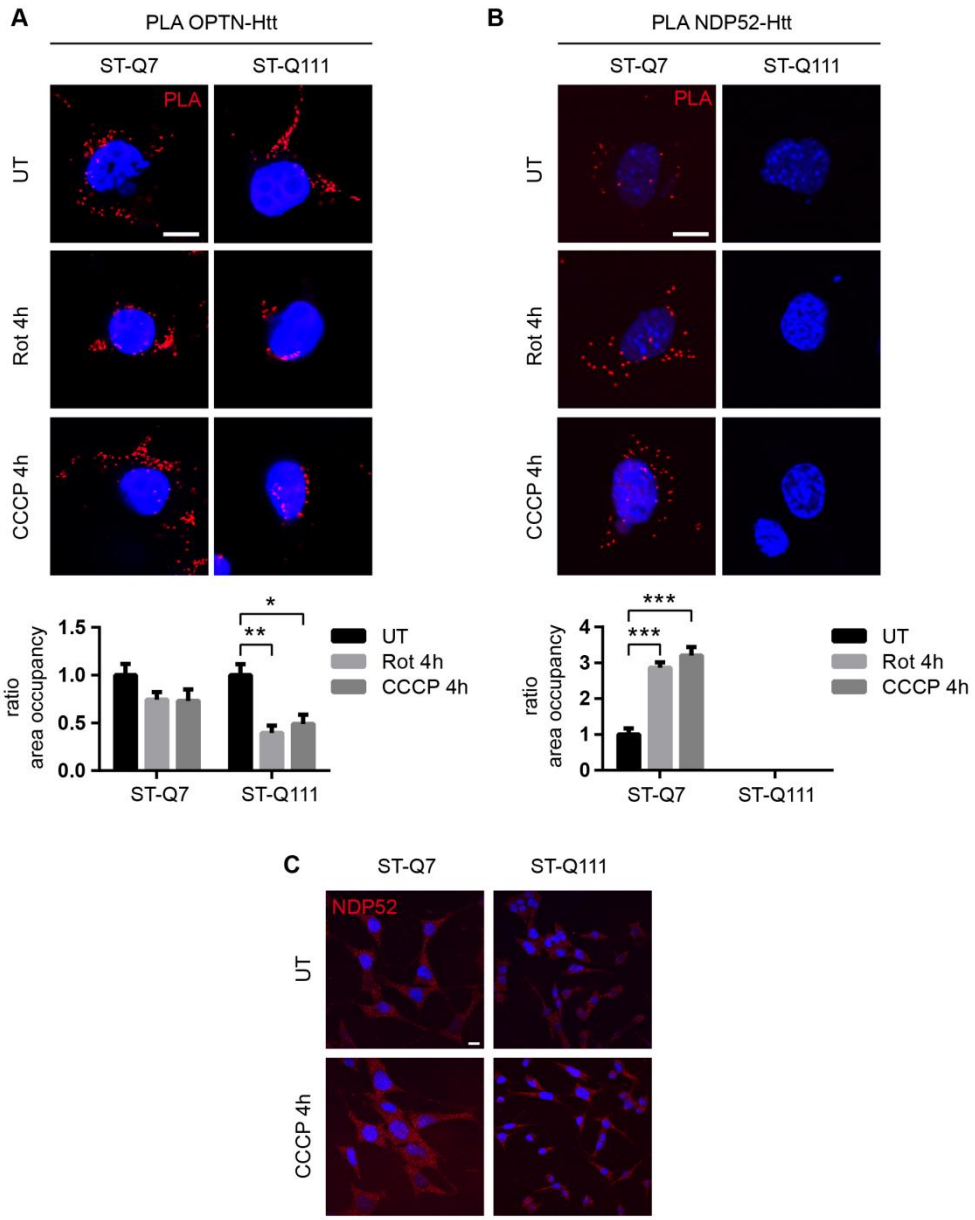

Figure 41. polyQ tract in mutant Htt affects the scaffolding role of Htt during mitophagy.

(**A**) OPTN-Htt interaction detected by PLA in ST-Q7 and ST-Q111 cells untreated (UT) or treated with rotenone (Rot, 1 µM, 4h) or CCCP (10 µM, 4h). 20 to 30 cells were analyzed per condition. (**B**) NDP52-Htt interaction detected by PLA in ST-Q7 and ST-Q111 cells UT or treated with Rot (1 µM, 4h) or CCCP (10 µM, 4h). 38 to 46 cells were analyzed per condition. (**C**) Representative images of NDP52 immunostained ST-Q7 and ST-Q111 cells UT or treated with CCCP (10 µM, 4h). (**A-C**) Scale bars: 10 µm. (**A-B**) PLA interaction was quantified as a ratio of area occupancy by the PLA signal represented as the fold change compared with ST-Q7 untreated condition. Data are presented as mean ± s.e.m. * $P < 0.05$, ** $P < 0.01$, *** $P < 0.001$ after two-way ANOVA test followed by Tukey's post hoc test.

4.2.6 polyQ tract in Htt affects the interaction of mitophagy receptors with the nascent autophagosome

As last step of substrate recognition during mitophagy, receptors interact directly and recruit LC3-II, the main component of the autophagosome membrane, allowing the elongation of the autophagosome membrane around mitochondria. Previously, it was shown that p62 could interact with the Htt complex (Rui et al., 2015) and the presence of the mutant form could interfere with this interaction (Martinez-Vicente et al., 2010). To analyze if the previously observed alterations in the interaction between Htt and the receptors could finally have a consequence in the ability of the receptors to recruit LC3-II, we studied the interaction of these receptors with LC3-II during mitophagy induction. First, we analyzed the interaction between the selective autophagy receptors p62 and NBRI with LC3-II by immunoprecipitation, since the level of these proteins allowed this method. By co-immunoprecipitation in ST-Q7 and ST-Q111 cells, we observed that the presence of mutant Htt dramatically impairs p62 and NBRI interaction with LC3-II (**Fig 42A**), further confirming the pivotal role of Htt as an scaffold for several components in the autophagy process. To take a closer look in the mitophagy process, we analyzed by PLA the interaction between the two essential mitophagy receptors OPTN and NDP52 with LC3. Upon depolarization, OPTN-LC3 interaction and NDP52-LC3 interaction was increased in differentiated ST-Q7 cells. Conversely, the presence of mutant polyQ tract hampered OPTN-LC3 interaction and decreased NDP52-LC3 interaction (**Fig. 42B and C**). These data are in agreement with the previous results showing both decreased interaction of ULK1 with the scaffolding Htt protein (**Fig. 39B**) as well as decreased interaction of Htt with OPTN and NDP52 (**Fig. 41A and B**). These results further indicate that the polyQ presence impairs the scaffolding ability of Htt, which facilitates autophagy receptors interaction with the nascent pre-autophagosomal structure.

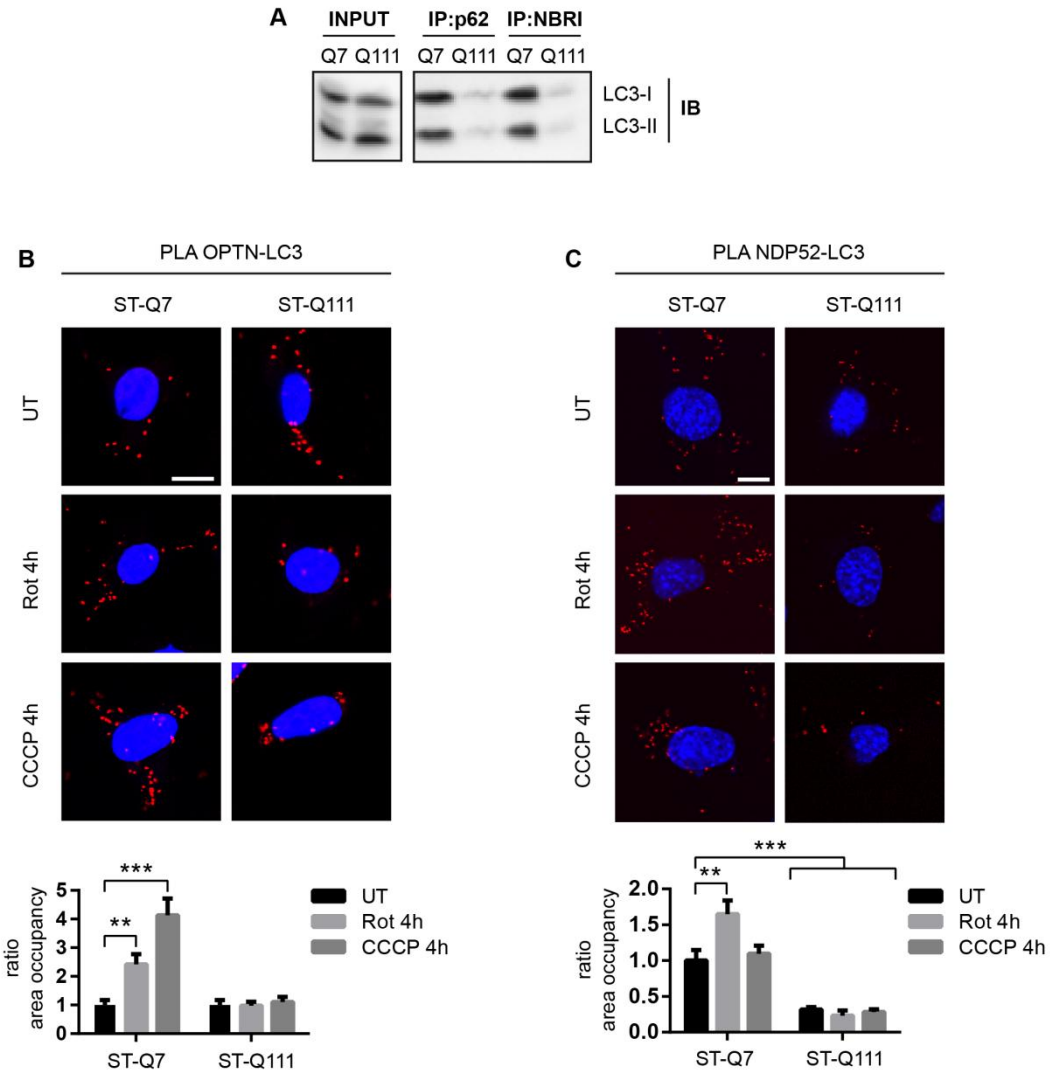

Figure 42. polyQ tract in Htt affects mitophagy receptors interaction with the nascent autophagosome.

(**A**) Representative images of immunoprecipitation of p62 and NBR1 in ST-Q7 and ST-Q111 and immunoblotting against LC3-II. (**B**) OPTN-LC3 interaction detected by PLA in ST-Q7 and ST-Q111 cells untreated (UT) or treated with rotenone (Rot, 1 µM, 4h) or CCCP (10 µM, 4h). 25 to 38 cells were analyzed per condition. (**C**) NDP52-LC3 interaction detected by PLA in ST-Q7 and ST-Q111 cells UT or treated with Rot (1 µM, 4h) or CCCP (10 µM, 4h). 25 to 45 cells were analyzed per condition. (**B-C**) Scale bars: 10 µm. PLA interaction was quantified as a ratio of area occupancy by the PLA signal represented as the fold change compared with ST-Q7 untreated condition. Data are presented as mean ± s.e.m. * P < 0.05, ** P < 0.01, *** P < 0.001 after two-way ANOVA test followed by Tukey's post hoc test.

4.2.7 Impaired mitophagy leads to accumulation of damaged mitochondria in ST-Q111 cells

At this point, we have already described an important impairment in several steps during mitophagy initiation when mutant Htt is present, thus affecting the ability of the neuron to respond to mitophagy induction upon depolarization. As a consequence of this lower efficiency of mitophagy after depolarization, an accumulation of damaged mitochondria can be observed in differentiated ST-Q111 neurons. The ratio between healthy mitochondria and total mitochondrial pool can be detected by using a mitochondrial probe sensible to mitochondrial membrane potential like TMRM, in parallel with a mitochondrial probe like MitoTracker® Deep Red as control of total mitochondria (healthy and unhealthy). The TMRM signal corrected by total amount of mitochondria with MitoTracker® Deep Red, indicate the amount of healthy mitochondria remaining in the cell after depolarization. We observed that this was higher in the control cells (ST-Q7) while mutant cells (ST-Q111) showed lower capacity to properly turn over damaged mitochondria upon depolarization. Consequently, differentiated ST-Q111 cells presented lower rates of healthy mitochondria after 24 hours of mild or acute depolarization (**Fig. 43A**).

Furthermore, we analyzed the mitochondrial function by measuring the oxygen consumption ratio (OCR) of differentiated striatal cells under basal conditions and after a respiration stress by using Seahorse technology. Initially, both differentiated neuronal cell lines presented similar basal respiration levels, which is strongly controlled by ATP turnover and to a lesser extent by substrate oxidation and proton leak. Inhibition of ATP synthase (complex V) with oligomycin caused an expected decrease in both ST-Q7 and ST-Q111 cells without significant differences. Addition of the uncoupling agent CCCP collapsed the proton gradient and caused an increase in the OCR until the maximum respiration rate is achieved. ST-Q111 cells clearly showed a lower rate of maximal respiration and lower spare capacity (ability of the cell to respond to increased energy demand) compared with control cells. These results indicate that mitochondria from ST-Q111 cells are bioenergeticaly less active and have lower ability to respond to an increased energy demand (**Fig. 43B and C**).

If cells were mildly depolarized with rotenone 4 hours and recovered for 24 hours, the remaining mitochondria from mutant ST-Q111 cells presented lower basal respiration, lower ATP production, lower maximal respiration and lower spare capacity compared to control cells under the same treatment (**Fig. 43D**). This assay clearly shows that as a consequence of inefficient induced mitophagy, the remaining pool of mitochondria present in the cell are

not fully healthy mitochondria, thus contributing to the general mitochondrial dysfunction observed in HD.

One of the main consequences of the cell inability to properly eliminate damaged mitochondria is the increase of reactive oxygen species (ROS), produced at least in part from the damaged mitochondria and detected by the fluorescent probes CellROX® Green (**Fig. 43E and F**) and CM-H_2DCFDA (**Fig 43G**). Both probes are cell-permeant and non-fluorescent in the reduced state, but upon oxidation with intracellular free radicals both reagents exhibit strong fluorescence. CellROX® is known to detect $^{\bullet}O_2^-$ (superoxide radical) and $OH^{\bullet}$ (hydroxyl radical) and CM-H_2DCFDA can react with several ROS including hydrogen peroxide, hydroxyl radicals and peroxynitrite. Data showed increased ROS levels in ST-Q111 cells compared with ST-Q7 cells, which might accumulate in part due to the decreased induced-mitophagy rate observed in these cells.

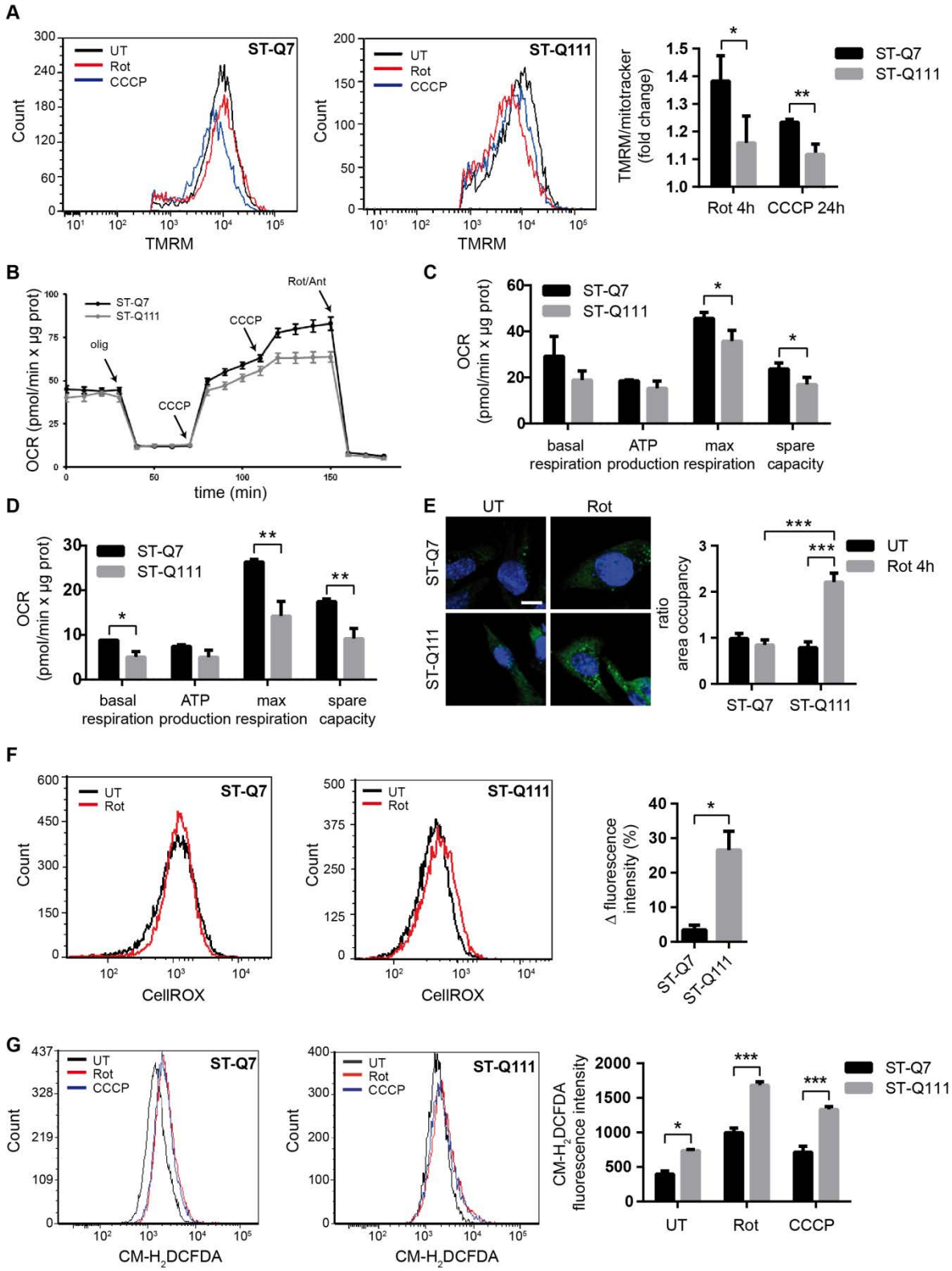

Figure 43. Impaired mitophagy leads to the accumulation of damaged mitochondria in ST-Q111 cells.

(**A**) Flow cytometry was used to determine TMRM and MitoTracker® DeepRed staining in ST-Q7 and ST-Q111 cells untreated (UT) or treated with rotenone (Rot, 1 µM, 4h) or CCCP (10 µM, 4h). Cells were added chloroquine with the rotenone and CCCP treatments (60 µM; n=3 independent

experiments). Quantification is represented as fold change compared with the corresponding UT condition. (**B**) Seahorse XF-24 instrument analysis of oxygen consumption rate (OCR). Mitochondrial respiration reflected by OCR levels was detected in ST-Q7 and ST-Q111 cells under basal conditions or following the addition of oligomycin (olig, 1 µM), the uncoupler CCCP (CCCP, 0.5 µM each time) and Rotenone and Antimycin (Rot/Ant, 1 µM) at the indicated times (n=3 independent experiments). (**C**) The rates of basal respiration, ATP production, maximal respiration and spare capacity were quantified by normalization of OCR level to the total protein OD values (n=3 independent experiments). (**D**) The rates of basal respiration, ATP production, maximal respiration and spare capacity in ST-Q7 and ST-Q111 cells after 4h of rotenone treatment and 24h of recovery were quantified by normalization of OCR level to the total protein OD values. (**E**) Representative images of CellROX® Green immunostained ST-Q7 and ST-Q111 cells UT or treated with Rot (1 µM, 4h). Scale bar: 10 µm. Intracellular ROS levels were quantified as a measure of the area fraction occupied by CellROX® staining and represented as the fold change compared with ST-Q7 UT. 44 to 80 cells were analyzed per condition. (**F**) Flow cytometry was used to determine CellROX® intensity in ST-Q7 and ST-Q111 cells UT or treated with Rot (1 µM, 4h). Intracellular ROS levels were quantified as a measure of CellROX® intensity and represented as the ratio between rotenone and untreated conditions (n=3 independent experiments). (**G**) Flow cytometry was used to determine CM-H_2DCFDA staining in ST-Q7 and ST-Q111 cells UT or treated with Rot (1 µM, 4h). Intracellular ROS levels were quantified as a measure of CM-H_2DCFDA intensity and represented as mean fluorescence intensity (n=3 independent experiments). (**A-G**) Data are presented as mean ± s.e.m. * $P < 0.05$, ** $P < 0.01$, *** $P < 0.001$ after (A; E; G) two-way ANOVA test followed by Tukey's post hoc test (C-D; F) Student's t test.

DISCUSSION

5 Discussion

PD and HD are two neurodegenerative disorders with some common traits. Both are movement disorders marked by aberrant protein aggregation in the brain, though the specific proteins that aggregate and types of neurons affected differ between them. Moreover, they can be viewed as mirror-images of each other; while in HD GABAergic medium spiny neurons in the striatum are the neuronal type that neuropreferentially degenerate, they are spared in PD. On the contrary, dopaminergic neurons that selectively degenerate in PD are spared in HD. Even though they have been described more than 100 years ago, there are still not current therapies that can modify the progression of both diseases, and drugs available only target the symptoms but not the neuodegenrative process itself. To develop a treatment that has an impact on the course of these diseases, it is necessary to understand the pathways that lead to cell dysfunction and death. Proteostatic defects, neuroinflammation, calcium dysregulation and mitochondrial dysfunction are some of the common pathways that underlie the pathology in these two neurodegenerative disorders. Nonetheless, effective drugs for neuroprotection may be applicable at all stages of the disease, but would rather be best started in the earliest phase detectable (**Fig. 44**). A paradigmatic example is the use of antiapoptotic drugs as a treatment for PD. Caspase inhibitors such as CEP-1347 and THC346 had very promising results in preclinical trials (Andringa et al., 2003; Saporito et al., 1999) but failed in clinical trials (Olanow et al., 2006; Parkinson Study Group PRECEPT Investigators, 2007). This could be explained because anti apoptotic drugs act too late in the degeneration process to have a disease-modifying effect. Therefore, we strongly believe that we have to focus on dysfunction taking place earlier in the deleterious cascade in order to find new therapeutic targets that could have a chance to slow or prevent the progression of neurodegeneration. Interestingly, the role of mitochondrial quality control in neuronal health is a recently growing subject for investigation, and it has been suggested to be central to maintain healthy mitochondria. For that reason, we have focused on two different mitochondrial quality control mechanisms that have not been studied in depth in PD and in HD. Whereas mutant Htt had previously been reported to impair mitochondrial protein import, less is known in the field of PD. In contrast, mitophagy has been extensively studied in the context of PD, due to the roles of PINK1 and Parkin proteins, while there is much less data about the effect of polyQ expansion on Htt's role in mitophagy.

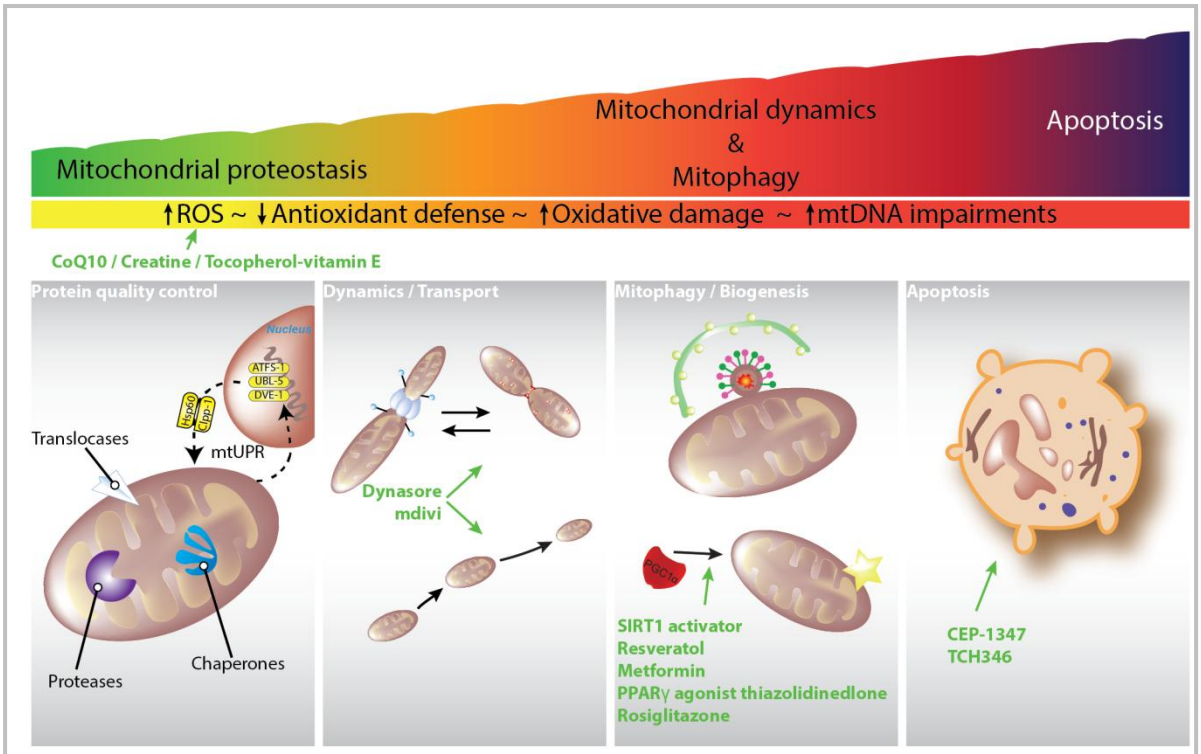

Figure 44. Schematic diagram depicting an hypothesized scenario responsible for mitochondrial dysfunction in PD and HD.

ROS are continuously produced *in vivo* by all body tissues. The presence of mitochondrial translocases, chaperones and proteases within the mitochondrial matrix and intermembrane space acts as a first line of defense against unfolded and oxidized soluble proteins. Mitochondrial unfolded protein response (mtUPR) is believed to be activated by cytosolic transcription factors (ATFS-1, UBL-5, DVE-1) which upregulate the expression of genes involved in mitochondrial proteostasis. To maintain a healthy network, mitochondrial are dynamic and can fuse, divide and move. Once the accumulation of mitochondrial defects exceeds a certain threshold, patches of mitochondria can be removed through the generation of mitochondrial-derived vesicles (MDVs), which transit to the lysosome. Upon complete mitochondrial dysfunction, the entire organelle can be targeted for degradation via mitophagy. When none of the rescue strategies are able to restore mitochondrial function, the cell enters in its ultimate destiny, apoptosis. Clinical trials using general caspase inhibitors such as CEP-1347 and TCH346 failed, maybe because it was too late in the process to intervene. Other compounds were tested in clinical trials, from fission inhibition using mdivi to PPARγ activation, but none were able to show clear treatment benefits. Interestingly, the role of mitochondrial quality control in neuronal health is a recently growing subject for investigation, indicating that mitochondrial quality control might be central to maintain healthy mitochondria.

5.1 Chapter I

Our work has focused on better characterize the mitochondrial protein import system in the context of PD with the aim of finding a putative therapeutic target that could be modulated. We have found that complex I inhibition leads to a mitochondrial protein import deficit, both *in vitro* and *in vivo*. This deficit is characterized by downregulation of key translocases protein levels together with decreased presence of nuclear-encoded mitochondrial proteins. This results in mitochondrial protein aggregation, hampered mtUPR activation, increased ROS production and loss of mitochondrial membrane potential. Overexpression of TOM20 on complex I inhibited cells restored mitochondrial protein import activity but only partially rescued mitochondrial membrane potential, ROS levels and cell death *in vitro*. In the MPTP mouse model, stereotaxically-delivered TOM20 did not restore mitochondrial protein import and could not protect against MPTP-induced neurodegeneration, [even exerting increased degree of nigrostriatal system demise]. Overexpression of TIM23 on complex I inhibited cells restored mitochondrial protein import but exhibited a milder effect *in vitro* compared with TOM20 regarding membrane potential, ROS production and cell death. Overexpression of TIM23 in the MPTP-mouse model was able to reestablish mitochondrial protein import and exerted a mild protection against degeneration of TH-positive neurons.

Mitochondrial protein import was previously described to be impaired in the context of HD. Yano *et al*. found that mutant Htt binds to TIM23 complex in the IMM in isolated brain mitochondria. As a consequence, protein import into mitochondria was inhibited in a manner dependent on the concentration and length of the Htt polyglutamine stretch. Synaptosomal mitochondria, a specific group of mitochondria with high energetic demands, from R6/2 mice exhibited markedly compromised protein import even at early disease stages, in comparison with non-synaptosomal mitochondria, suggesting that this defect is one of the earliest alterations present in the course of the disease. Furthermore, overexpression of the major subunits of TIM23 complex (TIM23, TIM50 and TIM17A) was able to improve metabolic health and neuronal survival in cortical neurons expressing mutant Htt (Yano et al., 2014). In the field of PD, α-synuclein has also been reported to impair mitochondrial protein import system. Devi *et al.* described a cryptic mitochondrial targeting sequence in α-synuclein and found that α-synuclein was imported into the mitochondria through the TOM complex. A component of the complex, TOM40, was reported to directly interact with α-synuclein. Mitochondrial α-synuclein accumulation was correlated with decreased complex I activity and elevated ROS in human fetal dopaminergic primary neuronal cells. Furthermore, mitochondria isolated from SN of PD patients presented higher levels of α-synuclein compared to control mitochondria and this correlated as well with decreased complex I

activity (Devi et al., 2008b). Some years after, TOM40 levels were found specifically decreased in SN from PD patients and α-synuclein transgenic mice. *In vitro* and *in vivo* overexpression of α-synuclein led to TOM40 downregulation, decreased mitochondrial mass and increased oxidative damage, whereas TOM40 overexpression decreased α-synuclein protein levels and reverse α-synuclein-induced mitochondrial toxicity (Bender et al., 2013). Shortly after, Di Maio *et al.* uncovered the presence of a mitochondrial protein import deficit in the context of PD. In their work, they observed decreased NDUFS3 staining in the rotenone rat model, in the AAV2-viral mediated overexpression of human α-synuclein rat model and in human PD brain samples. Upon analysis of different α-synuclein species on mitochondrial protein import, an interaction between those species and TOM20 was unraveled, in contradiction with the previously reported α-synuclein-TOM40 link. Specifically, some α-synuclein modified species interacted with TOM20 and prevented TOM20-TOM22 normal binding. In contrast to previous work, Di Maio and coworkers failed to find a specific α-synuclein-TOM40 interaction using PLA technology (Di Maio et al., 2016). To sum up, the few reports about mitochondrial protein import in PD have linked those defects to α-synuclein localization to mitochondria. In fact, α-synuclein has long been reported to interact with mitochondria in different experimental settings (Devi et al., 2008b; Li et al., 2007; Martin et al., 2006; Parihar et al., 2008) although its exact localization, binding mechanisms and dependence on mitochondrial membrane potential remains a matter of debate. Besides, whether α-synuclein hampers protein import into mitochondria through TOM40 or TOM20 interaction is also controversial. Therefore, there is a need to clarify the mechanisms leading to impaired mitochondrial protein import in a context of mitochondrial dysfunction independent of α-synuclein. This is the reason why we have worked with complex I deficient mice and neuronal cultures.

Here, we have not only characterized the expression of different nuclear-encoded mitochondrial proteins as a read-out of mitochondrial protein import *in vivo*, but also analyzed some key translocases proteins, important for the system. Moreover, we have controlled for mitochondrial mass changes to ensure that we were observing decreases in mitochondrial protein import and not only a reduction in mitochondrial mass. Regarding TIM23 and TOM20 protein levels, we have found both of them decreased in all the models analyzed (MPP^+-treated cells and MPTP-treated mice) and also in *post-mortem* human brain samples from PD patients. However, a previous study only found a specific decrease in TOM40 but not in TOM20 (Bender et al., 2013) in human samples, so more data is needed to clarify which of the components of the mitochondrial protein import system are actually hampered in the human context. We think that whereas working with *post-mortem* tissue strengthens the value of the results, caution must be taken to extrapolate those results. This

is because *post-mortem* samples likely reflect the end-stage of the disease and some alterations present in this kind of samples could be secondary thus, not reflecting the exact disease phenotype on a cellular level. For such, we propose to use other human-derived samples, as fibroblasts or iPSC cells, which in turn can be reprogrammed to neurons or other cellular types. This kind of samples are available at different stages of the disease and can be used to study mechanistic details, to elucidate signaling pathways and to identify novel therapeutic strategies (Zhang et al., 2017).

We have used complementary assays to characterize the consequences of complex I inhibition in BE(2)-M17 cells on mitochondrial protein import function. For such, we have analyzed the intramitochondrial processing and fluorescence intensity of an exogenous protein (mitoGFP) and also we have analyzed the presence of nuclear-encoded mitochondrial endogenous proteins. To assess whether the inhibition of mitochondrial protein import was direct, we isolated mitochondria an analyzed the effect of MPP^+ treatment on the import of OTC. With all these alternative approaches we have shown that complex I inhibition leads to a significant mitochondrial protein import deficiency.

We have also analyzed OXPHOS protein levels upon MPP^+ intoxication. Since MPP^+ is a complex I inhibitor (Cleeter et al., 1992) it impairs OXPHOS activity (Desai et al., 1996). Moreover, we have observed reduced protein levels of NDUFB8, SDHB, UQCRC2 and COX II, similar to other report also showing decreases in proteins from complex I, III and IV and no effects on complex V upon MPP^+ intoxication. Interestingly enough, authors show how the exposure to a low-dose of MPP^+ sustained over time specifically impairs mitochondrial translation activity in cells (Zhu et al., 2012). Therefore, is very tempting to speculate that in our model MPP^+ is exerting a double detrimental effect; on one side disrupts the mitochondrial protein import hampering the entry of the nuclear-encoded mitochondrial proteins, and, on the other side, downregulates the translation of the mitochondrial-encoded proteins. Moreover, MPP^+ intoxication also leads to protein misfolding inside mitochondria as shown by increased levels of detergent-insoluble subunits of respiratory chain complexes. Mitochondrial stress is able to elicit a response called mtUPR which is characterized by the transcriptional upregulation of mitochondrial proteases and chaperones (Fiorese et al., 2016; Haynes et al., 2010; Zhao et al., 2002). Indeed, we observed a ~2-fold increase in CLPX and HSP9 chaperones mRNA which is not translated into increased protein levels. It is apparent that import defects might impair the translocation of proteases and chaperones of mtUPR into the mitochondria and the subsequent mtUPR activation. Besides, HTRA2 protease deficiency in mice leads to protein misfolding in the mitochondria (Moisoi et al., 2009b) which could exemplify that a deficit in the mitochondrial quality control could lead to mitochondrial

protein aggregation. A recent report, though, has put into question the beneficial effects of long lasting mtUPR activation in the context of PD. In a *C. elegans* model of human α-synuclein authors observed that mtUPR response is highly activated. However, this was associated with enhanced dopaminergic neurotoxicity (Martinez et al., 2017b), highlighting the potential detrimental role of prolonged mtUPR activation. In fact, the current view encompasses the mtUPR response in an integrated mitochondria stress response (ISRmt) (Suomalainen and Battersby, 2017). This stress response leads to the activation of transcripts that encode proteins that are involved in the regulation of lipid and glucose metabolism, as well as the anabolic one-carbon cycle (Bao et al., 2016; Nikkanen et al., 2016). In a mouse model of mitochondrial myopathy, ISRmt is controlled by mTORC1 in muscle and rapamycin treatment downregulated all components of ISRmt and reversed the progression of the disease (Khan et al., 2017). This exemplifies that mitochondrial dysfunction can elicit an ISRmt, which upon long-term induction can have a detrimental effect.

To our knowledge, this is the first time that components of the mitochondrial protein import system are modulated as a potential target to prevent neurodegeneration in PD. Previous studies have focused on the study of the mechanism by which α-synuclein impairs import (Di Maio et al., 2016) or have used models in which there is no overt neurodegeneration (Bender et al., 2013). Knockdown of TOM40 or TIM23 in primary cortical and striatal neurons caused increased cell death (Yano et al., 2014), reinforcing the notion that mitochondrial protein import is essential for neuronal survival. We have used different strategies to increase translocases protein levels *in vitro*: transient overexpression of TIM23- or TOM20-plasmids and generation of stable cell lines. Upon transient delivery of TIM23 or TOM20 plasmids, we observed an increased cell death at basal levels, which could be due to a massive protein overexpression. Upon MPP^+ treatment there were no differences in cell death between vehicle, TIM23- or TOM20-overexpressing cells. Another report in which TIM23 was overexpressed did not show any basal toxicity. However, authors co-overexpressed TIM23 with TIM50 and TIM17A through a lentiviral-mediated strategy (Yano et al., 2014), which generally has better transfection efficiency rates and leads to sustained but lower protein expression levels. In fact, in the case of TOM20, when we used the stable cell line to assess MPP^+-induced cell death, we observed a partial protection against cell death (**Fig. 45**).

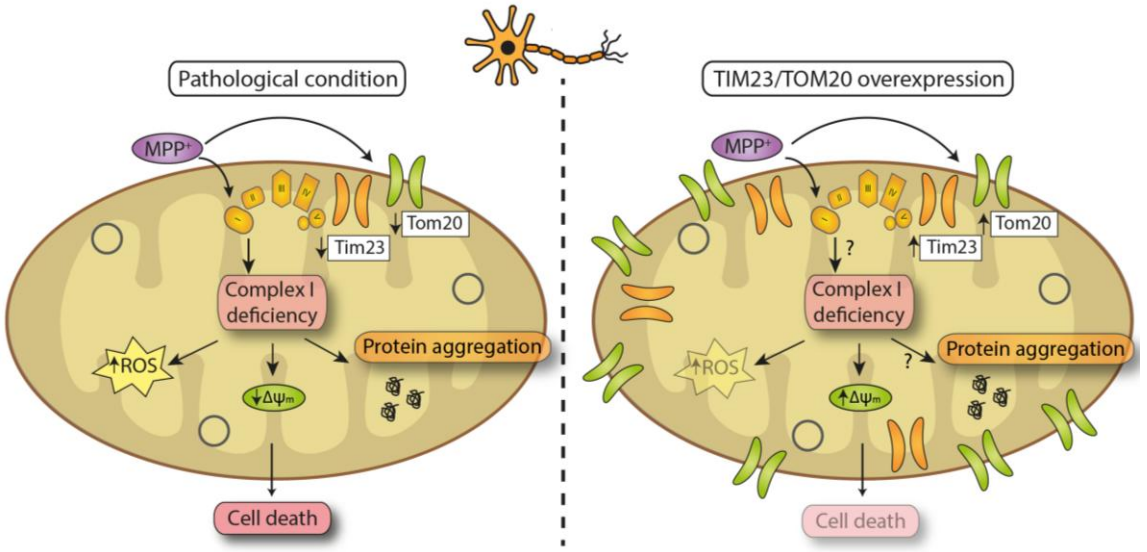

Figure 45. Schematic representation of TIM23/TOM20 protective role in MPP+- treated cells.

Pathological condition: MPP^+ intoxication *in vitro* leads to complex I deficiency and downregulation of TIM23 and TOM20 levels through an unknown mechanism. Upon complex I-deficiency, there is a loss of protein import and mitochondrial membrane potential ($\Delta\psi_m$) together with an increase in ROS production and protein aggregation. All together, this leads to mitochondrial dysfunction and cell death. **TIM23/TOM20 overexpression** partially reduces ROS production and restores mitochondrial protein import and membrane potential, possibly contributing to reduce cell death. We have not assessed complex I activity or protein aggregation upon TIM23/TOM20 overexpression (indicated by question marks).

Our studies have also focused on *in vivo* modulation of mitochondrial protein import system on PD-context. For such, we stereotaxically delivered AAV2/9-hTIM23 or AAV2/9-hTOM20 prior to the intoxication with the parkinsonian neurotoxin MPTP. TIM23 delivery *in vivo* restored mitochondrial import and exerted a slight degree of neuroprotection. Strikingly, TOM20 overexpression did not restore mitochondrial protein import activity nor protect against MPTP-induced neurodegeneration. Indeed, we observed even more cell death compared with MPTP-intoxication alone. Moreover, upon transient TOM20 overexpression but not TIM23, mitochondria appeared hyperfused and clusered around the nucleus. This effect on mitochondrial morphology was already reported by Yano and collaborators, showing that the glutamine-rich segment of TOM20 is essential for perinuclear mitochondrial aggregation (Yano et al., 1997). Authors also analyzed the structure of the mitochondrial aggregates and reported that they are in fact composed of individual round-shape mitochondria, confined to the aggregates but not fused (Yano et al., 1998). Importantly, TOM20 overexpression in COS-7 cells is linked to increased mitochondrial protein import

(Yano et al., 1997, 1998), in the same way that TOM20 overexpression in our cellular model also stimulates mitochondrial import, indicating that overexpression of only one component of the receptor complex may result in import stimulation. Intriguingly, authors reported that the same glutamine-rich regions that seemed responsible for mitochondrial aggregation are also essential for the stimulation of mitochondrial protein import (Yano et al., 1998).

However, *in vivo* results failed to show TOM20-mediated restoration on protein import. It is plausible that the long-lasting overexpression of TOM20, leading to high levels of protein expression *in vivo*, could explain its toxicity. Indeed, AAV2/9-TOM20 overexpressing SN neurons display mitochondrial aggregation. Aggregation and perinuclear clustering of mitochondria has been observed in relation to some forms of apoptotic cell death (De Vos et al., 1998; Suen et al., 2000; Yee et al., 2009) and also upon Bax (Desagher and Martinou, 2000), Bim (Puthalakath et al., 1999) and Bid (Li et al., 1998) induction. Moreover, perinuclear mitochondrial clustering is also present during the mitophagy process upon Parkin translocation to the mitochondria (Okatsu et al., 2010). Thus, we can hypothesize that the observed perinuclear mitochondrial clustering correlates with the increased cell death observed upon AAV2/9-hTOM20 overexpression. However, the exact mechanism by which TOM20 overexpression *in vivo* induces cell death is unclear. In any case, the contradicting results found here also pose a critic to the current PD models. In general, none of the up-to-date models can recapitulate all the features present in PD. Models can represent some aspects of PD pathology and the choice of the model will depend on what we want to study. In our case, we have worked with an *in vitro* model, the BE(2)-M17 dopaminergic cell line intoxicated with MPP^+, and an *in vivo* model, the MPTP mouse model. MPP^+ and MPTP have already demonstrated that cause mitochondrial dysfunction and cell death (Bové and Perier, 2012). We have moved from the mechanistic characterization of mitochondrial protein import impairment *in vitro*, towards an *in vivo* model because we wanted to study whether restoration of mitochondrial protein import through TIM23 and TOM20 overexpression could represent a therapeutic target in a more physiologic environment, in which several cell types are present and interact with each other. Even though we had promising results *in vitro* for both TIM23 and TOM20 to prevent cell death, this was partially attenuated in an *in viv*o environment (**Fig. 46**), highlighting the need for any therapeutic target to be tested in the context of a whole animal and not just *in vitro*. It is true, though, that even very promising therapies that have worked in different *in vivo* models have failed in clinical trials. Hence, there is an urgent need to fine-tune our current *in vivo* models in order to facilitate the translation of potential therapies to the clinic.

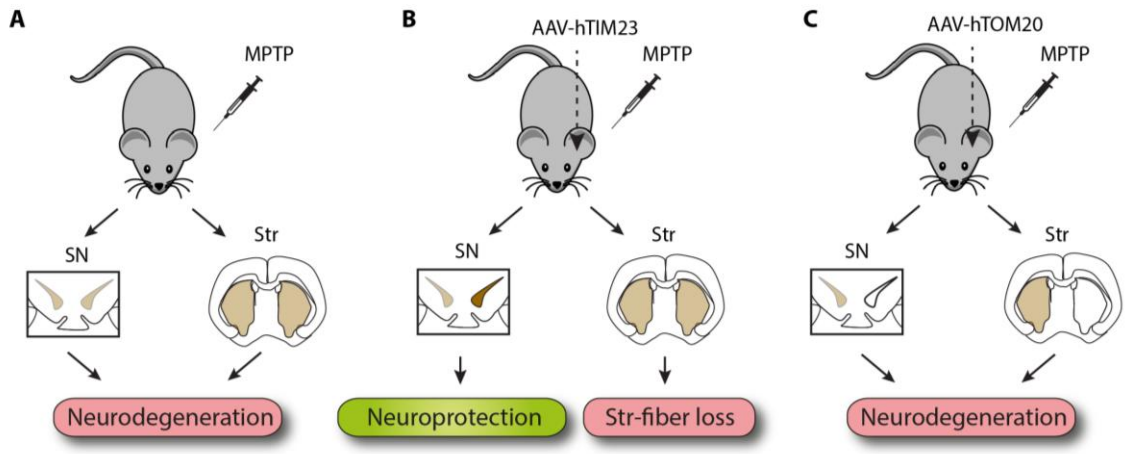

Figure 46. Schematic representation of the dopaminergic nigrostriatal system integrity upon different genetic manipulations in MPTP-treated mice.

A) MPTP treatment leads to striatal fiber loss and degeneration of SN TH-positive neurons, as represented with light brown color. **B**) AAV-hTIM23 overexpression in the right side of MPTP-intoxicated mice, only protects mildly against degeneration of SN TH-positive neurons (represented in bright brown color) but not against striatal-fiber loss. **C**) AAV-hTOM20 overexpression in the right side of MPTP-intoxicated mice does not protect against doapaminergic nigrostriatal system degeneration. Moreover, AAV-hTOM20 delivery leads to increased cell death in comparison to MPTP-intoxication only, as represented in white color.

In summary, our results have identified the disruption of mitochondrial protein import system as a key pathogenic event in the context of PD. Even though overexpression of single subunits of the translocases system has not been enough to fight against neurodegeneration, we strongly think that an strategy aimed to target several key elements in the pathway could have a major impact. Thus, identification of potential drugs/compounds able to boost mitochondrial protein import activity could represent a potential therapeutic strategy in the field of PD.

5.2 Chapter II

In the second chapter we have focused on the study of neuronal mitophagy in the context of HD. We have shown that in differentiated striatal cells and other neuronal cell lines, induced mitophagy is not driven by Parkin translocation to the mitochondria. Additionally, in the presence of mutant Htt, lower levels of induced mitophagy are observed, most likely because endogenous Htt participate as an scaffold protein in different steps of the mitophagy mechanism and the presence of the polyQ tract in mutant Htt impairs the following processes: (i) the ULK1 activation after release from the mTORC1 complex, (ii) the formation of the nucleation complex (beclin 1-Vps15-Vps34), (iii) the interaction between Htt and mitophagy adapters, (iv) the interaction of mitophagy adapters and the autophagosome membrane. As a consequence of the hampered mitophagy, damaged mitochondria accumulate leading to deficits in mitochondrial respiration and increased ROS production, which amplifies the cellular damage.

Our study is one of the few studies that has aimed to characterize mitophagy under conditions as close as possible to the physiological ones. First, we have used full-length Htt protein instead of exon1-constructs to study not only the gain of toxic function, due to the presence of the polyQ expansion, but also the loss of normal full length Htt function as an scaffolding protein due to the presence of the polyQ tract. The observed alterations in Htt interactions during induced mitophagy can only be achieved with full-length Htt, since most of the protein-protein interactions modulated by Htt cannot be studied just with Htt-exon1 constructs. As HD is regarded as a primarily toxic gain-of-function disease, most of the studies only use Htt-exon1 constructs. However, increasing lines of evidence (Schulte and Littleton, 2011; Van Raamsdonk et al., 2005; Zuccato et al., 2003) suggest a loss-of-function component in the pathology of HD, since wild type Htt has important activities in neurons and loss of these activities may play a role in HD. For instance, homozygous Htt knockout mice are embryonic lethal at pre-gastrulation stage (Duyao et al., 1995; Nasir et al., 1995; Zeitlin et al., 1995) while heterozygous knockout still show some physical and behavioral alterations (Nasir et al., 1995). These evidences have important consequences, regarding the need to study wild type Htt function and also therapeutic implications.

Second, we also have used differentiated striatal cells, since in contrast with dividing cells, neurons require basal and continuous autophagy activity for survival (Hara et al., 2006; Komatsu et al., 2006). Mitophagy, as one type of selective autophagy, is also essential for neurons to assurance the maintenance of the healthy mitochondrial pool and properly eliminate the damaged or old mitochondria that become a source of ROS and ultimately

contribute to cell death (Amadoro et al., 2014; Bolaños et al., 2010; Oliveira, 2011). Thus, is extremely important to study mitophagy and the consequences of mitophagy impairment in differentiated, non-dividing neurons. Third, most of the works studying mitophagy have employed artificial introduction, overexpression or deletions of the different proteins involved in this mechanism. Even though this approach is completely valid and has revealed crucial details of mitophagy process, when trying to reproduce these results in endogenous conditions in neurons authors have observed, instead, that other types of mitophagy might be taking place in neurons (Chu et al., 2013; Shi et al., 2014). Classically, endogenous Parkin translocation to mitochondria has not been detected in neuronal cell lines (Cai et al., 2012; Rakovic et al., 2013; Sterky et al., 2011; Van Laar et al., 2011). We have confirmed also these results in our striatal cell line. Only the artificial overexpression of Parkin together with a long-lasting and severe depolarization could reproduce the typical translocation of Parkin to mitochondria in less than 50% of differentiated striatal cells. This is in contrast to other neuroblastoma cells like SH-SY5Y and BE(2)-M17 which under these forced conditions presented almost 100% of cells with overexpressed-parkin cocalizing with mitochondria. These results suggest that the mitophagy process occurring in striatal cells might be Parkin-independent and, consequently, mitophagy probably takes place at a lower rate.

Finally, we have tried to induce mitophagy in a more subtle way. For such, we have used not only the classical m-clorophenyl hydrazone (CCCP) uncoupler to induce mitophagy, but also a mild, subtoxic rotenone concentration, which causes a more subtle mitochondrial damage. Ionophores such as CCCP, which induce a rapid and massive loss of the mitochondrial membrane potential in the entire mitochondrial pool, have been widely used to study damage-induced mitophagy (Ding and Yin, 2012; Vives-Bauza et al., 2010). However, the signaling pathways activated by CCCP treatment are ill-defined and do not reflect the mitochondrial dysfunctional state during chronic neurodegenerative disease (Grenier et al., 2013). For instance, giving the high dependence of neurons on mitochondrial respiration (Bolaños et al., 2010; Oliveira, 2011), it is not likely that a complete depolarization and degradation of the mitochondria pool might take place.

Initial work by Martínez-Vicente *et al*, described the presence of “empty autophagosomes” in HD cells, suggesting that mutant Htt impairs the cargo sequestration step, leading to inefficient cargo loading with lipid droplets and mitochondria being excluded from autophagic vacuoles (Martinez-Vicente et al., 2010). As a consequence of altered autophagy, chaperone-mediated autophagy is upregulated in HD striatal cells (Koga et al., 2011). Conversely, others argued that Htt was not required for autophagosome formation or cargo

loading. Instead, they pointed at defective autophagosome transport, which is disrupted upon polyQ presence, as the reason for undigested mitochondria, suggesting that misregulation of autophagosome transport leads to inefficient autophagosome maturation (Wong and Holzbaur, 2014). However, more recent work has unraveled the role of wild type Htt at the cargo recognition step in stress-induced selective autophagy due to its ability to act as a scaffold bringing together different proteins required for autophagy to take place (Ochaba et al., 2014; Rui et al., 2015). These works using Htt-knock out models and Htt-deletion constructs showed that endogenous Htt participates in cargo recognition by interacting with and facilitating p62 binding to ubiquitin-K63-modified cargos and LC3. Moreover, Htt also binds to ULK1, releasing its mTOR-mediated inhibition, thereby leading to its activation and interacting with Htt in a kinase-active form (Rui et al., 2015). Nevertheless, Htt is only implicated in some types of selective autophagy, such as mitophagy, aggrephagy and lipophagy and only in response to certain stresses, such as FCCP (carbonyl cyanide-4-(trifluoromethoxy)phenylhydrazone), UPS inhibition and lipotoxic stress but not starvation stress. All in all, this ability of Htt to physically interact with several partners provides structural stabilization to different protein complexes and allows the proximity required to trigger different cellular mechanisms. However, these works did not assess the consequences of the polyQ expansion in the scaffolding role of Htt, since they worked with Htt loss of function constructs and conditional knockouts.

In this thesis, our goal was to analyze in detail the mitophagy process in differentiated striatal neurons carrying wildtype and mutant Htt to understand the consequences and contribution of polyQ expansion to mitophagy mechanism (**Fig. 47**).

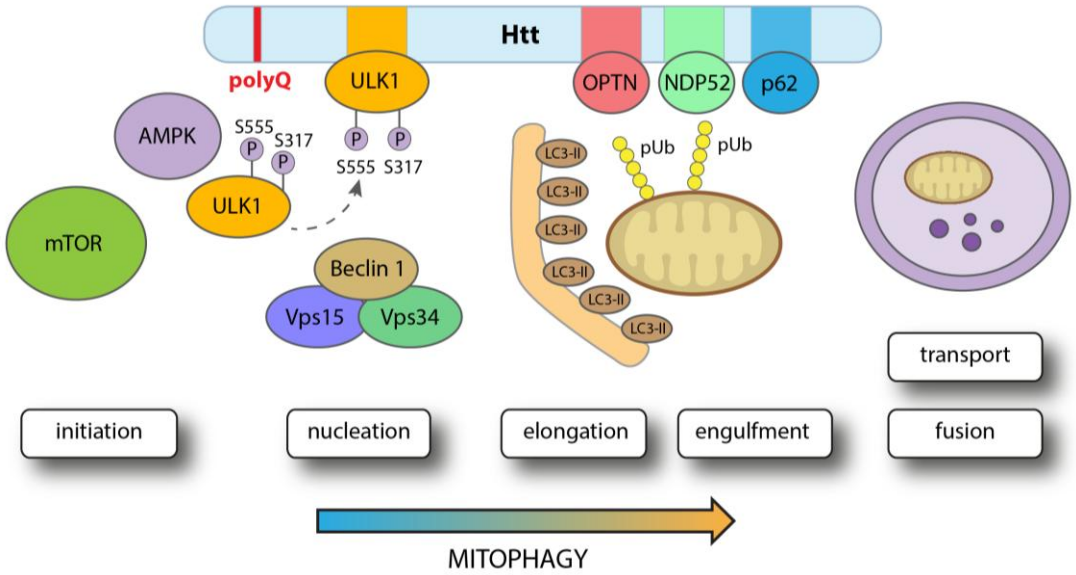

Figure 47. Schematic representation of mitophagy process with Htt acting as an scaffolding protein.

For autophagy activation, ULK1 has to be released from mTOR interaction and inhibition. AMPK phosphorylates ULK1 at S555 and S317; which acts as well as an activation signal. Htt competes with mTOR for ULK1 interaction. Moreover, the nucleation complex needs to be formed (Beclin 1-Vps15-Vps34) which activates de formation of the pre-autophagosomal structure. Damaged mitochondria are tagged with K63 ubiquitin chains that are phosphorylated (pUb). These signals in the cargo are recognized by mitophagy adapters (OPTN and NDP52) and general autophagy adapters (p62). Htt interacts with OPTN, NDP52 and p62, thus bringing together all the elements required for mitophagy to take place. Mitophagy adapters interact as well with LC3-II in the autophagosome membrane and tagged mitochondria are engulfed by autophagosomes and fused with lysosomes for degradation.

To understand the role of Htt particularly in mitophagy we analyzed different steps required for mitophagy mechanism. Despite our inability to observe Parkin translocation to mitochondria, we found that mitochondria was being ubiquitinated with the typical K-63 linkage, which signals for autophagy (Tan et al., 2008). PolyQ expansion in Htt did not interfere with this particular step, as previously reported (Khalil et al., 2015). This is in contrast with a previous report showing accumulation of ubiquitin K11, K48 and K63 chains in mouse neuroblastoma cell line and brains from R6/2 mice (Bennett et al., 2007). However, the increase in ubiquitin K63 chains *in vitro* was transient, bringing back together both observations.

One of the key proteins involved in autophagy initiation is ULK1, which has been shown to interact with Htt (Rui et al., 2015) and, in that way, release its mTOR-inactivating interaction.

Htt has been shown to have an important role in the release of ULK1 from mTORC1 by competing in the inhibitory binding of mTORC1 to ULK1. We confirmed in our neuronal model that the interaction of Htt with ULK1 is increased after the addition of mitochondrial uncouplers. On the contrary, in differentiated ST-Q111 cells, mutant Htt loses its ability to interact with ULK1 upon depolarization. This is translated in an increased ULK1-mTOR binding in mitophagy-inducing conditions and increased S757-inhibitory phosphorylation of ULK1. Another protein implicated in autophagy initiation is beclin 1. Beclin 1 forms a transient complex with Vps15 and the phosphatidylinositol 3 kinase Vps34, which generates phosphatidylinositol 3-phosphate (PtdIns3P). This complex, called the nucleation complex, is involved in autophagic vesicle nucleation (Kang et al., 2011; Kihara et al., 2001). Beclin 1 was shown to interact with the deubiquitinase ataxin 3 through its polyQ domain, thus protecting beclin 1 from proteasomal degradation. Moreover, beclin 1 binds more strongly to longer polyQ domains. In that way, Beclin 1 affinity to longer polyQ stretches displace normal binding of beclin 1 to ataxin 3 in the presence of mutant Htt, increasing beclin 1 degradation (Ashkenazi et al., 2017). Consistently, we have reported decreased interaction of beclin 1 with Vps15 in ST-Q111 cells, further confirming that the presence of mutant Htt alters different steps in mitophagy initiation.

Once mitochondria have been tagged for mitophagy, different mitophagy receptors can recognize dysfunctional mitochondria and act as a bridge between the autophagosome (LC3-II) and the cargo (mitochondria) (Stolz et al., 2014). In this context, it was previously described that the receptor for selective autophagy p62 was able to interact with Htt (Rui et al., 2015) and this interaction was altered in mutant Htt (Martinez-Vicente et al., 2010). As a result, p62 interaction with ubiquitin-K63 chains of the substrate and LC3 of the autophagosome was altered (Rui et al., 2015). Recently, the role of p62 in mitophagy has been questioned since p62 has been reported to be dispensable for mitophagy, while OPTN and NDP52 have been found to be the primary receptors for mitophagy (Lazarou et al., 2015b). Similarly, interactions between Htt and the essential mitophagy adaptors have already been described (del Toro et al., 2009; Hattula and Peränen, 2000) or predicted *in silico*. We have confirmed in our neuronal model that Htt binds not only to general autophagy adapters, p62 and NBRI, but also to specific mitophagy adapters, OPTN and NDP52 and that these interactions are lost in the presence of the polyQ stretch upon depolarization-induced mitophagy. Similarly, mutant Htt was previously reported to impair the interaction between optineurin/Rab8 complex (del Toro et al., 2009). The main consequence of the hampered interaction between the scaffolding protein Htt and the different receptors is that lower LC3-II is recruited to the targeted mitochondria, as demonstrated by the loss in OPTN and NDP52 interaction with LC3 in the presence of mutant Htt and mitochondrial uncouplers.

As a result, striatal cells carrying mutant Htt did not respond with the same efficiency to the elimination of damaged mitochondria and as a consequence higher number of these damaged mitochondria are accumulated in the neurons and become a new source of ROS. We are aware that in addition to the role of Htt in selective mitophagy described in this study, many other works have linked mutant Htt to mitochondrial dysfunction by alteration in other mitochondrial processes such as mitochondrial fusion/fission dynamics, mitochondrial protein import system, mitochondrial complex assembly and mitochondrial axonal transport (Guedes-Dias et al., 2016). These events might act simultaneously to the mitophagy impairment described in this work, and all together probably contribute to the pathogenic increase of mitochondrial dysfunction and ROS accumulation observed in neurons affected by HD (Johri and Beal, 2012).

In this work we have used only striatal cells, since we wanted to characterize at the molecular level all the interactions between wild type and mutant Htt with mitophagy key proteins. However, there are evidences *in vivo* that sustain our findings. For instance, using a mitoKeima transgenic mouse model in which human Htt transgene was expressed, decreased levels of mitophagy were observed in the dentate gyrus (Sun et al., 2015).

In contrast with our findings and previous publications by many other groups (Khalil et al., 2015; Martinez-Vicente et al., 2010; Wong and Holzbaur, 2014), a recent work reported that valosin-containing protein (VCP) binds preferentially to mutant Htt on mitochondria in striatal Q111 cells and VCP translocation to mitochondria mediates excessive mitochondrial turnover and subsequent cell death (Guo et al., 2016). However, our findings do not support the presence of an excessive mitochondrial clearance in basal conditions. In fact, to our knowledge, this is the only work in which mutant Htt has been linked with increased or excessive mitophagy, leading to a decrease in mitochondrial mass, energy and neuronal survival. Moreover, another report has shown that VCP translocation to mitochondria has a positive effect on mitochondrial respiration and prevents mitochondrial permeability transition pore (mPTP) opening in cardiomyocytes (Lizano et al., 2017). These differences could be explained by the intrinsic characteristics of each cellular type. Since we have worked with differentiated cells we cannot rule out that mutant Htt displays different roles on mitotic and postmitotic cells.

It is important to mention that we have measured the mitophagy process upon basal and depolarized-induced conditions. While mutant Htt impaired mitophagy induced by mild or strong mitochondrial damaging agents, it did not affect basal mitophagy taking place in striatal neuronal cells. Moreover, there are other types of mitophagy mediated by receptors

present in mitochondrial membranes (BNIP3, NIX, FUND1, AMBRA, cardiolipin, etc) as well as other forms of partial mitochondrial degradation (Martinez-Vicente, 2017) that have not been studied. All these forms of mitochondrial degradation may occur simultaneously or in response to specific stimulus and may contribute all together to the mantainance of a healthy mitochondrial network. Therefore, we cannot rule out that mutant Htt also affects these other mitophagy-related mechanisms.

In summary Htt can physically put together at the same time the active ULK1 complex, mitophagy receptors and LC3-II to facilitate depolarized-induced mitophagy process. Thus, when Htt is mutated, the inefficiency of mutant Htt to bind ULK1 and the receptors and therefore recruit LC3-II, will definitely affect the effectiveness of the neuronal mitophagy (**Fig. 48**).

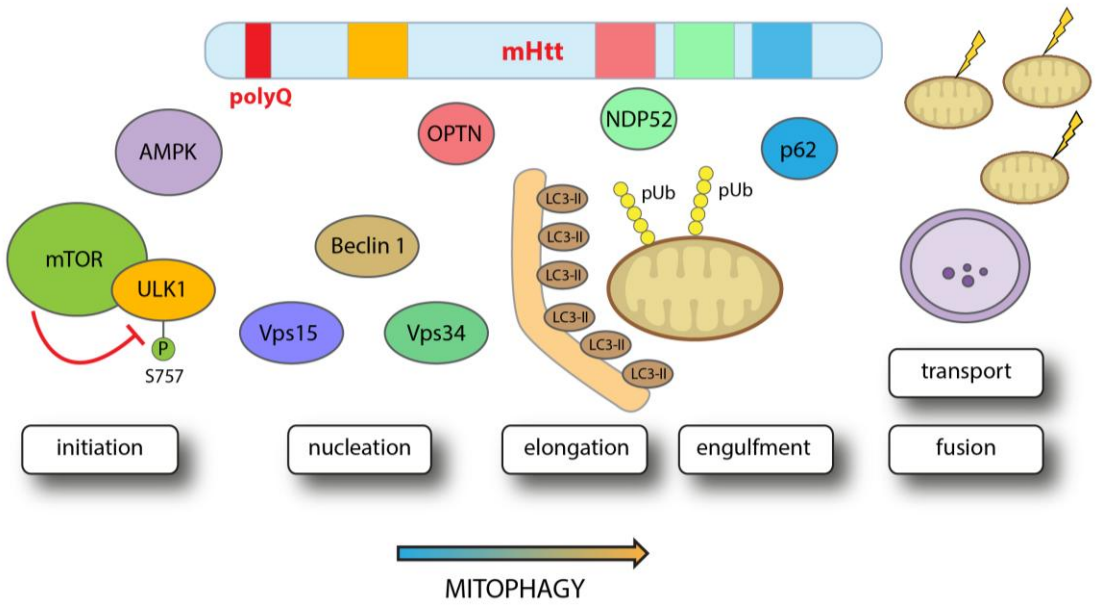

Figure 48. Schematic representation of the different steps where mutant Htt impairs induced-mitophagy.

When mitophagy is induced in the presence of mutant Htt (mHttt) ULK1 binds preferentially to mTOR, which phosphorylates ULK1 at S757. Moreover, the interaction between beclin 1 and Vps15 is reduced, suggesting that the formation of the nucleation complex is impaired. Mitochondria to be degraded are tagged with K63 ubiquitin chains that are phosphorylated (pUb). However, mitophagy adapters OPTN and NDP52, and the general autophagy adapter p62 do not interact with Htt. Besides, OPTN and NDP52 interact poorly with LC3-II in the autophagosome membrane. Mitochondria are less efficiently engulfed by the autophagosomes and degraded in the lysosomes. As a consequence, damaged mitochondria accumulate, leading to an increased ROS production and probably damaging more mitochondria.

5.3 Mitochondrial quality control and neurodegeneration: a potential therapeutic target?

Neurons are a type of cells with some particular features. They have high energy demands in order to (i) maintain membrane potential, (ii) re-establish the ion balance after the firing of an action potential, (iii) trigger the release and (iv) recapture of neurotransmitters. Moreover, neurons rely almost exclusively on the mitochondrial OXPHOS for energy production (Schönfeld and Reiser, 2013). On top of that, they are post-mitotic cells, meaning that their lifespan is similar to that of the whole organism. Therefore, it is apparent that they are more sensitive to the accumulation of oxidative damage compared to dividing cells and are more prone to accumulate defective mitochondria during ageing (Kowald and Kirkwood, 2000; Terman et al., 2010). It is not surprising, then, that impaired mitochondrial function has long been revealed as a common theme in neurodegenerative disorders, despite their phenotypic diversity (Schon and Przedborski, 2011).

In fact, some therapeutic strategies regarding mitochondria have advanced into clinical trials for both, PD and HD. Coenzyme Q10 and creatine were both aimed at improving overall function for HD patients. These two trials were the largest trials ever conducted in HD but closed prematurely owing to futility (Hersch et al., 2017; McGarry et al., 2017). The first clinical trial investigating drugs targeting mitochondrial function and oxidative stress in PD was the DATATOP study, in which selegiline, a monoamine oxidase B inhibitor, together with tocopherol, an antioxidant, were assessed. While the use of selegiline had a clear beneficial effect, tocopherol did not delay the onset of disability associated with PD (Parkinson Study Group, 1993). Similarly, creatine has also been tested in a clinical trial for PD, but the trial was again terminated due to futility reasons (Kieburtz et al., 2015). These are some examples of mitochondrial-based therapies that have gone into clinical trials. **Table 9** summarizes the major clinical trials targeting mitochondria in PD and HD. Unfortunately, none of them have had a positive result. Therefore, there is an urgent need to find new therapeutic targets for mitochondrial dysfunction.

Table 9. Therapeutic strategies targeting mitochondria in PD and HD

Disease	Therapeutic agent	Mechanism	Clinical outcome	Result	Reference
PD	Tocopherol (vitamin E)	Antioxidant	Time to levodopa.	Negative	Parkinson Study Group, 1993
PD	Coenzyme Q10	Bioenergetics	Rate of deterioration in UPDRS score from baseline	Negative	Beal et al., 2014
PD	Creatine	Bioenergetics	Clinical decline	Negative	Kieburtz et al., 2015
PD	Pioglitazone	PPARγ activator	Change in total UPDRS score	Negative	NINDS Exploratory Trials in Parkinson Disease (NET-PD) FS-ZONE Investigators, 2015
PD	Exenatide	Agonist of glucagon-like peptide 1 (GLP-1)	Difference in the UPDRS motor subscale part 3	Positive but unknown disease-modifiying effects	Athauda et al., 2017
PD	N-acetylcysteine	Antioxidant	Blood GSH/GSSG ratios and brain GSH levels.	Negative	Holmay et al., 2013
PD	Glutathione	Antioxidant	Change in total UPDRS score	Negative	Mischley et al., 2017
HD	Coenzyme Q10	Antioxidant	Change from baseline in TFC score combined with time to death.	Negative	McGarry et al., 2017
HD	Creatine	Bioenergetics	Change in TFC.	Negative	Hersch et al., 2017
HD	Resveratrol	Antioxidant	Change in caudate atrophy at 12 months.	Ongoing	

UPDRS: Unified Parkinson's Disease Rating Scale, TFC: total functional capacity

Noteworthy, clinical trials might also have failed due to factors implying the design of the trial itself. The first obstacle to overcome is the selection of the patients, because the heterogeneity of the populations studied can lead to confounding results. For instance, in PD there is now great interest in the use of defined populations with specific deficits, such as carriers of LRRK2 or glucocerebrosidase mutations, in order to reduce variability and increase the chance of detecting a treatment effect (Schapira and Olanow, 2004). Another important factor for patient selection is the disease stage. Patients in more advanced states are more accurately diagnosed but have less chances to see a benefit even if a drug is neuroprotective since they have less neurons left to preserve than early untreated patients (Kordower et al., 2013). For HD it is a bit different since it is a genetic disease and mutant Htt is present from the very first moment of the protein's expression. Therefore, the prodromal presymptomatic phase would be the ideal phase to start a putative treatment (Hersch and Rosas, 2008).

When attempting to find a neuroprotective therapy, attention in the study design has to be paid. In the past years, new study designs have been used to distinguish a disease-modifying effect from a symptomatic effect. However, to date, no intervention has proven sufficient to conclude that it has a disease-modifying effect (Olanow et al., 2017). Specifically in the field of PD there is also a need to develop new biomarkers that allow (i) earlier PD diagnosis (ii) higher accuracy in the diagnosis to minimize diagnostic errors in clinical trials and (iii) provide an objective measure of the underlying disease progression (Olanow et al., 2017; Schapira, 2013).

To sum up, the mitochondria-related molecules already tested are mostly antioxidants or molecules that target bioenergetics. These strategies have already failed in clinical trials, thus, in the next years new approaches will be needed to target mitochondrial dysfunction in neurodegenerative disorders. These disorders, despite their origin, progression and heterogeneity, all share mitochondrial dysfunction and ROS production (Bose and Beal, 2016; Moreira et al., 2010; Ross and Tabrizi, 2011). In some cases, there is a direct involvement of the genetic defect with mitochondria, such as in Friedreich's ataxia, while in others the link is more indirect, such as in PD, HD or Alzheimer's disease. Therefore, a mitochondrial-targeting therapy with efficacy for one disease may hold promise for several neurodegenerative disorders.

CONCLUSIONS

6 CONCLUSIONS

1. Mitochondrial protein import system is impaired in human midbrain *post-mortem* tissue from PD patients, complex I-deficient mice midbrain and in complex I-deficient neuroblastoma cells.
2. Complex I inhibition in neuroblastoma cells results in a general mitochondrial dysfunction, characterised by decreased OXPHOS protein levels, impaired mtUPR activation, mitochondrial membrane depolarization, increased ROS production and increased cell death.
3. Overexpression of key translocases proteins, TIM23 and TOM20, partially restores mitochondrial membrane potential, ROS production and partially protects against MPP^+-induced cell death.
4. TIM23 overexpression in MPTP mice restores mitochondrial protein import deficiency and partially protects against SN dopaminergic neuronal loss.
5. TOM20 overexpression in MPTP mice does not restore mitochondrial protein import deficiency and increases SN dopaminergic neuronal loss. Therefore, despite promising results *in vitro*, TOM20 is not a good therapeutic candidate for PD.
6. Mutant huntingtin impairs induced mitophagy in differentiated striatal cells.
7. Endogenous neuronal mitophagy is not mediated by Parkin translocation to the mitochondria.
8. Mutant huntingtin does not impair mitochondrial polyubiquitination.
9. The presence of mutant polyQ tract impairs the interaction of huntingtin with ULK1. Consequently, ULK1 activation is affected and favors that ULK1 remains inactive and attached to mTOR.
10. Beclin 1 - Vps15 interaction is also hampered in the presence of mutant huntingtin, affecting the formation of the nucleation complex.
11. Wild type huntingtin is able to bind to the essential mitophagy adapters OPTN and NDP52 and these interactions are impaired in the presence of mutant huntingtin. Therefore, OPTN/NDP52 interaction with LC3 decreases, avoiding the proper recognition and engulfment of the targeted mitochondria by the nascent autophagosome
12. Dysfunctional mitochondria accumulate in ST-Q111 cells. Therefore, mutant cells exhibit impaired mitochondrial respiration, depolarization and increased ROS production.

BIBLIOGRAPHY

7 Bibliography

Adams, K. L., and Palmer, J. D. (2003). Evolution of mitochondrial gene content: gene loss and transfer to the nucleus. *Mol. Phylogenet. Evol.* 29, 380–95.

Aharon-Peretz, J., Rosenbaum, H., and Gershoni-Baruch, R. (2004). Mutations in the Glucocerebrosidase Gene and Parkinson's Disease in Ashkenazi Jews. *N. Engl. J. Med.* 351, 1972–1977. doi:10.1056/NEJMoa033277.

Akutsu, M., Dikic, I., and Bremm, A. (2016). Ubiquitin chain diversity at a glance. *J. Cell Sci.* 129, 875–80. doi:10.1242/jcs.183954.

Alberts, B., Johnson, A., Lewis, J., Raff, M., Roberts, K., and Walter, P. (2002). *Molecular biology of the cell*. Garland Science.

Aldridge, J. E., Horibe, T., and Hoogenraad, N. J. (2007). Discovery of Genes Activated by the Mitochondrial Unfolded Protein Response (mtUPR) and Cognate Promoter Elements. *PLoS One* 2, e874. doi:10.1371/journal.pone.0000874.

Alvarez-Erviti, L., Rodriguez-Oroz, M. C., Cooper, J. M., Caballero, C., Ferrer, I., Obeso, J. A., et al. (2010). Chaperone-Mediated Autophagy Markers in Parkinson Disease Brains. *Arch. Neurol.* 67, 1464–72. doi:10.1001/archneurol.2010.198.

Amadoro, G., Corsetti, V., Florenzano, F., Atlante, A., Bobba, A., Nicolin, V., et al. (2014). Morphological and bioenergetic demands underlying the mitophagy in post-mitotic neurons: the pink-parkin pathway. *Front. Aging Neurosci.* 6, 18. doi:10.3389/fnagi.2014.00018.

Ambrose, C. M., Duyao, M. P., Barnes, G., Bates, G. P., Lin, C. S., Srinidhi, J., et al. (1994). Structure and expression of the Huntington's disease gene: evidence against simple inactivation due to an expanded CAG repeat. *Somat. Cell Mol. Genet.* 20, 27–38. Available at: http://www.ncbi.nlm.nih.gov/pubmed/8197474 [Accessed December 3, 2017].

Anand, R., Wai, T., Baker, M. J., Kladt, N., Schauss, A. C., Rugarli, E., et al. (2014). The i-AAA protease YME1L and OMA1 cleave OPA1 to balance mitochondrial fusion and fission. *J. Cell Biol.* 204, 919–29. doi:10.1083/jcb.201308006.

Anderson, S., Bankier, A. T., Barrell, B. G., de Bruijn, M. H., Coulson, A. R., Drouin, J., et al. (1981). Sequence and organization of the human mitochondrial genome. *Nature* 290, 457–65.

Andringa, G., Eshuis, S., Perentes, E., Maguire, R. P., Roth, D., Ibrahim, M., et al. (2003). TCH346 prevents motor symptoms and loss of striatal FDOPA uptake in bilaterally MPTP-treated primates. *Neurobiol. Dis.* 14, 205–217. doi:10.1016/S0969-9961(03)00125-6.

Anglade, P., Vyas, S., Javoy-Agid, F., Herrero, M. T., Michel, P. P., Marquez, J., et al. (1997). Apoptosis and autophagy in nigral neurons of patients with Parkinson's disease. *Histol. Histopathol.* 12, 25–31. Available at: http://www.ncbi.nlm.nih.gov/pubmed/9046040 [Accessed February 8, 2018].

Arrasate, M., and Finkbeiner, S. (2012). Protein aggregates in Huntington's disease. *Exp. Neurol.* 238, 1–11. doi:10.1016/j.expneurol.2011.12.013.

Ashkenazi, A., Bento, C. F., Ricketts, T., Vicinanza, M., Siddiqi, F., Pavel, M., et al. (2017). Polyglutamine tracts regulate beclin 1-dependent autophagy. *Nature* 545, 108–111. doi:10.1038/nature22078.

Ashrafi, G., Schlehe, J. S., LaVoie, M. J., and Schwarz, T. L. (2014). Mitophagy of damaged

mitochondria occurs locally in distal neuronal axons and requires PINK1 and Parkin. *J. Cell Biol.* 206, 655–70. doi:10.1083/jcb.201401070.

Athauda, D., Maclagan, K., Skene, S. S., Bajwa-Joseph, M., Letchford, D., Chowdhury, K., et al. (2017). Exenatide once weekly versus placebo in Parkinson's disease: a randomised, double-blind, placebo-controlled trial. *Lancet* 390, 1664–1675. doi:10.1016/S0140-6736(17)31585-4.

Axe, E. L., Walker, S. A., Manifava, M., Chandra, P., Roderick, H. L., Habermann, A., et al. (2008). Autophagosome formation from membrane compartments enriched in phosphatidylinositol 3-phosphate and dynamically connected to the endoplasmic reticulum. *J. Cell Biol.* 182, 685–701. doi:10.1083/jcb.200803137.

Bae, B.-I., Xu, H., Igarashi, S., Fujimuro, M., Agrawal, N., Taya, Y., et al. (2005). p53 Mediates Cellular Dysfunction and Behavioral Abnormalities in Huntington's Disease. *Neuron* 47, 29–41. doi:10.1016/J.NEURON.2005.06.005.

Baker, T. A., and Sauer, R. T. (2012). ClpXP, an ATP-powered unfolding and protein-degradation machine. *Biochim. Biophys. Acta - Mol. Cell Res.* 1823, 15–28. doi:10.1016/j.bbamcr.2011.06.007.

Banerjee, K., Sinha, M., Pham, C. L. L., Jana, S., Chanda, D., Cappai, R., et al. (2010). α-Synuclein induced membrane depolarization and loss of phosphorylation capacity of isolated rat brain mitochondria: Implications in Parkinson's disease. *FEBS Lett.* 584, 1571–1576. doi:10.1016/j.febslet.2010.03.012.

Bao, X. R., Ong, S.-E., Goldberger, O., Peng, J., Sharma, R., Thompson, D. A., et al. (2016). Mitochondrial dysfunction remodels one-carbon metabolism in human cells. *Elife* 5. doi:10.7554/eLife.10575.

Barsoum, M. J., Yuan, H., Gerencser, A. A., Liot, G., Kushnareva, Y., Gräber, S., et al. (2006). Nitric oxide-induced mitochondrial fission is regulated by dynamin-related GTPases in neurons. *EMBO J.* 25, 3900–3911. doi:10.1038/sj.emboj.7601253.

Bates, G. P., Dorsey, R., Gusella, J. F., Hayden, M. R., Kay, C., Leavitt, B. R., et al. (2015). Huntington disease. *Nat. Rev. Dis. Prim.* 1, 15005. doi:10.1038/nrdp.2015.5.

Bausewein, T., Mills, D. J., Langer, J. D., Nitschke, B., Nussberger, S., Kühlbrandt, W., et al. (2017). Cryo-EM Structure of the TOM Core Complex from Neurospora crassa. *Cell* 170, 693–700.e7. doi:10.1016/j.cell.2017.07.012.

Beal, M. F., Oakes, D., Shoulson, I., Henchcliffe, C., Galpern, W. R., Haas, R., et al. (2014). A Randomized Clinical Trial of High-Dosage Coenzyme Q10 in Early Parkinson Disease. *JAMA Neurol.* 71, 543. doi:10.1001/jamaneurol.2014.131.

Bender, A., Desplats, P., Spencer, B., Rockenstein, E., Adame, A., Elstner, M., et al. (2013). TOM40 mediates mitochondrial dysfunction induced by alpha-synuclein accumulation in Parkinson's disease. *PLoS One* 8, e62277. doi:10.1371/journal.pone.0062277.

Bender, A., Krishnan, K. J., Morris, C. M., Taylor, G. A., Reeve, A. K., Perry, R. H., et al. (2006). High levels of mitochondrial DNA deletions in substantia nigra neurons in aging and Parkinson disease. *Nat. Genet.* 38, 515–517. doi:10.1038/ng1769.

Bennett, E. J., Shaler, T. A., Woodman, B., Ryu, K.-Y., Zaitseva, T. S., Becker, C. H., et al. (2007). Global changes to the ubiquitin system in Huntington's disease. *Nature* 448, 704–708. doi:10.1038/nature06022.

Betarbet, R., Sherer, T. B., MacKenzie, G., Garcia-Osuna, M., Panov, A. V., and Greenamyre, J. T. (2000). Chronic systemic pesticide exposure reproduces features of Parkinson's disease. *Nat. Neurosci.* 3, 1301–1306. doi:10.1038/81834.

Bido, S., Soria, F. N., Fan, R. Z., Bezard, E., and Tieu, K. (2017). Mitochondrial division inhibitor-1 is neuroprotective in the A53T-α-synuclein rat model of Parkinson's disease.

Sci. Rep. 7, 7495. doi:10.1038/s41598-017-07181-0.

Bingol, B., and Sheng, M. (2016). Mechanisms of mitophagy: PINK1, Parkin, USP30 and beyond. *Free Radic. Biol. Med.* 100, 210–222. doi:10.1016/J.FREERADBIOMED.2016.04.015.

Bingol, B., Tea, J. S., Phu, L., Reichelt, M., Bakalarski, C. E., Song, Q., et al. (2014). The mitochondrial deubiquitinase USP30 opposes parkin-mediated mitophagy. *Nature* 510, 370–375. doi:10.1038/nature13418.

Birsa, N., Norkett, R., Wauer, T., Mevissen, T. E. T., Wu, H.-C., Foltynie, T., et al. (2014). Lysine 27 ubiquitination of the mitochondrial transport protein Miro is dependent on serine 65 of the Parkin ubiquitin ligase. *J. Biol. Chem.* 289, 14569–82. doi:10.1074/jbc.M114.563031.

Blin, O., Desnuelle, C., Rascol, O., Borg, M., Peyro Saint Paul, H., Azulay, J., et al. (1994). Mitochondrial respiratory failure in skeletal muscle from patients with Parkinson's disease and multiple system atrophy. *J. Neurol. Sci.* 125, 95–101. doi:10.1016/0022-510X(94)90248-8.

Bolaños, J. P., Almeida, A., and Moncada, S. (2010). Glycolysis: a bioenergetic or a survival pathway? *Trends Biochem. Sci.* 35, 145–149. doi:10.1016/j.tibs.2009.10.006.

Bonifati, V., Rizzu, P., van Baren, M. J., Schaap, O., Breedveld, G. J., Krieger, E., et al. (2003). Mutations in the DJ-1 Gene Associated with Autosomal Recessive Early-Onset Parkinsonism. *Science (80-.).* 299, 256–259. doi:10.1126/science.1077209.

Bose, A., and Beal, M. F. (2016). Mitochondrial dysfunction in Parkinson's disease. *J. Neurochem.* 139, 216–231. doi:10.1111/jnc.13731.

Bostantjopoulou, S., Katsarou, Z., Papadimitriou, A., Veletza, V., Hatzigeorgiou, G., and Lees, A. (2001). Clinical features of parkinsonian patients with the alpha-synuclein (G209A) mutation. *Mov. Disord.* 16, 1007–13. Available at: http://www.ncbi.nlm.nih.gov/pubmed/11748731 [Accessed February 8, 2018].

Bové, J., Martínez-Vicente, M., Dehay, B., Perier, C., Recasens, A., Bombrun, A., et al. (2014). BAX channel activity mediates lysosomal disruption linked to Parkinson disease. *Autophagy* 10, 889–900. doi:10.4161/auto.28286.

Bové, J., and Perier, C. (2012). Neurotoxin-based models of Parkinson's disease. *Neuroscience* 211, 51–76. doi:10.1016/j.neuroscience.2011.10.057.

Braak, H., Del Tredici, K., Rüb, U., de Vos, R. A. I., Jansen Steur, E. N. H., and Braak, E. (2003). Staging of brain pathology related to sporadic Parkinson's disease. *Neurobiol. Aging* 24, 197–211. Available at: http://www.ncbi.nlm.nih.gov/pubmed/12498954 [Accessed February 8, 2018].

Braak, H., Ghebremedhin, E., Rüb, U., Bratzke, H., and Del Tredici, K. (2004). Stages in the development of Parkinson's disease-related pathology. *Cell Tissue Res.* 318, 121–134. doi:10.1007/s00441-004-0956-9.

Brás, J., Guerreiro, R., and Hardy, J. (2015). SnapShot: Genetics of Parkinson's Disease. *Cell* 160, 570–570.e1. doi:10.1016/j.cell.2015.01.019.

Brennan, W. A., Bird, E. D., and Aprille, J. R. (1985). Regional mitochondrial respiratory activity in Huntington's disease brain. *J. Neurochem.* 44, 1948–50.

Broadley, S. A., and Hartl, F. U. (2008). Mitochondrial stress signaling: a pathway unfolds. *Trends Cell Biol.* 18, 1–4. doi:10.1016/j.tcb.2007.11.003.

Brooks, A. I., Chadwick, C. A., Gelbard, H. A., Cory-Slechta, D. A., and Federoff, H. J. (1999). Paraquat elicited neurobehavioral syndrome caused by dopaminergic neuron loss. *Brain Res.* 823, 1–10. Available at: http://www.ncbi.nlm.nih.gov/pubmed/10095006 [Accessed February 8, 2018].

Browne, S. E., Bowling, A. C., Macgarvey, U., Baik, M. J., Berger, S. C., Muquit, M. M. K., et al. (1997). Oxidative damage and metabolic dysfunction in Huntington's disease: Selective vulnerability of the basal ganglia. *Ann. Neurol.* 41, 646–653. doi:10.1002/ana.410410514.

Brownell, A.-L., Jenkins, B. G., Elmaleh, D. R., Deacon, T. W., Spealman, R. D., and Isacson, O. (1998). Combined PET/MRS brain studies show dynamic and long-term physiological changes in a primate model of Parkinson disease. *Nat. Med.* 4, 1308–1312. doi:10.1038/3300.

Burbulla, L. F., Schelling, C., Kato, H., Rapaport, D., Woitalla, D., Schiesling, C., et al. (2010). Dissecting the role of the mitochondrial chaperone mortalin in Parkinson's disease: functional impact of disease-related variants on mitochondrial homeostasis. *Hum. Mol. Genet.* 19, 4437–4452. doi:10.1093/hmg/ddq370.

Burchell, V. S., Nelson, D. E., Sanchez-Martinez, A., Delgado-Camprubi, M., Ivatt, R. M., Pogson, J. H., et al. (2013). The Parkinson's disease–linked proteins Fbxo7 and Parkin interact to mediate mitophagy. *Nat. Neurosci.* 16, 1257–1265. doi:10.1038/nn.3489.

Burman, J. L., Yu, S., Poole, A. C., Decal, R. B., and Pallanck, L. (2012). Analysis of neural subtypes reveals selective mitochondrial dysfunction in dopaminergic neurons from parkin mutants. *Proc. Natl. Acad. Sci.* 109, 10438–10443. doi:10.1073/pnas.1120688109.

Butler, E. K., Voigt, A., Lutz, A. K., Toegel, J. P., Gerhardt, E., Karsten, P., et al. (2012). The mitochondrial chaperone protein TRAP1 mitigates α-synuclein Toxicity. *PLoS Genet.* 8, e1002488. doi:10.1371/journal.pgen.1002488.

Cai, Q., Zakaria, H. M., Simone, A., and Sheng, Z.-H. (2012). Spatial parkin translocation and degradation of damaged mitochondria via mitophagy in live cortical neurons. *Curr. Biol.* 22, 545–552. doi:10.1016/j.cub.2012.02.005.

Callegari, S., Richter, F., Chojnacka, K., Jans, D. C., Lorenzi, I., Pacheu-Grau, D., et al. (2016). TIM29 is a subunit of the human carrier translocase required for protein transport. *FEBS Lett.* 590, 4147–4158. doi:10.1002/1873-3468.12450.

Camnasio, S., Carri, A. D., Lombardo, A., Grad, I., Mariotti, C., Castucci, A., et al. (2012). The first reported generation of several induced pluripotent stem cell lines from homozygous and heterozygous Huntington's disease patients demonstrates mutation related enhanced lysosomal activity. *Neurobiol. Dis.* 46, 41–51. doi:10.1016/j.nbd.2011.12.042.

Cattaneo, E., Zuccato, C., and Tartari, M. (2005). Normal huntingtin function: an alternative approach to Huntington's disease. *Nat. Rev. Neurosci.* 6, 919–930. doi:10.1038/nrn1806.

Cha, J.-H. J. (2007). Transcriptional signatures in Huntington's disease. *Prog. Neurobiol.* 83, 228–48. doi:10.1016/j.pneurobio.2007.03.004.

Chacinska, A., Koehler, C. M., Milenkovic, D., Lithgow, T., and Pfanner, N. (2009). Importing Mitochondrial Proteins: Machineries and Mechanisms. *Cell* 138, 628–644. doi:10.1016/j.cell.2009.08.005.

Chacinska, A., van der Laan, M., Mehnert, C. S., Guiard, B., Mick, D. U., Hutu, D. P., et al. (2010). Distinct Forms of Mitochondrial TOM-TIM Supercomplexes Define Signal-Dependent States of Preprotein Sorting. *Mol. Cell. Biol.* 30, 307–318. doi:10.1128/MCB.00749-09.

Chan, N. C., Salazar, A. M., Pham, A. H., Sweredoski, M. J., Kolawa, N. J., Graham, R. L. J., et al. (2011). Broad activation of the ubiquitin-proteasome system by Parkin is critical for mitophagy. *Hum. Mol. Genet.* 20, 1726–37. doi:10.1093/hmg/ddr048.

Chance, B., Sies, H., and Boveris, A. (1979). Hydroperoxide metabolism in mammalian organs. *Physiol. Rev.* 59, 527–605.

Chang, D. T. W., Rintoul, G. L., Pandipati, S., and Reynolds, I. J. (2006). Mutant huntingtin aggregates impair mitochondrial movement and trafficking in cortical neurons. *Neurobiol. Dis.* 22, 388–400. doi:10.1016/j.nbd.2005.12.007.

Chen, Y., and Dorn, G. W. (2013). PINK1-phosphorylated Mitofusin 2 is a parkin receptor for culling damaged mitochondria. *Science (80-.).* 340, 471–475. doi:10.1126/science.1231031.

Choi, S.-Y., Huang, P., Jenkins, G. M., Chan, D. C., Schiller, J., and Frohman, M. A. (2006). A common lipid links Mfn-mediated mitochondrial fusion and SNARE-regulated exocytosis. *Nat. Cell Biol.* 8, 1255–1262. doi:10.1038/ncb1487.

Choo, Y. S., Johnson, G. V. W., MacDonald, M., Detloff, P. J., and Lesort, M. (2004). Mutant huntingtin directly increases susceptibility of mitochondria to the calcium-induced permeability transition and cytochrome c release. *Hum. Mol. Genet.* 13, 1407–1420. doi:10.1093/hmg/ddh162.

Choubey, V., Safiulina, D., Vaarmann, A., Cagalinec, M., Wareski, P., Kuum, M., et al. (2011). Mutant A53T α-Synuclein Induces Neuronal Death by Increasing Mitochondrial Autophagy. *J. Biol. Chem.* 286, 10814–10824. doi:10.1074/jbc.M110.132514.

Chu, C. T., Ji, J., Dagda, R. K., Jiang, J. F., Tyurina, Y. Y., Kapralov, A. A., et al. (2013). Cardiolipin externalization to the outer mitochondrial membrane acts as an elimination signal for mitophagy in neuronal cells. *Nat. Cell Biol.* 15, 1197–1205. doi:10.1038/ncb2837.

Chu, Y., Dodiya, H., Aebischer, P., Olanow, C. W., and Kordower, J. H. (2009). Alterations in lysosomal and proteasomal markers in Parkinson's disease: Relationship to alpha-synuclein inclusions. *Neurobiol. Dis.* 35, 385–398. doi:10.1016/j.nbd.2009.05.023.

Chung, S. J., Kim, M.-J., Ryu, H.-S., Kim, J., Kim, Y. J., Kim, K., et al. (2017). Lack of association of mortalin (HSPA9) and other mitochondria-related genes with risk of Parkinson's and Alzheimer's diseases. *Neurobiol. Aging* 49, 215.e9-215.e10. doi:10.1016/j.neurobiolaging.2016.09.017.

Cipolat, S., Martins de Brito, O., Dal Zilio, B., and Scorrano, L. (2004). OPA1 requires mitofusin 1 to promote mitochondrial fusion. *Proc. Natl. Acad. Sci. U. S. A.* 101, 15927–32. doi:10.1073/pnas.0407043101.

Cisbani, G., and Cicchetti, F. (2012). An in vitro perspective on the molecular mechanisms underlying mutant huntingtin protein toxicity. *Cell Death Dis.* 3, e382–e382. doi:10.1038/cddis.2012.121.

Clausen, T., Kaiser, M., Huber, R., and Ehrmann, M. (2011). HTRA proteases: regulated proteolysis in protein quality control. *Nat. Rev. Mol. Cell Biol.* 12, 152–162. doi:10.1038/nrm3065.

Cleeter, M. W., Cooper, J. M., and Schapira, A. H. (1992). Irreversible inhibition of mitochondrial complex I by 1-methyl-4-phenylpyridinium: evidence for free radical involvement. *J. Neurochem.* 58, 786–9. Available at: http://www.ncbi.nlm.nih.gov/pubmed/1729421 [Accessed February 9, 2018].

Coelho, M., and Ferreira, J. J. (2012). Late-stage Parkinson disease. *Nat. Rev. Neurol.* 8, 435–442. doi:10.1038/nrneurol.2012.126.

Connolly, B. S., and Lang, A. E. (2014). Pharmacological Treatment of Parkinson Disease. *JAMA* 311, 1670. doi:10.1001/jama.2014.3654.

Cornelissen, T., Haddad, D., Wauters, F., Van Humbeeck, C., Mandemakers, W., Koentjoro, B., et al. (2014). The deubiquitinase USP15 antagonizes Parkin-mediated mitochondrial

ubiquitination and mitophagy. *Hum. Mol. Genet.* 23, 5227–5242. doi:10.1093/hmg/ddu244.

Court, F. A., and Coleman, M. P. (2012). Mitochondria as a central sensor for axonal degenerative stimuli. *Trends Neurosci.* 35, 364–372. doi:10.1016/j.tins.2012.04.001.

Coyle, J. T., and Schwarcz, R. (1976). Lesion of striatal neurons with kainic acid provides a model for Huntington's chorea. *Nature* 263, 244–246. doi:10.1038/263244a0.

Craufurd, D., Thompson, J. C., and Snowden, J. S. (2001). Behavioral changes in Huntington Disease. *Neuropsychiatry. Neuropsychol. Behav. Neurol.* 14, 219–26. Available at: http://www.ncbi.nlm.nih.gov/pubmed/11725215 [Accessed February 8, 2018].

Cuervo, A. M., and Macian, F. (2012). Autophagy, nutrition and immunology. *Mol. Aspects Med.* 33, 2–13. doi:10.1016/j.mam.2011.09.001.

Cui, L., Jeong, H., Borovecki, F., Parkhurst, C. N., Tanese, N., and Krainc, D. (2006). Transcriptional repression of PGC-1alpha by mutant huntingtin leads to mitochondrial dysfunction and neurodegeneration. *Cell* 127, 59–69. doi:10.1016/j.cell.2006.09.015.

Cui, M., Tang, X., Christian, W. V., Yoon, Y., and Tieu, K. (2010). Perturbations in Mitochondrial Dynamics Induced by Human Mutant PINK1 Can Be Rescued by the Mitochondrial Division Inhibitor mdivi-1. *J. Biol. Chem.* 285, 11740–11752. doi:10.1074/jbc.M109.066662.

Dai, Y., Clark, J., Zheng, K., Kujoth, G. C., Prolla, T. A., and Simon, D. K. (2014). Somatic mitochondrial DNA mutations do not increase neuronal vulnerability to MPTP in young POLG mutator mice. *Neurotoxicol. Teratol.* 46, 62–7. doi:10.1016/j.ntt.2014.10.004.

Damiano, M., Diguet, E., Malgorn, C., D'Aurelio, M., Galvan, L., Petit, F., et al. (2013). A role of mitochondrial complex II defects in genetic models of Huntington's disease expressing N-terminal fragments of mutant huntingtin. *Hum. Mol. Genet.* 22, 3869–3882. doi:10.1093/hmg/ddt242.

Davidzon, G., Greene, P., Mancuso, M., Klos, K. J., Ahlskog, J. E., Hirano, M., et al. (2006). Early-onset familial parkinsonism due to POLG mutations. *Ann. Neurol.* 59, 859–862. doi:10.1002/ana.20831.

Davies, S. W., Turmaine, M., Cozens, B. A., DiFiglia, M., Sharp, A. H., Ross, C. A., et al. (1997). Formation of neuronal intranuclear inclusions underlies the neurological dysfunction in mice transgenic for the HD mutation. *Cell* 90, 537–48. Available at: http://www.ncbi.nlm.nih.gov/pubmed/9267033 [Accessed February 8, 2018].

de Brito, O. M., and Scorrano, L. (2008). Mitofusin 2 tethers endoplasmic reticulum to mitochondria. *Nature* 456, 605–610. doi:10.1038/nature07534.

De Vos, K., Goossens, V., Boone, E., Vercammen, D., Vancompernolle, K., Vandenabeele, P., et al. (1998). The 55-kDa tumor necrosis factor receptor induces clustering of mitochondria through its membrane-proximal region. *J. Biol. Chem.* 273, 9673–80. doi:10.1074/JBC.273.16.9673.

Dehay, B., Bove, J., Rodriguez-Muela, N., Perier, C., Recasens, A., Boya, P., et al. (2010). Pathogenic Lysosomal Depletion in Parkinson's Disease. *J. Neurosci.* 30, 12535–12544. doi:10.1523/JNEUROSCI.1920-10.2010.

Dehay, B., Martinez-Vicente, M., Caldwell, G. A., Caldwell, K. A., Yue, Z., Cookson, M. R., et al. (2013). Lysosomal impairment in Parkinson's disease. *Mov. Disord.* 28, 725–732. doi:10.1002/mds.25462.

del Toro, D., Alberch, J., Lazaro-Dieguez, F., Martin-Ibanez, R., Xifro, X., Egea, G., et al. (2009). Mutant Huntingtin Impairs Post-Golgi Trafficking to Lysosomes by Delocalizing Optineurin/Rab8 Complex from the Golgi Apparatus. *Mol. Biol. Cell* 20, 1478–1492.

doi:10.1091/mbc.E08-07-0726.

Deng, H., Wang, P., and Jankovic, J. (2018). The genetics of Parkinson disease. *Ageing Res. Rev.* 42, 72–85. doi:10.1016/j.arr.2017.12.007.

Deng, Z., Purtell, K., Lachance, V., Wold, M. S., Chen, S., and Yue, Z. (2017). Autophagy Receptors and Neurodegenerative Diseases. *Trends Cell Biol.* 27, 491–504. doi:10.1016/J.TCB.2017.01.001.

Desagher, S., and Martinou, J. C. (2000). Mitochondria as the central control point of apoptosis. *Trends Cell Biol.* 10, 369–77. Available at: http://www.ncbi.nlm.nih.gov/pubmed/10932094 [Accessed February 9, 2018].

Desai, V. G., Feuers, R. J., Hart, R. W., and Ali, S. F. (1996). MPP+-induced neurotoxicity in mouse is age-dependent: evidenced by the selective inhibition of complexes of electron transport. *Brain Res.* 715, 1–8. doi:10.1016/0006-8993(95)01255-9.

Devi, L., Raghavendran, V., Prabhu, B. M., Avadhani, N. G., and Anandatheerthavarada, H. K. (2008a). Mitochondrial Import and Accumulation of ⎵-Synuclein Impair Complex I in Human Dopaminergic Neuronal Cultures and Parkinson Disease Brain * □ S. doi:10.1074/jbc.M710012200.

Devi, L., Raghavendran, V., Prabhu, B. M., Avadhani, N. G., and Anandatheerthavarada, H. K. (2008b). Mitochondrial import and accumulation of alpha-synuclein impair complex I in human dopaminergic neuronal cultures and Parkinson disease brain. *J. Biol. Chem.* 283, 9089–100. doi:10.1074/jbc.M710012200.

Di Bartolomeo, S., Corazzari, M., Nazio, F., Oliverio, S., Lisi, G., Antonioli, M., et al. (2010). The dynamic interaction of AMBRA1 with the dynein motor complex regulates mammalian autophagy. *J. Cell Biol.* 191, 155–168. doi:10.1083/jcb.201002100.

Di Maio, R., Barrett, P. J., Hoffman, E. K., Barrett, C. W., Zharikov, A., Borah, A., et al. (2016). α-Synuclein binds TOM20 and inhibits mitochondrial protein import in Parkinson's disease. *Sci. Transl. Med.* 8, 342ra78. doi:10.1126/scitranslmed.aaf3634.

Dickey, A. S., Pineda, V. V, Tsunemi, T., Liu, P. P., Miranda, H. C., Gilmore-Hall, S. K., et al. (2016). PPAR-δ is repressed in Huntington's disease, is required for normal neuronal function and can be targeted therapeutically. *Nat. Med.* 22, 37–45. doi:10.1038/nm.4003.

DiFiglia, M., Sapp, E., Chase, K. O., Davies, S. W., Bates, G. P., Vonsattel, J. P., et al. (1997). Aggregation of huntingtin in neuronal intranuclear inclusions and dystrophic neurites in brain. *Science* 277, 1990–3. Available at: http://www.ncbi.nlm.nih.gov/pubmed/9302293 [Accessed February 8, 2018].

Ding, W.-X., and Yin, X.-M. (2012). Mitophagy: mechanisms, pathophysiological roles, and analysis. *Biol. Chem.* 393, 547–64. doi:10.1515/hsz-2012-0119.

Dorsey, E. R., Beck, C. A., Darwin, K., Nichols, P., Brocht, A. F. D., Biglan, K. M., et al. (2013). Natural History of Huntington Disease. *JAMA Neurol.* 70, 1520–30. doi:10.1001/jamaneurol.2013.4408.

Dorsey, E. R., Constantinescu, R., Thompson, J. P., Biglan, K. M., Holloway, R. G., Kieburtz, K., et al. (2007). Projected number of people with Parkinson disease in the most populous nations, 2005 through 2030. *Neurology* 68, 384–386. doi:10.1212/01.wnl.0000247740.47667.03.

Dragatsis, I., Levine, M. S., and Zeitlin, S. (2000). Inactivation of Hdh in the brain and testis results in progressive neurodegeneration and sterility in mice. *Nat. Genet.* 26, 300–306. doi:10.1038/81593.

Duyao, M. P., Auerbach, A. B., Ryan, A., Persichetti, F., Barnes, G. T., McNeil, S. M., et al.

(1995). Inactivation of the mouse Huntington's disease gene homolog Hdh. *Science* 269, 407–10. Available at: http://www.ncbi.nlm.nih.gov/pubmed/7618107 [Accessed February 8, 2018].

Edvardson, S., Cinnamon, Y., Ta-Shma, A., Shaag, A., Yim, Y.-I., Zenvirt, S., et al. (2012). A Deleterious Mutation in DNAJC6 Encoding the Neuronal-Specific Clathrin-Uncoating Co-Chaperone Auxilin, Is Associated with Juvenile Parkinsonism. *PLoS One* 7, e36458. doi:10.1371/journal.pone.0036458.

Egan, D. F., Shackelford, D. B., Mihaylova, M. M., Gelino, S., Kohnz, R. A., Mair, W., et al. (2011). Phosphorylation of ULK1 (hATG1) by AMP-Activated Protein Kinase Connects Energy Sensing to Mitophagy. *Science (80-.).* 331, 456–461. doi:10.1126/science.1196371.

Ekstrand, M. I., Falkenberg, M., Rantanen, A., Park, C. B., Gaspari, M., Hultenby, K., et al. (2004). Mitochondrial transcription factor A regulates mtDNA copy number in mammals. *Hum. Mol. Genet.* 13, 935–944. doi:10.1093/hmg/ddh109.

El-Daher, M.-T., Hangen, E., Bruyere, J., Poizat, G., Al-Ramahi, I., Pardo, R., et al. (2015). Huntingtin proteolysis releases non-polyQ fragments that cause toxicity through dynamin 1 dysregulation. *EMBO J.* 34, 2255–2271. doi:10.15252/embj.201490808.

Fahn, S. (2003). Description of Parkinson's disease as a clinical syndrome. *Ann. N. Y. Acad. Sci.* 991, 1–14. Available at: http://www.ncbi.nlm.nih.gov/pubmed/12846969 [Accessed February 8, 2018].

Faou, P., and Hoogenraad, N. J. (2012). Tom34: A cytosolic cochaperone of the Hsp90/Hsp70 protein complex involved in mitochondrial protein import. *Biochim. Biophys. Acta - Mol. Cell Res.* 1823, 348–357. doi:10.1016/j.bbamcr.2011.12.001.

Fasano, A., Daniele, A., and Albanese, A. (2012). Treatment of motor and non-motor features of Parkinson's disease with deep brain stimulation. *Lancet Neurol.* 11, 429–442. doi:10.1016/S1474-4422(12)70049-2.

Fearnley, J. M., and Lees, A. J. (1991). Ageing and Parkinson's disease: substantia nigra regional selectivity. *Brain* 114 (Pt 5), 2283–301. Available at: http://www.ncbi.nlm.nih.gov/pubmed/1933245 [Accessed February 8, 2018].

Ferrante, R. J. (2009). Mouse models of Huntington's disease and methodological considerations for therapeutic trials. *Biochim. Biophys. Acta - Mol. Basis Dis.* 1792, 506–520. doi:10.1016/j.bbadis.2009.04.001.

Fiorese, C. J., Schulz, A. M., Lin, Y.-F., Rosin, N., Pellegrino, M. W., and Haynes, C. M. (2016). The Transcription Factor ATF5 Mediates a Mammalian Mitochondrial UPR. *Curr. Biol.* 26, 2037–2043. doi:10.1016/j.cub.2016.06.002.

Forman, H. J., Davies, K. J. A., and Ursini, F. (2014). How do nutritional antioxidants really work: nucleophilic tone and para-hormesis versus free radical scavenging in vivo. *Free Radic. Biol. Med.* 66, 24–35. doi:10.1016/j.freeradbiomed.2013.05.045.

Frank, S., Testa, C. M., Stamler, D., Kayson, E., Davis, C., Edmondson, M. C., et al. (2016). Effect of Deutetrabenazine on Chorea Among Patients With Huntington Disease. *JAMA* 316, 40. doi:10.1001/jama.2016.8655.

Freimann, K., Zschiedrich, K., Brüggemann, N., Grünewald, A., Pawlack, H., Hagenah, J., et al. (2013). Mortalin mutations are not a frequent cause of early-onset Parkinson disease. *Neurobiol. Aging* 34, 2694.e19-2694.e20. doi:10.1016/j.neurobiolaging.2013.05.021.

Frezza, C., Cipolat, S., and Scorrano, L. (2007). Organelle isolation: functional mitochondria from mouse liver, muscle and cultured filroblasts. *Nat. Protoc.* 2, 287–295. doi:10.1038/nprot.2006.478.

Friedman, J. R., Lackner, L. L., West, M., DiBenedetto, J. R., Nunnari, J., and Voeltz, G. K. (2011). ER tubules mark sites of mitochondrial division. *Science (80-.).* 334, 358–62. Available at: http://science.sciencemag.org/content/334/6054/358.full [Accessed November 12, 2017].

Funayama, M., Ohe, K., Amo, T., Furuya, N., Yamaguchi, J., Saiki, S., et al. (2015). CHCHD2 mutations in autosomal dominant late-onset Parkinson's disease: a genome-wide linkage and sequencing study. *Lancet Neurol.* 14, 274–282. doi:10.1016/S1474-4422(14)70266-2.

Gakh, O., Cavadini, P., and Isaya, G. (2002). Mitochondrial processing peptidases. *Biochim. Biophys. Acta* 1592, 63–77.

Ganley, I. G., Lam, D. H., Wang, J., Ding, X., Chen, S., and Jiang, X. (2009). ULK1·ATG13·FIP200 Complex Mediates mTOR Signaling and Is Essential for Autophagy. *J. Biol. Chem.* 284, 12297–12305. doi:10.1074/jbc.M900573200.

Gao, H.-M., Kotzbauer, P. T., Uryu, K., Leight, S., Trojanowski, J. Q., and Lee, V. M.-Y. (2008). Neuroinflammation and oxidation/nitration of alpha-synuclein linked to dopaminergic neurodegeneration. *J. Neurosci.* 28, 7687–98. doi:10.1523/JNEUROSCI.0143-07.2008.

Gao, H., Yang, W., Qi, Z., Lu, L., Duan, C., Zhao, C., et al. (2012). DJ-1 Protects Dopaminergic Neurons against Rotenone-Induced Apoptosis by Enhancing ERK-Dependent Mitophagy. *J. Mol. Biol.* 423, 232–248. doi:10.1016/j.jmb.2012.06.034.

Gauthier, L. R., Charrin, B. C., Borrell-Pagès, M., Dompierre, J. P., Rangone, H., Cordelières, F. P., et al. (2004). Huntingtin Controls Neurotrophic Support and Survival of Neurons by Enhancing BDNF Vesicular Transport along Microtubules. *Cell* 118, 127–138. doi:10.1016/j.cell.2004.06.018.

Gegg, M. E., Cooper, J. M., Chau, K.-Y., Rojo, M., Schapira, A. H. V., and Taanman, J.-W. (2010). Mitofusin 1 and mitofusin 2 are ubiquitinated in a PINK1/parkin-dependent manner upon induction of mitophagy. *Hum. Mol. Genet.* 19, 4861–4870. doi:10.1093/hmg/ddq419.

Geisler, S., Holmström, K. M., Skujat, D., Fiesel, F. C., Rothfuss, O. C., Kahle, P. J., et al. (2010). PINK1/Parkin-mediated mitophagy is dependent on VDAC1 and p62/SQSTM1. *Nat. Cell Biol.* 12, 119–131. doi:10.1038/ncb2012.

Gellerich, F. N., Gizatullina, Z., Nguyen, H. P., Trumbeckaite, S., Vielhaber, S., Seppet, E., et al. (2008). Impaired Regulation of Brain Mitochondria by Extramitochondrial Ca^{2+} in Transgenic Huntington Disease Rats. *J. Biol. Chem.* 283, 30715–30724. doi:10.1074/jbc.M709555200.

Gerdes, F., Tatsuta, T., and Langer, T. (2012). Mitochondrial AAA proteases — Towards a molecular understanding of membrane-bound proteolytic machines. *Biochim. Biophys. Acta - Mol. Cell Res.* 1823, 49–55. doi:10.1016/j.bbamcr.2011.09.015.

Gesualdi, N. M., Chirico, G., Pirozzi, G., Costantino, E., Landriscina, M., and Esposito, F. (2007). Tumor necrosis factor-associated protein 1 (TRAP-1) protects cells from oxidative stress and apoptosis. *Stress* 10, 342–350. doi:10.1080/10253890701314863.

Gines, S., Ivanova, E., Seong, I.-S., Saura, C. A., and MacDonald, M. E. (2003a). Enhanced Akt Signaling Is an Early Pro-survival Response That Reflects *N* -Methyl-D-aspartate Receptor Activation in Huntington's Disease Knock-in Striatal Cells. *J. Biol. Chem.* 278, 50514–50522. doi:10.1074/jbc.M309348200.

Gines, S., Seong, I. S., Fossale, E., Ivanova, E., Trettel, F., Gusella, J. F., et al. (2003b). Specific progressive cAMP reduction implicates energy deficit in presymptomatic Huntington's disease knock-in mice. *Hum. Mol. Genet.* 12, 497–508. Available at:

http://www.ncbi.nlm.nih.gov/pubmed/12588797 [Accessed February 8, 2018].
Gispert, S., Parganlija, D., Klinkenberg, M., Drose, S., Wittig, I., Mittelbronn, M., et al. (2013). Loss of mitochondrial peptidase Clpp leads to infertility, hearing loss plus growth retardation via accumulation of CLPX, mtDNA and inflammatory factors. *Hum. Mol. Genet.* 22, 4871–4887. doi:10.1093/hmg/ddt338.
Glick, B. S., Brandt, A., Cunningham, K., Müller, S., Hallberg, R. L., and Schatz, G. (1992). Cytochromes c1 and b2 are sorted to the intermembrane space of yeast mitochondria by a stop-transfer mechanism. *Cell* 69, 809–22. Available at: http://www.ncbi.nlm.nih.gov/pubmed/1350514 [Accessed February 7, 2018].
Gomez-Lazaro, M., Bonekamp, N. A., Galindo, M. F., Jordán, J., and Schrader, M. (2008). 6-Hydroxydopamine (6-OHDA) induces Drp1-dependent mitochondrial fragmentation in SH-SY5Y cells. *Free Radic. Biol. Med.* 44, 1960–1969. doi:10.1016/j.freeradbiomed.2008.03.009.
Gordon, D. M., Dancis, A., and Pain, D. (2000). Mechanisms of mitochondrial protein import. *Essays Biochem.* 36, 61–73.
Goswami, A. V., Samaddar, M., Sinha, D., Purushotham, J., and D'Silva, P. (2012). Enhanced J-protein interaction and compromised protein stability of mtHsp70 variants lead to mitochondrial dysfunction in Parkinson's disease. *Hum. Mol. Genet.* 21, 3317–3332. doi:10.1093/hmg/dds162.
Grafton, S. T., Mazziotta, J. C., Pahl, J. J., St George-Hyslop, P., Haines, J. L., Gusella, J., et al. (1992). Serial changes of cerebral glucose metabolism and caudate size in persons at risk for Huntington's disease. *Arch. Neurol.* 49, 1161–7.
Gray, C. W., Ward, R. V, Karran, E., Turconi, S., Rowles, A., Viglienghi, D., et al. (2000). Characterization of human HtrA2, a novel serine protease involved in the mammalian cellular stress response. *Eur. J. Biochem.* 267, 5699–710. Available at: http://www.ncbi.nlm.nih.gov/pubmed/10971580 [Accessed February 7, 2018].
Gray, M., Shirasaki, D. I., Cepeda, C., Andre, V. M., Wilburn, B., Lu, X.-H., et al. (2008). Full-Length Human Mutant Huntingtin with a Stable Polyglutamine Repeat Can Elicit Progressive and Selective Neuropathogenesis in BACHD Mice. *J. Neurosci.* 28, 6182–6195. doi:10.1523/JNEUROSCI.0857-08.2008.
Gray, M. W. (2012). Mitochondrial evolution. *Cold Spring Harb. Perspect. Biol.* 4, a011403. doi:10.1101/cshperspect.a011403.
Greene, J. C., Whitworth, A. J., Kuo, I., Andrews, L. A., Feany, M. B., and Pallanck, L. J. (2003). Mitochondrial pathology and apoptotic muscle degeneration in Drosophila parkin mutants. *Proc. Natl. Acad. Sci.* 100, 4078–4083. doi:10.1073/pnas.0737556100.
Grenier, K., McLelland, G.-L., and Fon, E. A. (2013). Parkin- and PINK1-Dependent Mitophagy in Neurons: Will the Real Pathway Please Stand Up? *Front. Neurol.* 4, 100. doi:10.3389/fneur.2013.00100.
Gu, M., Gash, M. T., Mann, V. M., Javoy-Agid, F., Cooper, J. M., and Schapira, A. H. (1996). Mitochondrial defect in Huntington's disease caudate nucleus. *Ann. Neurol.* 39, 385–9. doi:10.1002/ana.410390317.
Guedes-Dias, P., Pinho, B. R., Soares, T. R., de Proença, J., Duchen, M. R., and Oliveira, J. M. A. (2016). Mitochondrial dynamics and quality control in Huntington's disease. *Neurobiol. Dis.* 90, 51–57. doi:10.1016/j.nbd.2015.09.008.
Gumeni, S., and Trougakos, I. P. (2016). Cross Talk of Proteostasis and Mitostasis in Cellular Homeodynamics, Ageing, and Disease. *Oxid. Med. Cell. Longev.* 2016, 4587691. doi:10.1155/2016/4587691.
Gunawardena, S., Her, L.-S., Brusch, R. G., Laymon, R. A., Niesman, I. R., Gordesky-Gold,

B., et al. (2003). Disruption of axonal transport by loss of huntingtin or expression of pathogenic polyQ proteins in Drosophila. *Neuron* 40, 25–40.

Guo, M. (2012). Drosophila as a Model to Study Mitochondrial Dysfunction in Parkinson's Disease. *Cold Spring Harb. Perspect. Med.* 2, a009944–a009944. doi:10.1101/cshperspect.a009944.

Guo, X., Disatnik, M.-H., Monbureau, M., Shamloo, M., Mochly-Rosen, D., and Qi, X. (2013). Inhibition of mitochondrial fragmentation diminishes Huntington's disease-associated neurodegeneration. *J. Clin. Invest.* 123, 5371–88. doi:10.1172/JCI70911.

Guo, X., Sun, X., Hu, D., Wang, Y.-J., Fujioka, H., Vyas, R., et al. (2016). VCP recruitment to mitochondria causes mitophagy impairment and neurodegeneration in models of Huntington's disease. *Nat. Commun.* 7, 12646. doi:10.1038/ncomms12646.

Gusdon, A. M., Zhu, J., Van Houten, B., and Chu, C. T. (2012). ATP13A2 regulates mitochondrial bioenergetics through macroautophagy. *Neurobiol. Dis.* 45, 962–72. doi:10.1016/j.nbd.2011.12.015.

Gutekunst, C. A., Li, S. H., Yi, H., Ferrante, R. J., Li, X. J., and Hersch, S. M. (1998). The cellular and subcellular localization of huntingtin-associated protein 1 (HAP1): comparison with huntingtin in rat and human. *J. Neurosci.* 18, 7674–86.

Haas, R. H., Nasirian, F., Nakano, K., Ward, D., Pay, M., Hill, R., et al. (1995). Low platelet mitochondrial complex I and complex II/III activity in early untreated parkinson's disease. *Ann. Neurol.* 37, 714–722. doi:10.1002/ana.410370604.

Halliwell, B. (1996). Free radicals, proteins and DNA: oxidative damage versus redox regulation. *Biochem. Soc. Trans.* 24, 1023–7. Available at: http://www.ncbi.nlm.nih.gov/pubmed/8968505 [Accessed February 7, 2018].

Halliwell, B., and Gutteridge, J. M. (1984). Oxygen toxicity, oxygen radicals, transition metals and disease. *Biochem. J.* 219, 1–14.

Hantraye, P., Riche, D., Maziere, M., and Isacson, O. (1990). A primate model of Huntington's disease: behavioral and anatomical studies of unilateral excitotoxic lesions of the caudate-putamen in the baboon. *Exp. Neurol.* 108, 91–104. Available at: http://www.ncbi.nlm.nih.gov/pubmed/2139853 [Accessed January 23, 2018].

Hara, T., Nakamura, K., Matsui, M., Yamamoto, A., Nakahara, Y., Suzuki-migishima, R., et al. (2006). Suppression of basal autophagy in neural cells causes neurodegenerative disease in mice. 1–5. doi:10.1038/nature04724.

Hardie, D. G. (2007). AMP-activated/SNF1 protein kinases: conserved guardians of cellular energy. *Nat. Rev. Mol. Cell Biol.* 8, 774–785. doi:10.1038/nrm2249.

Hasegawa, E., Takeshige, K., Oishi, T., Murai, Y., and Minakami, S. (1990). 1-Methyl-4-phenylpyridinium (MPP+) induces NADH-dependent superoxide formation and enhances NADH-dependent lipid peroxidation in bovine heart submitochondrial particles. *Biochem. Biophys. Res. Commun.* 170, 1049–1055. doi:10.1016/0006-291X(90)90498-C.

Hatano, Y., Li, Y., Sato, K., Asakawa, S., Yamamura, Y., Tomiyama, H., et al. (2004). NovelPINK1 mutations in early-onset parkinsonism. *Ann. Neurol.* 56, 424–427. doi:10.1002/ana.20251.

Hattula, K., and Peränen, J. (2000). FIP-2, a coiled-coil protein, links Huntingtin to Rab8 and modulates cellular morphogenesis. *Curr. Biol.* 10, 1603–6. doi:10.1016/S0960-9822(00)00864-2.

Hayes, J. D., Flanagan, J. U., and Jowsey, I. R. (2005). Glutathione transferases. *Annu. Rev. Pharmacol. Toxicol.* 45, 51–88. doi:10.1146/annurev.pharmtox.45.120403.095857.

Haynes, C. M., Petrova, K., Benedetti, C., Yang, Y., and Ron, D. (2007). ClpP Mediates Activation of a Mitochondrial Unfolded Protein Response in C. elegans. *Dev. Cell* 13, 467–480. doi:10.1016/j.devcel.2007.07.016.

Haynes, C. M., and Ron, D. (2010). The mitochondrial UPR - protecting organelle protein homeostasis. *J. Cell Sci.* 123, 3849–3855. doi:10.1242/jcs.075119.

Haynes, C. M., Yang, Y., Blais, S. P., Neubert, T. A., and Ron, D. (2010). The Matrix Peptide Exporter HAF-1 Signals a Mitochondrial UPR by Activating the Transcription Factor ZC376.7 in C. elegans. *Mol. Cell* 37, 529–540. doi:10.1016/j.molcel.2010.01.015.

He, C., and Klionsky, D. J. (2009). Regulation Mechanisms and Signaling Pathways of Autophagy. *Annu. Rev. Genet.* 43, 67–93. doi:10.1146/annurev-genet-102808-114910.

He, R., Peng, J., Yuan, P., Xu, F., and Wei, W. (2015). Divergent roles of BECN1 in LC3 lipidation and autophagosomal function. *Autophagy* 11, 740–747. doi:10.1080/15548627.2015.1034404.

Hegde, R., Srinivasula, S. M., Zhang, Z., Wassell, R., Mukattash, R., Cilenti, L., et al. (2002). Identification of Omi/HtrA2 as a mitochondrial apoptotic serine protease that disrupts inhibitor of apoptosis protein-caspase interaction. *J. Biol. Chem.* 277, 432–8. doi:10.1074/jbc.M109721200.

Hely, M. A., Reid, W. G. J., Adena, M. A., Halliday, G. M., and Morris, J. G. L. (2008). The Sydney multicenter study of Parkinson's disease: The inevitability of dementia at 20 years. *Mov. Disord.* 23, 837–844. doi:10.1002/mds.21956.

Hendricks, A. E., Latourelle, J. C., Lunetta, K. L., Cupples, L. A., Wheeler, V., MacDonald, M. E., et al. (2009). Estimating the probability of de novo HD cases from transmissions of expanded penetrant CAG alleles in the Huntington disease gene from male carriers of high normal alleles (27-35 CAG). *Am. J. Med. Genet. Part A* 149A, 1375–1381. doi:10.1002/ajmg.a.32901.

Heo, J.-M., Ordureau, A., Paulo, J. A., Rinehart, J., and Harper, J. W. (2015). The PINK1-PARKIN Mitochondrial Ubiquitylation Pathway Drives a Program of OPTN/NDP52 Recruitment and TBK1 Activation to Promote Mitophagy. *Mol. Cell* 60, 7–20. doi:10.1016/j.molcel.2015.08.016.

Hernandez, D. G., Reed, X., and Singleton, A. B. (2016). Genetics in Parkinson disease: Mendelian versus non-Mendelian inheritance. *J. Neurochem.* 139, 59–74. doi:10.1111/jnc.13593.

Herrmann, J. M., and Riemer, J. (2010). The Intermembrane Space of Mitochondria. *Antioxid. Redox Signal.* 13, 1341–1358. doi:10.1089/ars.2009.3063.

Hersch, S. M., and Rosas, H. D. (2008). Neuroprotection for Huntington's disease: Ready, set, slow. *Neurotherapeutics* 5, 226–236. doi:10.1016/j.nurt.2008.01.003.

Hersch, S. M., Schifitto, G., Oakes, D., Bredlau, A.-L., Meyers, C. M., Nahin, R., et al. (2017). The CREST-E study of creatine for Huntington disease: A randomized controlled trial. *Neurology* 89, 594–601. doi:10.1212/WNL.0000000000004209.

Hirsch, E. C., and Hunot, S. (2009). Neuroinflammation in Parkinson's disease: a target for neuroprotection? *Lancet Neurol.* 8, 382–397. doi:10.1016/S1474-4422(09)70062-6.

Hirsch, E. C., Orieux, G., Muriel, M.-P., Francois, C., and Feger, J. (2003). Nondopaminergic neurons in Parkinson's disease. *Adv. Neurol.* 91, 29–37. Available at: http://www.ncbi.nlm.nih.gov/pubmed/12449099 [Accessed February 8, 2018].

Hoang, T., Choi, D.-K., Nagai, M., Wu, D.-C., Nagata, T., Prou, D., et al. (2009). Neuronal NOS and cyclooxygenase-2 contribute to DNA damage in a mouse model of Parkinson disease. *Free Radic. Biol. Med.* 47, 1049–56. doi:10.1016/j.freeradbiomed.2009.07.013.

Hodges, A., Strand, A. D., Aragaki, A. K., Kuhn, A., Sengstag, T., Hughes, G., et al. (2006). Regional and cellular gene expression changes in human Huntington's disease brain. *Hum. Mol. Genet.* 15, 965–977. doi:10.1093/hmg/ddl013.

Hodgson, J. G., Agopyan, N., Gutekunst, C. A., Leavitt, B. R., LePiane, F., Singaraja, R., et al. (1999). A YAC mouse model for Huntington's disease with full-length mutant huntingtin, cytoplasmic toxicity, and selective striatal neurodegeneration. *Neuron* 23, 181–92. Available at: http://www.ncbi.nlm.nih.gov/pubmed/10402204 [Accessed February 8, 2018].

Holmans, P. A., Massey, T. H., and Jones, L. (2017). Genetic modifiers of Mendelian disease: Huntington's disease and the trinucleotide repeat disorders. *Hum. Mol. Genet.* 26, R83–R90. doi:10.1093/hmg/ddx261.

Holmay, M. J., Terpstra, M., Coles, L. D., Mishra, U., Ahlskog, M., Öz, G., et al. (2013). N-acetylcysteine Boosts Brain and Blood Glutathione in Gaucher and Parkinson Diseases. *Clin. Neuropharmacol.* 36, 103–106. doi:10.1097/WNF.0b013e31829ae713.

Hoop, C. L., Lin, H.-K., Kar, K., Magyarfalvi, G., Lamley, J. M., Boatz, J. C., et al. (2016). Huntingtin exon 1 fibrils feature an interdigitated β-hairpin–based polyglutamine core. *Proc. Natl. Acad. Sci.* 113, 1546–1551. doi:10.1073/pnas.1521933113.

Horst, M., Oppliger, W., Rospert, S., Schönfeld, H. J., Schatz, G., and Azem, A. (1997). Sequential action of two hsp70 complexes during protein import into mitochondria. *EMBO J.* 16, 1842–1849. doi:10.1093/emboj/16.8.1842.

Hosokawa, N., Hara, T., Kaizuka, T., Kishi, C., Takamura, A., Miura, Y., et al. (2009). Nutrient-dependent mTORC1 Association with the ULK1-Atg13-FIP200 Complex Required for Autophagy. *Mol. Biol. Cell* 20, 1981–1991. doi:10.1091/mbc.E08-12-1248.

Hsieh, C.-H., Shaltouki, A., Gonzalez, A. E., Bettencourt da Cruz, A., Burbulla, L. F., St Lawrence, E., et al. (2016). Functional Impairment in Miro Degradation and Mitophagy Is a Shared Feature in Familial and Sporadic Parkinson's Disease. *Cell Stem Cell* 19, 709–724. doi:10.1016/j.stem.2016.08.002.

Huang, H., and Frohman, M. A. (2009). Lipid signaling on the mitochondrial surface. *Biochim. Biophys. Acta - Mol. Cell Biol. Lipids* 1791, 839–844. doi:10.1016/j.bbalip.2009.05.012.

Huntington, G. (1872). On chorea. *Med Surg Rep* 26, 317–21.

Huntington Study Group (2006). Tetrabenazine as antichorea therapy in Huntington disease: A randomized controlled trial. *Neurology* 66, 366–372. doi:10.1212/01.wnl.0000198586.85250.13.

Jackson-Lewis, V., Jakowec, M., Burke, R. E., and Przedborski, S. (1995). Time course and morphology of dopaminergic neuronal death caused by the neurotoxin 1-methyl-4-phenyl-1,2,3,6-tetrahydropyridine. *Neurodegeneration* 4, 257–69. Available at: http://www.ncbi.nlm.nih.gov/pubmed/8581558 [Accessed February 8, 2018].

Jackson-Lewis, V., and Przedborski, S. (2007). Protocol for the MPTP mouse model of Parkinson's disease. *Nat. Protoc.* 2, 141–151. doi:10.1038/nprot.2006.342.

Javitch, J. A., D'Amato, R. J., Strittmatter, S. M., and Snyder, S. H. (1985). Parkinsonism-inducing neurotoxin, N-methyl-4-phenyl-1,2,3,6 -tetrahydropyridine: uptake of the metabolite N-methyl-4-phenylpyridine by dopamine neurons explains selective toxicity. *Proc. Natl. Acad. Sci. U. S. A.* 82, 2173–7. Available at: http://www.ncbi.nlm.nih.gov/pubmed/3872460 [Accessed February 8, 2018].

Jenkins, B. G., Koroshetz, W. J., Beal, M. F., and Rosen, B. R. (1993). Evidence for impairment of energy metabolism in vivo in Huntington's disease using localized 1H NMR spectroscopy. *Neurology* 43, 2689–95.

Jeong, H., Then, F., Melia, T. J., Mazzulli, J. R., Cui, L., Savas, J. N., et al. (2009). Acetylation Targets Mutant Huntingtin to Autophagosomes for Degradation. *Cell* 137, 60–72. doi:10.1016/j.cell.2009.03.018.

Johri, A., and Beal, M. F. (2012). Antioxidants in Huntington's disease. *Biochim. Biophys. Acta - Mol. Basis Dis.* 1822, 664–674. doi:10.1016/j.bbadis.2011.11.014.

Jones, L., and Hughes, A. (2011). "Pathogenic Mechanisms in Huntington's Disease," in *International review of neurobiology*, 373–418. doi:10.1016/B978-0-12-381328-2.00015-8.

Joselin, A. P., Hewitt, S. J., Callaghan, S. M., Kim, R. H., Chung, Y.-H., Mak, T. W., et al. (2012). ROS-dependent regulation of Parkin and DJ-1 localization during oxidative stress in neurons. *Hum. Mol. Genet.* 21, 4888–4903. doi:10.1093/hmg/dds325.

Jung, C. H., Jun, C. B., Ro, S.-H., Kim, Y.-M., Otto, N. M., Cao, J., et al. (2009). ULK-Atg13-FIP200 Complexes Mediate mTOR Signaling to the Autophagy Machinery. *Mol. Biol. Cell* 20, 1992–2003. doi:10.1091/mbc.E08-12-1249.

Kalchman, M. A., Graham, R. K., Xia, G., Koide, H. B., Hodgson, J. G., Graham, K. C., et al. (1996). Huntingtin is ubiquitinated and interacts with a specific ubiquitin-conjugating enzyme. *J. Biol. Chem.* 271, 19385–94. doi:10.1074/JBC.271.32.19385.

Kamp, F., Exner, N., Lutz, A. K., Wender, N., Hegermann, J., Brunner, B., et al. (2010). Inhibition of mitochondrial fusion by α-synuclein is rescued by PINK1, Parkin and DJ-1. *EMBO J.* 29, 3571–3589. doi:10.1038/emboj.2010.223.

Kane, L. A., Lazarou, M., Fogel, A. I., Li, Y., Yamano, K., Sarraf, S. A., et al. (2014). PINK1 phosphorylates ubiquitin to activate Parkin E3 ubiquitin ligase activity. *J. Cell Biol.* 205, 143–153. doi:10.1083/jcb.201402104.

Kang, R., Zeh, H. J., Lotze, M. T., and Tang, D. (2011). The Beclin 1 network regulates autophagy and apoptosis. *Cell Death Differ.* 18, 571–80. doi:10.1038/cdd.2010.191.

Kang, Y., Baker, M. J., Liem, M., Louber, J., McKenzie, M., Atukorala, I., et al. (2016). Tim29 is a novel subunit of the human TIM22 translocase and is involved in complex assembly and stability. *Elife* 5. doi:10.7554/eLife.17463.

Kang, Y., Fielden, L. F., and Stojanovski, D. (2017a). Mitochondrial protein transport in health and disease. *Semin. Cell Dev. Biol.*, 1–12. doi:10.1016/j.semcdb.2017.07.028.

Kang, Y., Stroud, D. A., Baker, M. J., De Souza, D. P., Frazier, A. E., Liem, M., et al. (2017b). Sengers Syndrome-Associated Mitochondrial Acylglycerol Kinase Is a Subunit of the Human TIM22 Protein Import Complex. *Mol. Cell* 67, 457–470.e5. doi:10.1016/J.MOLCEL.2017.06.014.

Katayama, H., Kogure, T., Mizushima, N., Yoshimori, T., and Miyawaki, A. (2011). A Sensitive and Quantitative Technique for Detecting Autophagic Events Based on Lysosomal Delivery. *Chem. Biol.* 18, 1042–1052. doi:10.1016/j.chembiol.2011.05.013.

Kazlauskaite, A., Kondapalli, C., Gourlay, R., Campbell, D. G., Ritorto, M. S., Hofmann, K., et al. (2014). Parkin is activated by PINK1-dependent phosphorylation of ubiquitin at Ser65. *Biochem. J.* 460, 127–39. doi:10.1042/BJ20140334.

Keeney, P. M., Xie, J., Capaldi, R. A., and Bennett, J. P. (2006). Parkinson's Disease Brain Mitochondrial Complex I Has Oxidatively Damaged Subunits and Is Functionally Impaired and Misassembled. *J. Neurosci.* 26, 5256–5264. doi:10.1523/JNEUROSCI.0984-06.2006.

Kerscher, O., Holder, J., Srinivasan, M., Leung, R. S., and Jensen, R. E. (1997). The Tim54p-Tim22p complex mediates insertion of proteins into the mitochondrial inner membrane. *J. Cell Biol.* 139, 1663–75. Available at: http://www.ncbi.nlm.nih.gov/pubmed/9412462 [Accessed February 7, 2018].

Khalil, B., El Fissi, N., Aouane, A., Cabirol-Pol, M.-J., Rival, T., and Liévens, J.-C. (2015). PINK1-induced mitophagy promotes neuroprotection in Huntington's disease. *Cell Death Dis.* 6, e1617–e1617. doi:10.1038/cddis.2014.581.

Khan, N. A., Nikkanen, J., Yatsuga, S., Jackson, C., Wang, L., Pradhan, S., et al. (2017). mTORC1 Regulates Mitochondrial Integrated Stress Response and Mitochondrial Myopathy Progression. *Cell Metab.* 26, 419–428.e5. doi:10.1016/j.cmet.2017.07.007.

Kieburtz, K., Tilley, B. C., Elm, J. J., Babcock, D., Hauser, R., Ross, G. W., et al. (2015). Effect of Creatine Monohydrate on Clinical Progression in Patients With Parkinson Disease. *JAMA* 313, 584. doi:10.1001/jama.2015.120.

Kihara, A., Kabeya, Y., Ohsumi, Y., and Yoshimori, T. (2001). Beclin-phosphatidylinositol 3-kinase complex functions at the *trans* -Golgi network. *EMBO Rep.* 2, 330–335. doi:10.1093/embo-reports/kve061.

Kim, C., and Lee, S.-J. (2008). Controlling the mass action of α-synuclein in Parkinson's disease. *J. Neurochem.* 107, 303–316. doi:10.1111/j.1471-4159.2008.05612.x.

Kim, J., Kundu, M., Viollet, B., and Guan, K.-L. (2011). AMPK and mTOR regulate autophagy through direct phosphorylation of Ulk1. *Nat. Cell Biol.* 13, 132–141. doi:10.1038/ncb2152.

Kim, J., Moody, J. P., Edgerly, C. K., Bordiuk, O. L., Cormier, K., Smith, K., et al. (2010). Mitochondrial loss, dysfunction and altered dynamics in Huntington's disease. *Hum. Mol. Genet.* 19, 3919–35. doi:10.1093/hmg/ddq306.

Kim, Y. E., Hipp, M. S., Bracher, A., Hayer-Hartl, M., and Hartl, F. U. (2013). Molecular chaperone functions in protein folding and proteostasis. *Annu. Rev. Biochem.* 82, 323–55. doi:10.1146/annurev-biochem-060208-092442.

Kim, Y. J., Yi, Y., Sapp, E., Wang, Y., Cuiffo, B., Kegel, K. B., et al. (2001). Caspase 3-cleaved N-terminal fragments of wild-type and mutant huntingtin are present in normal and Huntington's disease brains, associate with membranes, and undergo calpain-dependent proteolysis. *Proc. Natl. Acad. Sci. U. S. A.* 98, 12784–9. doi:10.1073/pnas.221451398.

Kim, Y., Park, J., Kim, S., Song, S., Kwon, S.-K., Lee, S.-H., et al. (2008). PINK1 controls mitochondrial localization of Parkin through direct phosphorylation. *Biochem. Biophys. Res. Commun.* 377, 975–980. doi:10.1016/j.bbrc.2008.10.104.

Kinghorn, K. J., Castillo-Quan, J. I., Bartolome, F., Angelova, P. R., Li, L., Pope, S., et al. (2015). Loss of PLA2G6 leads to elevated mitochondrial lipid peroxidation and mitochondrial dysfunction. *Brain* 138, 1801–16. doi:10.1093/brain/awv132.

Kitada, T., Asakawa, S., Hattori, N., Matsumine, H., Yamamura, Y., Minoshima, S., et al. (1998). Mutations in the parkin gene cause autosomal recessive juvenile parkinsonism. *Nature* 392, 605–608. doi:10.1038/33416.

Klein, C., and Westenberger, A. (2012). Genetics of Parkinson's Disease. *Cold Spring Harb. Perspect. Med.* 2, a008888–a008888. doi:10.1101/cshperspect.a008888.

Klionsky, D. J., and Emr, S. D. (2000). Autophagy as a regulated pathway of cellular degradation. *Science* 290, 1717–21. Available at: http://www.ncbi.nlm.nih.gov/pubmed/11099404 [Accessed February 7, 2018].

Koehler, C. M., Merchant, S., Oppliger, W., Schmid, K., Jarosch, E., Dolfini, L., et al. (1998). Tim9p, an essential partner subunit of Tim10p for the import of mitochondrial carrier proteins. *EMBO J.* 17, 6477–6486. doi:10.1093/emboj/17.22.6477.

Koga, H., Martinez-Vicente, M., Arias, E., Kaushik, S., Sulzer, D., and Cuervo, A. M. (2011). Constitutive Upregulation of Chaperone-Mediated Autophagy in Huntington's Disease. *J. Neurosci.* 31, 18492–18505. doi:10.1523/JNEUROSCI.3219-11.2011.

Kogan, F. J., Nichols, W. K., and Gibb, J. W. (1976). Influence of methamphetamine on nigral and striatal tyrosine hydroxylase activity and on striatal dopamine levels. *Eur. J. Pharmacol.* 36, 363–71. Available at: http://www.ncbi.nlm.nih.gov/pubmed/6286 [Accessed February 8, 2018].

Koirala, S., Guo, Q., Kalia, R., Bui, H. T., Eckert, D. M., Frost, A., et al. (2013). Interchangeable adaptors regulate mitochondrial dynamin assembly for membrane scission. *Proc. Natl. Acad. Sci. U. S. A.* 110, E1342-51. doi:10.1073/pnas.1300855110.

Komatsu, M., Waguri, S., Chiba, T., Murata, S., Iwata, J. I., Tanida, I., et al. (2006). Loss of autophagy in the central nervous system causes neurodegeneration in mice. *Nature*.

Kordower, J. H., Olanow, C. W., Dodiya, H. B., Chu, Y., Beach, T. G., Adler, C. H., et al. (2013). Disease duration and the integrity of the nigrostriatal system in Parkinson's disease. *Brain* 136, 2419–2431. doi:10.1093/brain/awt192.

Kowald, A., and Kirkwood, T. B. L. (2000). Accumulation of Defective Mitochondria through Delayed Degradation of Damaged Organelles and Its Possible Role in the Ageing of Post-mitotic and Dividing Cells. *J. Theor. Biol.* 202, 145–160. doi:10.1006/jtbi.1999.1046.

Koyano, F., Okatsu, K., Kosako, H., Tamura, Y., Go, E., Kimura, M., et al. (2014). Ubiquitin is phosphorylated by PINK1 to activate parkin. *Nature* 510, 162–166. doi:10.1038/nature13392.

Kraytsberg, Y., Kudryavtseva, E., McKee, A. C., Geula, C., Kowall, N. W., and Khrapko, K. (2006). Mitochondrial DNA deletions are abundant and cause functional impairment in aged human substantia nigra neurons. *Nat. Genet.* 38, 518–520. doi:10.1038/ng1778.

Krebiehl, G., Ruckerbauer, S., Burbulla, L. F., Kieper, N., Maurer, B., Waak, J., et al. (2010). Reduced Basal Autophagy and Impaired Mitochondrial Dynamics Due to Loss of Parkinson's Disease-Associated Protein DJ-1. *PLoS One* 5, e9367. doi:10.1371/journal.pone.0009367.

Krebs, C. E., Karkheiran, S., Powell, J. C., Cao, M., Makarov, V., Darvish, H., et al. (2013). The Sac1 Domain of *SYNJ1* Identified Mutated in a Family with Early-Onset Progressive Parkinsonism with Generalized Seizures. *Hum. Mutat.* 34, 1200–1207. doi:10.1002/humu.22372.

Krige, D., Carroll, M. T., Cooper, J. M., Marsden, C. D., and Schapira, A. H. V. (1992). Platelet mitochondria function in Parkinson's disease. *Ann. Neurol.* 32, 782–788. doi:10.1002/ana.410320612.

Krüger, R., Sharma, M., Riess, O., Gasser, T., Van Broeckhoven, C., Theuns, J., et al. (2011). A large-scale genetic association study to evaluate the contribution of Omi/HtrA2 (PARK13) to Parkinson's disease. *Neurobiol. Aging* 32, 548.e9-18. doi:10.1016/j.neurobiolaging.2009.11.021.

Langston, J. W., Ballard, P., Tetrud, J. W., and Irwin, I. (1983). Chronic Parkinsonism in humans due to a product of meperidine-analog synthesis. *Science* 219, 979–80.

Larsson, N.-G. (2010). Somatic Mitochondrial DNA Mutations in Mammalian Aging. *Annu. Rev. Biochem.* 79, 683–706. doi:10.1146/annurev-biochem-060408-093701.

Lazarou, M., Jin, S. M., Kane, L. A., and Youle, R. J. (2012). Role of PINK1 Binding to the TOM Complex and Alternate Intracellular Membranes in Recruitment and Activation of the E3 Ligase Parkin. *Dev. Cell* 22, 320–333. doi:10.1016/j.devcel.2011.12.014.

Lazarou, M., Sliter, D. a., Kane, L. a., Sarraf, S. a., Wang, C., Burman, J. L., et al. (2015a). The ubiquitin kinase PINK1 recruits autophagy receptors to induce mitophagy. *Nature*. doi:10.1038/nature14893.

Lazarou, M., Sliter, D. A., Kane, L. A., Sarraf, S. A., Wang, C., Burman, J. L., et al. (2015b).

The ubiquitin kinase PINK1 recruits autophagy receptors to induce mitophagy. *Nature* 524, 309–314. doi:10.1038/nature14893.

Lee, J.-Y., Nagano, Y., Taylor, J. P., Lim, K. L., and Yao, T.-P. (2010a). Disease-causing mutations in Parkin impair mitochondrial ubiquitination, aggregation, and HDAC6-dependent mitophagy. *J. Cell Biol.* 189, 671–679. doi:10.1083/jcb.201001039.

Lee, J. W., Park, S., Takahashi, Y., and Wang, H.-G. (2010b). The Association of AMPK with ULK1 Regulates Autophagy. *PLoS One* 5, e15394. doi:10.1371/journal.pone.0015394.

Lee, Y., Dawson, V. L., and Dawson, T. M. (2012). Animal Models of Parkinson's Disease: Vertebrate Genetics. *Cold Spring Harb. Perspect. Med.* 2, a009324–a009324. doi:10.1101/cshperspect.a009324.

Legros, F., Malka, F., Frachon, P., Lombès, A., and Rojo, M. (2004). Organization and dynamics of human mitochondrial DNA. *J. Cell Sci.* 117, 2653–62. doi:10.1242/jcs.01134.

Li, H., Zhu, H., Xu, C., and Yuan, J. (1998). Cleavage of BID by Caspase 8 Mediates the Mitochondrial Damage in the Fas Pathway of Apoptosis. *Cell* 94, 491–501. doi:10.1016/S0092-8674(00)81590-1.

Li, S.-H., and Li, X.-J. (2004). Huntingtin-protein interactions and the pathogenesis of Huntington's disease. *Trends Genet.* 20, 146–54. doi:10.1016/j.tig.2004.01.008.

Li, W.-W., Yang, R., Guo, J.-C., Ren, H.-M., Zha, X.-L., Cheng, J.-S., et al. (2007). Localization of α-synuclein to mitochondria within midbrain of mice. *Neuroreport* 18, 1543–1546. doi:10.1097/WNR.0b013e3282f03db4.

Li, W., Serpell, L. C., Carter, W. J., Rubinsztein, D. C., and Huntington, J. A. (2006). Expression and Characterization of Full-length Human Huntingtin, an Elongated HEAT Repeat Protein. *J. Biol. Chem.* 281, 15916–15922. doi:10.1074/jbc.M511007200.

Li, Z., Okamoto, K.-I., Hayashi, Y., and Sheng, M. (2004). The Importance of Dendritic Mitochondria in the Morphogenesis and Plasticity of Spines and Synapses. *Cell* 119, 873–887. doi:10.1016/j.cell.2004.11.003.

Liesa, M., and Shirihai, O. S. (2013). Mitochondrial Dynamics in the Regulation of Nutrient Utilization and Energy Expenditure. *Cell Metab.* 17, 491–506. doi:10.1016/j.cmet.2013.03.002.

Lin, C.-H., Tallaksen-Greene, S., Chien, W.-M., Cearley, J. A., Jackson, W. S., Crouse, A. B., et al. (2001). Neurological abnormalities in a knock-in mouse model of Huntington's disease. *Hum. Mol. Genet.* 10, 137–144. doi:10.1093/hmg/10.2.137.

Lin, M. T., and Beal, M. F. (2006). Mitochondrial dysfunction and oxidative stress in neurodegenerative diseases. *Nature* 443, 787–795. doi:10.1038/nature05292.

Liochev, S. I. (2013). Reactive oxygen species and the free radical theory of aging. *Free Radic. Biol. Med.* 60, 1–4. doi:10.1016/J.FREERADBIOMED.2013.02.011.

Liot, G., Bossy, B., Lubitz, S., Kushnareva, Y., Sejbuk, N., and Bossy-Wetzel, E. (2009). Complex II inhibition by 3-NP causes mitochondrial fragmentation and neuronal cell death via an NMDA- and ROS-dependent pathway. *Cell Death Differ.* 16, 899–909. doi:10.1038/cdd.2009.22.

Liu, G., Zhang, C., Yin, J., Li, X., Cheng, F., Li, Y., et al. (2009a). α-Synuclein is differentially expressed in mitochondria from different rat brain regions and dose-dependently down-regulates complex I activity. *Neurosci. Lett.* 454, 187–192. doi:10.1016/J.NEULET.2009.02.056.

Liu, L., Feng, D., Chen, G., Chen, M., Zheng, Q., Song, P., et al. (2012). Mitochondrial outer-membrane protein FUNDC1 mediates hypoxia-induced mitophagy in mammalian cells. *Nat. Cell Biol.* 14, 177–185. doi:10.1038/ncb2422.

Liu, W., Vives-Bauza, C., Acín-Peréz-, R., Yamamoto, A., Tan, Y., Li, Y., et al. (2009b). PINK1 Defect Causes Mitochondrial Dysfunction, Proteasomal Deficit and α-Synuclein Aggregation in Cell Culture Models of Parkinson's Disease. *PLoS One* 4, e4597. doi:10.1371/journal.pone.0004597.

Lizano, P., Rashed, E., Stoll, S., Zhou, N., Wen, H., Hays, T. T., et al. (2017). The valosin-containing protein is a novel mediator of mitochondrial respiration and cell survival in the heart in vivo. *Sci. Rep.* 7, 46324. doi:10.1038/srep46324.

Loeb, V., Yakunin, E., Saada, A., and Sharon, R. (2010). The transgenic overexpression of alpha-synuclein and not its related pathology associates with complex I inhibition. *J. Biol. Chem.* 285, 7334–43. doi:10.1074/jbc.M109.061051.

Losón, O. C., Song, Z., Chen, H., and Chan, D. C. (2013). Fis1, Mff, MiD49, and MiD51 mediate Drp1 recruitment in mitochondrial fission. *Mol. Biol. Cell* 24, 659–67. doi:10.1091/mbc.E12-10-0721.

Luoma, P., Melberg, A., Rinne, J. O., Kaukonen, J. A., Nupponen, N. N., Chalmers, R. M., et al. (2004). Parkinsonism, premature menopause, and mitochondrial DNA polymerase γ mutations: clinical and molecular genetic study. *Lancet* 364, 875–882. doi:10.1016/S0140-6736(04)16983-3.

Luthi-Carter, R., and Cha, J.-H. J. (2003). Mechanisms of transcriptional dysregulation in Huntington's disease. *Clin. Neurosci. Res.* 3, 165–177. doi:10.1016/S1566-2772(03)00059-8.

MacAskill, A. F., Atkin, T. A., and Kittler, J. T. (2010). Mitochondrial trafficking and the provision of energy and calcium buffering at excitatory synapses. *Eur. J. Neurosci.* 32, 231–240. doi:10.1111/j.1460-9568.2010.07345.x.

MacVicar, T., and Langer, T. (2016). OPA1 processing in cell death and disease – the long and short of it. *J. Cell Sci.* 129, 2297–2306. doi:10.1242/jcs.159186.

Madhavan, L., Ourednik, V., and Ourednik, J. (2008). Neural Stem/Progenitor Cells Initiate the Formation of Cellular Networks That Provide Neuroprotection by Growth Factor-Modulated Antioxidant Expression. *Stem Cells* 26, 254–265. doi:10.1634/stemcells.2007-0221.

Maguire, J. J., Tyurina, Y. Y., Mohammadyani, D., Kapralov, A. A., Anthonymuthu, T. S., Qu, F., et al. (2017). Known unknowns of cardiolipin signaling: The best is yet to come. *Biochim. Biophys. Acta - Mol. Cell Biol. Lipids* 1862, 8–24. doi:10.1016/j.bbalip.2016.08.001.

Mangiarini, L., Sathasivam, K., Seller, M., Cozens, B., Harper, A., Hetherington, C., et al. (1996). Exon 1 of the HD gene with an expanded CAG repeat is sufficient to cause a progressive neurological phenotype in transgenic mice. *Cell* 87, 493–506. Available at: http://www.ncbi.nlm.nih.gov/pubmed/8898202 [Accessed February 8, 2018].

Margulis, L. (1970). *Origin of eukaryotic cells*. New Haven (Connecticut): Yale University Press.

Martin, D. D. O., Ladha, S., Ehrnhoefer, D. E., and Hayden, M. R. (2014). Autophagy in Huntington disease and huntingtin in autophagy. *Trends Neurosci.*, 1–10. doi:10.1016/j.tins.2014.09.003.

Martin, L. J., Pan, Y., Price, A. C., Sterling, W., Copeland, N. G., Jenkins, N. A., et al. (2006). Parkinson's Disease -Synuclein Transgenic Mice Develop Neuronal Mitochondrial Degeneration and Cell Death. *J. Neurosci.* 26, 41–50. doi:10.1523/JNEUROSCI.4308-05.2006.

Martinez-Vicente, M. (2015). Autophagy in neurodegenerative diseases: From pathogenic dysfunction to therapeutic modulation. *Semin. Cell Dev. Biol.* 40, 115–126.

doi:10.1016/j.semcdb.2015.03.005.
Martinez-Vicente, M. (2017). Neuronal Mitophagy in Neurodegenerative Diseases. *Front. Mol. Neurosci.* 10, 64. doi:10.3389/fnmol.2017.00064.
Martinez-Vicente, M., Talloczy, Z., Wong, E., Tang, G., Koga, H., Kaushik, S., et al. (2010). Cargo recognition failure is responsible for inefficient autophagy in Huntington's disease. *Nat. Neurosci.* 13, 567–76. doi:10.1038/nn.2528.
Martinez, B. A., Caldwell, K. A., and Caldwell, G. A. (2017a). C . elegans as a model system to accelerate discovery for Parkinson disease. *Curr. Opin. Genet. Dev.* 44, 102–109. doi:10.1016/j.gde.2017.02.011.
Martinez, B. A., Petersen, D. A., Gaeta, A. L., Stanley, S. P., Caldwell, G. A., and Caldwell, K. A. (2017b). Dysregulation of the Mitochondrial Unfolded Protein Response Induces Non-Apoptotic Dopaminergic Neurodegeneration in C. elegans Models of Parkinson's Disease. *J. Neurosci.* 37, 11085–11100. doi:10.1523/JNEUROSCI.1294-17.2017.
Martins, L. M., Morrison, A., Klupsch, K., Fedele, V., Moisoi, N., Teismann, P., et al. (2004). Neuroprotective Role of the Reaper-Related Serine Protease HtrA2/Omi Revealed by Targeted Deletion in Mice. *Mol. Cell. Biol.* 24, 9848–9862. doi:10.1128/MCB.24.22.9848-9862.2004.
Martinus, R. D., Garth, G. P., Webster, T. L., Cartwright, P., Naylor, D. J., Høj, P. B., et al. (1996). Selective induction of mitochondrial chaperones in response to loss of the mitochondrial genome. *Eur. J. Biochem.* 240, 98–103.
Matsuda, N., Sato, S., Shiba, K., Okatsu, K., Saisho, K., Gautier, C. A., et al. (2010). PINK1 stabilized by mitochondrial depolarization recruits Parkin to damaged mitochondria and activates latent Parkin for mitophagy. *J. Cell Biol.* 189, 211–221. doi:10.1083/jcb.200910140.
Matsunaga, K., Morita, E., Saitoh, T., Akira, S., Ktistakis, N. T., Izumi, T., et al. (2010). Autophagy requires endoplasmic reticulum targeting of the PI3-kinase complex via Atg14L. *J. Cell Biol.* 190, 511–21. doi:10.1083/jcb.200911141.
Matsushima, Y., Goto, Y., and Kaguni, L. S. (2010). Mitochondrial Lon protease regulates mitochondrial DNA copy number and transcription by selective degradation of mitochondrial transcription factor A (TFAM). *Proc. Natl. Acad. Sci. U. S. A.* 107, 18410–5. doi:10.1073/pnas.1008924107.
McGarry, A., McDermott, M., Kieburtz, K., de Blieck, E. A., Beal, F., Marder, K., et al. (2017). A randomized, double-blind, placebo-controlled trial of coenzyme Q10 in Huntington disease. *Neurology* 88, 152–159. doi:10.1212/WNL.0000000000003478.
McLelland, G.-L., Soubannier, V., Chen, C. X., McBride, H. M., and Fon, E. A. (2014). Parkin and PINK1 function in a vesicular trafficking pathway regulating mitochondrial quality control. *EMBO J.* 33, 282–95. doi:10.1002/embj.201385902.
McWilliams, T. G., and Muqit, M. M. (2017). PINK1 and Parkin: emerging themes in mitochondrial homeostasis. *Curr. Opin. Cell Biol.* 45, 83–91. doi:10.1016/j.ceb.2017.03.013.
McWilliams, T. G., Prescott, A. R., Montava-Garriga, L., Ball, G., Singh, F., Barini, E., et al. (2018). Basal Mitophagy Occurs Independently of PINK1 in Mouse Tissues of High Metabolic Demand. *Cell Metab.* 27, 439–449.e5. doi:10.1016/j.cmet.2017.12.008.
Menalled, L. B., Sison, J. D., Dragatsis, I., Zeitlin, S., and Chesselet, M.-F. (2003). Time course of early motor and neuropathological anomalies in a knock-in mouse model of Huntington's disease with 140 CAG repeats. *J. Comp. Neurol.* 465, 11–26. doi:10.1002/cne.10776.
Mesecke, N., Terziyska, N., Kozany, C., Baumann, F., Neupert, W., Hell, K., et al. (2005). A

disulfide relay system in the intermembrane space of mitochondria that mediates protein import. *Cell* 121, 1059–69. doi:10.1016/j.cell.2005.04.011.

Meuer, K., Suppanz, I. E., Lingor, P., Planchamp, V., Göricke, B., Fichtner, L., et al. (2007). Cyclin-dependent kinase 5 is an upstream regulator of mitochondrial fission during neuronal apoptosis. *Cell Death Differ.* 14, 651–661. doi:10.1038/sj.cdd.4402087.

Mischley, L. K., Lau, R. C., Shankland, E. G., Wilbur, T. K., and Padowski, J. M. (2017). Phase IIb Study of Intranasal Glutathione in Parkinson's Disease. *J. Parkinsons. Dis.* 7, 289–299. doi:10.3233/JPD-161040.

Misgeld, T., and Schwarz, T. L. (2017). Mitostasis in Neurons: Maintaining Mitochondria in an Extended Cellular Architecture. *Neuron* 96, 651–666. doi:10.1016/j.neuron.2017.09.055.

Mishra, P., and Chan, D. C. (2014). Mitochondrial dynamics and inheritance during cell division, development and disease. *Nat. Rev. Mol. Cell Biol.* 15, 634–46. doi:10.1038/nrm3877.

Mitchell, P. (1961). Coupling of phosphorylation to electron and hydrogen transfer by a chemi-osmotic type of mechanism. *Nature* 191, 144–8. Available at: http://www.ncbi.nlm.nih.gov/pubmed/13771349 [Accessed February 7, 2018].

Miwa, S., Lawless, C., and von Zglinicki, T. (2008). Mitochondrial turnover in liver is fast *in vivo* and is accelerated by dietary restriction: application of a simple dynamic model. *Aging Cell* 7, 920–923. doi:10.1111/j.1474-9726.2008.00426.x.

Mochel, F., Durant, B., Meng, X., O'Callaghan, J., Yu, H., Brouillet, E., et al. (2012). Early Alterations of Brain Cellular Energy Homeostasis in Huntington Disease Models. *J. Biol. Chem.* 287, 1361–1370. doi:10.1074/jbc.M111.309849.

Model, K., Meisinger, C., and Kühlbrandt, W. (2008). Cryo-Electron Microscopy Structure of a Yeast Mitochondrial Preprotein Translocase. *J. Mol. Biol.* 383, 1049–1057. doi:10.1016/j.jmb.2008.07.087.

Moisoi, N., Klupsch, K., Fedele, V., East, P., Sharma, S., Renton, A., et al. (2009a). Mitochondrial dysfunction triggered by loss of HtrA2 results in the activation of a brain-specific transcriptional stress response. *Cell Death Differ.* 16, 449–464. doi:10.1038/cdd.2008.166.

Moisoi, N., Klupsch, K., Fedele, V., East, P., Sharma, S., Renton, A., et al. (2009b). Mitochondrial dysfunction triggered by loss of HtrA2 results in the activation of a brain-specific transcriptional stress response. *Cell Death Differ.* 16, 449–464. doi:10.1038/cdd.2008.166.

Mokranjac, D., and Neupert, W. (2007). "Protein Import Into Isolated Mitochondria," in (Humana Press), 277–286. doi:10.1007/978-1-59745-365-3_20.

Mokranjac, D., and Neupert, W. (2010). The many faces of the mitochondrial TIM23 complex. *Biochim. Biophys. Acta - Bioenerg.* 1797, 1045–1054. doi:10.1016/j.bbabio.2010.01.026.

Morais, V. A., Verstreken, P., Roethig, A., Smet, J., Snellinx, A., Vanbrabant, M., et al. (2009). Parkinson's disease mutations in PINK1 result in decreased Complex I activity and deficient synaptic function. *EMBO Mol. Med.* 1, 99–111. doi:10.1002/emmm.200900006.

Moreira, P. I., Carvalho, C., Zhu, X., Smith, M. A., and Perry, G. (2010). Mitochondrial dysfunction is a trigger of Alzheimer's disease pathophysiology. *Biochim. Biophys. Acta - Mol. Basis Dis.* 1802, 2–10. doi:10.1016/j.bbadis.2009.10.006.

Morfini, G. A., You, Y.-M., Pollema, S. L., Kaminska, A., Liu, K., Yoshioka, K., et al. (2009). Pathogenic huntingtin inhibits fast axonal transport by activating JNK3 and

phosphorylating kinesin. *Nat. Neurosci.* 12, 864–871. doi:10.1038/nn.2346.

Mossmann, D., Vögtle, F.-N., Taskin, A. A., Teixeira, P. F., Ring, J., Burkhart, J. M., et al. (2014). Amyloid-β peptide induces mitochondrial dysfunction by inhibition of preprotein maturation. *Cell Metab.* 20, 662–9. doi:10.1016/j.cmet.2014.07.024.

Müftüoglu, M., Elibol, B., Dalmızrak, Ö., Ercan, A., Kulaksız, G., Ögüs, H., et al. (2004). Mitochondrial complex I and IV activities in leukocytes from patients with parkin mutations. *Mov. Disord.* 19, 544–548. doi:10.1002/mds.10695.

Naia, L., Ferreira, I. L., Cunha-Oliveira, T., Duarte, A. I., Ribeiro, M., Rosenstock, T. R., et al. (2015). Activation of IGF-1 and Insulin Signaling Pathways Ameliorate Mitochondrial Function and Energy Metabolism in Huntington's Disease Human Lymphoblasts. *Mol. Neurobiol.* 51, 331–348. doi:10.1007/s12035-014-8735-4.

Naia, L., Ribeiro, M., Rodrigues, J., Duarte, A. I., Lopes, C., Rosenstock, T. R., et al. (2016). Insulin and IGF-1 regularize energy metabolites in neural cells expressing full-length mutant huntingtin. *Neuropeptides* 58, 73–81. doi:10.1016/j.npep.2016.01.009.

Nakai, M., Mori, A., Watanabe, A., and Mitsumoto, Y. (2003). 1-methyl-4-phenylpyridinium (MPP+) decreases mitochondrial oxidation-reduction (REDOX) activity and membrane potential (Deltapsi(m)) in rat striatum. *Exp. Neurol.* 179, 103–10. Available at: http://www.ncbi.nlm.nih.gov/pubmed/12504872 [Accessed January 11, 2018].

Nakamura, K., Nemani, V. M., Azarbal, F., Skibinski, G., Levy, J. M., Egami, K., et al. (2011). Direct Membrane Association Drives Mitochondrial Fission by the Parkinson Disease-associated Protein α-Synuclein. *J. Biol. Chem.* 286, 20710–20726. doi:10.1074/jbc.M110.213538.

Napoli, E., Wong, S., Hung, C., Ross-Inta, C., Bomdica, P., and Giulivi, C. (2013). Defective mitochondrial disulfide relay system, altered mitochondrial morphology and function in Huntington's disease. *Hum. Mol. Genet.* 22, 989–1004. doi:10.1093/hmg/dds503.

Narendra, D., Kane, L. A., Hauser, D. N., Fearnley, I. M., and Youle, R. J. (2010a). p62/SQSTM1 is required for Parkin-induced mitochondrial clustering but not mitophagy; VDAC1 is dispensable for both. *Autophagy* 6, 1090–106. doi:10.4161/AUTO.6.8.13426.

Narendra, D. P., Jin, S. M., Tanaka, A., Suen, D.-F., Gautier, C. A., Shen, J., et al. (2010b). PINK1 Is Selectively Stabilized on Impaired Mitochondria to Activate Parkin. *PLoS Biol.* 8, e1000298. doi:10.1371/journal.pbio.1000298.

Nargund, A. M., Pellegrino, M. W., Fiorese, C. J., Baker, B. M., and Haynes, C. M. (2012). Mitochondrial Import Efficiency of ATFS-1 Regulates Mitochondrial UPR Activation. *Science (80-.).* 337, 587–590. doi:10.1126/science.1223560.

Nasir, J., Floresco, S. B., O'Kusky, J. R., Diewert, V. M., Richman, J. M., Zeisler, J., et al. (1995). Targeted disruption of the Huntington's disease gene results in embryonic lethality and behavioral and morphological changes in heterozygotes. *Cell* 81, 811–823. doi:10.1016/0092-8674(95)90542-1.

Neupert, W., and Herrmann, J. M. (2007). Translocation of proteins into mitochondria. *Annu. Rev. Biochem.* 76, 723–49. doi:10.1146/annurev.biochem.76.052705.163409.

Ng, C.-H., Guan, M. S. H., Koh, C., Ouyang, X., Yu, F., Tan, E.-K., et al. (2012). AMP Kinase Activation Mitigates Dopaminergic Dysfunction and Mitochondrial Abnormalities in Drosophila Models of Parkinson's Disease. *J. Neurosci.* 32, 14311–14317. doi:10.1523/JNEUROSCI.0499-12.2012.

Ngo, H. B., Kaiser, J. T., and Chan, D. C. (2011). The mitochondrial transcription and packaging factor Tfam imposes a U-turn on mitochondrial DNA. *Nat. Struct. Mol. Biol.* 18, 1290–1296. doi:10.1038/nsmb.2159.

Nicklas, W. J., Vyas, I., and Heikkila, R. E. (1985). Inhibition of NADH-linked oxidation in

brain mitochondria by 1-methyl-4-phenyl-pyridine, a metabolite of the neurotoxin, 1-methyl-4-phenyl-1,2,5,6-tetrahydropyridine. *Life Sci.* 36, 2503–8. Available at: http://www.ncbi.nlm.nih.gov/pubmed/2861548 [Accessed February 9, 2018].

Nikkanen, J., Forsström, S., Euro, L., Paetau, I., Kohnz, R. A., Wang, L., et al. (2016). Mitochondrial DNA Replication Defects Disturb Cellular dNTP Pools and Remodel One-Carbon Metabolism. *Cell Metab.* 23, 635–648. doi:10.1016/J.CMET.2016.01.019.

NINDS Exploratory Trials in Parkinson Disease (NET-PD) FS-ZONE Investigators (2015). Pioglitazone in early Parkinson's disease: a phase 2, multicentre, double-blind, randomised trial. *Lancet Neurol.* 14, 795–803. doi:10.1016/S1474-4422(15)00144-1.

Niu, J., Yu, M., Wang, C., and Xu, Z. (2012). Leucine-rich repeat kinase 2 disturbs mitochondrial dynamics via Dynamin-like protein. *J. Neurochem.* 122, 650–658. doi:10.1111/j.1471-4159.2012.07809.x.

Novak, I., Kirkin, V., McEwan, D. G., Zhang, J., Wild, P., Rozenknop, A., et al. (2010). Nix is a selective autophagy receptor for mitochondrial clearance. *EMBO Rep.* 11, 45–51. doi:10.1038/embor.2009.256.

Nunnari, J., and Suomalainen, A. (2012). Mitochondria: In Sickness and in Health. *Cell* 148, 1145–1159. doi:10.1016/j.cell.2012.02.035.

O'Donnell, K. C., Lulla, A., Stahl, M. C., Wheat, N. D., Bronstein, J. M., and Sagasti, A. (2014). Axon degeneration and PGC-1 -mediated protection in a zebrafish model of -synuclein toxicity. *Dis. Model. Mech.* 7, 571–582. doi:10.1242/dmm.013185.

O'Rourke, B. (2007). Mitochondrial Ion Channels. *Annu. Rev. Physiol.* 69, 19–49. doi:10.1146/annurev.physiol.69.031905.163804.

O'Toole, M., Latham, R., Baqri, R. M., and Miller, K. E. (2008). Modeling mitochondrial dynamics during in vivo axonal elongation. *J. Theor. Biol.* 255, 369–377. doi:10.1016/j.jtbi.2008.09.009.

Ochaba, J., Lukacsovich, T., Csikos, G., Zheng, S., Margulis, J., Salazar, L., et al. (2014). Potential function for the Huntingtin protein as a scaffold for selective autophagy. *Proc. Natl. Acad. Sci. U. S. A.* 111, 16889–94. doi:10.1073/pnas.1420103111.

Oertel, W. H. (2017). Recent advances in treating Parkinson's disease. *F1000Research* 6, 260. doi:10.12688/f1000research.10100.1.

Okamoto, T., Ishida, R., Yamamoto, H., Tanabe-Ishida, M., Haga, A., Takahashi, H., et al. (2015). Functional structure and physiological functions of mammalian wild-type HSP60. *Arch. Biochem. Biophys.* 586, 10–19. doi:10.1016/j.abb.2015.09.022.

Okatsu, K., Saisho, K., Shimanuki, M., Nakada, K., Shitara, H., Sou, Y., et al. (2010). p62/SQSTM1 cooperates with Parkin for perinuclear clustering of depolarized mitochondria. *Genes to Cells* 15, no-no. doi:10.1111/j.1365-2443.2010.01426.x.

Olanow, C. W., Kieburtz, K., and Katz, R. (2017). Clinical approaches to the development of a neuroprotective therapy for PD. *Exp. Neurol.* 298, 246–251. doi:10.1016/j.expneurol.2017.06.018.

Olanow, C. W., Schapira, A. H., LeWitt, P. A., Kieburtz, K., Sauer, D., Olivieri, G., et al. (2006). TCH346 as a neuroprotective drug in Parkinson's disease: a double-blind, randomised, controlled trial. *Lancet Neurol.* 5, 1013–1020. doi:10.1016/S1474-4422(06)70602-0.

Olichon, A., Guillou, E., Delettre, C., Landes, T., Arnauné-Pelloquin, L., Emorine, L. J., et al. (2006). Mitochondrial dynamics and disease, OPA1. *Biochim. Biophys. Acta - Mol. Cell Res.* 1763, 500–509. doi:10.1016/j.bbamcr.2006.04.003.

Oliveira, J. M. A. (2011). Techniques to investigate neuronal mitochondrial function and its pharmacological modulation. *Curr. Drug Targets* 12, 762–73. Available at:

http://www.ncbi.nlm.nih.gov/pubmed/21275887 [Accessed February 9, 2018].

Orr, A. L., Li, S., Wang, C.-E., Li, H., Wang, J., Rong, J., et al. (2008). N-Terminal Mutant Huntingtin Associates with Mitochondria and Impairs Mitochondrial Trafficking. *J. Neurosci.* 28, 2783–2792. doi:10.1523/JNEUROSCI.0106-08.2008.

Ortega, Z., and Lucas, J. J. (2014). Ubiquitin-proteasome system involvement in Huntington's disease. *Front. Mol. Neurosci.* 7, 77. doi:10.3389/fnmol.2014.00077.

Osellame, L. D., Singh, A. P., Stroud, D. A., Palmer, C. S., Stojanovski, D., Ramachandran, R., et al. (2016). Cooperative and independent roles of the Drp1 adaptors Mff, MiD49 and MiD51 in mitochondrial fission. *J. Cell Sci.* 129, 2170–2181. doi:10.1242/jcs.185165.

Pacelli, C., De Rasmo, D., Signorile, A., Grattagliano, I., di Tullio, G., D'Orazio, A., et al. (2011). Mitochondrial defect and PGC-1α dysfunction in parkin-associated familial Parkinson's disease. *Biochim. Biophys. Acta - Mol. Basis Dis.* 1812, 1041–1053. doi:10.1016/j.bbadis.2010.12.022.

Paisan-Ruiz, C., Bhatia, K. P., Li, A., Hernandez, D., Davis, M., Wood, N. W., et al. (2008). Characterization of PLA2G6 as a locus for dystonia-parkinsonism. *Ann. Neurol.* 65, 19–23. doi:10.1002/ana.21415.

Paisán-Ruíz, C., Jain, S., Evans, E. W., Gilks, W. P., Simón, J., van der Brug, M., et al. (2004). Cloning of the Gene Containing Mutations that Cause PARK8-Linked Parkinson's Disease. *Neuron* 44, 595–600. doi:10.1016/j.neuron.2004.10.023.

Panov, A. V., Gutekunst, C.-A., Leavitt, B. R., Hayden, M. R., Burke, J. R., Strittmatter, W. J., et al. (2002). Early mitochondrial calcium defects in Huntington's disease are a direct effect of polyglutamines. *Nat. Neurosci.* 5, 731–736. doi:10.1038/nn884.

Panov, A. V, Burke, J. R., Strittmatter, W. J., and Greenamyre, J. T. (2003). In vitro effects of polyglutamine tracts on Ca2+-dependent depolarization of rat and human mitochondria: relevance to Huntington's disease. *Arch. Biochem. Biophys.* 410, 1–6. Available at: http://www.ncbi.nlm.nih.gov/pubmed/12559971 [Accessed December 10, 2017].

Papoutsi, M., Labuschagne, I., Tabrizi, S. J., and Stout, J. C. (2014). The cognitive burden in Huntington's disease: Pathology, phenotype, and mechanisms of compensation. *Mov. Disord.* 29, 673–683. doi:10.1002/mds.25864.

Parihar, M. S., Parihar, A., Fujita, M., Hashimoto, M., and Ghafourifar, P. (2008). Mitochondrial association of alpha-synuclein causes oxidative stress. *Cell. Mol. Life Sci.* 65, 1272–1284. doi:10.1007/s00018-008-7589-1.

Parker, W. D., Boyson, S. J., and Parks, J. K. (1989). Abnormalities of the electron transport chain in idiopathic parkinson's disease. *Ann. Neurol.* 26, 719–723. doi:10.1002/ana.410260606.

Parker, W. D., Parks, J. K., Swerdlow, R. H., and Swerdlow, R. H. (2008). Complex I deficiency in Parkinson's disease frontal cortex. *Brain Res.* 1189, 215–8. doi:10.1016/j.brainres.2007.10.061.

Parkinson, J. (2002). An Essay on the Shaking Palsy. *J. Neuropsychiatry Clin. Neurosci.* 14, 223–236. doi:10.1176/jnp.14.2.223.

Parkinson Study Group (1993). Effects of Tocopherol and Deprenyl on the Progression of Disability in Early Parkinson's Disease. *N. Engl. J. Med.* 328, 176–183. doi:10.1056/NEJM199301213280305.

Parkinson Study Group PRECEPT Investigators (2007). Mixed lineage kinase inhibitor CEP-1347 fails to delay disability in early Parkinson disease. *Neurology* 69, 1480–1490. doi:10.1212/01.wnl.0000277648.63931.c0.

Pascale, E., Di Battista, M. E., Rubino, A., Purcaro, C., Valente, M., Fattapposta, F., et al.

(2016). Genetic Architecture of MAPT Gene Region in Parkinson Disease Subtypes. *Front. Cell. Neurosci.* 10, 96. doi:10.3389/fncel.2016.00096.

Perier, C., Bender, A., García-Arumí, E., Melià, M. J., Bové, J., Laub, C., et al. (2013). Accumulation of mitochondrial DNA deletions within dopaminergic neurons triggers neuroprotective mechanisms. *Brain* 136, 2369–2378. doi:10.1093/brain/awt196.

Perier, C., Bové, J., Dehay, B., Jackson-Lewis, V., Rabinovitch, P. S., Przedborski, S., et al. (2010). AIF deficiency sensitizes dopaminergic neurons to parkinsonian neurotoxins. *Ann. Neurol.* 68, 184–92. doi:10.1002/ana.22034.

Perier, C., Bove, J., Wu, D.-C., Dehay, B., Choi, D.-K., Jackson-Lewis, V., et al. (2007). Two molecular pathways initiate mitochondria-dependent dopaminergic neurodegeneration in experimental Parkinson's disease. *Proc. Natl. Acad. Sci.* 104, 8161–8166. doi:10.1073/pnas.0609874104.

Perier, C., Tieu, K., Guegan, C., Caspersen, C., Jackson-Lewis, V., Carelli, V., et al. (2005a). Complex I deficiency primes Bax-dependent neuronal apoptosis through mitochondrial oxidative damage. *Proc. Natl. Acad. Sci.* 102, 19126–19131. doi:10.1073/pnas.0508215102.

Perier, C., Tieu, K., Guegan, C., Caspersen, C., Jackson-Lewis, V., Carelli, V., et al. (2005b). Complex I deficiency primes Bax-dependent neuronal apoptosis through mitochondrial oxidative damage. *Proc. Natl. Acad. Sci.* 102, 19126–19131. doi:10.1073/pnas.0508215102.

Perier, C., and Vila, M. (2012). Mitochondrial Biology and Parkinson's Disease. *Cold Spring Harb. Perspect. Med.* 2, a009332–a009332. doi:10.1101/cshperspect.a009332.

Perluigi, M., Poon, H. F., Maragos, W., Pierce, W. M., Klein, J. B., Calabrese, V., et al. (2005). Proteomic Analysis of Protein Expression and Oxidative Modification in R6/2 Transgenic Mice. *Mol. Cell. Proteomics* 4, 1849–1861. doi:10.1074/mcp.M500090-MCP200.

Perry, J. J. P., Shin, D. S., Getzoff, E. D., and Tainer, J. A. (2010). The structural biochemistry of the superoxide dismutases. *Biochim. Biophys. Acta - Proteins Proteomics* 1804, 245–262. doi:10.1016/j.bbapap.2009.11.004.

Peters-Libeu, C., Miller, J., Rutenber, E., Newhouse, Y., Krishnan, P., Cheung, K., et al. (2012). Disease-Associated Polyglutamine Stretches in Monomeric Huntingtin Adopt a Compact Structure. *J. Mol. Biol.* 421, 587–600. doi:10.1016/j.jmb.2012.01.034.

Pfanner, N., and Neupert, W. (1990). The Mitochondrial Protein Import Apparatus. *Annu. Rev. Biochem.* 59, 331–353. doi:10.1146/annurev.bi.59.070190.001555.

Pickrell, A. M., and Youle, R. J. (2015). The Roles of PINK1, Parkin, and Mitochondrial Fidelity in Parkinson's Disease. *Neuron* 85, 257–273. doi:10.1016/j.neuron.2014.12.007.

Ploumi, C., Daskalaki, I., and Tavernarakis, N. (2017). Mitochondrial biogenesis and clearance: a balancing act. *FEBS J.* 284, 183–195. doi:10.1111/febs.13820.

Polymeropoulos, M. H., Lavedan, C., Leroy, E., Ide, S. E., Dehejia, A., Dutra, A., et al. (1997). Mutation in the alpha-synuclein gene identified in families with Parkinson's disease. *Science* 276, 2045–7. Available at: http://www.ncbi.nlm.nih.gov/pubmed/9197268 [Accessed December 7, 2017].

Pont-Sunyer, C., Hotter, A., Gaig, C., Seppi, K., Compta, Y., Katzenschlager, R., et al. (2015). The Onset of Nonmotor Symptoms in Parkinson's disease (The ONSET PDStudy). *Mov. Disord.* 30, 229–237. doi:10.1002/mds.26077.

Porras, G., Li, Q., and Bezard, E. (2012). Modeling Parkinson's Disease in Primates: The MPTP Model. *Cold Spring Harb. Perspect. Med.* 2, a009308–a009308.

doi:10.1101/cshperspect.a009308.
Prasai, K. (2017). Regulation of mitochondrial structure and function by protein import: A current review. *Pathophysiology* 24, 107–122. doi:10.1016/j.pathophys.2017.03.001.
Pringsheim, T., Jette, N., Frolkis, A., and Steeves, T. D. L. (2014). The prevalence of Parkinson's disease: A systematic review and meta-analysis. *Mov. Disord.* 29, 1583–1590. doi:10.1002/mds.25945.
Puthalakath, H., Huang, D. C., O'Reilly, L. A., King, S. M., and Strasser, A. (1999). The proapoptotic activity of the Bcl-2 family member Bim is regulated by interaction with the dynein motor complex. *Mol. Cell* 3, 287–96. Available at: http://www.ncbi.nlm.nih.gov/pubmed/10198631 [Accessed February 9, 2018].
Quirós, P. M., Español, Y., Acín-Pérez, R., Rodríguez, F., Bárcena, C., Watanabe, K., et al. (2014). ATP-Dependent Lon Protease Controls Tumor Bioenergetics by Reprogramming Mitochondrial Activity. *Cell Rep.* 8, 542–556. doi:10.1016/j.celrep.2014.06.018.
Quirós, P. M., Langer, T., and López-Otín, C. (2015). New roles for mitochondrial proteases in health, ageing and disease. *Nat. Rev. Mol. Cell Biol.* 16, 345–359. doi:10.1038/nrm3984.
Rakovic, A., Shurkewitsch, K., Seibler, P., Grünewald, A., Zanon, A., Hagenah, J., et al. (2013). Phosphatase and tensin homolog (PTEN)-induced putative kinase 1 (PINK1)-dependent ubiquitination of endogenous Parkin attenuates mitophagy: study in human primary fibroblasts and induced pluripotent stem cell-derived neurons. *J. Biol. Chem.* 288, 2223–37. doi:10.1074/jbc.M112.391680.
Ramirez, A., Heimbach, A., Gründemann, J., Stiller, B., Hampshire, D., Cid, L. P., et al. (2006). Hereditary parkinsonism with dementia is caused by mutations in ATP13A2, encoding a lysosomal type 5 P-type ATPase. *Nat. Genet.* 38, 1184–1191. doi:10.1038/ng1884.
Ramonet, D., Perier, C., Recasens, A., Dehay, B., Bové, J., Costa, V., et al. (2013). Optic atrophy 1 mediates mitochondria remodeling and dopaminergic neurodegeneration linked to complex I deficiency. *Cell Death Differ.* 20, 77–85. doi:10.1038/cdd.2012.95.
Ransohoff, R. M. (2016). How neuroinflammation contributes to neurodegeneration. *Science (80-.).* 353, 777–783. doi:10.1126/science.aag2590.
Rappold, P. M., Cui, M., Grima, J. C., Fan, R. Z., de Mesy-Bentley, K. L., Chen, L., et al. (2014). Drp1 inhibition attenuates neurotoxicity and dopamine release deficits in vivo. *Nat. Commun.* 5, 5244. doi:10.1038/ncomms6244.
Ravikumar, B., Vacher, C., Berger, Z., Davies, J. E., Luo, S., Oroz, L. G., et al. (2004). Inhibition of mTOR induces autophagy and reduces toxicity of polyglutamine expansions in fly and mouse models of Huntington disease. *Nat. Genet.* 36, 585–595. doi:10.1038/ng1362.
Recasens, A., Dehay, B., Bové, J., Carballo-Carbajal, I., Dovero, S., Pérez-Villalba, A., et al. (2014). Lewy body extracts from Parkinson disease brains trigger α-synuclein pathology and neurodegeneration in mice and monkeys. *Ann. Neurol.* 75, 351–362. doi:10.1002/ana.24066.
Reiner, A., Albin, R. L., Anderson, K. D., D'Amato, C. J., Penney, J. B., and Young, A. B. (1988). Differential loss of striatal projection neurons in Huntington disease. *Proc. Natl. Acad. Sci. U. S. A.* 85, 5733–7. Available at: http://www.ncbi.nlm.nih.gov/pubmed/2456581 [Accessed February 8, 2018].
Rhee, S. G., Chae, H. Z., and Kim, K. (2005). Peroxiredoxins: a historical overview and speculative preview of novel mechanisms and emerging concepts in cell signaling. *Free*

Radic. Biol. Med. 38, 1543–52. doi:10.1016/j.freeradbiomed.2005.02.026.

Richter, B., Sliter, D. A., Herhaus, L., Stolz, A., Wang, C., Beli, P., et al. (2016). Phosphorylation of OPTN by TBK1 enhances its binding to Ub chains and promotes selective autophagy of damaged mitochondria. *Proc. Natl. Acad. Sci. U. S. A.* 113, 4039–44. doi:10.1073/pnas.1523926113.

Ritch, J. J., Valencia, A., Alexander, J., Sapp, E., Gatune, L., Sangrey, G. R., et al. (2012). Multiple phenotypes in Huntington disease mouse neural stem cells. *Mol. Cell. Neurosci.* 50, 70–81. doi:10.1016/j.mcn.2012.03.011.

Roberts, R. F., Tang, M. Y., Fon, E. A., and Durcan, T. M. (2016). Defending the mitochondria: The pathways of mitophagy and mitochondrial-derived vesicles. *Int. J. Biochem. Cell Biol.* 79, 427–436. doi:10.1016/j.biocel.2016.07.020.

Roise, D., Theiler, F., Horvath, S. J., Tomich, J. M., Richards, J. H., Allison, D. S., et al. (1988). Amphiphilicity is essential for mitochondrial presequence function. *EMBO J.* 7, 649–53. Available at: http://www.ncbi.nlm.nih.gov/pubmed/3396537 [Accessed February 7, 2018].

Ross, C. A., Aylward, E. H., Wild, E. J., Langbehn, D. R., Long, J. D., Warner, J. H., et al. (2014). Huntington disease: natural history, biomarkers and prospects for therapeutics. *Nat. Rev. Neurol.* 10, 204–216. doi:10.1038/nrneurol.2014.24.

Ross, C. A., and Tabrizi, S. J. (2011). Huntington's disease: from molecular pathogenesis to clinical treatment. *Lancet Neurol.* 10, 83–98. doi:10.1016/S1474-4422(10)70245-3.

Rossetti, Z. L., Sotgiu, A., Sharp, D. E., Hadjiconstantinou, M., and Neff, N. H. (1988). 1-Methyl-4-phenyl-1,2,3,6-tetrahydropyridine (MPTP) and free radicals in vitro. *Biochem. Pharmacol.* 37, 4573–4. Available at: http://www.ncbi.nlm.nih.gov/pubmed/2849450 [Accessed February 9, 2018].

Rubinsztein, D. C., and C., D. (2003). How does the Huntington's disease mutation damage cells? *Sci. Aging Knowledge Environ.* 2003, PE26. doi:10.1126/sageke.2003.37.pe26.

Rubio-Cosials, A., Sydow, J. F., Jiménez-Menéndez, N., Fernández-Millán, P., Montoya, J., Jacobs, H. T., et al. (2011). Human mitochondrial transcription factor A induces a U-turn structure in the light strand promoter. *Nat. Struct. Mol. Biol.* 18, 1281–1289. doi:10.1038/nsmb.2160.

Rugarli, E. I., and Langer, T. (2012). Mitochondrial quality control: a matter of life and death for neurons. *EMBO J.* 31, 1336–1349. doi:10.1038/emboj.2012.38.

Rui, Y.-N., Xu, Z., Patel, B., Chen, Z., Chen, D., Tito, A., et al. (2015). Huntingtin functions as a scaffold for selective macroautophagy. *Nat. Cell Biol.* 17, 262–275. doi:10.1038/ncb3101.

Russell, R. C., Tian, Y., Yuan, H., Park, H. W., Chang, Y.-Y., Kim, J., et al. (2013). ULK1 induces autophagy by phosphorylating Beclin-1 and activating VPS34 lipid kinase. *Nat. Cell Biol.* 15, 741–750. doi:10.1038/ncb2757.

Rutherford, J. C., and Bird, A. J. (2004). Metal-responsive transcription factors that regulate iron, zinc, and copper homeostasis in eukaryotic cells. *Eukaryot. Cell* 3, 1–13. Available at: http://www.pubmedcentral.nih.gov/articlerender.fcgi?artid=PMC329510 [Accessed December 10, 2017].

Saha, S., Guillily, M. D., Ferree, A., Lanceta, J., Chan, D., Ghosh, J., et al. (2009). LRRK2 Modulates Vulnerability to Mitochondrial Dysfunction in Caenorhabditis elegans. *J. Neurosci.* 29, 9210–9218. doi:10.1523/JNEUROSCI.2281-09.2009.

Sanders, L. H., McCoy, J., Hu, X., Mastroberardino, P. G., Dickinson, B. C., Chang, C. J., et al. (2014). Mitochondrial DNA damage: Molecular marker of vulnerable nigral neurons in Parkinson's disease. *Neurobiol. Dis.* 70, 214–223. doi:10.1016/j.nbd.2014.06.014.

Sandoval, H., Thiagarajan, P., Dasgupta, S. K., Schumacher, A., Prchal, J. T., Chen, M., et al. (2008). Essential role for Nix in autophagic maturation of erythroid cells. *Nature* 454, 232–235. doi:10.1038/nature07006.

Saporito, M. S., Brown, E. M., Miller, M. S., and Carswell, S. (1999). CEP-1347/KT-7515, an inhibitor of c-jun N-terminal kinase activation, attenuates the 1-methyl-4-phenyl tetrahydropyridine-mediated loss of nigrostriatal dopaminergic neurons In vivo. *J. Pharmacol. Exp. Ther.* 288, 421–7. Available at: http://www.ncbi.nlm.nih.gov/pubmed/9918541 [Accessed February 3, 2018].

Sarkar, S., and Rubinsztein, D. C. (2008). Huntington's disease: degradation of mutant huntingtin by autophagy. *FEBS J.* 275, 4263–4270. doi:10.1111/j.1742-4658.2008.06562.x.

Sarraf, S. A., Raman, M., Guarani-Pereira, V., Sowa, M. E., Huttlin, E. L., Gygi, S. P., et al. (2013). Landscape of the PARKIN-dependent ubiquitylome in response to mitochondrial depolarization. *Nature* 496, 372–376. doi:10.1038/nature12043.

Scarffe, L. A., Stevens, D. A., Dawson, V. L., and Dawson, T. M. (2014). Parkin and PINK1: much more than mitophagy. *Trends Neurosci.* 37, 315–24. doi:10.1016/j.tins.2014.03.004.

Scarpulla, R. C. (2006). Nuclear control of respiratory gene expression in mammalian cells. *J. Cell. Biochem.* 97, 673–683. doi:10.1002/jcb.20743.

Scarpulla, R. C. (2008). Nuclear Control of Respiratory Chain Expression by Nuclear Respiratory Factors and PGC-1-Related Coactivator. *Ann. N. Y. Acad. Sci.* 1147, 321–334. doi:10.1196/annals.1427.006.

Scarpulla, R. C. (2011). Metabolic control of mitochondrial biogenesis through the PGC-1 family regulatory network. *Biochim. Biophys. Acta - Mol. Cell Res.* 1813, 1269–1278. doi:10.1016/j.bbamcr.2010.09.019.

Schapira, A. H., Cooper, J. M., Dexter, D., Clark, J. B., Jenner, P., and Marsden, C. D. (1990). Mitochondrial complex I deficiency in Parkinson's disease. *J. Neurochem.* 54, 823–7.

Schapira, A. H. V. (2013). Recent developments in biomarkers in Parkinson disease. *Curr. Opin. Neurol.* 26, 395–400. doi:10.1097/WCO.0b013e3283633741.

Schapira, A. H. V., Chaudhuri, K. R., and Jenner, P. (2017). Non-motor features of Parkinson disease. *Nat. Rev. Neurosci.* 18, 435–450. doi:10.1038/nrn.2017.62.

Schapira, A. H. V., and Olanow, C. W. (2004). Neuroprotection in Parkinson Disease. *JAMA* 291, 358. doi:10.1001/jama.291.3.358.

Schilling, G., Becher, M. W., Sharp, A. H., Jinnah, H. A., Duan, K., Kotzuk, J. A., et al. (1999). Intranuclear inclusions and neuritic aggregates in transgenic mice expressing a mutant N-terminal fragment of huntingtin. *Hum. Mol. Genet.* 8, 397–407. Available at: http://www.ncbi.nlm.nih.gov/pubmed/9949199 [Accessed February 8, 2018].

Schon, E. A., and Przedborski, S. (2011). Mitochondria: The Next (Neurode)Generation. *Neuron* 70, 1033–1053. doi:10.1016/j.neuron.2011.06.003.

Schönfeld, P., and Reiser, G. (2013). Why does Brain Metabolism not Favor Burning of Fatty Acids to Provide Energy? - Reflections on Disadvantages of the Use of Free Fatty Acids as Fuel for Brain. *J. Cereb. Blood Flow Metab.* 33, 1493–1499. doi:10.1038/jcbfm.2013.128.

Schulte, J., and Littleton, J. T. (2011). The biological function of the Huntingtin protein and its relevance to Huntington's Disease pathology. *Curr. Trends Neurol.* 5, 65–78. Available at: http://www.ncbi.nlm.nih.gov/pubmed/22180703 [Accessed February 10, 2018].

Schwarcz, R., Guidetti, P., Sathyasaikumar, K. V, and Muchowski, P. J. (2010). Of mice, rats

and men: Revisiting the quinolinic acid hypothesis of Huntington's disease. *Prog. Neurobiol.* 90, 230–45. doi:10.1016/j.pneurobio.2009.04.005.

Schweers, R. L., Zhang, J., Randall, M. S., Loyd, M. R., Li, W., Dorsey, F. C., et al. (2007). NIX is required for programmed mitochondrial clearance during reticulocyte maturation. *Proc. Natl. Acad. Sci.* 104, 19500–19505. doi:10.1073/pnas.0708818104.

Sebastián, D., Palacín, M., and Zorzano, A. (2017). Mitochondrial Dynamics: Coupling Mitochondrial Fitness with Healthy Aging. *Trends Mol. Med.* 23, 201–215. doi:10.1016/j.molmed.2017.01.003.

Sena, L. A., and Chandel, N. S. (2012). Physiological roles of mitochondrial reactive oxygen species. *Mol. Cell* 48, 158–67. doi:10.1016/j.molcel.2012.09.025.

Seong, I. S., Ivanova, E., Lee, J.-M., Choo, Y. S., Fossale, E., Anderson, M., et al. (2005). HD CAG repeat implicates a dominant property of huntingtin in mitochondrial energy metabolism. *Hum. Mol. Genet.* 14, 2871–2880. doi:10.1093/hmg/ddi319.

Seredenina, T., and Luthi-Carter, R. (2012). What have we learned from gene expression profiles in Huntington's disease? *Neurobiol. Dis.* 45, 83–98. doi:10.1016/j.nbd.2011.07.001.

Sheng, Z.-H., and Cai, Q. (2012). Mitochondrial transport in neurons: impact on synaptic homeostasis and neurodegeneration. *Nat. Rev. Neurosci.* 13, 77–93. doi:10.1038/nrn3156.

Shi, R.-Y., Zhu, S.-H., Li, V., Gibson, S. B., Xu, X.-S., and Kong, J.-M. (2014). BNIP3 Interacting with LC3 Triggers Excessive Mitophagy in Delayed Neuronal Death in Stroke. *CNS Neurosci. Ther.* 20, 1045–1055. doi:10.1111/cns.12325.

Shiba-Fukushima, K., Imai, Y., Yoshida, S., Ishihama, Y., Kanao, T., Sato, S., et al. (2012). PINK1-mediated phosphorylation of the Parkin ubiquitin-like domain primes mitochondrial translocation of Parkin and regulates mitophagy. *Sci. Rep.* 2, 1002. doi:10.1038/srep01002.

Shin, J.-H., Ko, H. S., Kang, H., Lee, Y., Lee, Y.-I., Pletinkova, O., et al. (2011). PARIS (ZNF746) Repression of PGC-1α Contributes to Neurodegeneration in Parkinson's Disease. *Cell* 144, 689–702. doi:10.1016/j.cell.2011.02.010.

Shirendeb, U. P., Calkins, M. J., Manczak, M., Anekonda, V., Dufour, B., McBride, J. L., et al. (2012). Mutant huntingtin's interaction with mitochondrial protein Drp1 impairs mitochondrial biogenesis and causes defective axonal transport and synaptic degeneration in Huntington's disease. *Hum. Mol. Genet.* 21, 406–420. doi:10.1093/hmg/ddr475.

Shirendeb, U., Reddy, A. P., Manczak, M., Calkins, M. J., Mao, P., Tagle, D. A., et al. (2011). Abnormal mitochondrial dynamics, mitochondrial loss and mutant huntingtin oligomers in Huntington's disease: implications for selective neuronal damage. *Hum. Mol. Genet.* 20, 1438–55. doi:10.1093/hmg/ddr024.

Shojaee, S., Sina, F., Banihosseini, S. S., Kazemi, M. H., Kalhor, R., Shahidi, G.-A., et al. (2008). Genome-wide Linkage Analysis of a Parkinsonian-Pyramidal Syndrome Pedigree by 500 K SNP Arrays. *Am. J. Hum. Genet.* 82, 1375–1384. doi:10.1016/j.ajhg.2008.05.005.

Siddiqui, A., Rivera-Sánchez, S., Castro, M. del R., Acevedo-Torres, K., Rane, A., Torres-Ramos, C. A., et al. (2012). Mitochondrial DNA damage Is associated with reduced mitochondrial bioenergetics in Huntington's disease. *Free Radic. Biol. Med.* 53, 1478–1488. doi:10.1016/j.freeradbiomed.2012.06.008.

Simon-Sanchez, J., and Singleton, A. B. (2008a). Sequencing analysis of OMI/HTRA2 shows previously reported pathogenic mutations in neurologically normal controls.

Hum. Mol. Genet. 17, 1988–1993. doi:10.1093/hmg/ddn096.

Simon-Sanchez, J., and Singleton, A. B. (2008b). Sequencing analysis of OMI/HTRA2 shows previously reported pathogenic mutations in neurologically normal controls. *Hum. Mol. Genet.* 17, 1988–1993. doi:10.1093/hmg/ddn096.

Singleton, A. B., Farrer, M., Johnson, J., Singleton, A., Hague, S., Kachergus, J., et al. (2003). -Synuclein Locus Triplication Causes Parkinson's Disease. *Science (80-.).* 302, 841–841. doi:10.1126/science.1090278.

Sokol, A. M., Sztolsztener, M. E., Wasilewski, M., Heinz, E., and Chacinska, A. (2014). Mitochondrial protein translocases for survival and wellbeing. *FEBS Lett.* 588, 2484–2495. doi:10.1016/j.febslet.2014.05.028.

Song, H. Y., Dunbar, J. D., Zhang, Y. X., Guo, D., and Donner, D. B. (1995). Identification of a protein with homology to hsp90 that binds the type 1 tumor necrosis factor receptor. *J. Biol. Chem.* 270, 3574–81.

Song, W., Chen, J., Petrilli, A., Liot, G., Klinglmayr, E., Zhou, Y., et al. (2011). Mutant huntingtin binds the mitochondrial fission GTPase dynamin-related protein-1 and increases its enzymatic activity. *Nat. Med.* 17, 377–382. doi:10.1038/nm.2313.

Sorolla, M. A., Rodríguez-Colman, M. J., Tamarit, J., Ortega, Z., Lucas, J. J., Ferrer, I., et al. (2010). Protein oxidation in Huntington disease affects energy production and vitamin B6 metabolism. *Free Radic. Biol. Med.* 49, 612–21. doi:10.1016/j.freeradbiomed.2010.05.016.

Soubannier, V., McLelland, G.-L., Zunino, R., Braschi, E., Rippstein, P., Fon, E. A., et al. (2012). A Vesicular Transport Pathway Shuttles Cargo from Mitochondria to Lysosomes. *Curr. Biol.* 22, 135–141. doi:10.1016/j.cub.2011.11.057.

St-Pierre, J., Drori, S., Uldry, M., Silvaggi, J. M., Rhee, J., Jäger, S., et al. (2006). Suppression of Reactive Oxygen Species and Neurodegeneration by the PGC-1 Transcriptional Coactivators. *Cell* 127, 397–408. doi:10.1016/j.cell.2006.09.024.

Stack, E. C., Matson, W. R., and Ferrante, R. J. (2008). Evidence of oxidant damage in Huntington's disease: translational strategies using antioxidants. *Ann. N. Y. Acad. Sci.* 1147, 79–92. doi:10.1196/annals.1427.008.

Sterky, F. H., Lee, S., Wibom, R., Olson, L., and Larsson, N.-G. (2011). Impaired mitochondrial transport and Parkin-independent degeneration of respiratory chain-deficient dopamine neurons in vivo. *Proc. Natl. Acad. Sci. U. S. A.* 108, 12937–42. doi:10.1073/pnas.1103295108.

Stevens, D. A., Lee, Y., Kang, H. C., Lee, B. D., Lee, Y.-I., Bower, A., et al. (2015). Parkin loss leads to PARIS-dependent declines in mitochondrial mass and respiration. *Proc. Natl. Acad. Sci.* 112, 11696–11701. doi:10.1073/pnas.1500624112.

Stojanovski, D., Bohnert, M., Pfanner, N., and van der Laan, M. (2012). Mechanisms of protein sorting in mitochondria. *Cold Spring Harb. Perspect. Biol.* 4. doi:10.1101/cshperspect.a011320.

Stojanovski, D., Ryan, M. T., Wojtkowska, M., Kmita, H., Stojanovski, D., Ryan, M. T., et al. (2017). "Mitochondria Protein Import: Methods," in *eLS* (Chichester, UK: John Wiley & Sons, Ltd), 1–6. doi:10.1002/9780470015902.a0002617.pub3.

Stolz, A., Ernst, A., and Dikic, I. (2014). Cargo recognition and trafficking in selective autophagy. *Nat. Cell Biol.* 16, 495–501. doi:10.1038/ncb2979.

Stout, J. C., Paulsen, J. S., Queller, S., Solomon, A. C., Whitlock, K. B., Campbell, J. C., et al. (2011). Neurocognitive signs in prodromal Huntington disease. *Neuropsychology* 25, 1–14. doi:10.1037/a0020937.

Strauss, K. M., Martins, L. M., Plun-Favreau, H., Marx, F. P., Kautzmann, S., Berg, D., et al.

(2005). Loss of function mutations in the gene encoding Omi/HtrA2 in Parkinson's disease. *Hum. Mol. Genet.* 14, 2099–2111. doi:10.1093/hmg/ddi215.

Su, Y.-C., and Qi, X. (2013). Inhibition of excessive mitochondrial fission reduced aberrant autophagy and neuronal damage caused by LRRK2 G2019S mutation. *Hum. Mol. Genet.* 22, 4545–4561. doi:10.1093/hmg/ddt301.

Suen, Y. K., Fung, K. P., Choy, Y. M., Lee, C. Y., Chan, C. W., and Kong, S. K. (2000). Concanavalin A induced apoptosis in murine macrophage PU5-1.8 cells through clustering of mitochondria and release of cytochrome c. *Apoptosis* 5, 369–77. Available at: http://www.ncbi.nlm.nih.gov/pubmed/11227218 [Accessed February 9, 2018].

Sun, N., Yun, J., Liu, J., Malide, D., Liu, C., Rovira, I. I., et al. (2015). Measuring In Vivo Mitophagy. *Mol. Cell* 60, 685–696. doi:10.1016/j.molcel.2015.10.009.

Suomalainen, A., and Battersby, B. J. (2017). Mitochondrial diseases: the contribution of organelle stress responses to pathology. *Nat. Rev. Mol. Cell Biol.* 19, 77–92. doi:10.1038/nrm.2017.66.

Swerdlow, R. H., Parks, J. K., Miller, S. W., Davis, R. E., Tuttle, J. B., Trimmer, P. A., et al. (1996). Origin and functional consequences of the complex I defect in Parkinson's disease. *Ann. Neurol.* 40, 663–671. doi:10.1002/ana.410400417.

Szargel, R., Shani, V., Abd Elghani, F., Mekies, L. N., Liani, E., Rott, R., et al. (2016). The PINK1, synphilin-1 and SIAH-1 complex constitutes a novel mitophagy pathway. *Hum. Mol. Genet.* 25, 3476–3490. doi:10.1093/hmg/ddw189.

Tabrizi, S. J., Cleeter, M. W., Xuereb, J., Taanman, J. W., Cooper, J. M., and Schapira, A. H. (1999). Biochemical abnormalities and excitotoxicity in Huntington's disease brain. *Ann. Neurol.* 45, 25–32.

Tabrizi, S. J., Langbehn, D. R., Leavitt, B. R., Roos, R. A., Durr, A., Craufurd, D., et al. (2009). Biological and clinical manifestations of Huntington's disease in the longitudinal TRACK-HD study: cross-sectional analysis of baseline data. *Lancet Neurol.* 8, 791–801. doi:10.1016/S1474-4422(09)70170-X.

Tabrizi, S. J., Scahill, R. I., Owen, G., Durr, A., Leavitt, B. R., Roos, R. A., et al. (2013). Predictors of phenotypic progression and disease onset in premanifest and early-stage Huntington's disease in the TRACK-HD study: analysis of 36-month observational data. *Lancet Neurol.* 12, 637–649. doi:10.1016/S1474-4422(13)70088-7.

Tai, H.-C., and Schuman, E. M. (2008). Ubiquitin, the proteasome and protein degradation in neuronal function and dysfunction. *Nat. Rev. Neurosci.* 9, 826–838. doi:10.1038/nrn2499.

Tan, J. M. M., Wong, E. S. P., Kirkpatrick, D. S., Pletnikova, O., Ko, H. S., Tay, S.-P., et al. (2008). Lysine 63-linked ubiquitination promotes the formation and autophagic clearance of protein inclusions associated with neurodegenerative diseases. *Hum. Mol. Genet.* 17, 431–439. doi:10.1093/hmg/ddm320.

Tanaka, A., Cleland, M. M., Xu, S., Narendra, D. P., Suen, D.-F., Karbowski, M., et al. (2010). Proteasome and p97 mediate mitophagy and degradation of mitofusins induced by Parkin. *J. Cell Biol.* 191, 1367–1380. doi:10.1083/jcb.201007013.

Tassa, A., Roux, M. P., Attaix, D., and Bechet, D. M. (2003). Class III phosphoinositide 3-kinase--Beclin1 complex mediates the amino acid-dependent regulation of autophagy in C2C12 myotubes. *Biochem. J.* 376, 577–86. doi:10.1042/BJ20030826.

Tatton, N. A., and Kish, S. J. (1997). In situ detection of apoptotic nuclei in the substantia nigra compacta of 1-methyl-4-phenyl-1,2,3,6-tetrahydropyridine-treated mice using terminal deoxynucleotidyl transferase labelling and acridine orange staining. *Neuroscience* 77, 1037–48. Available at: http://www.ncbi.nlm.nih.gov/pubmed/9130785

[Accessed February 8, 2018].
Tayebi, N., Callahan, M., Madike, V., Stubblefield, B. K., Orvisky, E., Krasnewich, D., et al. (2001). Gaucher Disease and Parkinsonism: A Phenotypic and Genotypic Characterization. *Mol. Genet. Metab.* 73, 313–321. doi:10.1006/mgme.2001.3201.
Tenreiro, S., Franssens, V., Winderickx, J., and Outeiro, T. F. (2017). Yeast models of Parkinson's disease-associated molecular pathologies. *Curr. Opin. Genet. Dev.* 44, 74–83. doi:10.1016/j.gde.2017.01.013.
Terman, A., Kurz, T., Navratil, M., Arriaga, E. A., and Brunk, U. T. (2010). Mitochondrial Turnover and Aging of Long-Lived Postmitotic Cells: The Mitochondrial–Lysosomal Axis Theory of Aging. *Antioxid. Redox Signal.* 12, 503–535. doi:10.1089/ars.2009.2598.
Terzioglu, M., and Galter, D. (2008). Parkinson's disease: genetic versus toxin-induced rodent models. *FEBS J.* 275, 1384–1391. doi:10.1111/j.1742-4658.2008.06302.x.
The Huntington's Disease Collaborative Research Group. (1993). A novel gene containing a trinucleotide repeat that is expanded and unstable on Huntington's disease chromosomes. The Huntington's Disease Collaborative Research Group. *Cell* 72, 971–83. Available at: http://www.ncbi.nlm.nih.gov/pubmed/8458085 [Accessed February 8, 2018].
Trettel, F., Rigamonti, D., Hilditch-Maguire, P., Wheeler, V. C., Sharp, A. H., Persichetti, F., et al. (2000). Dominant phenotypes produced by the HD mutation in STHdh(Q111) striatal cells. *Hum. Mol. Genet.* 9, 2799–809. Available at: http://www.ncbi.nlm.nih.gov/pubmed/11092756 [Accessed January 23, 2018].
Trushina, E., Dyer, R. B., Badger, J. D., Ure, D., Eide, L., Tran, D. D., et al. (2004). Mutant huntingtin impairs axonal trafficking in mammalian neurons in vivo and in vitro. *Mol. Cell. Biol.* 24, 8195–209. doi:10.1128/MCB.24.18.8195-8209.2004.
Uversky, V. N. (2007). Neuropathology, biochemistry, and biophysics of ?-synuclein aggregation. *J. Neurochem.* 0, 070710052154012–??? doi:10.1111/j.1471-4159.2007.04764.x.
Valente, E. M., Abou-Sleiman, P. M., Caputo, V., Muqit, M. M. K., Harvey, K., Gispert, S., et al. (2004). Hereditary Early-Onset Parkinson's Disease Caused by Mutations in PINK1. *Science (80-.).* 304, 1158–1160. doi:10.1126/science.1096284.
van der Laan, M., Horvath, S. E., and Pfanner, N. (2016). Mitochondrial contact site and cristae organizing system. *Curr. Opin. Cell Biol.* 41, 33–42. doi:10.1016/j.ceb.2016.03.013.
van der Laan, M., Hutu, D. P., and Rehling, P. (2010). On the mechanism of preprotein import by the mitochondrial presequence translocase. *Biochim. Biophys. Acta - Mol. Cell Res.* 1803, 732–739. doi:10.1016/J.BBAMCR.2010.01.013.
Van Laar, V. S., Arnold, B., Cassady, S. J., Chu, C. T., Burton, E. A., and Berman, S. B. (2011). Bioenergetics of neurons inhibit the translocation response of Parkin following rapid mitochondrial depolarization. *Hum. Mol. Genet.* 20, 927–40. doi:10.1093/hmg/ddq531.
Van Raamsdonk, J. M., Pearson, J., Rogers, D. A., Bissada, N., Vogl, A. W., Hayden, M. R., et al. (2005). Loss of wild-type huntingtin influences motor dysfunction and survival in the YAC128 mouse model of Huntington disease. *Hum. Mol. Genet.* 14, 1379–1392. doi:10.1093/hmg/ddi147.
Ventura, I., Russo, M. T., De Nuccio, C., De Luca, G., Degan, P., Bernardo, A., et al. (2013). hMTH1 expression protects mitochondria from Huntington's disease-like impairment. *Neurobiol. Dis.* 49, 148–58. doi:10.1016/j.nbd.2012.09.002.
Verhagen, A. M., Silke, J., Ekert, P. G., Pakusch, M., Kaufmann, H., Connolly, L. M., et al.

(2002). HtrA2 Promotes Cell Death through Its Serine Protease Activity and Its Ability to Antagonize Inhibitor of Apoptosis Proteins. *J. Biol. Chem.* 277, 445–454. doi:10.1074/jbc.M109891200.

Vila, M., Jackson-Lewis, V., Vukosavic, S., Djaldetti, R., Liberatore, G., Offen, D., et al. (2001). Bax ablation prevents dopaminergic neurodegeneration in the 1-methyl- 4-phenyl-1,2,3,6-tetrahydropyridine mouse model of Parkinson's disease. *Proc. Natl. Acad. Sci.* 98, 2837–2842. doi:10.1073/pnas.051633998.

Vila, M., and Przedborski, S. (2003). Targeting programmed cell death in neurodegenerative diseases. *Nat. Rev. Neurosci.* 4, 365–375. doi:10.1038/nrn1100.

Vilariño-Güell, C., Wider, C., Ross, O. A., Dachsel, J. C., Kachergus, J. M., Lincoln, S. J., et al. (2011). VPS35 Mutations in Parkinson Disease. *Am. J. Hum. Genet.* 89, 162–167. doi:10.1016/j.ajhg.2011.06.001.

Virbasius, C. A., Virbasius, J. V, and Scarpulla, R. C. (1993). NRF-1, an activator involved in nuclear-mitochondrial interactions, utilizes a new DNA-binding domain conserved in a family of developmental regulators. *Genes Dev.* 7, 2431–45.

Vives-Bauza, C., Zhou, C., Huang, Y., Cui, M., de Vries, R. L. A., Kim, J., et al. (2010). PINK1-dependent recruitment of Parkin to mitochondria in mitophagy. *Proc. Natl. Acad. Sci.* 107, 378–383. doi:10.1073/pnas.0911187107.

Vogel, F., Bornhövd, C., Neupert, W., and Reichert, A. S. (2006). Dynamic subcompartmentalization of the mitochondrial inner membrane. *J. Cell Biol.* 175, 237–47. doi:10.1083/jcb.200605138.

Vögtle, F.-N., Wortelkamp, S., Zahedi, R. P., Becker, D., Leidhold, C., Gevaert, K., et al. (2009). Global Analysis of the Mitochondrial N-Proteome Identifies a Processing Peptidase Critical for Protein Stability. *Cell* 139, 428–439. doi:10.1016/j.cell.2009.07.045.

Vukotic, M., Nolte, H., König, T., Saita, S., Ananjew, M., Krüger, M., et al. (2017). Acylglycerol Kinase Mutated in Sengers Syndrome Is a Subunit of the TIM22 Protein Translocase in Mitochondria. *Mol. Cell* 67, 471–483.e7. doi:10.1016/J.MOLCEL.2017.06.013.

Waelter, S., Boeddrich, A., Lurz, R., Scherzinger, E., Lueder, G., Lehrach, H., et al. (2001). Accumulation of mutant huntingtin fragments in aggresome-like inclusion bodies as a result of insufficient protein degradation. *Mol. Biol. Cell* 12, 1393–407. Available at: http://www.ncbi.nlm.nih.gov/pubmed/11359930 [Accessed February 2, 2018].

Wai, T., Garcia-Prieto, J., Baker, M. J., Merkwirth, C., Benit, P., Rustin, P., et al. (2015). Imbalanced OPA1 processing and mitochondrial fragmentation cause heart failure in mice. *Science (80-.).* 350, aad0116-aad0116. doi:10.1126/science.aad0116.

Wai, T., and Langer, T. (2016). Mitochondrial Dynamics and Metabolic Regulation. *Trends Endocrinol. Metab.* 27, 105–117. doi:10.1016/j.tem.2015.12.001.

Waldvogel, H. J., Kim, E. H., Tippett, L. J., Vonsattel, J.-P. G., and Faull, R. L. (2014). "The Neuropathology of Huntington's Disease," in *Current topics in behavioral neurosciences*, 33–80. doi:10.1007/7854_2014_354.

Wang, C.-E., Tydlacka, S., Orr, A. L., Yang, S.-H., Graham, R. K., Hayden, M. R., et al. (2008). Accumulation of N-terminal mutant huntingtin in mouse and monkey models implicated as a pathogenic mechanism in Huntington's disease. *Hum. Mol. Genet.* 17, 2738–2751. doi:10.1093/hmg/ddn175.

Wang, W., Wang, X., Fujioka, H., Hoppel, C., Whone, A. L., Caldwell, M. A., et al. (2015a). Parkinson's disease–associated mutant VPS35 causes mitochondrial dysfunction by recycling DLP1 complexes. *Nat. Med.* 22, 54–63. doi:10.1038/nm.3983.

Wang, X., Petrie, T. G., Liu, Y., Liu, J., Fujioka, H., and Zhu, X. (2012a). Parkinson's disease-associated DJ-1 mutations impair mitochondrial dynamics and cause mitochondrial dysfunction. *J. Neurochem.* 121, 830–839. doi:10.1111/j.1471-4159.2012.07734.x.

Wang, X., Winter, D., Ashrafi, G., Schlehe, J., Wong, Y. L., Selkoe, D., et al. (2011). PINK1 and Parkin target Miro for phosphorylation and degradation to arrest mitochondrial motility. *Cell* 147, 893–906. doi:10.1016/j.cell.2011.10.018.

Wang, X., Yan, M. H., Fujioka, H., Liu, J., Wilson-Delfosse, A., Chen, S. G., et al. (2012b). LRRK2 regulates mitochondrial dynamics and function through direct interaction with DLP1. *Hum. Mol. Genet.* 21, 1931–1944. doi:10.1093/hmg/dds003.

Wang, Y., Serricchio, M., Jauregui, M., Shanbhag, R., Stoltz, T., Di Paolo, C. T., et al. (2015b). Deubiquitinating enzymes regulate PARK2-mediated mitophagy. *Autophagy* 11, 595–606. doi:10.1080/15548627.2015.1034408.

Wasilewski, M., Chojnacka, K., and Chacinska, A. (2017). Protein trafficking at the crossroads to mitochondria. *Biochim. Biophys. Acta - Mol. Cell Res.* 1864, 125–137. doi:10.1016/J.BBAMCR.2016.10.019.

Webb, C. T., Gorman, M. A., Lazarou, M., Ryan, M. T., and Gulbis, J. M. (2006). Crystal Structure of the Mitochondrial Chaperone TIM9•10 Reveals a Six-Bladed α-Propeller. *Mol. Cell* 21, 123–133. doi:10.1016/j.molcel.2005.11.010.

Wellington, C. L., Ellerby, L. M., Gutekunst, C.-A., Rogers, D., Warby, S., Graham, R. K., et al. (2002). Caspase cleavage of mutant huntingtin precedes neurodegeneration in Huntington's disease. *J. Neurosci.* 22, 7862–72. Available at: http://www.ncbi.nlm.nih.gov/pubmed/12223539 [Accessed February 8, 2018].

Weydt, P., Pineda, V. V, Torrence, A. E., Libby, R. T., Satterfield, T. F., Lazarowski, E. R., et al. (2006). Thermoregulatory and metabolic defects in Huntington's disease transgenic mice implicate PGC-1alpha in Huntington's disease neurodegeneration. *Cell Metab.* 4, 349–62. doi:10.1016/j.cmet.2006.10.004.

Wheeler, V. C., Gutekunst, C.-A., Vrbanac, V., Lebel, L.-A., Schilling, G., Hersch, S., et al. (2002). Early phenotypes that presage late-onset neurodegenerative disease allow testing of modifiers in Hdh CAG knock-in mice. *Hum. Mol. Genet.* 11, 633–640. doi:10.1093/hmg/11.6.633.

Wheeler, V. C., White, J. K., Gutekunst, C. A., Vrbanac, V., Weaver, M., Li, X. J., et al. (2000). Long glutamine tracts cause nuclear localization of a novel form of huntingtin in medium spiny striatal neurons in HdhQ92 and HdhQ111 knock-in mice. *Hum. Mol. Genet.* 9, 503–13. Available at: http://www.ncbi.nlm.nih.gov/pubmed/10699173 [Accessed February 8, 2018].

Wiedemann, N., Frazier, A. E., and Pfanner, N. (2004). The protein import machinery of mitochondria. *J. Biol. Chem.* 279, 14473–6. doi:10.1074/jbc.R400003200.

Wiedemann, N., Kozjak, V., Chacinska, A., Schönfisch, B., Rospert, S., Ryan, M. T., et al. (2003). Machinery for protein sorting and assembly in the mitochondrial outer membrane. *Nature* 424, 565–571. doi:10.1038/nature01753.

Wiedemann, N., and Pfanner, N. (2017). Mitochondrial Machineries for Protein Import and Assembly. *Annu. Rev. Biochem.* 86, 685–714. doi:10.1146/annurev-biochem-060815-014352.

Wild, P., McEwan, D. G., and Dikic, I. (2014). The LC3 interactome at a glance. *J. Cell Sci.* 127, 3–9. doi:10.1242/jcs.140426.

Wong, Y. C., and Holzbaur, E. L. F. (2014). The regulation of autophagosome dynamics by huntingtin and HAP1 is disrupted by expression of mutant huntingtin, leading to

defective cargo degradation. *J. Neurosci.* 34, 1293–305. doi:10.1523/JNEUROSCI.1870-13.2014.

Wu, Z., Puigserver, P., Andersson, U., Zhang, C., Adelmant, G., Mootha, V., et al. (1999). Mechanisms Controlling Mitochondrial Biogenesis and Respiration through the Thermogenic Coactivator PGC-1. *Cell* 98, 115–124. doi:10.1016/S0092-8674(00)80611-X.

Wüllner, U., Pakzaban, P., Brownell, A. L., Hantraye, P., Burns, L., Shoup, T., et al. (1994). Dopamine terminal loss and onset of motor symptoms in MPTP-treated monkeys: a positron emission tomography study with 11C-CFT. *Exp. Neurol.* 126, 305–9. Available at: http://www.ncbi.nlm.nih.gov/pubmed/7925829 [Accessed February 8, 2018].

Xifró, X., García-Martínez, J. M., del Toro, D., Alberch, J., and Pérez-Navarro, E. (2008). Calcineurin is involved in the early activation of NMDA-mediated cell death in mutant huntingtin knock-in striatal cells. *J. Neurochem.* 105, 1596–1612. doi:10.1111/j.1471-4159.2008.05252.x.

Yamano, K., Matsuda, N., and Tanaka, K. (2016). The ubiquitin signal and autophagy: an orchestrated dance leading to mitochondrial degradation. *EMBO Rep.* 17, 300–16. doi:10.15252/embr.201541486.

Yano, H., Baranov, S. V, Baranova, O. V, Kim, J., Pan, Y., Yablonska, S., et al. (2014). Inhibition of mitochondrial protein import by mutant huntingtin. *Nat. Neurosci.* 17, 822–31. doi:10.1038/nn.3721.

Yano, M., Kanazawa, M., Terada, K., Namchai, C., Yamaizumi, M., Hanson, B., et al. (1997). Visualization of mitochondrial protein import in cultured mammalian cells with green fluorescent protein and effects of overexpression of the human import receptor Tom20. *J. Biol. Chem.* 272, 8459–65. doi:10.1074/JBC.272.13.8459.

Yano, M., Kanazawa, M., Terada, K., Takeya, M., Hoogenraad, N., and Mori, M. (1998). Functional analysis of human mitochondrial receptor Tom20 for protein import into mitochondria. *J. Biol. Chem.* 273, 26844–51. doi:10.1074/JBC.273.41.26844.

Yee, K. S., Wilkinson, S., James, J., Ryan, K. M., and Vousden, K. H. (2009). PUMA- and Bax-induced autophagy contributes to apoptosis. *Cell Death Differ.* 16, 1135–45. doi:10.1038/cdd.2009.28.

Yoshii, S. R., and Mizushima, N. (2015). Autophagy machinery in the context of mammalian mitophagy. *Biochim. Biophys. Acta - Mol. Cell Res.* 1853, 2797–2801. doi:10.1016/j.bbamcr.2015.01.013.

Young, J. C., Hoogenraad, N. J., and Hartl, F. U. (2003). Molecular chaperones Hsp90 and Hsp70 deliver preproteins to the mitochondrial import receptor Tom70. *Cell* 112, 41–50.

Zarranz, J. J., Alegre, J., Gómez-Esteban, J. C., Lezcano, E., Ros, R., Ampuero, I., et al. (2004). The new mutation, E46K, of α-synuclein causes parkinson and Lewy body dementia. *Ann. Neurol.* 55, 164–173. doi:10.1002/ana.10795.

Zeitlin, S., Liu, J.-P., Chapman, D. L., Papaioannou, V. E., and Efstratiadis, A. (1995). Increased apoptosis and early embryonic lethality in mice nullizygous for the Huntington's disease gene homologue. *Nat. Genet.* 11, 155–163. doi:10.1038/ng1095-155.

Zhang, J., and Ney, P. A. (2009). Role of BNIP3 and NIX in cell death, autophagy, and mitophagy. *Cell Death Differ.* 16, 939–946. doi:10.1038/cdd.2009.16.

Zhang, Q., Chen, W., Tan, S., and Lin, T. (2017). Stem Cells for Modeling and Therapy of Parkinson's Disease. *Hum. Gene Ther.* 28, 85–98. doi:10.1089/hum.2016.116.

Zhao, Q., Wang, J., Levichkin, I. V, Stasinopoulos, S., Ryan, M. T., and Hoogenraad, N. J. (2002). A mitochondrial specific stress response in mammalian cells. *EMBO J.* 21,

4411–9. Available at: http://www.pubmedcentral.nih.gov/articlerender.fcgi?artid=PMC126185 [Accessed November 19, 2017].

Zheng, B., Liao, Z., Locascio, J. J., Lesniak, K. A., Roderick, S. S., Watt, M. L., et al. (2010). PGC-1 , A Potential Therapeutic Target for Early Intervention in Parkinson's Disease. *Sci. Transl. Med.* 2, 52ra73-52ra73. doi:10.1126/scitranslmed.3001059.

Zhu, J. H., Gusdon, A. M., Cimen, H., Van Houten, B., Koc, E., and Chu, C. T. (2012). Impaired mitochondrial biogenesis contributes to depletion of functional mitochondria in chronic MPP+ toxicity: dual roles for ERK1/2. *Cell Death Dis.* 3, e312. doi:10.1038/cddis.2012.46.

Zimprich, A., Benet-Pagès, A., Struhal, W., Graf, E., Eck, S. H., Offman, M. N., et al. (2011). A Mutation in VPS35, Encoding a Subunit of the Retromer Complex, Causes Late-Onset Parkinson Disease. *Am. J. Hum. Genet.* 89, 168–175. doi:10.1016/j.ajhg.2011.06.008.

Zimprich, A., Biskup, S., Leitner, P., Lichtner, P., Farrer, M., Lincoln, S., et al. (2004). Mutations in LRRK2 Cause Autosomal-Dominant Parkinsonism with Pleomorphic Pathology. *Neuron* 44, 601–607. doi:10.1016/j.neuron.2004.11.005.

Ziviani, E., Tao, R. N., and Whitworth, A. J. (2010). Drosophila Parkin requires PINK1 for mitochondrial translocation and ubiquitinates Mitofusin. *Proc. Natl. Acad. Sci.* 107, 5018–5023. doi:10.1073/pnas.0913485107.

Zuccato, C., Tartari, M., Crotti, A., Goffredo, D., Valenza, M., Conti, L., et al. (2003). Huntingtin interacts with REST/NRSF to modulate the transcription of NRSE-controlled neuronal genes. *Nat. Genet.* 35, 76–83. doi:10.1038/ng1219.

Züchner, S., Mersiyanova, I. V, Muglia, M., Bissar-Tadmouri, N., Rochelle, J., Dadali, E. L., et al. (2004). Mutations in the mitochondrial GTPase mitofusin 2 cause Charcot-Marie-Tooth neuropathy type 2A. *Nat. Genet.* 36, 449–451. doi:10.1038/ng1341.